MECHANISMS AND KINETICS OF BINARY ALKALI SILICATE GLASS CORROSION

By

EDWIN CLARK ETHRIDGE

A DISSERTATION PRESENTED TO THE GRADUATE COUNCIL OF
THE UNIVERSITY OF FLORIDA
IN PARTIAL FULFILLMENT OF THE REQUIREMENTS FOR THE
DEGREE OF DOCTOR OF PHILOSOPHY

UNIVERSITY OF FLORIDA

1977

To Mom and Dad

ACKNOWLEDGEMENTS

The author wishes to recognize his father for instilling an interest in science at an early age and Morris Dilmore for introducing the author to Materials Science. Special thanks to to Andy Walker and Jack Gary for assisting with some of the data collecting and figure drawing and to Eddie Clark for helpful discussions. The author is especially indebted to his advisor, L. L. Hench, for providing guidance and invaluable encouragement throughout the entire study and to the rest of the committee for criticisms and suggestions. Finally, the author wishes to thank his wife, Julie, for typing the many drafts and the final copy of the dissertation.

This research was financed in part by the National Institute of Dental Research, contract number N01-DE-32421.

TABLE OF CONTENTS

LIST OF TABLES

LIST OF FIGURES

Abstract of Dissertation Presented to the Graduate Council of the University of Florida in Partial Fulfillment of the Requirements for the Degree of Doctor of Philosophy

MECHANISMS AND KINETICS OF BINARY ALKALI SILICATE GLASS CORROSION

By

Edwin Clark Ethridge

June, 1977

Chairman: Larry L. Hench
Major Department: Materials Science and Engineering

An extensive critical review of the glass corrosion and related literature is presented. Many irregularities are noted and some of the previously reported information is reinterpreted. Specific questions are raised which are discussed in detail.

Differences are shown to exist between the corrosion of glass powders and the corrosion of bulk glass surfaces. For glass grains, dissolution kinetics of $t^{\frac{1}{2}}$ and t^{1} are found to be only limiting conditions at short and long times respectively. Bulk glass surfaces, however, have these two conditions for long periods of time and have a sharp transition from $t^{\frac{1}{2}}$ to t^{1} kinetics when the pH exceeds approximately 9.5. The data from the corrosion of glass grains indicate that concentration cell effects exist which can produce anomalous results.

Variations of the surface area of glass to volume of solution (A/V) on glass corrosion kinetics are investigated. For bulk glass surfaces graphs of $\log$ Q vs. $\log$ A/V (at a given time of corrosion) and graphs of $\log t$ (time to reach a given concentration of glass constituent in solution) vs. $\log$ A/V yield results which are in agreement with derived equations. The corrosion of glass grains, however, yields results inconsistent with the derived equations. This is attributed to the change in the effective surface area of the glass grains as corrosion proceeds.

Many glasses in the Li_2O-, Na_2O-, and K_2O-SiO_2 systems are corroded using bulk glass surfaces and static test conditions. Reaction rate constants are determined for the leaching of alkali ions and for the extraction of silica during the $t^{\frac{1}{2}}$ regime. Concentrations of alkali ions and silica in solution are used to calculate the corrosion parameters alpha and epsilon. Corroded glass surfaces are examined by infrared reflection spectroscopy (IRRS) and techniques are developed for compositional analysis of corroded binary alkali silicate glass surfaces and for the determination of the leached layer compositional profiles. An equation is developed for calculating the thickness of the leached layer (X) from the surface composition and epsilon and calculated values of X are verified to be within experimental error. Another equation is developed for calculating the thickness of glass totally dissolved from the surface (X_1).

The kinetics of binary alkali silicate glass corrosion are followed with solution data, corrosion parameters, IRRS, surface

composition, leached layer profiles, X, X_1 and X/X_1. A general sequence of events is described for the corrosion of these glasses.

The temperature dependent corrosion kinetics for two glasses are presented. The same kinetic sequence of events occurs at 30°C, 50°C, and 100°C and only the time sequence to obtain equivalent extents of corrosion is changed. The time-temperature dependence does, however, depend on the composition of the glass.

Graphs of *log* (time to reach a critical extent of corrosion) vs. *log* A/V and temperature studies are discussed in terms of the possible long term prediction of corrosion and the study of nuclear waste containing glasses.

Evidence is presented which indicates that the surface of most corroded glasses undergoes a transformation induced by strain from the ion exchange reaction in which many silanol groups combine during a dehydration reaction to form new silicon bridging oxygen bonds.

Interdiffusion coefficients are calculated for the ion exchange reaction. The results indicate that the interdiffusion process is controlled by the diffusion of alkali ions out of the glass and by the openness of the leached layer.

A model is proposed for the $t^{\frac{1}{2}}$ dependent release of silica into acidic and neutral solutions. Diffusion coefficients are calculated which support a model in which Si-O bonds are attacked by OH^- ions from solution and free silanol groups are produced which diffuse through the transformed porous vitreous silica like leached layer.

CHAPTER I

INTRODUCTION

The chemical durability of a glass is a term which expresses the intrinsic resistance of the glass to decomposition by its surrounding environment. An American Society for Testing Materials (ASTM) definition for the chemical durability of glass is "The lasting quality (both physical and chemical) of a glass surface. It is frequently evaluated after prolonged weathering or storing, in terms of chemical and physical changes in the glass surface, or in terms of changes in the contents of a vessel."[1] Holland[2] stated that most silicate glasses in general use have very good chemical durability which has led many workers to erroneously treat glass as an inert substance. Glass, however, is not inert, optical glass can become stained by the atmosphere,[2] plate glass can be ruined by storing horizontally in cyclic condensation conditions,[3] and some glass containers degrade and produce a silicate precipitate in the contents.[3] The reaction of glass with water is also important from an engineering design standpoint since the mechanical strength, optical properties, or the surface electrical conductivity may be influenced.[4] Not all reactions between a glass surface and aqueous solution are detrimental. A calcium phosphate containing glass has been developed which undergoes surface chemical reactions producing a surface which resembles bone

and cementum. Such glasses have proved to be prime candidate materials for artificial bones[5-8] and dental implants.[9-10]

In general the broad classification of chemical durability can be subdivided into weathering and glass corrosion. The ASTM definition for weathering is the "attack of a glass surface by atmospheric elements."[11] Bacon[3] describes several effects of weathering of glasses. The storing of sheet glass with surfaces in contact can form cells in which moisture is trapped leading to severe attack of the glass surface. The effect on installed window panes can be two-fold. If the glass surface becomes soiled, moisture can be retained causing an accumulation of reaction products leading to alkaline conditions which etch the surface. If the window surface is clean and is rinsed by rain water the reaction products are washed away and weathering is not apparent. In this case the weathering can actually enhance the chemical durability of the surface by producing a leached surface rich in silica.

The weathering of bottles is another problem.[3] If bottles are stored in a warehouse in which cycles of temperature and humidity cause alternate condensation and evaporation of moisture on the surface, severe weathering can occur. If the weathering is slight, then the inside surface is only slightly clouded and disappears after rinsing or filling with a liquid. If the weathering is severe, glistening flakes of siliceous gel can become detached and float in the liquid. The weathering resistance can be enhanced by storing the glass containers in a suitable warehouse and/or by the incorporation of Al_2O_3 into the glass composition to enhance the weathering resistance.

Glass corrosion is the term applied to the reaction of a glass with aqueous solutions. A recent problem associated with glass corrosion involves the containment of highly radioactive wastes within a glassy matrix structure. It is hoped that these radioactive wastes can be prevented from entering the biosphere by limiting their rate of leaching from the glass.

The attack by water on glass is a decomposition reaction and should not be confused with true solubility.[3] From a study of the equilibrium conditions involving complex silicates and water over a range of temperatures and pressures, Morey[12] concluded that true phase equilibrium does not exist at ordinary temperatures for systems such as minerals, glasses and ceramic bodies. Therefore, glass corrosion is not a simple dissolution of glass in water. It involves the penetration of glass by water and the subsequent decomposition of the complex silicate matrix. The rate of the attack, not the final equilibrium condition, is of greatest technological importance.[13]

In principle there are three ways in which a glass may react during aqueous corrosion.[2] The first is for one or more of the glass constituents to preferentially dissolve leaving a leached layer on the surface of the glass. An example is the dealkalinization of the glass surface producing a surface depleted in alkali ions. A second way that a glass may corrode is by congruent dissolution such that the corrosion products appear in solution in the same proportions as in the bulk glass composition. Incongruent dissolution is a third possible way in which a glass may corrode. Oishi et al.[14] coined the term "incongruent dissolution" to describe the dissolution of a multicomponent

system with the precipitation of another phase at the interface. This can occur if any of the constituents in the liquid are unstable with respect to the surface.[15]

Purpose of the Dissertation

Many reviews of glass corrosion have appeared in the literature. Most of them approach the subject from an empirical standpoint describing the technological significance of the relative chemical durability of glasses of different compositions. A critical review of glass corrosion has never been prepared which examines the mechanisms controlling the extraction of each glass constituent at the different stages of corrosion. The first objective of this dissertation is to present such a critical review.

In Chapter II the use of "accelerated" corrosion tests are discussed. A conclusion of this section of Chapter II is that more work needs to be done to confirm the reliability and applicability of the two methods of accelerating glass corrosion. In Chapter IV the corrosion of glass grains will be compared with the corrosion of bulk glass surfaces (planar polished glass surface with a known ratio of the surface area of glass to volume of solution). Conclusions will be drawn concerning the usefulness of different corrosion tests in the study of glass corrosion processes.

Weyl and Marboe[16] recognized that the typical glass corrosion investigations (i.e. using glass grains and high temperature) are

conducted under conditions which do not resemble in any way the conditions under which the glass will be used. They wrote that it is illogical to test glasses at 100°C when they are used at ordinary temperatures. Chapter VI reports the results of an investigation into the effect of temperature on the acceleration of glass corrosion to determine if high temperature studies can be justifiably extrapolated to lower temperature in-service use.

It is not known from previous studies whether changing the glass surface area to solution volume ratio (A/V) has an effect on the corrosion process. Discrepancies which exist in the literature may be due to differences in the ratio of surface area to solution volume and they are clarified by a mathematical technique in Chapter V. Several ways of plotting corrosion data vs. A/V are discussed with reference to long term prediction of glass corrosion.

The first step in a systematic investigation of glass corrosion should involve a study of the simplest glass forming systems such as the binary alkali silicate glasses. By studying a binary alkali silicate system one can determine the effect of increasing numbers of non-bridging oxygen ions on the corrosion behavior in the absence of competing effects. Comparing such effects between different binary alkali silicate systems makes it possible to relate the size of the modifying alkali ions to the corrosion behavior.

According to several reviews of glass corrosion, there is a need for a more systematic investigation of the corrosion processes. Paraphrasing Weyl,[17] before it is possible to link the properties of glass with its structure it is necessary to accumulate sufficient experimental

data concerning the properties of systematically varied glasses. In a review of the state of the science of glass corrosion Das[18] stated, "A study between water and glass is incomplete if the reaction is not studied systematically with varying time, temperature and composition."[18] A purpose of this dissertation research has been to examine the corrosion behavior of several glasses in three binary alkali silicate systems over a wide range of compositions and times in order to characterize completely their corrosion behavior.

Douglas and El-Shamy[19] investigated the corrosion behavior of a few binary alkali silicates; however, several irregularities in their results exist which are discussed in Chapter IV. The cause of some of the irregularities is attributed to the fact that glass powders were used. As will be seen in Chapter IV, the corrosion of bulk glass surfaces yields data which are more representative of the properties of the glass. For this reason the data for the binary alkali silicate glasses in this investigation were obtained using the technique developed by Sanders and Hench.[20,21]

It is believed that as long as the concentrations of alkali and silica in solution are below 10^{-4} and 10^{-5} mole/l, respectively, the diffusion processes operating in glass corrosion remain in control.[22] Another objective of this dissertation has been to determine precisely when and why the root time dependence characteristic of diffusional processes changesover to a linear time dependence. Doremus[23] asked whether the dissolution rates become precisely linear with time or whether they continue to increase. This question is addressed in Chapter VI.

Rana and Douglas said, "For the time being it would appear more profitable to accumulate more experimental evidence and to consider the contribution of the reactions between the hydroxyl and hydronium ions and the silica network to the reaction kinetics."[24] Considerable data are accumulated in this dissertation on the corrosion of three binary alkali silicate glass systems. These data are strong evidence that the mechanisms of corrosion change as the pH of the aqueous solution changes with time. In Chapter VI a unified theory is proposed for the corrosion of the binary alkali silicate glasses.

Infrared reflection spectroscopy (IRRS) is a very useful tool for investigating the composition and structure of glass surfaces. Sanders et. al [25] demonstrated its usefulness in the study of the corrosion of a lithium disilicate glass (33L). In Chapters VII and VIII the use of IRRS to investigate the changes occurring in the surface during the corrosion of many binary alkali silicate glasses is discussed.

The diffusion of various species into or out of a glass during corrosion has been the object of discussion in some of the corrosion literature. In his book, Doremus said that the diffusion of water into glass and the subsequent reaction with internal Si-O-Si bonds needs further confirmation.[23] He also stated that the importance of hydration of the surface and the replacement of ions on the surface by smaller H^+ ions can be assessed only by further work.[23] In another book, Frischat[26] listed the need for the determination of self-consistent diffusion coefficients for the attack of glasses by aqueous solution as one topic for further work and investigation. In Chapter IX interdiffusion coefficients are reported for the ion exchange

process. These values are related to the hydration of the surface as well as to the penetration of H^+ (or H_3O^+) ions and the leaching of alkali ions. Diffusion coefficients have also been determined for the extraction of silica from the glass and are related to the diffusion of OH^- ions into the glass surface.

Several things need to be explained before the general review begins. Throughout the discussion the phrase "in the surface" will be used. Since there is no well-defined water bulk glass interface, the term "in the surface" will refer to the region between the water phase and the bulk glass.

An explanation of the notation used to designate the composition of the silicate glasses under discussion is also needed. This notation consists of numbers and letters (L = Li_2O, N = Na_2O, K = K_2O, C = CaO) referring to the mole % of a constituent and a letter designating the particular constituent. The balance in each case will be understood to be SiO_2. For example, the respective compositions of 33L and 20N10C are 33 mole % Li_2O - 67 mole % SiO_2 and 20 mole % Na_2O - 10 mole % CaO - 70 mole % SiO_2.

CHAPTER II

CRITICAL REVIEW OF GLASS CORROSION AND RELATED TOPICS

Glass Structure

Zachariasen proposed that the structure of glass is a continuous random network of silicon-oxygen-silicon bonds.[27] He wrote that the ultimate general requirement for the formation of glass is that an extended three dimensional network be produced which lacks long range order and has an energy similar to a crystalline network. These restrictions require certain conditions based on the coordination of anions around cations. According to this theory the coordination number for a cation is derived on a geometrical basis, assuming that the ions are spherical, relating the radius of the cation to the radius of the anion (i.e. radium ratio). This continuous random network theory is a good first approximation for the structure of glass but it does not allow the prediction of the properties of simple glasses.[17]

Weyl proposed a more atomistic approach to the chemistry of glass based on the principles of crystal chemistry involving the polarization of ions.[17] Weyl said that,

> . . . the work of Warren, Goldschmidt and Zachariasen . . . demonstrated that there is no major difference between the structure of silicate glasses and of related crystalline materials except that in crystals a long-range order exists which is absent in liquids and in glasses. The short-range order around a certain atom, however, is very similar for

> the vitreous state and for crystals. This discovery is of greatest significance since the short range order determines the chemistry of solids. Furthermore, it makes possible the use of the principles of crystal chemistry for exploring the structure and the properties of glasses.[28]

A short summary of Weyl's approach[17] deserves some mention. According to this approach the concept of "bond strength" seems to be meaningless when applied to glass. When an ion is formed from an atom, two energy changes are involved. There is the formation of a preferred outer electron shell and the creation of a potential field. These two effects counteract one another so that the formation of many ions requires the screening and neutralization of their potential fields. An example of this is the formation of NaCl. After the Na^+ and Cl^- ions are formed, their fields must be screened. The combination of the two ions to form a NaCl molecule does not completely screen the potential fields, however, and the molecule remains reactive. This leads to the combination of these ions to form a crystal. Therefore, the forces which lead to the formation of chemical compounds are precisely the same as those which cause crystallization or polymerization differing only in magnitude.

According to this theory the Na^+ ion not only has to be linked to one anion but must also be surrounded by them (equally linked to all anions in 1st coordination sphere) to be stable. The concept of the coordination number in crystal chemistry arises from the need of a number of anions to adequately screen each cation and vice versa. The coordination number is determined by two factors, the size of the anion and its polarizability (where the polarizability of an ion is the

ability of an ion to adjust its electronic configurations and force fields to suit the environment). The rigidity of the coordination requirement of an ion is determined by its polarizability such that the coordination requirements become more important as the polarizability of the ion decreases. Since anions are more polarizable than cations and large cations are more polarizable than small cations, coordination requirements are more strict for small cations than for larger cations and anions.

The formation of silicate glasses can be considered an aggregation or polymerization process which results from the coordination requirement of the Si^{4+} in the structure. In vitreous silica where each O^{2-} ion is exposed to two Si^{4+} ions the coordination of O^{2-} ions around Si^{4+} ions is four.

The coordination requirements of a cation is also affected by the polarizability of the anion. Anions which are more polarizable are better screeners since their electron cloud can be deformed more easily allowing the electron density around the cation to become more evenly distributed. Weyl said,

> The number of oxygen ions which are required for the screening of an Si^{4+} ion depends on their polarizability which, in turn, is a function of the second coordination sphere. According to K. Fajans the polarizability of an anion is decreased if its electron cloud is tightened under the influence of strong positive fields. This effect, which has been called contrapolarization by V. M. Goldschmidt, plays a decisive role in determining the coordination number of a cation.[29]

If the contrapolarization is produced by cations weaker than Si^{4+} (i.e. Na^{+}, Ca^{+}) the coordination remains four. If, however, the O^{2-} ions are deformed by stronger positive fields (i.e. H^{+}, P^{5+}) they have

a lower polarizability so that more than four O^{2-} ions may be required for screening the Si^{4+} ion.

Oxygen ions in pure silica have a low polarizability since their electron clouds are attracted by the strong fields of the two adjoining Si^{4+} ions. However, the contrapolarizing effect of an alkali ion can make the O^{2-} ion more polarizable. Since O^{2-} ions contrapolarized by alkali ions have a higher polarizability than O^{2-} ions between two Si^{4+} ions, they can better screen the Si^{4+} ions. Weyl described this as the driving force for the formation of the alkali silicates. Each of the alkali ions exerts a different contrapolarizing effect. The alkali ions produce contrapolarizing effects such that the screening of the Si^{4+} ions by the O^{2-} ions decreases for alkali ions in the order $K^+ > Na^+ > Li^+$.[17]

The extent of screening of the central cation (Si^{4+}) affects its chemical reactivity. Anything which decreases the screening of the cation (i.e. increasing the cation-anion distance, increasing the contrapolarizing effect on the anion) increases the chemical reactivity. This is significant to glass corrosion and will be discussed later.

Vitreous Silica and Water

Since silicate glasses contain large percentages of SiO_2 it seems most logical to begin the study of glass corrosion with an investigation of the reactions between water and vitreous silica. This will give an understanding of the reactions between water and the silica network in the absence of network modifying constituents.

Physical chemists have contributed a considerable amount of information on the reactions of vitreous silica with water. Alexander et al.[30] investigated the solubility of amorphous silica at various values of pH. A relatively constant solubility of 0.012 - 0.014% was observed over the pH range of 5 to 8. Above a pH of about 9, however, the value increased rapidly to about 0.5% at a pH of 11. This change in solubility with pH was explained on the basis of the equilibrium equation,

$$Si(OH)_4 + OH^- = Si(OH)_3O^- + H_2O \qquad (1)$$

assuming that the concentration of $Si(OH)_4$ does not change with pH. Roller and Ervin[31] found the equilibrium constant for the above equation at 30°C to be,

$$\frac{[H^+][Si(OH)_3O^-]}{[Si(OH)_4]} = 10^{-9.8} \qquad (2)$$

for the total solubility of silica including monomeric silicic acid and silicate ions, S_t, and the concentration of monosilicic acid, S_m,

$$\frac{[H^+][S_t - S_m]}{[S_m]} = 10^{-9.8} \qquad (3)$$

$$pH - \log\left(\frac{S_t - S_m}{S_m}\right) = 9.8 \qquad (4)$$

Alexander et al.[30] substituted S_m = 0.012% into Eq. 4 and calculated values of pH. It was shown that these calculated values were in reasonably good agreement with the experimental values. This is evidence that the concentration of $Si(OH)_4$ in equilibrium with the solid phase is not affected by the pH of the solution.

Greenberg and Price[32] examined the solubility of silica in electrolyte solutions. It was observed that sodium chloride solutions in the concentration range of 0.0001 to 0.10N and sodium sulfate solutions in the concentration range of 0.005 to 0.20N produce no appreciable effect on the solubility of silica. The solubility at 25°C for these cases was found to be 0.0018M which was in good agreement with Alexander et al.[30] When the sodium chloride concentration is increased to 1N the solubility is reduced only slightly to 0.0016M.

Several investigators have studied the kinetics for the solution of silica in water. O'Connor and Greenberg[33] developed a model surface reaction which is controlled by a combination of the removal and addition of silica groups. According to this model the rate of solution is,

$$\frac{dc}{dt} = k_1 S \tag{5}$$

and the rate of polymerization,

$$-\frac{dc}{dt} = k_2 c S \tag{6}$$

The net change is,

$$\frac{dc}{dt} = (k_1 - k_2 c) \cdot S \qquad (7)$$

where c is the concentration of monosilicic acid at a given time t, k_1 and k_2 are rate constants and S is the surface area per unit volume of solution. At equilibrium, dc/dt is zero so that,

$$K = \frac{k_1}{k_2} = C_e \qquad (8)$$

where C_e is the equilibrium concentration of silicic acid. Rearranging and substituting into Eq. 7 yields,

$$\frac{dc}{dt} = k_2 S \, (C_e - C) \qquad (9)$$

Integrating one obtains,

$$\log\left(\frac{C_e - C}{C_e}\right) = -(k_2 S t) \qquad (10)$$

O'Connor and Greenberg[33] point out that Eq. 9 is in the same form as that obtained by assuming that a diffusion step is rate determining. They used data obtained by Lucas and Doland[34] for the dissolution of quartz to test Eq. 10. In all cases they obtained linear relations for $\log (C_e - C)/C_e$ vs. t as predicted by the equation. This is good evidence for the model that the dissolution of vitreous silica is

controlled by a balance of the competing reactions of dissolution and repolymerization; in other words, an incongruent dissolution process.

Jörgensen[35] investigated the dissolution kinetics of amorphous silica in 1M $NaClO_4$. He also observed a dissolution behavior which indicated that one solid phase dissolves with the subsequent precipitation of a more stable phase. Early X-ray measurements suggested a surface structure similar to cristobalite or tridymite.[36] But, Jörgensen[35] was skeptical of these X-ray results since the solubility of cristobalite is about 3 or 4 times lower than that observed.

In alkaline solution above a pH of about 11 it is possible to neglect the term k_2CS from Eq. 7 since the rate of polymerization is negligible. After integrating one obtains:

$$C_p^{1/3} = C_{p_o}^{1/3} - k_3 t \qquad (11)$$

where C_{p_o} is the concentration of polymer at $t = 0$ and k_3 is a constant. O'Connor and Greenberg[33] tested this theory for the dissolution of silica in alkaline media (0.025M NaOH) and obtained a linear relation for $C_p^{1/3}$ vs. t confirming the depolymerization process.

A specific study of the polymerization and depolymerization of silicic acid was carried out by Greenberg and Sinclair[37] and Greenberg[38] respectively. Two possible mechanisms exist for the polymerization of silicic acid:

$$2\ Si(OH)_4 \rightleftarrows Si(OH)_3OSi(OH)_3 + H_2O \qquad (12)$$

$$Si(OH)_3O^- + Si(OH)_4 \rightleftarrows Si(OH)_3OSi(OH)_3 + OH^- \qquad (13)$$

The actual mechanism in control should be consistent with all the available information concerning the process.

1. The reaction does not occur at high pH where depolymerization occurs and where ionized silanol groups repel each other.
2. The reaction is slow at low pH.
3. The reaction proceeds at a maximum rate in a pH range of 8-9.
4. As the silicate ion concentration increases the rate of reaction increases.

At low pH the slow rate of polymerization can be attributed to the low constant silicate ion concentration. Since the proportion of ionized to unionized silanol groups in this range is very low, polymerization proceeds by the first mechanism (Eq. 12).

At values of pH greater than 9 the proportion of ionized silicate ions is significant. However, as the pH increases the concentration of OH^- ions increases. This drives the second mechanism (Eq. 13) in reverse resulting in depolymerization. Since the proportions of ionized to unionized silanol groups at high pH is very large, repulsion of the ionized groups would also tend to prevent polymerization from occurring.

For the pH range 8-9 some silicate ions exist in solution along with the constant concentration of unionized silanol groups.[30] The

maximum rate of polymerization in this range is, therefore, due to the sum of the two mechanisms occurring simultaneously.

There are two different activation energies for the polymerization reaction.[39] In acidic solution it is 9-11 Kcal/mole and can be considered the activation energy for the first mechanism (Eq. 12). In alkaline solution the activation energy is 24 Kcal/mole and is attributed to the second mechanism (Eq. 13).

Greenberg[38] attributed the depolymerization process to a reaction similar to the reverse of Eq. 13,

$$\equiv Si\text{-}O\text{-}Si\equiv + OH^- \rightleftarrows \equiv Si\text{-}OH + {}^-O\text{-}Si\equiv \qquad (14)$$

With this mechanism, OH^- ions must diffuse into the silica structure to hydrolyze the network with subsequent diffusion of the low molecular weight silicic acid molecules away from the surface into the liquid phases. The activation energy for the depolymerization reaction is the same in neutral water and alkaline solutions (pH > 11),[33] however, it varies from 18 Kcal/mole[33] to 21.5 Kcal/mole[38] depending on the form of silica. Differences in the activation energies as well as the rates of depolymerization[38] with various forms of silica indicate that the strength of the silicon bridging oxygen bond markedly affects the rate of depolymerization.

Polymerization and depolymerization reactions similar to Eqs. 12 and 14 will be discussed in terms of corrosion of silicate glasses in later chapters.

Kinetics of Glass Corrosion

Charles[40] noted that there is a big difference between the attack by water on fused silica and on commercial glasses. While fused silica and quartz are nearly insoluble in water at neutral pH and moderate temperatures, most commercial glasses are quite reactive releasing large quantities of glass constituents into solution. Charles attributed this difference in behavior to the terminal structures (non-bridging oxygen atoms) produced by the alkali ions and the other modifiers in the glass network.

The first logical step for studying the corrosion of glass is to investigate the effect of additions of various concentrations of different glass modifiers to vitreous silica. In this way one can ascertain the significance of the terminal structures produced by different modifiers on glass corrosion. There is, however, very little systematic data on the aqueous reaction with binary glasses. Most investigators have been primarily interested in examining the effects of adding third constituents to the binary alkali silicate glasses. The results of various corrosion studies will, therefore, be discussed from a qualitative standpoint even though results are difficult to correlate because of the many different compositions and types of tests reported in the literature.

Many of the early investigators of glass corrosion found that the extraction of alkali from a glass followed a parabolic course during early corrosion times.[41-44] An ion exchange reaction was proposed to

account for the leaching of Na^+ ions and the preservation of electroneutrality at the surface:[45]

$$Na^+_{gl} + H_3O^+(\text{or } H^+)_{liq} \rightleftarrows Na^+_{liq} + H_3O^+(\text{or } H^+)_{gl} \qquad (15)$$

Lyle[46] suggested that the leaching of sodium was controlled by the rate of diffusion of sodium through a hydrated surface on the glass and that the rate of leaching should be proportional to the sodium concentration gradient in the glass surface. Lyle modeled the time release of alkali ions into solution by the kinetic equation,

$$Q^A = k't \qquad (16)$$

where Q is the quantity of alkali leached after a given length of time, t, while A and k' are constants. For a root time dependence to hold A must equal 2. Lyle[46] found that for the conditions studied A was not always equal to 2 but depended on the glass used.

The time release of silica into solution follows the same type of behavior; however, it is not as clearly established as the leaching of sodium. The kinetic equation for the leaching of alkali and the release of silica in solution given by Lyle[46] was altered slightly by Rana and Douglas[47] to the more commonly used form.

$$Q = kt^a \qquad (17)$$

Where Q is the quantity of glass constituent released after time t, while k and a are the reaction rate constant and reaction rate exponent respectively. Taking the logarithm of Eq. 17 yields,

$$\log Q = \log k + a \log t \qquad (18)$$

The slope of a plot of $\log Q$ vs. $\log t$, therefore, gives the reaction rate exponent, a.

Zagar and Schmillmöller[48] studied the corrosion of a series of technical glasses and observed that with some glass constituents a parabolic time dependence was obvious. With others it was uncertain and apparently was not present with silica. Slopes of $\log Q$ vs. $\log t$ for silica were greater than 0.5, however, they approached a value of 1.0 at 100°C. The slopes for Ca^{2+} were lower than 0.5 while those for Na^{+} and K^{+} were higher than 0.5. Their conclusion was that during water attack of glass, two reaction mechanisms occurring at the same time determine the extraction. At temperatures below about 80°C diffusion is predominant while above 80°C direct corrosion on the glass framework is decisive.[48]

The work of Rana and Douglas[47] contradicts the above conclusion. For both the leaching of alkali and the extraction of silica the root time behavior is described as the limiting relation for sufficiently short times and low enough temperatures. However, for longer times and higher temperatures the limiting relation for all constituents is a linear variation with time.[47]

Rana and Douglas[47] found that at short enough times, the rate of leaching of alkali ions follows a root time dependence. This is even true for the very soluble 25K glass at 1°C for the first few minutes of reaction.[19] During the root time regime the ratio of alkali to silica in solution is much greater than the ratio in the bulk glass, demonstrating that the surface of the glass is depleted in alkali. At longer times they found that a linear time dependence for the removal of alkali ions becomes the limiting condition. When this occurs the ratio of alkali to silica in the solution approximately equals the ratio in the glass for both binary alkali silicate glasses and ternary alkali silicate glasses with CaO. Rana and Douglas[47] made note of the two different regions of behavior and referred to the short time region as the first mechanism (varying as $t^{\frac{1}{2}}$) and that at long times as the second mechanism (varying at t^{1}). The change from the first to the second mechanism was said to take place over a time interval so that there is no clear way to determine exactly where the changeover takes place. The approximate time of this changeover in kinetics can be estimated and it occurs at shorter times and higher temperatures for the less durable glasses.

Das and Douglas[49] studied the corrosion of glasses over a wide range of compositions and temperatures confirming the results of Rana and Douglas.[47] Some of their data plotted as $\log$ Q vs. $\log t$ yielded a series of gentle curves with slopes of 0.5 at short times and 1.0 at long times.[47] At intermediate times the slope gradually changed from the two extremes over several orders of magnitude of time. The transition between the two regions was attributed to the development

of a highly siliceous layer with channels which increase the effective surface area present to aqueous solution. In Chapter IV this mechanism is shown to be unlikely in light of new evidence provided in this dissertation.

Lyle[46] used the glass container corrosion data of Bacon and Burch[50,51] to construct a plot of $\log [Na^+]$ in solution vs. $\log t$. He found that straight lines existed over two or more orders of magnitude of time and the slopes did not change as the temperature was increased. An obvious feature of these plots was not reported by Lyle.[46] The slopes for one bottle were 0.53, 0.50, 0.48, and 0.47 at four different temperatures. These values are essentially 0.5, demonstrating that a diffusion controlled mechanism was dominant. For another bottle sample the slopes were 1.0 for each of the four temperatures and were constant over two or more orders of magnitude. This is in disagreement with the results of Rana and Douglas[47] who found that the values of ½ and 1 for the slope were merely limiting conditions at short and long times respectively. A clue to the reason for the difference lies in the type of test used to obtain the data. Rana and Douglas[47] used glass grains while Bacon and Burch[50,51] used glass containers. This inconsistency is discussed in more detail in the section of this chapter dealing with different experimental tests.

Equilibrium pH

An equilibrium at the leached layer solution interface was described by Douglas and El-Shamy.[19] One can express the ion exchange reaction on the glass surface as,

$$\equiv Si\text{-}OR_{g\ell} + H^+ \rightleftarrows \equiv Si\text{-}OH_{g\ell} + R^+ \qquad (19)$$

For solutions less than pH 9 $\equiv Si\text{-}OR_{g\ell}$ can be assumed to be completely dissociated[40] and the acid equilibrium constant can be written as,

$$\frac{[\equiv Si\text{-}O^-][H_3O^+]}{[\equiv Si\text{-}OH]} = k_a \qquad (20)$$

The dissociation of silica at the surface is expressed in Eq. 14 which has a corresponding base constant,

$$\frac{[\equiv Si\text{-}OH][OH^-]}{[\equiv Si\text{-}O^-]} = k_b \qquad (21)$$

where the terms in brackets represent the activities of the species indicated and k_b is the base constant for the silanol group. One can assume that the acid constant for surface silanol groups has the same acid constant as the dissociation step for orthosilicic acid as has been suggested by Iler.[36] Since one is mainly concerned with

the conjugate acid-base system this assumption is probably valid[52] and Eq. 20 can be rewritten as,

$$\frac{[\equiv Si\text{-}O^-]}{[\equiv Si\text{-}OH]} = 10^{(-9.8 + pH)} \qquad (22)$$

If one assumes that activity coefficients are unity in Eq. 22, one can determine the relative occupancy of the surface sites by H^+ ions. Douglas and El-Shamy[19] calculated the mole fraction of surface sites occupied by H^+ ions at various values of pH. This information is reproduced in Table I. One can see that at values of pH less than 9, most of the surface sites are not ionized, however, at values greater than about 10 most of them are ionized.

Budd and Frankiewiez[53] discovered a property of the glass surface during corrosion which they called the "equilibrium pH." They used a procedure in which glass grains are crushed under aqueous solution while the pH is measured. The procedure is continued until there is no immediate increase or decrease in the pH. This equilibrium is arrived at both from initially high and low pH solutions. At low pH, excess H_3O^+ (H^+) ions are taken up by the glass, while OH^- ions are taken up at high pH. The equilibrium pH is said to be a dynamic equilibrium between the uptake of H_3O^+ and OH^- ions by the glass.

The uptake of OH^- and H_3O^+ ions can be thought of as proceeding by the reactions given by Eq. 14 and Eq. 19 respectively. From the

Table I. Mole Fraction of Surface Silanol Sites Occupied by H^+ at Various Values of pH.

pH	Mole Fraction of Surface Sites Occupied by H^+
5	1.00
6	1.00
7	1.00
8	0.98
9	0.86
10	0.39
11	0.06
12	0.01
13	0.00

Source: After Douglas and El-Shamy.[19]

equilibrium relations for these two reactions (Eq. 20 and 21) and the equilibrium expression for water,

$$[H_3O^+]\,[OH^-] = k_w = 10^{-14} \tag{23}$$

it follows that,

$$[\equiv Si\text{-}OH]_{g\ell} = \left(\frac{k_w}{k_a k_b}\right)^{1/2} \tag{24}$$

and,

$$[OH^-]_{liq} = K\,[\equiv Si\text{-}O^-]_{g\ell} \tag{25}$$

so that when fresh glass surface is exposed, the activities of H_3O^+, OH^- and $\equiv S\text{-}O^-$ adjust until Eq. 25 is satisfied.[53]

According to Eq. 25, as the number of nonbridging oxygen centers increase, the equilibrium pH should increase. The addition of alumina to a soda lime silica glass coordinates nonbridging oxygen atoms and thereby reducing the oxygen ion activity of the glass. One would expect the equilibrium pH to be lower for a soda lime silica glass without alumina than one that contains alumina. This was confirmed experimentally.[53]

Das[54] noted that the oxygen ion activity per mole of SiO_2, $[Si\text{-}O^-]$, can be calculated if the concentration of Na_2O in the glass,

x, and the activity coefficient for O^{2-} ions associated with Na^{+} ions, [Si-ONa] are known,

$$[Si\text{-}O^{-}] = \frac{2x[Si\text{-}ONa]}{(100-x)} \qquad (26)$$

If it is assumed that the value for [Si-ONa] is constant for the binary alkali silicate glasses, substituting Eq. 26 into Eq. 25 and rearranging yields,

$$pH = K' + \ell og \left(\frac{2x}{100-x}\right) \qquad (27)$$

This implies that a linear relation should exist between the equilibrium pH and the logarithm of 2x/(100-x). Such a relation was verified experimentally for Na_2O-SiO_2 glasses[54] and a similar relation was observed for multicomponent glasses in the system Na_2O-CaO-Al_2O_3-SiO_2.[54]

Budd and Frankiewicz's[53] concept of the equilibrium pH has not been related to glass corrosion. It is a subject which might, however, aid the prediction of the corrosion behavior of a glass under different conditions.

Diffusion

As described above the leaching of alkali ions from a glass surface at short times follows a parabolic rate which decreases with corrosion time.[22] Keppler and Thomas-Welzow[55] and Keppler[56] recognized that

some type of diffusion mechanism represented the slowest process. It is worthwhile to first examine the diffusion of ions in the bulk glass to establish a foundation upon which to base the discussions of diffusion controlled corrosion mechanisms.

The Na^+ ion is the most mobile ion in glass at temperatures bwlow the fictive temperature.[57] Lithium ions are also quite mobile in oxide glasses, however, the larger K^+ ions and smaller H^+ ions have a much lower mobility.[58] Frischat[45] described the aspects of ionic diffusion in glasses and tabulated all of the available data. A list with activation energies and diffusion coefficients for some of the ions important in understanding glass corrosion is given in Table II.

The diffusion of monovalent cations (alkali ions, H^+ and H_3O^+) in glass is limited by two factors, the extent of interaction with the network (O^{2-} ions) and the openness of the structure. The size and the ionic field strength (charge/radius^2) of the ion determine which of these two factors is more important. Small cations (H^+ and to a lesser extent the Li^+ ion) have a large ionic strength so they interact strongly with the network. The significance of ionic field strength to diffusion of an ion can be understood by comparing the Na^+ and Ca^{2+} ions which are nearly equal in size (.96Å and .99Å respectively). The very large field strength of the Ca^{2+} ion causes it to have a diffusion rate seven orders of magnitude slower than the Na^+ ion. The large ions (K^+, H_3O^+) interact less with the network but their size limits the diffusion from one site to another making the diffusion coefficient a function of the openness of the glass

Table II. List of Activation Energies and Diffusion Coefficients for Diffusion in Silicate Glasses.

Glass	Diffusing ion	Temp. Range(°C)	$Q\left(\frac{Kcal}{mol}\right)$	$D_o\left(\frac{cm^2}{s}\right)$	$D^*_{50°C}\left(\frac{cm^2}{s}\right)$	Reference
Vit. SiO_2 **	Na^+	250-600	26.9	1.3×10^{0}	1.1×10^{-18}	59
Vit. SiO_2 ***	Na^+	170-250	28.2	2.1×10^{0}	2.3×10^{-19}	60
Vit. SiO_2 ***	Na^+	250-600	25.8	3.7×10^{-1}	1.7×10^{-18}	60
5N	Na^+	300-500	26.2	8.7×10^{-3}	2.1×10^{-20}	61
7.5N	Na^+	300-500	20.6	8.9×10^{-3}	1.3×10^{-16}	61
10N	Na^+	300-500	19.3	5.5×10^{-3}	5.8×10^{-16}	61,62≠
12.6N	Na^+	250-400	18.7	2.5×10^{-3}	6.7×10^{-16}	45
13N	Na^+	300-500	17.2	1.2×10^{-3}	3.3×10^{-15}	63
14.8N	Na^+	250-400	18.5	3.5×10^{-3}	1.3×10^{-15}	45
16.7N	Na^+	200-500	21.4	3.8×10^{-3}	1.1×10^{-17}	64
17.4N	Na^+	250-450	16.3	8.0×10^{-4}	8.8×10^{-15}	65
20N	Na^+	300-500	18.3	4.0×10^{-3}	1.8×10^{-15}	61,62≠
22N	Na^+	250-400	16.5	6.6×10^{-4}	5.3×10^{-15}	45
25N	Na^+	250-500	16.7	5.4×10^{-3}	3.1×10^{-14}	61,62≠, 66,68
30N	Na^+	300-500	16.1	2.0×10^{-3}	3.0×10^{-14}	61
33N	Na^+	100-400	15.1	3.0×10^{-3}	2.2×10^{-13}	62,66≠, 69
10K	K^+	300-500	19.4	2.0×10^{-4}	1.8×10^{-17}	61
15K	K^+	300-500	19.3	5.3×10^{-4}	5.6×10^{-17}	61
20K	K^+	300-500	18.5	3.8×10^{-4}	1.4×10^{-16}	61
25K	K^+	250-450	17.1	3.7×10^{-4}	4.8×10^{-16}	67,68≠
27K	K^+	300-500	18.2	2.4×10^{-3}	1.4×10^{-15}	61

Table II - continued.

Glass	Diffusing ion	Temp. Range(°C)	Q $\left(\frac{\text{Kcal}}{\text{mol}}\right)$	$D_o \left(\frac{\text{cm}^2}{\text{S}}\right)$	$D^*_{50°C} \left(\frac{\text{cm}^2}{\text{S}}\right)$	Reference
33.3K	K^+	300-500	16.0	9.3×10^{-4}	1.6×10^{-14}	61
33L	Li^+	450	12-16	--	--	70
Vit. SiO_2 ≠	K^+	500-900	7.35	2.5×10^{-3}	2.9×10^{-8}	71
CsO-SiO_2 ≠≠	H^+	--	Very low	--	--	45
Vit. SiO_2***	OH^-	1000	≠≠≠	3.9×10^{-7}	4.2×10^{-19}	72
Vit. SiO_2**	OH^-	1000	≠≠≠	1.0×10^{-6}	1.1×10^{-18}	73
Vit. SiO_2	OH^-(in)	600-1000	18.3	1.0×10^{-6}	5.0×10^{-19}	73
Vit. SiO_2	OH^-(out)	600-1000	17.3	2.7×10^{-7}	6.3×10^{-19}	74

Source: Edited and averaged from Frischat.[45]

---

*extrapolated

**Vitreous silica with ≃ 1300 PPM OH

***Vitreous silica with ≃ 130 PPM OH

≠Averaged values

≠Surface diffusion

≠≠20% Cs - 80% SiO_2 containing water

≠≠≠Estimated assuming Q = 17.8 Kcal/mole

structure. The Na^+ ion has an optimum size for diffusion in most glasses. It is large enough such that it does not interact significantly with the O^{2-} ions yet it is small enough to diffuse through the structure.

The relative ratios for the diffusion of different monovalent cations illustrates this point. The relative ratios for many glasses have been tabulated by Doremus[58] and a list of the more pertinent ratios is given in Table III. In vitreous silica and Na_2O containing glasses, the diffusion coefficient for the Na^+ ion is much greater than all of the other univalent cations, illustrating the above description. In the K_2O containing glasses the diffusion coefficient for the Na^+ ion is slightly less than that for the K^+ ion. This is due to the fact that K_2O containing glasses have a more open structure to compensate for the large K^+ ions. The dominating factor limiting the diffusion of Na^+ and K^+ ions in these glasses is, therefore, their interaction with the O^{2-} ions so that the cation with the lowest field strength (K^+) diffuses fastest.

The diffusion coefficient is affected by the concentration of alkali ions. In general an increase in the concentration of alkali oxide increases the diffusion coefficient and decreases the activation energy.[45,75] For glasses in the Na_2O-SiO_2 system it has been suggested that a relation exists between the diffusion coefficient and the Na_2O concentration in the glass,

$$D_{Na} = a \exp(bC_{Na}) \qquad (28)$$

Table III. Ratios of Diffusion Coefficients of Monovalent Ions in Silicate Glasses.

Glass	Temp. Range(°C)	Ions A - B	$\frac{D_A}{D_B}$	Reference
Vit. SiO_2*	380	Na-Li	6.7	76
Vit. SiO_2*	380	Na-K	>500	76
Spectrosil	380	Na-Li	33	76
Spectrosil	380	Na-K	1400	76
Vitreosil**	1000	Na-H	$\approx 10^4$	77
13N	415	Na-K	25	78
20N	415	Na-K	39	78
25N	415	Na-K	48	78
13K	415	Na-K	0.5	78
20K	415	Na-K	0.5	78
25K	415	Na-K	0.6	78
Na_2O-CaO-SiO_2≠	350	Na-H	1800	57
Na_2O-CaO-SiO_2≠	350	Na-K	1400	57
K_2O-CaO-SiO_2≠≠	350	K-H	2	57

Source: After Doremus.[58]

*GE 204, $\approx 10^{-4}$ Na^+ and K^+/mole

**$\approx 10^{-4}$ Na^+/mole

≠13 mole % Na_2O

≠≠12.5 mole % K_2O

where C_{Na} is the molar concentration of Na_2O while a and b are constants.[79] There is much disagreement, however, among the absolute values for the diffusion coefficients for the binary alkali silicate glass systems obtained by different investigators. Such discrepancies are probably produced by differences in the microstructure, annealing and trace concentration of water which are known to cause order of magnitude variations in diffusion coefficients.[79]

The diffusion of protons in vitreous silica containing trace concentrations of water is characterized by a very low mobility and is considerably less than that for alkali ions. Sendt[80] observed H^+ ion mobilities 40 and 20 times smaller than for Li^+ ions in Na_2O-CaO-SiO_2 and K_2O-CaO-SiO_2 glasses, respectively. The mobility of H^+ ions is also much smaller than that for Na^+ ions. Sendt found that H^+ ions were strongly attached to O^{2-} ions and were difficult to replace by Na^+ ions even at 300°C.[80] Recently Baucke[81] determined the diffusion coefficients for H^+ and Li^+ ions in the bulk of a glass electrode material. The protons were found to have a mobility 10^3 - 10^4 times smaller than that for Li^+ ions.

The diffusion of protons may involve two different processes.[16] In some cases it is like the migration of Na^+ ions while in others it is more like electronic conduction than a material transport process. This is probably related to the two ways in which the H^+ ion can be screened by O^{2-} ions within the glass structure.[82] The H^+ ion can completely penetrate into the electron cloud of the O^{2-} ion and it can be coordinated between two O^{2-} ions. The significance of these two screening mechanisms has not been discussed in any detail, however.

Rana and Douglas[47] were among many to confirm the parabolic dependence for the leaching of alkali ions into solution as given by Eq. 17 for which α is equal to $\frac{1}{2}$,

$$Q = kt^{\frac{1}{2}} \tag{29}$$

Holland[2] stated that if this is a diffusion controlled process then traditional diffusion analysis must be valid. If one assumes for the moment that the diffusion of the alkali ions in the surface of the glass controls the dealkalinization process, a solution must be obtained from Fick's law for a non-stationary state of flow,[2]

$$\frac{\partial c}{\partial t} = D \frac{\partial^2 c}{\partial x^2} \tag{30}$$

where c is the concentration of alkali ions in the glass at time, t, at a location, x, from the surface of the glass with a diffusion coefficient, D. A solution of Eq. 30 for a semi-infinite body is a model for the dealkalization of a thick glass,[2]

$$c = \frac{1}{(\pi D t)^{\frac{1}{2}}} \int_0^{\infty} f(x') \exp\left[-\frac{(x-x')^2}{40t}\right] dx' \tag{31}$$

where the solution-leached layer interface is at $x = 0$. If the concentration, c, is zero at time = 0 and $x = 0$, then the quantity of alkali removed at time, t, is,

$$Q = 2c_o \left(\frac{Dt}{\pi}\right)^{\frac{1}{2}} \tag{32}$$

Equating Eq. 29 and Eq. 32 solving for the diffusion coefficient yields,

$$k = 2c_o \left(\frac{D}{\pi}\right)^{\frac{1}{2}} \tag{33}$$

and

$$D = \frac{\pi}{4}\left(\frac{k^2}{c_o^2}\right) \tag{34}$$

The preservation of electrical neutrality at the glass surface requires that as alkali ions leach out of the glass, H_3O^+ (H^+) ions must interdiffuse into the glass from solution. This ion exchange reaction (Eq. 15) has an interdiffusion coefficient, $\bar{D}$, associated with the process,[2]

$$\bar{D} = \frac{D_A D_B}{n_A D_A + n_B D_B} \tag{35}$$

where D_i is the tracer diffusion coefficient and $n_i = c_i/(c_A + c_B)$ for either the A or B ion. If the diffusion coefficient of one ion is much larger than the other, then an electrical charge is developed at the surface. This produces an electrical potential gradient that slows down the faster diffusing ion and speeds up the slower one so that the fluxes of the two ions are equal and opposite. The ultimate controlling condition for interdiffusion is determined by the smaller of $n_A D_A$ or $n_B D_B$.

It was the thesis of Douglas and Isard[83] and Rana and Douglas[84] that if diffusion controls the release of alkali ions into solution then one would expect a correlation with some other diffusional based process such as electrical conduction. Douglas and Isard[83] were the first to attempt to correlate these two processes. They modeled the glass structure as a fixed silica network with Na^+ ions free to diffuse from interstice to interstice after acquiring the proper activation energy. It was assumed that the diffusion of the alkali ion (i.e. Na^+) is much smaller than the interdiffusing species. In this case the interdiffusion coefficient is approximately equal to the diffusion coefficient of the alkali ion.

Using an equation similar to Eq. 34 Douglas and Isard[83] calculated the interdiffusion coefficient, $\bar{D}$, from leaching experiments for a commercial glass and compared it with the diffusion coefficient for Na^+ ions obtained from electrical conduction measurements, D_c. The discrepancy was small, $\bar{D}/D_c = 1/3$, considering the model adopted.

Beattie[85] calculated the interdiffusion coefficient for several multicomponent glasses of the systems Na_2O-CaO-Al_2O_3-SiO_2 and Na_2O-CaO-B_2O_3-SiO_2 assuming that the rate controlling process for the ion exchange process is the diffusion of Na^+ ions in the glass network. His calculated interdiffusion coefficients were in same order of magnitude as the values for tracer diffusion of sodium found in the literature.

This work by Beattie[85] and Douglas and Isard[83] indicates that the corrosion behavior of glass can be predicted from bulk diffusion data. Therefore, a glass with the largest electrical resistivity should have

the best resistance to the dealkalinization process. This conclusion is not always true. It has been clearly demonstrated in the literature [84,86-88] that glasses containing K_2O have a higher electrical resistivity than glasses with Na_2O, however, they are less resistant to dealkalinization.

A more detailed analysis of the interdiffusion coefficients for a range of glasses revealed that there are real differences between the two diffusion coefficients[84] with $\bar{D}/D_c$ ranging from 1.5 to 64,000, see Tables IV and V. Rana and Douglas stated that there is clearly a more complicated process going on than was described in the simple theory of Douglas and Isard.[83] In contrast to the large differences in diffusion coefficients, the activation energies for the two processes differ only by small amounts which are attributed to experimental error. The glasses with Na_2O consistently have activation energies for interdiffusion larger than those for conduction while with glasses containing K_2O the trend is reversed. Rana and Douglas also observed that as the concentration of CaO in the glasses is increased the activation energies for both conduction and ion exchange increases. They noted, however, that in view of the large values for $\bar{D}/D_c$ one should use caution when interpreting these activation energies as diffusion activation energies. If this is the case then it seems as if the ion exchange process is concentration dependent with water possibly being an additional component.[84] Rana and Douglas asked the question as to whether or not the diffusion mathematics could be modified to account for the large value of $\bar{D}/D_c$.

Table IV. Diffusion Coefficients and Activation Energies of Na^+ for Interdiffusion ($\bar{D}$,E_R) and for Electrical Conduction (D_c,E_c) in Na_2O Containing Glasses.

	T(°C)	$\bar{D}\left[10^{-14}\right]\frac{cm^2}{s}$	$D_c\left[10^{-14}\right]\frac{cm^2}{s}$	$\frac{\bar{D}}{D_c}$	E_R $\frac{Kcal}{mol}$	E_c $\frac{Kcal}{mol}$
15N	60	153	2.4	64	20.3	15.8
	68.4	300	5.2	57		
	83.4	990	0.14	72		
	100.1	4200	0.38	112		
15N5C	61.6	1.0	0.057	18	22.4	16.3
	70.5	3.0	0.11	27		
	83.8	12	0.28	41		
	99.6	36	0.76	47		
15N10C	61.6	0.12	0.082	1.46	23.5	17.2
	70.5	0.51	0.17	3.0		
	83.8	1.1	0.45	2.6		
	99.6	3.9	1.3	3.0		
15N15C	60.6	2.6	0.012	214	25.2	19.2
	68.6	12	0.025	465		
	83.4	52	0.089	590		
	100.1	220	0.31	703		

Source: After Rana and Douglas.[84]

Table V. Diffusion Coefficients and Activation Energies of K^+ for Interdiffusion ($\bar{D}$,E_R) and for Electrical Conduction (D_c,E_c) in K_2O Containing Glasses.

	T(°C)	$\bar{D}$ $[10^{-14}]\frac{cm^2}{s}$	D_c $[10^{-17}]\frac{cm^2}{s}$	$\frac{\bar{D}}{D_c}$ 10^2	E_R $\frac{Kcal}{mol}$	D_c $\frac{Kcal}{mol}$
15K	31.6	160	2.5	640	16.3	18.5
	48.0	650	12	540		
	49.7	730	14	510		
15K5C	51.4	33	1.1	320	16.6	18.8
	59.2	56	2.0	280		
	70.9	180	6.1	300		
	75.1	200	8.5	230		
15K10C	60.3	1.5	7.1	2.09	16.8	19.0
	70.0	2.6	17	1.48		
	81.7	7.1	42	1.68		
15K15C	49.4	0.18	0.22	8.3	17.3	20.1
	59.1	0.32	0.56	5.6		
	69.2	0.79	1.4	5.6		
	81.9	1.8	4.2	4.3		

Source: After Rana and Douglas.[84]

The large values of $\bar{D}/D_c$ pose a problem when one tries to correlate ionic conduction in a bulk glass with the ion exchange process. The assumption necessary for such a comparison that most probably is violated is the assumption that the diffusion coefficient remains constant with the corrosion process. Frischat[45] criticized such comparisons. He said,

> Even if the true binary interdiffusion coefficients of the ion exchange have been determined it can be expected that this value is a function of concentration. Differences in radii between Na^+ and H^+ or H_3O^+ are not negligible. On the other hand the self diffusion coefficient of Na^+ also varies strongly in a mixed system. According to these facts, which most authors seem to have overlooked when making these comparisons, coincidence even between these true D from leaching and D from Na self-diffusion in the base glass can be obtained only under very restricted conditions (i.e. a narrow range of composition and $D_{H^+} >> D_{Na^+}$). If, however, corrosion of the glass network cannot be neglected there is no basis at all for such a comparison.[89]

Even though the interdiffusion coefficients cannot be correlated with ionic diffusion coefficients from conductivity measurements, some other correlations are significant. Das and Douglas[49] found a relation between the reaction rate constant for the leaching of alkali ($Q_{A^+}/\sqrt{t}$) and the logarithm of the ratio of the two diffusion coefficients, ℓog ($\bar{D}/D_c$). Several ternary glasses with the general formula 5% M - 15% Na_2O - 80% SiO_2 were studied (where % M stands for the mole percent of the third constituent). The general trend was for the data to belong to one of two categories. Glasses with third constituents which according to radius ratio considerations are expected to have six nearest neighbor oxygens (Pb, Ca, Sr, Ba and Cu), lie on one straight line while those expected to have four nearest neighbor oxygens (Cd, Mg, Al, Ti, Zn and Zr) lie on a second straight line. This implies that

the root time dependence of extraction and the $\ell og\ \bar{D}/D_c$ depends upon the configuration of the glass structure and the hydrated layer.[90]

When either the reaction rate constant or $\ell og\ (\bar{D}/D_c)$ is plotted against the ionic radius of the third constituent a trend results.[90] Das said "Points appear to lie on three well defined lines at various temperatures which extend over approximate ranges of ionic radii 0.31 - 0.60 Å, 0.60 - 1.0 Å and 1.0 - 1.6 Å."[91] These branches correspond roughly to regions of tetrahedral, octahedral and cubic coordination of the modifier cations respectively. Each range contained points corresponding to cations with different valency except for univalency. There also appears to be a maximum - minimum effect within each radius range with the smallest cation within any range having a larger reaction rate constant and $\ell og\ (\bar{D}/D_c)$, indicating faster corrosion. This indicates that the smaller ions pose the least obstruction to the path of diffusion for the alkali ions.[77]

As pointed out above, because of the large differences in the ratio $\bar{D}/D$ for some glasses, the interdiffusion coefficients are difficult to interpret and they are only an indirect indicator of the ion exchange reaction in the surface of the glass. A more direct determination of the interdiffusion coefficient can be obtained by analysis of the composition profile of the corroded glass surface. This will be discussed in detail in a later section of this chapter.

The hydration of a glass surface is another important process which occurs during corrosion. The process of hydration is usually studied by infrared spectroscopy by monitoring the absorption peaks

due to Si-OH and SiO-H bonds. Infrared spectroscopy as well as other surface analysis techniques are discussed in a later section.

The nature of the diffusing species involved in surface hydration has not been as well established.[92] Drury et al. emphasized, "Protons, hydrogen atoms and molecules, hydroxyl ions, oxygen atoms and ions, and water molecules could each conceivably play a part in the diffusion mechanism."[93] Drury et al.[92] proposed two models for the diffusion of water in vitreous silica which are consistent with all available data. In the first model, diffusion occurs by a proton jump followed by the jump of a hydroxyl group with the diffusing species being H^+ and OH^- ions.

The first model is represented by Eq. 36, 37 and 38,

$$\equiv Si\text{-}OH + HO\text{-}Si\equiv \rightleftarrows \equiv Si\text{-}OH + {}^-O\text{-}Si\equiv + H^+ \rightleftarrows \equiv Si\text{-}O\text{-}Si\equiv + H^+ + OH^- \quad (36)$$

$$\equiv Si\text{-}O\text{-}Si + H^+ \rightleftarrows \equiv Si^+ + HO\text{-}Si\equiv \quad (37)$$

$$\equiv Si^+ + OH^- \rightleftarrows \equiv Si\text{-}OH \quad (38)$$

The H^+ and OH^- ions become separated (Eq. 36) and diffuse independently to another $\equiv Si\text{-}O\text{-}Si\equiv$ site where one of the ions attacks a Si-O bond. This is followed by the addition of the other ion (Eqs. 37 and 38).

The hydration of a glass by separation of H^+ and OH^- ions can occur in two ways.[16] One way is for hydrolysis to be initiated by the addition of an OH^- ion. This requires that the glass contain a

cation (Si^{4+}) which can increase its coordination.[82] The OH^- ion penetration is followed by the penetration of an H^+ ion. The other way for hydrolysis to occur is by the penetration of a H^+ ion to a polarizable anion (O^{2-}) followed by the addition of a OH^- ion. For the second sequence to occur the anion must be sufficiently polarizable to provide better screening for the proton than it received in the water.[82]

The second model proposes that water molecules diffuse through the glass network until they find a favorable Si-O-Si site to react with. Further diffusion occurs by the recombination of H^+ and OH^- ions to produce the H_2O molecule as the diffusing species. The second model is represented by Eqs. 39 and 40.

$$\equiv Si\text{-}OH + HO\text{-}Si\equiv \rightleftarrows \equiv Si\text{-}O\text{-}Si\equiv + H_2O \qquad (39)$$

$$H_2O + \equiv Si\text{-}O\text{-}Si\equiv \rightleftarrows \equiv Si(O\text{-}H)\text{-}O\text{-}Si\equiv \rightleftarrows \equiv Si(OH) + HO\text{-}Si\equiv \qquad (40)$$

According to Drury et al.[92] the assignment of Model I at high temperatures and Model II at low temperatures is consistent with observations for vitreous silica.

The activation energy in the temperature range of 600° - 1200°C for the diffusion of water (in the form of Si-OH) into vitreous silica is 18.3 Kcal/mole for entry 17.3 Kcal/mole for removal.[74] This led

Doremus to favor the mechanism in which molecular water is the diffusing species.[58] Doremus[58] related a mathematical treatment of Crank's[94] to the diffusion of water in glass. Crank considered the diffusion of a material which is present in a much lower concentration of reacted specie (Si-OH groups), C_r, and the concentration of diffusing specie, C_i,

$$C_r = K(C_i)^{\frac{1}{2}} \tag{41}$$

An effective diffusion coefficient, D_e, was derived for the process,

$$D_e = 2D\left(\frac{C_r}{K^2}\right) \tag{42}$$

Doremus[58] used a solution of the diffusion equation for this dependence[95] and compared it with the Si-OH profile determined by Roberts and Roberts.[96,97] An excellent fit was obtained leading Doremus[58] to conclude that the molecular diffusion and reaction of water is the correct model.

Experimental evidence also supports the hydration of silica at low temperatures by the first model.[16] The equilibrium solubility of silicic acid in solution decreases with increasing acidity of the solution; however, at short times hydration is accelerated by acidic solutions. Weyl and Marboe[16] said that this indicates that in acid solutions the solution process is initiated by proton penetration to O^{2-} ions. In dilute alkaline solutions the reverse is the case so that the initial penetration is by the OH^- into the glass.[16]

Diffusion profiles of "water" into Vitreosil using tritiated water were obtained by Drury et al.[92] Using the Matano method[94] they determined the diffusion coefficient as a function of concentration. In the temperature range 700° - 1200°C the diffusion coefficient increases with increasing water content. The concentration dependence of the diffusion coefficient is, however, very small at the lower temperature.[92]

It has been demonstrated that the solubility of hydroxyl groups from the vapor phase into glass is proportional to the square root of the partial pressure of water vapor in the atmosphere at elevated temperatures. According to chemical kinetics, such a $p_{H_2O}^{\frac{1}{2}}$ dependence dictates that two hydroxyl groups are produced[92] from each with the overall reaction being the same as Eq. 39.[98] The hydroxyl groups are probably segregated in pairs and very few water molecules are present.[92]

The above models account for the hydration of vitreous silica. However, for glasses containing alkali ions as a glass constituent, the combined movement of alkali ions to the surface of the glass and the movement of H^+ ions into the glass surface must occur. It is, therefore, not necessary for OH^- ions to diffuse into the glass surface since the electrical neutrality condition is preserved by the ion exchange process. This makes it difficult to separate the process of hydration from the process of glass corrosion. A more detailed discussion is included in a later section.

For the binary alkali silicate glasses, the rate of hydrolysis increases with decreasing field strength of the alkali ion so that the hygroscopicity increases in the order Li_2O-SiO_2 < Na_2O-SiO_2 < K_2O-

SiO_2.[16] Addition of other oxides greatly reduces the hygroscopicity[99] by "tightening the O^{2-} ions."[16] Nonbridging oxygens are much more polarizable than bridging oxygens since they are associated with the weaker field of an alkali ion. The alkali silicate glasses can therefore hydrolyze rapidly since a proton can enter and become associated with these polarizable nonbridging oxygen ions.[82]

Weyl and Marboe[82] compared the hydration of these glasses to the hydration of $CaCO_3$ and $MgCO_3$. They said that the small Mg^{2+} ions exert a stronger tightening effect upon the $(CO_3)^{2-}$ ions than the larger Ca^{2+} ions making proton penetration more difficult. The rate of hydrolysis is, therefore, dependent on the rate of proton penetration which increases with increasing polarizability of the O^{2-} ion.[82]

The solubility of water in molten silicates also increases as the concentration of alkali oxide increases[58] and for a given concentration the solubility increases in the order $Li_2O < Na_2O < K_2O$. These effects may be partially explained by hydrogen bonding since it increases in the same order. Another factor is the weakening of the Si-O bonds by the addition of alkali oxide (i.e. decreased viscosity, shift of IR peaks to lower frequency).[16] A weakened Si-O bond results in a greater reactivity with water and a shift of Eq. 40 to the right.

Glass Composition

The enhancement of the chemical durability of a glass by altering its composition is of technological importance as long as other

desirable properties are not significantly changed. A paradoxical fact is that a water soluble alkali silicate glass is made much more resistant to aqueous attack by the addition of soluble CaO in place of relatively insoluble SiO_2.[16] Rana and Douglas[47] demonstrated that when CaO is substituted for SiO_2 in binary alkali silicate glasses, there is a progressive decrease in the rate of alkali leaching into neutral solution as the concentration of CaO in the glass increases. The extraction of silica under neutral conditions is at a minimum for a glass with 10% CaO. As the corrosion solution became more alkaline, the rate of alkali extraction also has a minimum rate with the 10% CaO glass composition. The progressive reduced rate of leaching of alkali during Mechanism I ($t^{\frac{1}{2}}$ regime) for CaO containing glasses must be due to the decreased interdiffusion through the leached layer because of the presence of Ca^{2+} ions. It is interesting to note that the reactivity of the silica network occurs at a Na_2O : CaO ratio (1.50) very close to the value Das[54] derived for the minimum oxygen ion activity and the value observed for the minimum equilibrium pH (1.25).

A list of the effects of substituting various constituents in a glass composition is given in Table VI. As can be seen the effect depends on the type of corrosion conditions (acid vs. alkali solutions) as well as the particular glass constituent monitored in the solution (alkali vs. silica). Some of the better inhibitors to acid and alkaline attack are ZrO_2, TiO_2, ZnO, Al_2O_3 and CaO. Weyl[100] described the effect of these cations on reducing the rate of corrosion. He said

Table VI. The Effects of Substituting One Glass Constituent By Another on the Chemical Durability.

Modifier	Substitution	Glass Composition (balance SiO_2)	Effect
CaO	0-15% SiO_2*	15% Na_2O* or 15% K_2O	Maximum durability of silica extraction in neutral solution at 10% CaO.[47]
			Progressive decrease of alkali extraction in neutral solution.[47]
			Maximum resistance to silica and alkali extraction in alkaline solution at 10% CaO.[47]
CaO	4-25% SiO_2	18% Na_2O	Dramatic continuous decrease in total extracted glass constituents in water.[101]
BaO	0-2% SiO_2	14% Na_2O** 12% (CaO + MgO)	Little effect on acid or water resistance.[3]
BaO	>2% SiO_2	"	Mildly detrimental effect.[3]
BaO	18-40% SiO_2	18% Na_2O	Continuous decrease in total constituents.[101]
MgO	0-15% SiO_2	18% Na_2O	Significant decrease in total extracted glass constituents in water with minimum at 9% MgO.[101]
MgO	0-12% CaO	16% Na_2O 12% (MgO + CaO)	Progression resistance to acid solution.[3]

Table VI - continued.

Modifier	Substitution	Glass Composition (balance SiO_2)	Effect
MgO	0-12% CaO	16% Na_2O 12% (MgO + CaO)	Decreasing water resistance with minimum at 6%.[3]
MgO	12% CaO	"	Greater water resistance than with 6% CaO.[3]
ZnO	6-30% SiO_2	18% Na_2O	Dramatic continuous decrease in total extracted constituents in water.[101]
PbO	18-38% SiO_2	18% Na_2O	Minimum total extracted glass constituents in water at 30% PbO.[101]
Al_2O_3	2-15% SiO_2	18% Na_2O	Dramatic continuous decrease in total extracted glass constituents in water.[101]
B_2O_2	0-16% SiO_2	18% Na_2O	Significant decrease in total extracted glass constituents with minimum at 7% B_2O_3.[101]
B_2O_3	0-5% SiO_2	10-12% Na_2O 16-14% (CaO + MgO)	Very little effect.[3]
B_2O_3	0-5% CaO-MgO	"	Very little effect.[3]
B_2O_3	0-5% Na_2O	"	Substantial increase in chemical durability.[3]
Fe_2O_3	0-5% SiO_2	11-12% Na_2O 16-14% (CaO + MgO)	Slightly increased water resistance.[3]

Table VI - continued.

Modifier	Substitution	Glass Composition (balance SiO_2)	Effect
Fe_2O_3	0-5% (CaO-MgO)	11-12% Na_2O 16-14% (CaO + MgO)	Detrimental to acid resistance, slightly beneficial to water resistance.[3]
ZrO_2	0-8% SiO_2	12% Na_2O 12% CaO	Enormous and progressive increase in resistance to alkaline solution.[3]
P_2O_5	1-2% SiO_2	12% Na_2O** 11% (CaO + MgO)	Little effect.[3]
P_2O_5	1-2% (CaO + MgO)	"	Little effect.[3]
F	1.1% SiO_2	16.5% Na_2O 10% (CaO + MgO)	Increased acid and water resistance.[3]
F	2% SiO_2	"	Less beneficial to increasing acid resistance.[3]
F	3.6% SiO_2	"	Detrimental to acid resistance.[3]
MgO, BaO and SrO	5% SiO_2*	15% Na_2O*	Reduction in alkali extraction during neutral and alkaline attack. Reduction in silica extraction in neutral water, accelerated silica extraction from alkaline attack.[49]
PbO, CdO CuO, CaO	5% SiO_2*	15% Na_2O*	Reduction in alkali and silica extraction in neutral and alkaline attack.[49]

Table VI - continued.

Modifier	Substitution	Glass Composition (balance SiO_2)	Effect
ZnO, TiO_2 and Al_2O_3	5% SiO_2*	15% Na_2O*	Large reduction in alkali and silica extraction during neutral and alkaline attack.[49]
ZrO_2	5% SiO_2*	15% Na_2O*	Greatest reduction in alkali and silica extraction during neutral and alkaline attack.[49]

*Mole %

**Commercial glass with balance SiO_2 and other constituents.

that the optimum reduction in attack of the silica network by alkaline solution is obtained by substituting small quantities of cations for alkali whose potential field is slightly weaker than that of the Si^{4+} ion, but is sufficiently strong to require screening by OH^- ions rather than by neutral water molecules. Large divalent ions, such as Ba^{2+}, are not useful since their potential fields are too weak and can be hydrated in solution without need for additional screening. Ca^{2+} and Mg^{2+} ions are much more effective for reducing the attack. This is due to their not being able to be adequately screened by water and their tendency to polymerize in aqueous solution as evidenced by their low solubility.[101]

The increased alkaline durability with glasses containing Ca^{2+} or Ma^{2+} can be explained in terms of an increased coordination of the O^{2-} ions in the glass.[82] The addition of CaO to a glass adds one polarizable O^{2-} ion but ties up several polarizable O^{2-} ions. These O^{2-} ions are tightened by three cations, one Si^{4+}, one Na^+ and one Ca^{2+}. This increase in the coordination number of the O^{2-} ions is responsible for the drastic improvement of the chemical durability of alkali silicate glasses. Oxides such as Al_2O_3, MgO, CaO and B_2O_3 are effective additives for this reason.[82]

Zn^{2+}, Al^{3+}, Ti^{4+} and Zr^{4+} are much better additives for preventing corrosion during the second mechanism.[102] The reason was explained by Weyl[101] on the basis of their pronounced tendencies to polymerize. The potential fields of Zr^{4+} and Ti^{4+} are so strong that they cannot exist in solution. Four OH^- ions plus additional water molecules can

neutalize the charge but they cannot completely screen the two ions. Their need for a large number of OH^- ions in the first coordination sphere causes them to polymerize to form colloidal hydroxides or copolymerize with silicic acid at a glass surface.

Bacon[3] reviewed the development of the more durable glasses. A glass developed in 1919 by Corning (Pyrex 7740®) was long used for severe conditions and dominated the scientific glassware field. It has an excellent acid resistance and low thermal expansion.[3] Pyrex owes its chemical resistance to the fact that the glass phase separates. This phase separation isolates phases rich in alkali (with a low chemical durability) inside a continuous phase rich in silica (with a high chemical durability).

Fused quartz glass is also available which has a high softening temperature, low expansion and excellent acid resistance. It is good for acidic conditions but it is expensive and is attacked severely by alkaline solutions. In 1944 a technique was devised for producing a glass called Vycor® with properties much like fused quartz. A borosilicate glass is melted and formed into the desired shape. it is then treated with a hot acid solution which leaches out a continuous glassy phase with low chemical durability, leaving a continuous SiO_2 rich skeleton with a high chemical durability. The porous body is then fired to consolidate the pores and to shrink the body to its final

---

®Corning

®Vycor

size. The result is a glass with HF, acid and alkaline resistance superior to Pyrex.

The need for a glass more resistant to alkaline solution led to the development of Corning's 7280 glass. Inclusion of a large percentage of ZrO_2 in this glass gives it a far superior resistance to alkaline solution than Pyrex®, Vycor® and fused quartz. The compositions of these glasses are given in Table III.

Glass Surface

The reaction of gases with the glass surface has been used to lower the chemical reactivity of the surface. One such effect occurs when a glass melt is exposed to CO_2. An increase in the chemical durability of a soda lime glass results and has been attributed to the absorption of CO_2 into the glass surface and a decrease in the alkalinity of the glass surface.[103] The presence of SO_2 in the atmosphere over the melt, however, has no effect on the glass durability.

Cousen and Peddle[104,105] were among the first to show that annealing of bottles in open-fixed lehrs greatly increases their chemical durability by exposure to sulfurous fumes. This is attributed to the dealkalization of the surface by a reaction with SO_2. There are basically four conditions during annealing, each of which produces different results in the glass surface. A glass can

Table VII. Compositions of Chemically Resistant Glasses (Weight %).

	Pyrex Corning's 7740	Vycor Corning	Corning's 7280
SiO_2	80.3	96+	71.3
Na_2O	4.2	trace	11.5
Li_2O	--	--	0.8
K_2O	--	--	0.1
$CaO \cdot MgO$	0.1	--	0.2
Al_2O_3	2.4	trace	--
B_2O_3	13.0	3	--
ZrO_2	--	--	15.8

Source: After Bacon.[3]

be annealed under anhydrous or hydrous conditions with or without an SO_2 atomophere. Because of a similarity between the processes which occur under these conditions and those of glass corrosion an understanding of them is useful.

At the temperature of annealing, Na^+ ions diffuse to the surface of a glass under the driving force of surface tension.[106,107] These Na^+ ions can accumulate on the surface increasing the surface concentration or they can be removed by another process to produce an alkali deficient surface. The outcome is determined by the difference in the rate at which the Na^+ ions diffuse to the surface and the rate at which they are removed from the surface by volatilization or reaction with SO_2.

Under anhydrous conditions the surface becomes depleted of sodium. This means that the rate of volatilization or reaction is faster than the diffusion of sodium to the surface. Douglas and Isard[83] found that the activation energy for an anhydrous high temperature (600 - 1000°C) sulfuring treatment is very large, being 2.6 ev. This indicates that the reaction is controlled by the diffusion of O^{2-} ions with the Na^+ ions to preserve electrical neutrality. They proposed the following mechanism for the dealkalization of a glass surface under anhydrous sulfuring conditions.

$$Na_2O_{glass} + SO_2 + \tfrac{1}{2}O_2 \rightleftarrows Na_2SO_4 \qquad (53)$$

The diffusion of sodium to the surface is much faster in an atmosphere containing water than under anhydrous conditions.[83] Water

present in the atmosphere provides a supply of H^+ ions at the surface which readily exchange with the Na^+ ions in the glass. This ion exchange reaction proceeds much more rapidly than the diffusion of Na_2O to the surface. The reaction, however, is much slower than predicted by electrical conductivity measurements.[83] This is due to the esterification of the surface (see Eq. 39) with the elimination of water producing a surface resembling vitreous silica. This esterification process was described as a type of phase separation.[83] The rate of sodium diffusion to the surface under hydrous conditions is so rapid that the surface can actually become enriched in sodium.

Douglas and Isard conclude,

> The type of diffusion process involved is governed by the condition that the electrical neutrality of the glass must be maintained. It is concluded that: (a) the reaction with water involves the exchange of sodium ions by hydrogen ions and that the reaction is limited by the rate of diffusion of sodium ions to the surface; (b) the reaction with sulphur dioxide at 20 - 100°C in gas saturated with water vapor involves the same process and proceeds at the same speed as the reaction with water; (c) at 100 - 600°C (and in atmospheres not saturated with water vapor below 100°C) the sulphur-dioxide reaction is limited by the rate of diffusion of sodium through a compacted layer of glass at the surface which arises from a secondary dehydration process; (d) with anhydrous reagents the sulphur-dioxide reaction involves the simultaneous diffusion of sodium ions and oxygen ions to the glass surface, and the speed is limited by the rate of diffusion of oxygen ions; above about 700°C this process predominates over ion exchange.[108]

Bacon and Calcamuggio[109] investigated the difference in chemical durability of glasses formed in either wet or dry air free of SO_2. It was observed that exposure of a bottle to moist air is detrimental to its chemical durability while exposure to dry air is beneficial. They proposed a limiting mechanism for the anhydrous condition which

is different from the mechanism proposed by Douglas and Isard.[83] In the absence of water vapor Na^+ ions diffuse from the surface and vaporize so that the escape of alkali from the surface exceeds its arrival from the bulk glass. This produces a significant decrease in the surface alkalinity. it was postulated that under these conditions the diffusion of Na^+ ions to the surface is controlled by the diffusion of H^+ ions into the glass and their availability at the surface. When water is present in the air it supplies H^+ ions which can penetrate the glass surface to replace Na^+ ions. This is in agreement with the observation that the rate of alkali diffusion to the surface increases as the humidity increases.[109]

The presence of moisture in the air increases the rate of alkali diffusion but it does not increase the volatility of sodium at the surface. Therefore, sodium becomes concentrated at the surface. This was verified by Pantano[110] using Auger electron spectroscopy. He demonstrated that when a glass is exposed to air with water vapor, the concentration of sodium on the surface is higher than in the bulk. Under this layer exists a relatively sodium depleted region. This proves that the tendency is for sodium to diffuse from the glass, however, the low rate of volatilization produces a sodium rich surface.

Corrosion Tests

Corrosion tests may be categorized as to whether they are based on analyzing the state of the glass or the state of the solution. The

glass can be studied as a formed article such as bottles, with or without a surface treatment (i.e. SO_2 treatment or rinsing), as crushed grains or as a polished flat surface. Each type of test has its advantages. THe use of an actual article such as a bottle makes the extrapolation of results to actual use more meaningful. Weyl and Marboe stated, "From a technical point of view the major problem in examining the chemical durability of glasses is the difficulty in measuring this property under conditions identical with those encountered in the practical use."[111]

The corrosion of commercial glass containers is a slow process which requires long periods of time to obtain meaningful information; therefore, accelerated corrosion tests have been used by most authors. These tests accomplish the acceleration or apparent acceleration of corrosion by two means. One way is to run the tests at a temperature higher than will be used in service. This is an actual acceleration of the corrosion processes. The other way is to use glass grains with a large surface area per unit volume of test solution. This permits the more rapid determination of reaction products which are extracted from the large surface area into the relatively small volume of solution.

Many different tests using glass grains have had technological importance by permitting the determination of the relative chemical durability between different glass compositions. The Corning Miniature Powder method,[112] the DIN method,[112] the American Ceramic Society's Tentative Method No. 1,[113] the U.S. Standard ASTM method,[112] the U.S.P. test,[54] and the Sheffield Grain Method[114] fall into this category. In

many cases the measurement of only one glass constituent in solution at one time and one temperature is made. Since the conditions are different for each test, comparison of results is usually meaningless.

Glass grains have even been used in more systematic scientific studies of corrosion processes. Two reasons were given for the use of glass grains.[112] The first was that glass grains enable the exposure of more surface area to the solution yielding a higher (and more easily detectable) concentration of glass constituents in solution and the second was to minimize the effect of accidental surface treatments of the glass.[112] However, there are many problems associated with the use of glass grains for scientific investigations which must be considered.

Glass grains are usually prepared by crushing larger pieces of glass in a porcelain or steel mortar with a vertical crushing method. After the grains are crushed they are sieved through meshes with limiting sieve sizes to give a particular particle mesh size range. Many investigators then wash the grains in CCl_4 to remove fine particles which are adherent to the larger grains. High impact crushing of the grains, has recently been found to lead to the formation of agglomerates of the small particles.[115] Sykes[115] said that is is necessary to scour the grains under dry ether to break down the agglomerates to eliminate the error they produce.

There are other problems associated with using glass grains for accelerated corrosion studies. One problem is from the contamination of the grains by heavy metals whose ions are known to have a large

influence on the corrosion of glass.[116,117] Traces of copper in the corrosion solution have a marked inhibiting effect at concentrations as low as 0.002 ppm.[118] Contamination could easily come from the sieving of the grains producing erroneous results.

Another disadvantage of the corrosion of glass powders arises from their size. Clark[119] recognized that a geometrical factor is needed in the kinetic equation related to the leaching of alkali ions since the area of the surface plane supplying the alkali ions decreases continuously with corrosion time. For 25 μm powders which develop a 1 μm leached layer, a 25% change in area is observed and the error increases as the leached layer becomes thicker.

The introduction of air bubbles through shaking or stirring the grains may also influence the results. Morey et al.[120] found that a glass is very susceptible to attack at the solution-air-glass interface. Quartz grains which were stirred in water dissolved 400 ppm of silica into solution (compared with 6 ppm at equilibrium). This is attributed to the formation of air-solution-quartz lines which are very reactive.

Glass grains have many sharp edges and fractured surfaces which make them different from the containers they are modeled to test.[121] Weyl and Marboe recognized that, "All extraction methods used for accelerated tests on glass powder suffer from the same shortcoming: the surface tested is that of the fractured glass, which can be very different from the actual surface used."[122]

Uncertainty as to the actual surface area of glass powders makes the calculation of the surface area of glass to volume of solution

ratio an approximation. There is also the problem of cell concentration effects effectively increasing the surface area to volume ratio locally within the mass of powder. It is not surprising then that a comparison of results using glass grains and actual containers in some cases yield different results.[50]

In order to eliminate many of the problems associated with corrosion studies utilizing glass grains, a new corrosion testing procedure was developed by Sanders and Hench.[20,21,123] The test is a static corrosion procedure which models the corrosion in a crack tip of abraded glass, the corrosion of two panes of glass stored in a high humidity or the leaching of glass bottles initially containing neutral aqueous solution. With this test a planar glass surface is corroded by securing it over a Teflon® corrosion cell filled with corrosion solution. This procedure has several significant advantages over the corrosion of glass grains and bottles. One of the important advantages is that the surface of the sample is well characterized and very reproducible. Holland[2] recognized that when experiments are performed using grains and bottles an allowance needs to be made for the weathering of the surface before the test is conducted. Such a consideration is not needed with the Sanders' method. A fresh glass surface is prepared just before corrosion by polishing the sample with dry 600 grit SiC paper. The polish gives the sample a reproducible surface

®Dupont

finish with a composition equal to that of the bulk glsss. Unlike the glass grains, the sample size is large enough that the surface is amendable to a new analytical technique, infrared reflection spectroscopy. This tool is especially suited for the study of glass surfaces and will be described in detail later.

An objective of this dissertation is to examine the use of powders as an accelerated corrosion procedure. The results are to be compared with those from the Sanders' test[20,21] (see Chapter IV).

One of the problems associated with glass corrosion is the correlation of accelerated test results with service applications. A great majority of the published data on the chemical durability of glass has been obtained using distilled water as the leaching solution. Bacon and Burch[50,51] were among the first to point out, however, that results from tests using distilled water can be misleading and bear little relation to the service behavior of the glasses tested. The conditions under which the glass will be in service should dictate the type of corrosion solution for the test. The test solution may be a distilled or deionized solution, dilute acid, dilute alkaline or a solution buffered to a specific pH. The addition of other anions and cations to the distilled water can have additional acceleration or inhibition effects. These effects will be discussed in another section.

It appears that accelerated tests using an acid solution produce results that can be used to predict the resistance of glasses to acid solution in commercial applications.[44] Keppler and Thomas-Welzow[55] proposed that the reaction rate constant be used to measure the chemical

durability for conditions in which the root time dependence exists during the entire process (acid solution).

Glasses with good acid resistance do not necessarily exhibit such good resistance to alkaline solution.[44] The resistance of different glasses to initially acidic, neutral and alkaline solutions may occur in different orders so they need to be determined separately.[35]

The only way of truly accelerating the corrosion of a glass surface is to increase the temperature of the test. Lyle[46] was the first and only investigator to attempt to correlate tests at elevated temperatures to commercial applications at lower temperatures. He noted that the data from accelerated tests should be correlated with service behavior only when the chemical attack was of about the same magnitude in the two cases. Almost "perfect" duplications of chemical attack is achieved at particular times and temperatures. Lyle said, "Seven hours at 95°C, two days at 75°C, three weeks at 50°C and one year at room temperature are, for most glasses, mutually equivalent. It would seem then that some definite relations of time and temperature exist and that these relations may be expressed by an equation of the proper form."[124]

Lyle[46] derived a relation between the time and temperature of corrosion that can be used as a tool for the prediction of accelerated corrosion studies. From Eq. 17 and an Arrehenius equation he derived,

$$\left(\frac{1}{a}\right) \log Q = \log t - \left(\frac{b}{T}\right) + c \qquad (43)$$

Using data form several sources Lyle found that the value of b = 5080. A simplification of Eq. 43 was derived such that one can determine the time and temperature necessary to model service conditions. If t_1 and T_1 are the time and temperature for service conditons, t_2 and T_2 for the conditions of an accelerated test can be determined from,

$$\log t_1 - \log t_2 = b\left(\frac{T_2-T_1}{T_2T_1}\right) \qquad (44)$$

To model the service conditions at 27°C for one year the time required to test at 100°C would be approximately four hours.

Lyle[46] stated that the use of the equation should be limited to data on the attack by water on soda-lime-silica type glasses. The data do not always fit exactly but in many cases the agreement between the calculated and observed results is excellent.

This analysis is dependent on the assumption that the activation energies for the leaching process are the same for the different glasses. This assumption is not too bad for the commercial soda-lime-silica glasses but one should not expect this relation to hold for all glasses. Another objective of this dissertation is to examine the temperature dependence of the corrosion of some of the binary alkali silicate glasses and to determine values for the constant, b in Eq. 43 (see Chapter VI).

Surface Area to Volume of Solution Ratio

The ratio of the surface area of the glass exposed to corrosion to the volume of corrosion solution (A/V ratio) is an important corrosion variable that has virtually been ignored by previous investigagors, except Sanders and Hench[21] and Dilmore.[124] All the tests with glass grains are based on the assumption that increasing the A/V ratio has no effect on the kinetics of corrosion. Such an assumption may not be valid.

The concept of the A/V ratio has technological significance. Different size containers have different A/V ratios. If the capacity of the container (volume of solution) is reduced by ½ the amount of surface area exposed per unit of volume is increased by 26%[3] This means that under the same conditions of exposure, higher concentrations of corrosion products will accumulate in the smaller container. But if the corrosion kinetics are changed because of the change in the A/V ratio, an entirely different process may occur in the two containers. The weathering of plate glass and the corrosion in a crack tip are two instances when the A/V ratio is much larger than with the corrosion of bottles. It should be noted that most likely, one set of corrosion conditions (one A/V ratio) probably will not adequately model these two conditions.

Very little information has appeared in the literature concerning tests where the A/V ratio is varied. One way in which the A/V ratio may be varied is to increase the weight of a particular mesh range of grains in a constant volume of corrosion solution. This assumes that

the surface area of the carefully prepared grains is proportional to their weight. El-Shamy and Douglas[52] confirmed this assumption to be valid for 1 to 3 g of glass grains in 100 ml of solution.

The instances in the literature which report the results of varying the A/V ratio conflict with one another. Dimbleby and Turner[106] found that for a Na_2O-MgO-SiO_2 glass, a four fold increase of the glass surface area only doubled the weight loss. Rexer [125] also found that the rate of leaching was not proportional to the surface area of the glass. El-Shamy and Douglas,[52] on the other hand, reported that for 25K glass grains the quantity of alkali and silica in solution was slightly more than doubled by doubling the surface area of the glass. These data indicate that changes in the A/V ratio affect the kinetics differently depending on the glass and/or the A/V ratio range under study. By direct investigation of the surface corrosion of a 33L glass Sanders and Hench[123] found that the rate of leaching of the surface was more rapid when the A/V ratio is decreased.

The objective of Chapter V is to examine the effect of changes in the A/V ratio on the corrosion processes. Data from both bulk glass surfaces (i.e. Sanders' test) and from glass powder studies are compared. The results are related to the kinetic equations.

Assessment of Changes in the Solution

In the older papers the principle method of assessing the amount of attack on the glass was by measuring changes in the electrical

conductivity of the attacking solution with time.[126] These tests assumed that the alkali ions were the sole contributors to the conductivity of the solution. As the concentration of silica in solution increases, however, the tendency is for the electrical conductivity to decrease. These two opposing effects on the electrical conductivity yield lower values than would be obtained if only sodium is in solution. Estimates of the kinetics of leaching of sodium into solution are, therefore, underestimated if only electrical conductivity measurements are used.[126]

Rana and Douglas[47] emphasized the need for complete analysis of the corrosion solution for all the corrosion products. Each wet chemical analysis technique used should be specific for the glass constituent being tested and the test should be independent of the other glass constituents in solution. Rana and Douglas initiated the use of flame spectrochemical analysis for the determination of the alkali ions, colorimetry for silica and titration against a standard EDTA solution for calcium.

Flame spectrochemical analysis techniques work on the principle that when a solution containing certain elements is aspirated into a flame certain characteristic wavelengths of light are emitted (atomic emission) or absorbed (atomic absorption). Changes from the base line intensity at these wavelengths are detected by a spectrometer and indicated on a meter or a strip chart. Calibration curves are obtained using solutions of known concentrations of each element. Linear relations essentially independent of the concentration of silicon and calcium are obtained for low concentrations of alkali ions.[47]

The determination of the concentration of silicic acid in solution is based on the silico-molybdic acid complex with ammonium molybdate.[127] The yellow complex is reduced to molybdenum blue by Na_2SO_3 and the intensity of the absorption at 700 μm is measured and compared with a calibration curve obtained from solutions of known silica concentrations.

The pH of the corrosion solution is another factor which should be determined along with the concentration of glass constituents. The combination of the weak acid (hydrosilicic acid) and the strong base (sodium hydroxide) in the corrosion solution produced some buffering characteristics such that the pH does not depend on absolute concentrations of any corrosion product but rather on the relative activity of each.[40] Since the pH of the solution greatly affects the leaching of alkali ions and the breakdown of the silica network it is essential that the pH of the corrosion solution be included in the discussions of the corrosion processes. Frequently the pH of the corroding solution is ignored leading to the misinterpretation of results.[53]

It is usually assumed that silica in dilute alkaline solution is in the form of silicic acid, H_2SiO_3, or in the ionized form $HSiO_3^-$.[31] This has led some investigators to believe that a rearrangement of bonds during corrosion is necessary since the species in solution are chemically different from the original glass.[53] Following the orthosilicate terminology, one can also express the silicon containing species in solution as orthosilicic acid and its ionized forms ($Si(OH)_4$, $Si(OH)_3O^-$ and $Si(OH)_2O^{2-}$).

Weyl[17] stated that even the orthosilicate molecule, $Si(OH)_4$, is unstable in solution. This is due to the strong contrapolarization by the H^+ ions which prevent the four O^{2-} ions from completely screening the Si^{4+} ion. Because of the similarity of the OH^- ion and the F^- ion and since there is a coordination of six F^- ions around the Si^{4+} ion, Weyl[101] suggested that the Si^{4+} ion in solution should have a coordination of six. Although six OH^- ions could screen the Si^{4+} ion most effectively, the $Si(OH)_4$ molecule can hydrate by adding two water molecules and probably screen the Si^{4+} ion adequately.

The accumulation of Na^+ ions in solution and the increase in pH led early investigators to believe that sodium hydroxide is a reaction product. Sodium hydroxide is an impractical reaction product due to the degree of ionization; however, an alkali (sodium) silicate is possible as a reaction product. After the silicate ion becomes ionized,

$$Si(OH)_4(H_2O)_2 + OH^- \rightleftarrows Si(OH)_3(H_2O)_2O^- + H_2O \qquad (45)$$

a sodium ion could combine according to,

$$Si(OH)_3(H_2O)_2O^- + Na^+ \rightleftarrows Si(OH)_3(H_2O)_2ONa \qquad (46)$$

This reaction product would be favored since the contrapolarizing effect of the Na^+ ion would permit the O^{2-} ion to more effectively screen the Si^{4+} ion than when a H^+ ion is present. The degree of hydrolysis should not be considered to be unity, however, since

Harman[128] demonstrated that the percent hydrolysis is 4.8% for 0.1N sodium metasilicate (first dissociation constant, $k_1 = 10^{-9.4}$) and Bogue[129] found it to be 27.8% for a 0.01N solution.

In order to determine the corrosion products from glass corrosion, Wang and Tooley[130] used what they termed a "simulated extract approach." After corroding a glass for a while they determined the precise concentrations of the different glass constituents in the extract. Simulated extract solutions were prepared using different substances which had the same total concentration as the real extract solution. Fresh glass samples were corroded using each of the simulated extracts and the real extract. Their thesis was that a simulated extract which exhibited the same corrosion rate as the real extract should contain the same constients as the real extract. The reaction products between the glass and water should be identical to the substances used to prepare the extract.

It was the conclusion of Wang and Tooley[130] that the constituents in solution following the corrosion of a soda lime silica glass are sodium metasilicate, calcium metasilicate and metasilicic acid. These conclusions are supported by the fact that the metasilicate salts have smaller heats of formation than the other possible reaction products. In another study Wang and Tooley[130] found that sodium metasilicate exhibited the greatest attack on glass while metasilicic acid showed the least attack. Calcium metasilicate and water had about equal rates of attack.

The conclusions of Wang and Tooley[130] failed to take into consideration the pH of the simulated extract solutions. If the

initial solutions had different values of pH one would expect different rates of reaction. This leaves some uncertainty as to their conclusions.

Ratios of Glass Constituents in Solution

Some glass constituents leach out of a glass much more rapidly than others. The result is that the proportion of glass constituents in solution do not equal those in the bulk glass. One of the first papers to make note of this difference was published by Mylius and Foerster.[86,87] They observed that the extracted solutions from most glasses contain a much larger alkali to silica ratio than in the bulk glass. The ratios from the binary glasses, however, are nearly the same in solution and in the glass. This is an indication that the binary glasses dissolve congruently.

Due to the limited corrosion conditions, Mylius and Foerster did not observe that the ratio of alkali to silica in the solution is also much less than the ratio in the glass under less severe conditions. Douglas and El-Shamy[19] studied the corrosion of glass over a wider range of conditions and made several generalizations about the alkali to silica ratio in solution. They concluded that the ratio decreases with time, temperature, alkali content of the glass, or replacement of the alkali ion of the glass by an ion of greater ionic radius. At longer times the ratio in solution approaches the ratio in the bulk glass but never becomes equal even at the longest corrosion time.[19]

The rate at which each of the glass constituents leaches into solution determines the magnitude of the ratio of glass constituents in solution. Differences in the ratios of constituents in solution at two different conditions, therefore, indicate differences in the rates at which the two constituents are leaching. For example it was determined that the ratio of sodium to silica in solution tended qualitatively to vary with the pH of the solution[131] being much greater for acidic solution than for alkaline solution.[19,52] At low pH the alkali to silica ratio in solution is very large since the alkali leaches much more rapidly than the silica. As the pH increases the alkali to silica ratio in solution decreases since the rate of alkali leaching decreases and the rate of silica extraction increases. The pH dependence of the extraction of glass constituents is discussed in the next section.

Several authors defined and calculated corrosion parameters to facilitate the discussion of the differences in the ratio of glass constituents in solution and in the bulk glass. Wang and Tooley[132] subtracted the ratio of alkali to silica in the glass from the same ratio in the solution to obtain a solution parameter, N,

$$N_{Na} = \left(\frac{Na}{Si}\right)_{extract} - \left(\frac{Na}{Si}\right)_{glass} \qquad (47)$$

A similar praameter was calculated for calcium,

$$N_{Ca} = \left(\frac{Ca}{Si}\right)_{extract} - \left(\frac{Ca}{Si}\right)_{glass} \qquad (48)$$

Values of N = 0 indicate that the ratio of modifying cations to silica in solution is equal to that in the glass. Values of N > 0 mean that the cations are leached preferentially to silica with the surface being depleted of the cation. The values of N calculated from their data indicate that N_{Na} is positive while N_{Ca} is close to zero. This is further evidence that sodium is preferentially leached from the surface. A value of N_{Ca} close to zero implies that the removal of Ca from the glass is due primarily to breakdown of the glass network in much the same way that silica is removed.

Schmidt[133] introduced a normalized corrosion parameter which he designated as alpha,

$$\alpha = \frac{N_{SiO_2}}{N_{R_2O}} \cdot \frac{1}{m} \tag{49}$$

where N is the amount of glass constituent that dissolves from the surface (mole/cm^2) of a binary alkali silicate glass with the composition $R_2O \cdot mSiO_2$. If alpha is equal to zero for a set of corrosion conditions, the implication is that the alkali in the glass preferentially leaches out of the glass and none of the silica goes into solution. At the other extreme when alpha equals one there is congruent dissolution of the glass with the ratio of alkali to silica in solution equal to that in the bulk glass. Intermediate values of alpha indicate the degree of selective leaching of the alkali ions with respect to the breakdown of the silica network and the release of silica into solution.

An equation for alpha was derived by Sanders[4] in terms of the concentration of glass constituents in parts per million (PPM). This equation is in error by a factor of 2, see Appendix A. The author prefers a more straight forward way of calculating alpha using the molar concentration of each glass constituent,

$$\alpha = \frac{2M_{SiO_2}}{M_{R+}} \cdot \frac{n}{m} \tag{50}$$

where M is the molar concentration of each glass constituent in solution for the binary $nR_2O \cdot mSiO_2$ (n and m are in mole %).

Sanders and Hench[21] introduced another glass corrosion parameter called epsilon. Epsilon is a measure of the excess silica left on the surface of the glass due to the leaching of the alkali ions. As will be discussed later, epsilon is proportional to the area of the leached layer profile (composition vs. distance into the glass). The expression derived by Sanders and Hench[21] for epsilon in terms of alpha and the PPM of silica in solution is,

$$\varepsilon = PPM_{SiO_2} \cdot \frac{1-\alpha}{\alpha} \tag{51}$$

Epsilon can also be expressed in molar terms by,

$$\varepsilon = M_{SiO_2} \cdot \frac{1-\alpha}{\alpha} \tag{52}$$

Schmidt[133] calculated alpha for glasses in the soda-silicate system at one time and temperature (1 hour at 100°C). He found that glasses with more than a critical concentration of 20 mole % Na_2O had an alpha equal to 1, but as the composition of the glass decreased below this critical concentration alpha decreased precipitously to zero.

Sanders and Hench[21] demonstrated that Schmidt[133] is in error. The critical factor is not the composition, but rather the time of corrosion. Even though the equation Sanders used to calculate alpha (and subsequently epsilon) is in error, the conclusions reached by Sanders and Hench[21] are valid for a hypothetical set of corrosion conditions. During the early period of corrosion the ratio of alkali to silica in the solution is much larger than in the glass. This is indicated by a very small value for alpha. As corrosion proceeds an increase in the rate at which silica goes into solution or a decrease in the leaching rate of alkali cause alpha to increase. These changes are accompanied by an increase in the value of epsilon indicating that the thickness of the leached layer is increasing. As corrosion proceeds alpha increases until it finally equals 1. At this same time epsilon equals zero indicating that the leached layer has dissolved. Longer times yield an alpha equal to 1 and epsilon equal to zero which show that congruent dissolution occurs.

At short times alpha has a smaller value as the temperature increases. Sanders and Hench[21] attributed this to a reaction between a highly reactive scratched glass surface. At longer times the order

is reversed and is probably due to the more rapid kinetics at high temperatures. Since alpha increases and approaches 1 at long times due to the increase in pH, an increase in temperature would be expected to make alpha increase faster.

An objective of this dissertation is to examine the changes in the corrosion parameters for a variety of glasses in the three alkali silicate glass systems (Li_2O-, Na_2O- and K_2O-SiO_2) in order to determine the actual sequence of changes which occur with corrosion time (for static corrosion conditions). Another objective is to determine whether the very durable glasses corrode by processes similar to the less durable glasses. Thus, this comparison should establish whether variations in durability of binary alkali silicates are due only to differences in kinetics or also involve different mechanisms.

Effects of the Solution on Glass Corrosion

The state of the attacking solution has a marked influence on the corrosion behavior of a glass. The pH of the solution probably has the greatest effect on the corrosion kinetics and complicates interpretation since the pH changes during the process of corrosion under static, unreplenished conditions.

Berger[134] was one of the first to recognize that it is necessary to distinguish between the attack of a vessel by acid, water or alkaline solution. The acid attack is characterized by a decreasing

rate of extraction with time while water and alkaline attack is usually much more severe. Hubbard and Hamilton[135] found that with most glasses, etching of the surface becomes severe in solutions of pH > 10 while the solutions with 2 < pH < 10 demonstrated very little etching.

The pH dependence for several binary glasses was investigated by Douglas and El-Shamy.[19,40] In general the rate of alkali extraction decreases only slightly for pH increasing from 1 to 9. Above a pH of 9, however, the rate of extraction decreases dramatically with increasing pH. This trend is also observed for some Na_2O-CaO-SiO_2 glasses and a glass electrode composition. The rate of silica extraction from glass surfaces also depends on the pH of the solution. Douglas and El-Shamy[19] observed that the extraction of silica from vitreous silica is independent of pH from 1 to 9. At values of pH > 9, however, the extraction of silica increases greatly with increasing pH. A similar trend is observed for 14K. The pH independent silica extraction range is, however, from 1 to approximately 7. Above a value of 7 the rate of silica extraction increases with increasing pH.

The aqueous attack of glass is very sensitive to small concentrations of some ionic species in solution producing one of two effects. They act as inhibitors of glass corrosion or they can accelerate the attack.

Trace concentrations of some metals in the aqueous solution produce inhibiting effects. Observations of Herman[118] and others[116,136,137] indicate that minute traces of copper and other heavy metal ions in solution or on the surface of a glass greatly reduce

the rate of extraction of alkali ions. Significant inhibiting effects have been observed for 0.002 PPM $CuSO_4$, 0.02 PPM $FeSO_4$ and 0.01 PPM $Fe_2(SO_4)_3$.[137]

The presence of alkali halides in neutral solution is also known to decrease the rate of extraction of alkali from a glass (22N6C). The effect was greatest for KCl and LiCl and least for NaCl.[117] Wiegel[117] described this as an antagonistic effect upon the gel structure. In a more mechanistic explanation, Weyl and Marboe[16] proposed that neutral salts decrease the passage of Na^+ ions through the gel by dehydration and formation of oxobridges (≡Si-O-Si≡ groups). This can also be thought of as a mixed alkali effect since the solutions with K^+ and Li^+ demonstrate the largest effect for a glass containing Na^+. A similar description was offered for the decreased rate of leaching of alkali ions when small concentrations of heavy metal ions are in solution. These heavy metal ions are thought to act as catalysts in the leached layer changing silanol groups into oxobridges reducing the permeability of the protective film.[16]

Devaux and Aubel[138] found that Ca^{2+} ions reversibly adsorb onto the glass surface. After rinsing glass wool with water, Ca^{2+} ions from calcium sulfate solution adsorb onto the surface in sufficient quantities to form a monolayer. After a prolonged leaching period in acid solution the glass adsorbs Ca^{2+} ions into the surface. A treatment of this Ca^{2+} rich surface with NaCl or KCl solution releases the Ca^{2+} ions which are replaced by alkali ions. The glass can be made to reversibly adsorb Ca^{2+}, H^+, K^+, Na^+, NH_4^+ and quinine.

Multivalent ions are strong adsorbers on a glass surface and their effect can be observed at very low concentrations. For example, Al^{3+} ions at a concentration of 10^{-5}M reverse the surface charge of quartz from negative to positive[139] and they adsorb so strongly that it is very difficult to remove them from the surface of quartz.

Some of the heavy metal ion glass modifiers which reduce the rate of leaching of alkali ions into acid and neutral solution are also very effective at reducing the rate of attack on the silica network. Geffcken[140] observed that small amounts of potassium silicate, and ions of some bivalent and trivalent metals (Ca^{2+}, Ba^{2+}, Zn^{2+}, Al^{3+}, Be^{2+}) greatly reduce the alkaline attack of the silica network. This led to the use of solutions containing some of these ions in commercial bottle washers in order to reduce the degradation in appearance of the bottles.[3]

Weyl stated that for an agent to be an inhibitor of alkaline attack of the silica network, it must form insoluble complexes on the surface.[141] He made a correlation between the effectiveness of these inhibitors and their field strength. Weyl recognized that there were limitations to this correlation due to the variation of the ionic radius with polarization and also to the intrinsic differences related to the outer electron shells of the ions.

In other experimental work, Hudson and Bacon[142] examined the ability of several inhibiting agents in solution to reduce the alkaline attack of glass. They found that complexes of Be^{2+}, pyrogallol ($C_6H_6O_3$) and Zn^{2+} are outstanding inhibiting agents while

Sr^{2+}, Sb^{3+}, Ba^{2+}, Al^{3+} and Pb^{2+} are not quite as effective. Complexes of Bi^{3+}, Cu^{2+}, Mg^{2+} and Zr^{4+} are precipitated by alkaline solution so their inhibiting effect is minimal. Three ions Mg^{2+}, Si^{4+} and Sn^{4+} do not reduce attack on the silica network at all.

Hudson and Bacon[142] found a correlation between the effectiveness of soluble divalent metal ions at reducing silica attack and their ionic strength which is similar to that proposed by Weyl.[141] No general correlation is observed, however, between the effectiveness of all of the inhibitors and their field strengths. Since some of the ionic species are not very soluble it is difficult for them to find their way to the glass surface to inhibit the attack. This is, therefore, another limiting condition of Weyl's theory.

A fairly good correlation between the inhibiting ability of a cation and its field strength was observed by Das.[102] In this study the ions were included in the glass composition so that there was no problem with getting the ions into solution and to the surface. As can be seen in Figure 1, there is a general trend to less silica extracted in any given time as the field strength of the cation increases. This will be discussed later in detail.

One can gain an insight as to the reasons for the inhibition effect by examining Iler's work in the effects of soluble aluminum on the solubility of silica.[139] Iler used aluminum citrate solutions at a pH where citrate has little or no effect on the dissolution of silica. As the concentration of aluminum citrate increased, the rate of silica dissolution is drastically reduced. He also found that as aluminum citrate is added to saturated solutions of silica

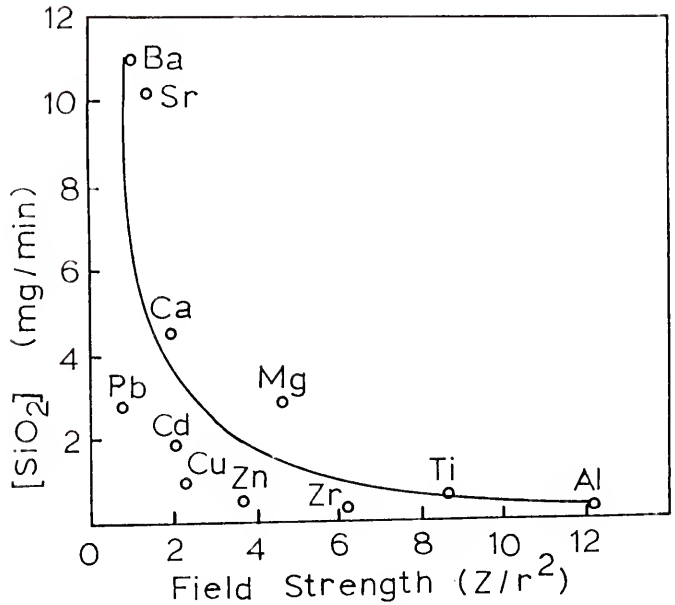

Fig. 1. Rate of silica extraction (at 84°C) vs. field strength of the indicated ions from glasses containing oxides of the elements indicated. After Das.[102]

the concentration of silica in the solution decreased. The aluminum ion complex adsorbs on the surface of the silica after which, if the silica concentration in solution is large enough, silica is removed from solution to form an alumino-silicate complex. It is suggested that the solubility of silica in dependent on the ratio of silica to alumina in the surface, each aluminosilicate site reducing the rate of silica dissolution of the silica surface surrounding it.[139] Iler concluded, "There is little question that in weakly alkaline solutions, silica is adsorbed on alumina or alumina on silica, forming an alumino-silicate surface that is much less soluble than either oxide alone."[143]

A possible mechanism is as follows; the Si^{4+} ion normally has a four fold coordination and is screened by four O^{2-} ions. The screening is not complete, however, as evidenced by the finite solubility of a complex of Si^{4+} in aqueous solution. The Al^{3+} ion also has a four fold coordination which completely screens its positive charge. The contrapolarization of an O^{2-} ion (shared between a Al^{3+} and Si^{4+} ion) by the Al^{3+} permits more of the electron cloud of the O^{2-} to screen the Si^{4+} ion. The more polarizable O^{2-} ion sufficiently screens the Si^{4+} ion such that it need not have any more screening from water and, therefore, the Si^{4+} ions surrounding the Al^{3+} are less soluble than Si^{4+} ions not under the influence of the Al^{3+} ion.

Certain chemical species in solution are known to accelerate the attack of the silica network. Most notably among these are the organic chelators. Ernsberger[144] described the attack by chelators on the glass surface. He said, "If the complex formed is water soluble, the

effect anticipated is an increase of the attack rate over that observed with the same solution in the absence of the agent in question, and, if insoluble, a decrease. . . . Chelating agents which might reasonably be expected to have an influence on the rate of attack of glass by aqueous solutions include those which are able to form stable complexes with the "protective" cations, e.g., Al^{3+} and Mg^{2+}, and especially those able to form complexes with the silicon ion itself."[145]

Ernsberger[144] investigated the effects of the two chelators EDTA (ethylene diamine tetracetic acid) and catechol (O-dihydroxy benzene) on the attack of the silica network over a pH range of approximately 9-13. Both of the chelators greatly increase the attack of the silica network of a commercial soda lime glass. EDTA is observed to produce a five fold increase in the attack of the glass at concentrations of 0.02% by weight. The rate of attack increases with pH to a maximum at approximately 12.5. This increase is attributed to the increase of the concentration of ionized chelator to the point of complete ionization. The addition of phosphates or carbonates shift this maximum to approximately 10.5.

Bacon and Raggon[121] examined the effects of citrate and other structurally similar organic anions on promoting attack of a commercial soda lime glass. The concentration of each ion in solution was 4% and the pH was adjusted to a value of 7. The observed behavior for each anion ranges from only slightly more reactive than neutral water to much more reactive in the order: lactate, benzoate, acetate (EDTA), succinate, ascorbate, malate, versene, tartrate, oxalate, gluconate,

fluoride and citrate. The solution containing sodium citrate is the most corrosive towards several types of glasses as well as silica. Bacon and Raggon explained,

> All the organic anions which substantially promote attack in the present work form known complexes with calcium. Of these, citrate, oxalate, tartrate, and ethylene diamine tetraacetate are known to form complexes with aluminum as well. This will not account, however, for the action of citrate and gluconate on relatively pure forms of silica. It seems very probable that this action is attributable to the formation by silicon of soluble complexes with these anions.[146]

Of the glasses tested by Bacon and Raggon a high zirconia and a zinc borosilicate glass tend to have the best resistance to citrate solutions.[121] The attack by citrate on the silica structure can be avoided by reducing the pH to around 5.[121]

The rate of silica removed into a solution with chelators is a linear function of time[144] indicating that an interfacial reaction mechanism must be the controlling step. Ernsberger[144] described the chelator catechol as being,

> . . . sterically adapted to react with the silicon ion itself. In the ionized state, catechol furnishes a pair of singly charged oxygen anions in sufficiently close proximity to each other that both ions can enter the first coordination sphere of the silicon ion without strain. . . . The extra stability conferred by the chelated structure has the effect of weakening the oxygen bridges which bind the surface silicon ions to the underlying silica network. The result is an increase in the rate at which silicon atoms are released from the network.[147]

Surface Analysis

Solution data can be used to obtain information indirectly about the surface of a corroded glass. A more direct method is to examine the surface itself. Three of the oldest ways of assessing the attack of a glass from changes in the surface are the measurement of weight loss, interferometry and the dimming test.[126] From the weight loss an idea of the total amount of the various extracted constituents is obtained. The absorption of water, however, presents a complicating factor and the total weight can in some cases actually increase. The other two methods give an idea of the appearance of the glass surface but nothing can be conveyed about the mechanisms of extraction.

There are four modern analytical techniques which can yield information about the corroded glass surface by direct analysis.[148] They comprise electron microscopy (EM),[20,148] electron microprobe analysis (EMP),[148,149] infrared reflection spectroscopy (IRRS),[21,123,148] and Auger electron spectroscopy (AES).[81,148,150] Each technique permits the analysis of a different aspect of the corroded glass surface. With electron microscopy one can observe the morphology of the surface while EMP, IRRS and AES permit the chemical analysis of the surface.

Electron microscopy techniques including scanning electron microscopy[151,152] and replica electron microscopy[153] have provided useful information about glass corrosion, weathering and sulfuring of surfaces. Studies of weathered plate glass indicate that a "porous structure" evolves.[154] Small craters are formed on the order of 0.1 μm

in diameter and increase in size as weathering is accelerated.[154] Another useful investigation explored the corrosion of abraded (33L) glass surfaces. The corrosion of glasses with surfaces abraded with 120 or 320 grit SiC paper produces etching of the scratches. Glasses abraded with 600 grit, however, are significantly less severely attacked and appeared much like the freshly abraded surface.[20]

The three surface chemical analysis techniques yield averaged information from their respective sampling depths. Electrons from the EMP penetrate to a depth of approximately 1.5 μm.[148] This is rather large when one considers the corrosion of relatively chemically durable glasses. The penetration depth can in fact be deeper than the corroded layer after short corrosion times. Infrared reflection spectroscopy has a smaller sampling depth than EMP analysis (approximately 0.5 μm) which permits the analysis of thinner corrosion films. This technique is especially well suited for the investigation of binary alkali silicate glasses.[25,155] The third analytical tool is Auger electron spectroscopy. This instrument provides information on the Angstrom scale with the escape depth for the Auger electron being in the range of 5 Å.[148] Each of the three techniques has advantages and disadvantages which are listed in Table VIII.

Of the three tehcniques listed above, structural information can only be obtained with IRRS. Infrared spectroscopy is a widely used analytical method based on the empirical foundation that observed maxima can be related to atomic groups of a known structure.[156] Peaks due to particular structural groups occur in narrow spectral regions

Table VIII. Advantages and Disadvantages of Electron Microprobe Analysis, Auger Electron Spectroscopy and Infrared Reflection Spectroscopy for Analyzing Glass Surfaces.

	Advantages	Disadvantages
EMP	1. Standard chemical analysis procedures.[157] 2. Profiles across cross-sections of thick leached layers.[21]	1. Requires a vacuum to operate. 2. Time loss to prepare sample. 3. Vacuum and electron effects on the sample.[149] 4. Large sampling depth.[148] 5. Cannot detect lithium.
AES	1. Very small (10-50Å) sampling depth.[148] 2. Semi-qualitative chemical analysis.[158,159] 3. Profiles of thin leached layers by ion milling.[160]	1. Requires a vacuum. 2. Time loss to prepare sample. 3. Vacuum and ion milling effects.[158,161] 4. Slow ion milling rate.
IRRS	1. No vacuum required. 2. Sampling depth[148] less than EMP. 3. Test does not affect the sample. 4. Qualitative chemical analysis of multicomponent glasses (Quantitative analysis of binary glasses) as well as structural information.[155] 5. Rapid analysis 6. Inexpensive	1. No quantitative analysis of multicomponent glasses.

so that the structure of a material may be estimated by comparison of its spectra with the spectra obtained from compounds with known structures. Infrared spectroscopy is also particularly useful in the study of glass since it is sensitive to the local positioning of atoms and the strength of the chemical bonds between them.[25]

Since the use of standard transmission infrared analysis of glass becomes impractical at frequencies lower than approximately 2000 cm^{-1} (4 to 5 μm)[162] infrared reflection spectroscopy (IRRS) has been used to study the structure of glass in the 1100 cm^{-1} (9 to 10 μm) region where a very strong vibration band of silica exists.[25,161,163,164,165]

Much information can be obtained from true infrared spectra if band-broadening effects of anharmonic coupling of vibrational modes are absent.[162] The curves represent distribution functions with the ordinate proportional to the number of vibrations at a given frequency. The frequency range over which the vibrations spread out are represented by the band width which also indicates the spread of the force constants.

For a rigorous interpretation of reflection spectra it is necessary to separate the effects caused by the optical properties n and k.[164] This can be accomplished by use of polarized radiation or by using two angles of incidence. It has been assumed for simple glasses that the maxima which are observed occur at wavelengths very close to the natural periods of vibration and there is evidence that this is valid for most cases.[25,163,164]

The peaks of interest on a typical infrared reflection spectra for a binary alkali silicate glass are designated by the letters shown

on Fig. 2. Simon and McMahon[162] assigned the strong peak at 1050 cm^{-1} to the stretch of a Si-O bond where the oxygen atom is part of the network (silicon bridging oxygen bond). THis peak is called the S peak. On the lower frequency side of this peak is another peak which appears when alkali oxide is added to vitreous silica. This peak at around 940 cm^{-1} is due to the stretch of a Si-O bond where the oxygen is a nonbridging oxygen (silicon nonbridging oxygen stretch peak) and it is given the designation NS.[162]

Using infrared reflection spectroscopy, Simon and McMahon[162] investigated the effect of adding alkali oxide to vitreous silica. They said,

> Upon the addition of a small percentage (less than approximately 10 mole %) of a metal oxide, the type of structure and the force constant of the Si-O-Si bond remain practically unchanged. When the amount of added oxide is increased up to approximately 25 mole %, the changes produced in the structure appear to depend not only on the amount but on the kind of oxide added. Finally, when the amount of added oxide exceeds a certain limit, the changes in the spectra indicate a profound change in the structure of the glass, largely independent of the kind of cation involved.[162]

As alkali oxide is added to vitreous silica the S peak becomes broader, decreases in intensity and shifts to a lower frequency. A new peak (NS peak) appears first as a shoulder on the S peak and later as a distinguishable separate peak. The extent of change associated with the addition of alkali oxide to the glass varies with the particular alkali. For a given concentration of alkali oxide added to vitreous silica the extent of change is in the order $K_2O > Na_2O > Li_2O$.[25]

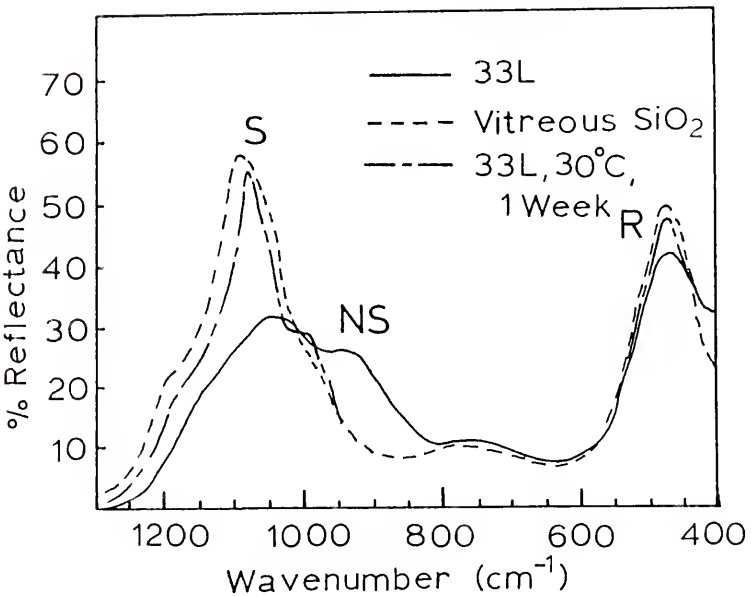

Fig. 2. Infrared reflection spectra for vitreous silica, 33L and 33L corroded for 1 week at 30°C.

Charles[166] said that at the transformation temperature the boundaries of the miscibility gaps for the Na_2O-SiO_2 and Li_2O-SiO_2 systems are 20 and 33 mole percent. Sanders et al.[25] argued that even though the consolute temperature of the K_2O-SiO_2 system is below the glass transformation temperature, it is thermodynamically probable and it should be closer to vitreous silica than for the Na_2O-SiO_2 system. The fact that for kinetic reasons the miscibility does not take place in the K_2O-SiO_2 system does not negate the possibility of local segregation of nonbridging oxygen atoms around the alkali atoms.[25]

A theoretical argument set forth by Sanders et al.[25] predicted that a plot of the reflectance should be directly proportional to the concentration of alkali oxide in the glass. Actual plots yield straight lines with a discontinuity. The discontinuities for each system occur at approximately the same composition (20, 25 and 33 mole % for the K_2O-, Na_2O- and Li_2O-SiO_2 systems respectively) as a discontinuity in the plot of wavenumber shifts vs. composition (20, 24 and 32 mole % for the K_2O-, Na_2O- and Li_2O-SiO_2 systems).[155] Sanders et al.[25] related these discontinuities to the depletion of the vibrational species of the high silica phase. They concluded that the discontinuities in plots of reflectance and wavenumber vs. composition detect both actual phase separation and the tendency towards phase separation.

The S peak at approximately 1100 cm^{-1} decreases in frequency as alkali oxide is added.[156,167] This indicates that the Si-O bond

force constant is decreased, weakening the structural bonding, by the cationic field of the network modifier.[162] This has been given as evidence for the decrease in elastic moduli and strength of Na_2O-SiO_2 glasses as the concentrations of Na_2O increases.[167] Peak frequency shifts have been used for the compositional analysis of the binary sodium silicate glasses[155,163] and multicomponent glasses.[155,164,165,168,169]

Certain changes in the IRRS spectra take place after corroding a glass, especially a binary alkali silicate glass. Figure 2 includes a spectrum for a 33L glass after corroding with deionized water for 1 week at 30°C using the Sanders' method.[21] One can see that after corroding the sample the silicon-bridging oxygen stretching peak (S peak) sharpens, increases in intensity[21] and shifts to a larger wavenumber.[155] This is accompanied by a decrease of intensity[21] as well as a shift to a lower wavenumber[155] for the silicon nonbridging oxygen stretching peak (NS) at around 940 cm^{-1}. These changes produce a spectrum which more closely resembles that of vitreous silica than the original glass. This is direct evidence of the leaching of alkali ions from the surface from direct analysis of the surface.

Clark et al.[155] demonstrated that shifts of the silicon bridging oxygen stretch peak from IRRS spectra could be used to follow glass corrosion and to obtain the composition of the surface of a corroded glass. Since glasses can undergo rather severe roughening during corrosion[20] a scattering of the reflected beam results, causing the whole spectrum to be lower than expected. The frequency of the

various peaks, however, are independent of the surface roughness so that shifts of the peaks can be used without accounting for surface roughness. Using plots of S peak wavenumber vs. Na_2O concentration in the glass obtained from freshly abraded samples as a calibration curve, Clark et al.[155] determined the surface concentration of Na_2O for the glasses 20N and 20N10C corroded at various corrosion times. Good agreement was obtained between the surface sodium concentrations obtained by this procedure and electron microprobe analysis.

There are a few more spectral changes which can be observed in IRRS analysis.[21] A silicon bridging oxygen rocking peak (R) at around 580 cm^{-1} increases in intensity as the leaching continues indicating an increase of the SiO_2 content of the surface. The region between the S and NS peaks decreases with corrosion. This is attributed to the loss of alkali ions responsible for coupling the two peaks. At long times after much leaching a peak attributed to the bending of silicon bridging oxygen atoms appears at around 800 cm^{-1}.

A similarity between the structures of silica gel and the binary alkali silicate glasses was demonstrated by Zarzycki and Naudin using infrared spectroscopy.[170] Two major peaks are observed at 1100 and 950 cm^{-1} corresponding precisely to the silicon bridging oxygen (S) and silicon nonbridging oxygen peaks (NS). A peak for fused silica at 930 cm^{-1} has also been attributed to the presence of OH^- ions and it can be developed if finely powdered quartz is exposed to water. This data indicates that the H^+ ion acts as a network modifier, being analogous to the alkali ions. After a heat treatment, Zarzycki and

Naudin[170] noted that the NS peak shifted to shorter wavelength and decreased in intensity. They attributed this to the calcination of the gel with the removal of some of the Si-OH groups as water (Eq. 54). They postulated that some of the remaining protons participated in hydrogen bonding between Si-OH groups and bridging oxygen ions. When this hydrogen bonding occurs, the proton changes its way of screening from penetrating into the electron cloud of the nonbridging O^{2-} ion to assuming a position where it is screened by the two O^{2-} ions. In this manner it acts like a network former having a coordination of two contributing to the strength of the structure.[170]

There are three so called "water" peaks which occur in silicate glasses in the regions 3650 - 3400 cm^{-1} (2.75-2.95 μ), 3000 - 2600 cm^{-1} (3.35-3.85 μ) and 2450 cm^{-1} (4.25 μ).[171,172] The strongest bond of SiO-H vibration[173] is that at approximately 3745 cm^{-1} (2.7 μ) and is attributed to the vibration of the hydroxyl group in the glass.[174] Hydrogen bonding of Si-OH groups produces a general decrease in the frequency of the assymmetric stretching for SiO-H bonds and a broadening of the contour of the peaks.[98] The peaks in the bond regions at lower frequency (wavenumber) than 3745 cm^{-1} are, therefore, attributed to hydrogen bonding.

Using the peaks at 3700 cm^{-1} (2.7 μ) and 2780 cm^{-1} (3.6 μ) corresponding to the hydrogen bonded and unbonded SiO-H groups respectively, Scholze[175] estimated the percentage of silanol groups involved in hydrogen bonding. These values appear in Table IX. The tendency towards hydrogen bonding of the SiO-H groups in the binary alkali

Table IX. Percentage of Hydrogen Bonded SiO-H Groups in Some Binary Alkali Silicate Glasses.

Glass	% H-Bonded SiO-H Groups
25L	35
30L	40
25N	93
25K	97

Source: After Scholze.[175]

silicate glasses increases in the order Li_2O-SiO_2 < Na_2O-SiO_2 < K_2O-SiO_2. In another study the two peaks at 3401 cm^{-1} and 2857 cm^{-1} corresponding to weakly and strongly H-bonded groups respectively, were used to observe the diffusion of "water" into glass.[176] As corrosion of the glass proceeds, both peaks increase in intensity but the strongly hydrogen bonded SiO-H peaks increase more slowly. Scholze concluded that more "water" diffuses to these unbonded (or weakly bonded) positions than to strongly hydrogen bonded positions.[176] Rana and Douglas[84] stated that Adams[176] calculated water diffusion coefficients which were in agreement with those obtained by Beattie[85] for the interdiffusion process. This indicates that Scholze[175] was monitoring the ion exchange process and the diffusion of H^+ ions into the glass to replace alkali ions thereby forming Si-OH groups.

The leached layer on the surface of a glass provides a diffusion barrier for the leaching of alkali ions out of the glass.[49] Evidence for this is provided by the fact that the leaching of alkali ions into acid or neutral solution slows down with time, following a root time dependence. The result of this leaching process is the production of a protonated glass surface. The nature of this layer has not, at the present, been explained with respect to the body of corrosion literature. An understanding, however, of the complicated process of alkali leaching requires a more specific examination of the leached layer.

Douglas and Isard[83] proposed that the protonated surface of a glass might undergo a phase separation process, eliminating water

from the surface. Such a process is known to exist at higher temperatures and even below room temperature for organosilicon compounds.[83] During glass corrosion the replacement of Na^+ ions by H^+ ions produces incompletely screened Si^{4+} ions.[101] In silica gels this need for more complete screening of the Si^{4+} ions serves as the driving force for a polymerization reaction.[101] As the polymerization reaction proceeds, the removal of water molecules produces a tension within the network which contracts the gel.

Weyl[101] felt, however, that the Si^{4+} ions with silanol groups, in the leached layer of a corroded glass satisfied their need for more screening by water molecules through hydrolysis of the surface. The resultant swelling of the leached layer was thought to be the reason the rate of diffusion slowed down.

Weyl's[101] theory was modified later in Weyl and Marboe's book.[16] They felt that a polymerization process could occur in the leached layer on the surface of a corroded glass. Several factors affecting such a structural change were discussed. As the corrosion time increases, the leached layer not only increases in thickness but also ol-bridges (≡Si-OH ··· HO-Si≡) transform to oxo-bridges (≡Si-O-Si≡) which produces an efficient barrier to leaching. This transformation is believed to increase with time and temperature and is catalyzed by heavy metal ions which prefer oxo- to ol-bridges. The presence of alkali ions in solution prevent this transformation from going to completion which renders the leached layer more permeable to alkali ions.

The above process was discussed by Das[90] in connection with experimental data. In reference to the differences in behavior of cations with different coordination requirements he concluded that the lower field strength and the greater polarizability of a cation having a higher coordination number makes it possible for the cation to increase its distance from the O^{2-} ions, so that their electrons can screen the Si^{4+} ions more effectively thereby reducing the tendency of polymerization to a compact layer.[90]

Some experimental evidence supports the idea that a polymerization reaction occurs on the surface of a leached glass. By using X-ray amorphous scattering techniques, Hill [177] and Gould and Hill[178] obtained pair function distribution curves for leached 20K, 25K and 33K glasses. Peak shifts of the main maxima to lower S values indicate that the interatomic distances (i.e. Si-1^{st}O, Si-1^{st}Si, Si-2^{nd}O, etc.) decrease slightly, as the glasses are leached, to values close to those obtained for vitreous silica. Gokularathnam et al.[179] demonstrated that a concentration of water up to 0.12% has little effect on the pair distribution function of vitreous silica. Silicic acid with 12% water, on the other hand, has a different short range order than vitreous silica. The Si-1^{st}O distance is larger and the Si-1^{st}Si interaction is much weaker than in vitreous silica. This implies that the structure of the silica rich leached layer on corroded glasses more closely resembles vitreous silica than a hydrated silica structure like silica gel.[180]

If it does in fact occur, the extent of the dehydration reaction is probably limited. Douglas and Isard[83] conducted a leaching experiment which was interrupted by a heat treatment at about 500°C. An interruption of the leaching process with no heat treatment had little effect on the test; however, heating the glass produced a large effect. The heat treatment completely dehydrated the surface greatly reducing the mobility of the Na^+ ions. It was found that even a heat treatment does not completely dehydrate a glass surface. A soda lime silica glass heated for one hour at 1200°C in the presence of water had a surface with 2.5% water.[181]

Surface Corrosion Profiles

Much speculation has been generated concerning the nature of the leached layer on the surface of corroded glasses. The first fact that was deduced form solution data was that alkali ions leach from the surface faster than the rate of attack of the silica network.

Das[90] used a schematic diagram to describe the corrosion of a glass surface, see Fig. 3a. The leached layer on the surface of the glass is represented by the region $(X_2 + X)$. With further corrosion, X_2 glass is extracted so that the leached layer becomes $(X + X_1)$. The amounts of alkali and silica extracted are represented by,

$$dQ_A = K_1 X_1 \qquad (54)$$

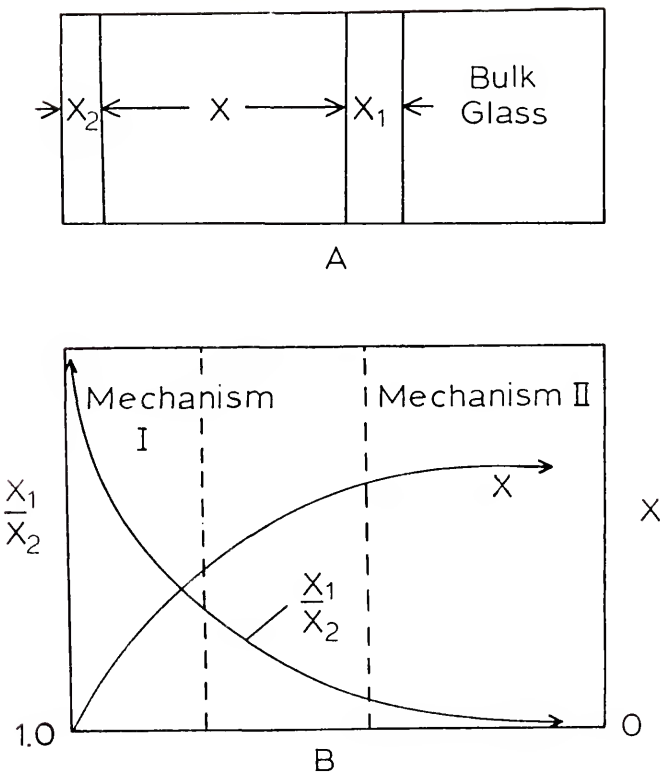

Fig. 3. Schematic diagram of a corroded glass surface (A) and the general sequence of events during corrosion (B). After Das.[90]

$$dQ_S = K_2 X_2 \tag{55}$$

where Q_A and Q_S are the amounts of alkali and silica respectively extracted while K_1 and K_2 are constants for the glass. Das then wrote an expression for the ratios of the extracted glass constituents,

$$\frac{dQ_A}{dQ_S} = K\left(\frac{X_1}{X_2}\right) \tag{56}$$

Das described the general sequence of events during the corrosion of commercial soda lime glass, see Fig. 3b.[90] At the beginning of the reaction, when only a little alkali has been extracted, X_1/X_2 is at infinity. This ratio was said to decrease from infinity during the first mechanism and then become constant during the second mechansism. The value of X assumes a positive value as soon as the ion exchange begins.[90] Since the rate at which alkali leaches is faster than the dissolution of silica, X increases with time during the first mechanism but at a decreasing rate. This increase continues until some time during the second mechanism when it becomes constant and the steady state model proposed by Lyle[46] comes into effect.

Das said, "in order that X should remain constant, X_1/X_2 should have a value of 1, in other words the alkali to silica ratio in the extract should be the same as that in the glass, which is not so in actual practice. X would, therefore, still increase during the second mechanism though at a decreasing rate."[182]

This is not precisely correct. It is true that in order for X to remain constant X_1/X_2 should equal 1, but this does not imply that the alkali to silica ratio in the solution should be the same as in the glass. If this last statement were true then there would be no reason to assume that X will increase during the second mechanism and there is no reason to have to propose an effective increase of the surface area of the glass by the formation of channels as Das does. The alkali to silica ratio cannot be used as an indication of whether or not X is constant. Some other corrosion parameter is needed.

Sanders and Hench[21] proposed a method for determining the thickness of the leached layer. Using the value of the corrosion parameter epsilon (excess silica on the surface) and the surface area of the glass to the volume of solution ratio (A/V) they defined the quantity S as,

$$S = \varepsilon \frac{V}{A} \tag{57}$$

where the units for S are (g excess SiO_2/cm^2 surface), ε (g excess SiO_2 x $10^{-3}/\ell$ solution) and V/A (cm).

The author prefers to think of S as a special type of epsilon,

$$\varepsilon' = \varepsilon \frac{V}{A} (10^{-3}) \tag{58}$$

If one assumes a linear composition profile as in Fig. 4 one can see that the product of the film thickness and the compositional difference between the bulk and the surface yields a quantity whose units are mole SiO_2/cm^2. These are precisely the same units as for ε' and implies that ε' is proportional to this product and ε' is proportional to the area under the composition profile. An equation is derived in Appendix E for the thickness of the leached layer using these quantities.

There are several techniques by which surface profiles may be determined directly from the surface of the glass.[45] For most of the methods the leached layer has to be relatively thick to get any meaningful data. Grinding techniques have been developed which allow the removal of layers 2 - 3 μm thick and an HF technique can get down to 0.2 - 0.3 μm thick layers. The material from each removed layer is analyzed by wet analysis to obtain an averaged composition for the layer. Electron probe microanalysis has also been used to obtain a composition profile across a cross section of corroded glass.[21] The limiting condition for this technique is the size of the electron beam (1 μm in diameter) and the diffusion of alkali ions out from under the beam.[149] The combined use of ion milling and Auger electron spectroscopy makes it possible to examine corrosion films 40 - 50 Å thick.[150,160]

Dobos[183] examined the concentration distribution in the leached layer of a 28N4Ba glass and found two distinct regions. The outer region contained much water with a positive concentration

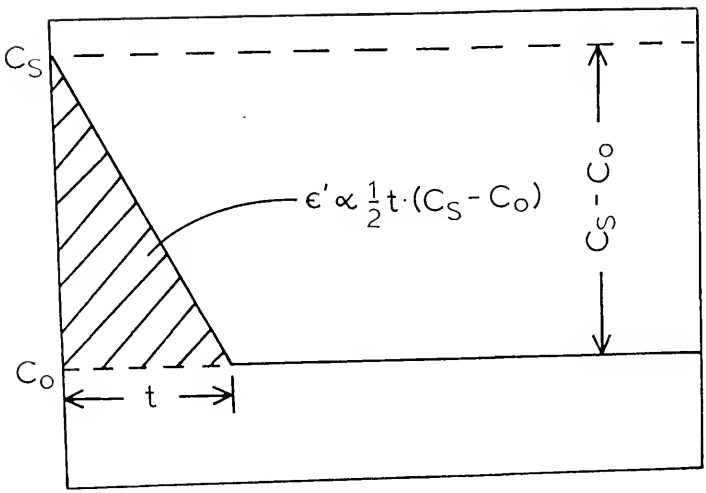

Fig. 4. Schematic diagram indicating that ϵ' is proportional to the area under the silica composition profile on the surface of a corroded glass.

gradient from the interior of the leached layer to the glass surface. This swollen part of the surface layer was said to possess a "micro-heterogeneous structure."[184] The inner layer contained much less water and H^+ ions which had diffused ahead of the water.[183]

Boksay et al.[22] used the HF technique for the stepwise dissolution of the leached layer on the surface of several corroded glasses, of which one had the same composition as studied by Dobos.[183] It was their conclusion that the leached layer formed under short time diffusion controlled conditions and had two steady state regions with respect to the alkali concentration.[22,81,185] A schematic representation of this appears in Fig. 5. Nearest the surface of the glass the alkali concentration gradient is low and nearly linear. Close to the bulk glass the sodium concentration gradient changes rapidly as the sodium concentration changes from a low value to that measured in the bulk. The diffusion coefficient must, therefore, have a large value in the outer region which decreases abruptly within the second region. This indicates that a structural transformation in the leached layer probably occurs when the sodium concentration of the leached layer has been depleted to a certain value.[22] Boksay et al.[22] felt that this structural transformation was caused by the diffusion of OH^- ions into the glass and their need for a larger space than the Na^+ ions.

The author tends to believe that it is not the diffusion of OH^- ions into the glass but rather the replacement of alkali ions with H^+ ions producing a protonated surface with many Si-OH groups which

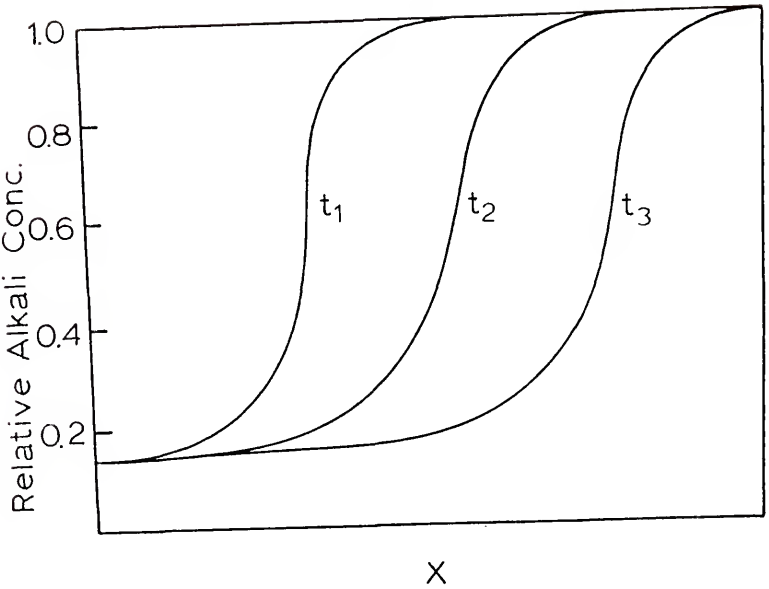

Fig. 5. The relative concentration of alkali in the leached layer of a corroded glass as a function of depth into the surface, X, for increasing corrosion times ($t_1 < t_2 < t_3$). After Boksay et al.[22]

causes this transformation. This outer region would be much more open than the bulk glass and alkali ions would rapidly diffuse through it. The Si-OH groups are also precisely the species detected when measuring the concentration of water in glass and it is more likely that this is the "water" that Dobos[183] reported as being in high concentration in the region of the leached layer.

Boksay et al. derived[22] a relation for calculating the mole fraction of alkali ions in the leached layer of a glass during the steady state process as described by Lyle.[46] Assuming a constant network solution rate, v, and a constant interdiffusion coefficient, D, the alkali mole fraction, n, as a function of the distance, X, from the leached layer solution interface into the glass is,

$$n = 1-\exp\left(-\frac{aX}{D}\right) \qquad (59)$$

This relation was found to be in good agreement with the experimentally determined composition profile indicating that at least in this case D is independent of $\bar{n}$. Boksay attributed this to the nearly identical size of the K^+ ion (1.33 Å) and the H_3O^+ ion (1.26 Å) in the glass tested.

Diffusion coefficients can be determined directly from composition profiles. The values for the diffusion coefficient determined in this way are limited, however, by the resolution of the method used to determine the profiles. The real maximum concentration gradients could be greater than those actually determined so that the actual diffusion

coefficient could be smaller. Each of the different procedures described earlier for determining composition profiles has a different minimum surface sampling depth which limits the minimum detectable diffusion coefficient. The HF, EMP and AES procedures have a minimum attainable diffusion coefficient determination of 10^{-14}, 10^{-16} and 10^{-18} cm^2/s respectively.

Boksay et al.[22] demonstrated how it is possible to calculate the diffusion coefficient from a composition profile. Using the equation,

$$D = a\sum_{i=0}^{K} \Delta X_i \cdot (1-\bar{n}_i) \qquad (60)$$

where the mole fraction of alkali, $\bar{n}_i$, is known for a particular layer fraction, i, of thickness, ΔX_i, they calculated the interdiffusion coefficient for a glass in the steady state condition to be very large, $D = 2.1 \times 10^{-5}$ (cm^2/s).

Using an analysis similar to Boksay et al., Baucke[81] derived a relation to determine the diffusion coefficient for lithium within the leached layer of glasses corroded in acid solution. Knowing the difference in alkali concentration from the bulk to the surface C^o_{Li}-C^s_{Li}, the dissolution rate of the silica network, v, and the maximum concentration gradient in the leached layer, $\frac{dC_{Li}}{dX}$, the interdiffusion coefficient, $\bar{D}$, is,

$$\bar{D} = \frac{(C^o_{Li}-C^s_{Li})}{\frac{dC_{Li}}{dX}} v \qquad (61)$$

The interdiffusion coefficients for the ion exchange of H^+ ions for Li^+ ions in a glass electrode membrane were determined by Baucke.[81] He found that this interdiffusion coefficient is two orders of magnitude lower than for the diffusion of Li^+ ions in the bulk glass. Since protons (H^+ ions) have a much lower mobility than Li^+ ions in this glass, the low interdiffusion coefficient was attributed to the low diffusion coefficient of the protons. Baucke determined that within the region $0.3C^o_{Si} \leq C_{Li} \leq 0.5C^o_{Li}$ the interdiffusion coefficient is a minimum. This indicates that a structure much like the bulk glass is preserved in the leached layer down to a Li^+ ion concentration of at least $0.3C^o_{Li}$. At Li^+ ion concentrations lower than $0.3C^o_{Li}$ the structure is increasingly changed such that the diffusion coefficients are higher. The smaller of either $C_{R^+}D_{R^+}$ or $D_{H^+}D_{H^+}$ limits the magnitude of the interdiffusion coefficient, see Eq. 35. If $C_{R^+}D_{R^+} \leq C_{H^+}D_{H^+}$ then the leaching process is controlled by the diffusion of alkali ions (R^+). But, since hydrolysis of the silicate network can generate more Si-OH groups, the concentration of protons can be more than expected merely from the ion exchange reaction, $C_H \geq C^o_{Li} - C_{Li}$ and such an analysis may be difficult.

Mechanisms

Many people have described the so called "mechanisms" of glass corrosion. A list of the significant advances in the understanding of glass corrosion are listed in Table X. In most studies only one

Table X. Significant Advances in Understanding Glass Corrosion.

Type of Glass	Solution	Test Model	Observations	Reference
Multicomponent as formed	Neutral water	Stagnant	$t^{1/2}$ kinetics to 0.0002 N (Na_2O) in solution	83
Multicomponent polished surface	Alkaline (NaOH)	Stagnant, stirred	t^{1} kinetics	186
Multicomponent as formed, bottles	Alkaline	Stagnant	Inhibitors of alkaline attack	142
Multicomponent as formed, bottles	Neutral water	Stagnant	Inhibiting effect of anions	121
Multicomponent as formed, bulk surface	Range of pH	Stagnant	Accelerated attack by chelators	144
Multicomponent as formed and SO_2 treated bottles	Water	Stagnant	Relate $t^{1/2}$ to Na^+ diffusion	83
Multicomponent as formed, bottles	Atmospheric water	Weathering	H^+ diffusion controlled corrosion	109
Multicomponent as formed, bottles and powders	Water, acid and alkaline	Stagnant	Different results with different tests, solutions and compositions	50,51
Multicomponent as formed bottled	Used data of Bacon and Burch[50,51]		$\log$ [NaOH] vs. $\log t$, slopes of 0.5 and 1.0 over several orders of magnitude	46
NCS, powder	Water	Stagnant	Equilibrium pH as a function of composition	187
NCS. powder	Water	Discontinuous flow	$t^{1/2}$ at short times, incorrectly described t^{1} at long times for 15N	47

Table X - continued.

Type of Glass	Solution	Test Model	Observations	Reference
NCS and KCS, powder	Water	Discontinuous flow	Differences between D (electrical cond.) and D (ion exchange)	84
LS, NS, KS, powder	Water	Stagnant	Limiting conditions of $t^{\frac{1}{2}}$ at short times and t^{1} at long times. Effect of pH on alkali and silica extraction	19
15K, powder	Buffered pH 0-12.6	Stagnant	$t^{\frac{1}{2}}$ leaching of K^{+} at all values of pH	40
33L, polished glass surface	Water	Stagnant	Calculation of epsilon. Applied IRRS to study corrosion	21

corrosion process is described for one set of conditions (i.e. leaching of alkali ions into neutral water). To formulate a mechanism for each type of corrosion process it is necessary to recognize the limitations of the testing procedures used to obtain the data as well as possible influences from the test conditions on the corrosion process. There is a need to avoid limiting the scale of the tests since observations applicable under some conditions are not applicable under others. This has led to many errors in the literature. Much has been learned for the corrosion of glass under specific conditions but none has addressed the specific mechanisms for each process in control under different conditions.

Most studies of glass corrosion behavior have dealt with a kinetic analysis of glass constituents going into the corroding solution. An early study was conducted by Burch and Bacon[50,51] on the leaching of Na^+ from bottles. They observed that the leaching of Na^+ seemed to follow a complicated regime. Corrosion by a weakly acidic solution produced plots which were mostly parabola-like with a decreasing rate of leaching with time. However, one plot seemed to be linear and another increasing with time. But since these plots were constructed with only three data points the later two cases are likely to be due to experimental error. When neutral water was used for the test solution the attack was similar to acid attack but accelerated at longer times for a few bottles. Speaking of these results Weyl and Marboe said that these kind of results indicate how futile it is to describe the results by mathematical expressions

covering the effects of time and temperature on the aqueous attack of glasses.[16] The author disagrees with this statement. The corrosion of glass is a complicated process and can seem almost impossible to interpret for such a small set of data. However, if a more systematic examination of the process is undertaken much can be learned from the kinetic data.

Douglas and El-Shamy[19] studied in detail the corrosion of glass grains of a variety of compositions from three binary alkali silicate systems. Values for the reaction rate constants, k, and the reaction rate exponents, a, (Eq. 17) were determined for the extraction of alkali and silica from these glasses for several temperatures. In general, the values of both parameters increase as the alkali content of the glass increases (at constant temperature) and they increase as the size of the alkali ion increases (for a constant temperature and composition). The values of a range from ½ to 1 for most of the cases but in some cases a is slightly greater than 1 for the K_2O-SiO_2 glasses. Since the values of a are not precisely ½ or 1, the values for k are only apparent reaction rate constants.

Das and Douglas recognized that ½ and 1 are limiting conditions for the corrosion of glass and, "The time and temperature dependence of simple binary glasses of low chemical durability and ternary glasses of high chemical durability can be seen to fall into the same general type of process."[188]

The limiting conditions of ½ and 1 for the reaction rate exponent for the corrosion in a solution of limited volume implies that two

different mechanisms control the process. At short times the value of ½ implies a diffusion controlled mechanism while the value of 1 at long times indicates an interface controlled process.

Selective Leaching

The corrosion of binary alkali silicate glasses is the simplest case to consider. For these glasses the only glass constituent to be selectively leached are the alkali ions. An ion exchange mechanism was confirmed by Douglas and Isard[83] who calculated that without the diffusion of counter ions, the electrical double layer produced would permit 100 times less sodium to diffuse out than was observed. The ion exchange mechanism also accounts for the increase in pH of the attacking solution with time. Since H^+ (H_3O^+) ions are constantly depleted from solution as in Eq. 15, the concentration of OH^- ions must increase according to the mass balance reaction,

$$2H_2O \rightleftharpoons H_3O^+ + OH^- \qquad (62)$$

Limiting conditions result because one reaction mechanism in the chain of events becomes much slower than all of the others. One can represent a sequence of events which must occur for the extraction of any one glass constituent by the schematic in Fig. 6.

The rate of alkali leaching is controlled by the slowest of one of the following. Diffusion of H^+ (H_3O^+) ions from the bulk water to the water leached layer interface (1,2), interaction of H^+ (H_3O^+) at the water leached layer interface (3), diffusion of H^+ (H_3O^+) into

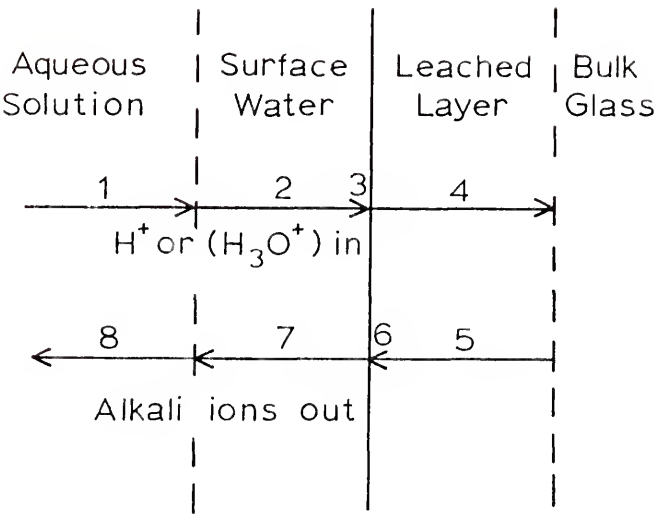

Fig. 6. Schematic representation of the processes involved in selective leaching of a binary alkali silicate glass.

the glass (4), diffusion of alkali ions (R^+) from the bulk glass to the leached layer water interface (5), solution interaction at the leached layer water interface (6), or diffusion of R^+ ions away from the glass surface into solution (7,8). Which mechanism controls the leaching of alkali ions depends on the boundary conditions of the experiment.

It is general knowledge that the leaching of alkali ions into neutral solution with low concentrations of reaction products (pH < 10, static or continuous flow test conditions) follows a root time dependence. This eliminates the possibility that the controlling step is transfer across the leached layer solution interface (steps 3,6). The controlling mechanism is, therefore, either the diffusion in the solution or in the glass. One would expect the alkali and H^+ (H_3O^+) ions to diffuse much slower in the glass than in the solution. This was confirmed by El-Shamy[189] using an "interruption test."

The procedure for this test is to first leach a glass in solution. It is then removed from the solution (interrupted) for a period of time and then reimmersed into solution. According to this test, for a process controlled by diffusion within the leached layer, the rate of leaching immediately after reimmersion is greater than prior to the interruption. The interruption provides time for the concentration gradient within the leached layer to change. A process controlled by the movement across an aqueous film has no change in the rate of leaching since there is no concentration gradient in the leached layer.

El-Shamy[189] observed an interruption point for the leaching of K^+ ions from a 15K glass at a pH of approximately 10. This is evidence that the rate determining step for dealkalization is interdiffusion within the leached layer rather than diffusion in the solution phase. Further proof of this mechanism is the fact that a leached layer forms on the surface of the glass. Therefore, for these conditions, steps 1, 2, 8 and 9 in Fig. 6 can be eliminated.

There is much ambiguity as to whether the specie diffusing into the glass to exchange for the alkali ions is H^+ or H_3O^+. It has been assumed by some[90,135] that the Na^+ ion is replaced by H_3O^+ ions since "their sizes are identical". Weyl and Marboe[190] proposed that the first step of the ion exchange process is H^+ ion penetration. It is helpful to examine the first steps of the ion exchange process in order to get an idea of which species are actually involved.

Das[90] proposed the following mechanism for the ion exchange reaction for glasses containing soda,

$$\equiv Si\text{-}O\text{-}Na^+_{g\ell} + H_3O^+_{sol} \rightleftarrows \equiv Si\text{-}O\text{---}H\text{---}O(H)_{g\ell} + Na^+_{sol} \qquad (63)$$

$$\rightleftarrows \equiv Si\text{-}O\text{-}H_{g\ell} + H_2O_{g\ell} + Na^+_{sol}$$

There is a problem if one assumes that H_3O^+ is the interdiffusing species. Since water does not exist in the molecular form in glass except as a possible diffusion species, it would react with the network to form two Si-OH groups as in Eq. 38 or 40. Therefore, for

every alkali ion replaced, there would be three Si-OH groups formed. If the surface of a binary alkali silicate with 33 mole % alkali oxide glass leaches completely, then each Si^{4+} ion would have three Si-OH groups. The continuous silica network would be destroyed and the leached layer would not exist. Since leached layers with very low Li^{+} ion concentration form on 33L[21] proton penetration is more likely.

Proton penetration is supported by hydration theory. It is known that vitreous silica hydrates by one of two processes, either proton or OH^{-} ion penetration followed by OH^{-} ion or proton migration respectively. The corrosion of glass produces a negative potential which causes protons to penetrate the surface to replace the alkali ions at $Si\text{-}O^{-}$ sites. This could be considered a hydration process since Si-OH groups are being formed. It is not like the hydration of vitreous silica, however, since it does not require the second step of hydrolysis (OH^{-} ion penetration) to preserve electrical neutrality. Therefore the "hydrolysis" of multicomponent glasses is not nearly as slow as the hydrolysis of vitreous silica.

The alkali ions which leach from the glass during the initial stages must, therefore, be replaced primarily by H^{+} ions. As the ion exchange process proceeds, the number of Si-OH groups increases. Glasses containing a sufficient concentration of H^{+} ions in the bulk or in the surface are protonic conductors. Weyl and Marboe[16] describe protonic conduction in glass as being similar to that in water. In this process protons jump from one O^{2-} ion to another without a major activation energy. The low activation energy for proton diffusion in

glass is low, being 8 Kcal/mole for a $CsO\text{-}SiO_2$ glass.[70] Further into the leached layer, close to the bulk glass it cannot be considered a protonic conductor and the H^+ ion diffusion may be low.

Ionic diffusion of alkali ions in the hydrated surface of a glass is much larger than that in a dry surface. This was demonstrated by Eisenman[191] using radioactive tracers of sodium and potassium. The mobility of sodium and potassium atoms in the hydrated surface is very large with sodium 5-10 times more mobile than potassium. In a dry surface, however, the alkalis are much less mobile with potassium 1000 times less mobile than sodium.[192]

Doremus[23] recognized that the difference in mobilities in the dry and hydrated surfaces could be due to one of two reasons. One possible reason is that the replacement of alkali ions by H^+ ions would produce a more open network for alkali ions to diffuse. Another possible reason is that some water molecules could diffuse in and react with the network producing a weakened structure through which the alkali ions could diffuse.

Eisenman[191] produced a protonated surface on a glass for which he determined the mobility of sodium atoms through the surface under dry conditions. The sodium diffusion coefficient was not larger in this protonated surface than in the bulk glass. This indicates that the much smaller H^+ ions do not produce a structure significantly more open to alkali diffusion. It appears, therefore, that it is the reaction with water that weakens the network increasing the mobility of the alkali ions. One would expect this to affect the larger K^+

ions more than Na^+ or Li^+ ions.[58] The importance of these effects can be assessed only by further work.

There is also much ambiguity as to whether the alkali ions diffusing out or the H^+ ions diffusing in limits the ion exchange process. It was assumed by Beattie[85] and others[53] that the interdiffusion process is limited by the diffusion of Na^+ ions. Baucke,[81] however, found that for a selective glass electrode the diffusion of H^+ ions controls the ion exchange process.

The structure of the leached layer is a key to understanding the ion exchange process and the overall glass corrosion process. It is the structure of the leached layer which determines the diffusion rate of each of the species important to glass corrosion. This will be discussed later.

Silica Dissolution

The ion exchange reaction has been postulated by many to be "the meahanism" of corrosion. This is not precisely true. It does qualitatively explain the leaching of alkali ions but it does not account for the dissolution of the silica network.

Douglas and El-Shamy[19] stated, "the rate of extraction of silica at any time is profoundly related to the amount of alkali in both the glass and the leaching solution; the effect of alkali ions in one cannot be separated from the effect of those in the other."[193] They conducted an experiment to show that the alkali ion concentration in solution is very important in the breakdown of the silica structure. In one test glass grains were corroded in water; in another

similar test a resin was added to remove alkali ions from solution. The concentration of silica in solution was determined to be lower in the test with the resin. It was concluded that, "Factors which are likely to affect the alkali level in the leaching solution--have a strong influence on the rate of extraction of silica from glass."[194] Douglas and El-Shamy seem to have overlooked an important point. The resin which removed Na^+ ions from solution also removed an equal number of OH^- ions.

$$(Resin)SO_2OH + Na^+ + OH^- \rightleftarrows (Resin)SO_2ONa + H_2O \qquad (64)$$

Their data indicates that the pH of the attacking solutions in both of these cases was above a value of 9. In view of their experiments which demonstrate faster silica extraction rates at values of pH > 9, it is likely that the removal of OH^- ions from solution for this test is more important than the removal of Na^+ ions. This is supported by the fact that the solubility of vitreous silica decreases[32] to a concentration of 1.0N Na^+ thereby contradicting Douglas and El-Shamy's[19] conclusion.

Douglas and El-Shamy also wrote, "The amount of silica removed from the glass or left in the glass depends on the rate of removal of alkali and not on the quantity of alkali removed."[194] This statement was based on an observation that at the late stage of corrosion (after a long time in linear time dependence) the rate at which the alkali leached and the silica was extracted decreased

and became close to zero. It may be that when the concentration of reaction products becomes as concentrated as it was in these tests the equilibrium pH is reached and this is likely to slow down the dissolution process.

Charles[40] was the first to discuss a mechanism for the aqueous attack of silica. His explanation has been widely accepted and quoted elsewhere.[195] He stated that there are two structures which are important to the corrosion of glass. The unending silica network is one and the nonbridging oxygen terminal structures associated with the alkali ions is the other. At moderate temperatures (up to 300°C) fused silica remains essentially unaltered and has a specific equilibrium concentration. On the other hand, glasses containing alkali oxides (which impart the terminal structure) undergo rather severe decomposition. He concluded that the degradation of the glass structure is dependent very much on these terminal structures. Following this reasoning he wrote equations to describe the process.

Charles recognized that at neutral pH and at moderate temperatures (less than 100°C), direct attack by water (Eq. 42) is not significant. This is demonstrated by the fact that fused quartz and quartz crystals are virtually insoluble in water.[40] He proposed that there are at least two processes involved in the silica attack which are interrelated. The attack of glass by superheated steam is triggered by the exchange of H^+ for Na^+ (alkali ions) in the glass,

$$\equiv Si\text{-}O\text{-}Na + H_2O \rightleftarrows \equiv Si\text{-}OH + Na^+ + OH^- \qquad (65)$$

To facilitate the diffusion of Na^+ ions to the surface, water dissociates, releasing a H^+ ion which penetrates the glass to satisfy the electroneutrality condition. A higher concentration of Na^+ and OH^- ions are produced on the surface.

Charles[40] said that free OH^- ions are produced by Eq. 65 which permit the important step in glass dissolution,

$$\equiv Si\text{-}O\text{-}Si\equiv + OH^- \rightleftarrows \equiv Si\text{-}OH + {}^-O\text{-}Si\equiv \qquad (66)$$

The ionized silanol group produced in this reaction is free to dissociate another surface water molecule,

$$\equiv Si\text{-}O^- + H_2O \rightleftarrows \equiv Si\text{-}OH + OH^- \qquad (67)$$

The net effect of these three reactions is an increase of the pH in the surface and broken Si-O-Si bonds. An autocatalytic effect results causing an acceleration of corrosion with time.

He said that one could be tempted to bypass the first step, Eq. 66, by writing Eq. 40 but such a reaction has little significance in glass dissolution at low pH and low temperatures since quartz and fused silica have such a low solubility in water.

Budd[196] presented a theoretical description of the mechanisms of attack by different reagents on glass. There are basically two types of attack. Electrophilic reagents attack a negative dipole such as the oxygen atoms while nucleophilic reagents attack positive dipoles

(the silicon atoms). Different reagents possess different degrees of attacking ability. The OH^- ion and O^{2-} are strongly nucleophilic while F^- ions and H_2O are moderately and weakly nucleophilic respectively. The H_3O^+ and H^+ ions are considered to be strongly electrophilic. Budd[196] used such a description to describe the attack of water on the silica network at high temperatures.

$$\equiv Si\text{-}O\text{-}Si\equiv \rightleftarrows \equiv Si^{\delta+}\cdots O^{\delta-}Si\equiv \rightleftarrows \equiv Si(OH)\text{-}Si\equiv \qquad (68)$$

One hydrogen atom of the water molecule electrophilically attacks the O^{2-} ion of the network while the oxygen atom of the water molecule nucleophilically attacks the Si^{4+} ion. Energetically Eq. 68 is the most favorable mechanism for the attack by water on the silica network[196] and it is common for organosilicon compounds at moderate temperatures (even below room temperature).[185] Without the formation of an intermediate structure it is necessary to break a Si-O-Si bond followed by the attack by water. Such a process requires a very large activation energy, 50 Kcal/mole,[197] and is very unlikely.[196]

A schematic representation of the sequence of events which must occur for the dissolution of silica appears in Fig. 7. A chemical species must diffuse through the solution to the glass surface, 1, and possibly into the glass to some extent, 3, where it reacts with the silica network (2 or 4). The new chemical species must then diffuse out of the surface, 5, and then through the solution, 6.

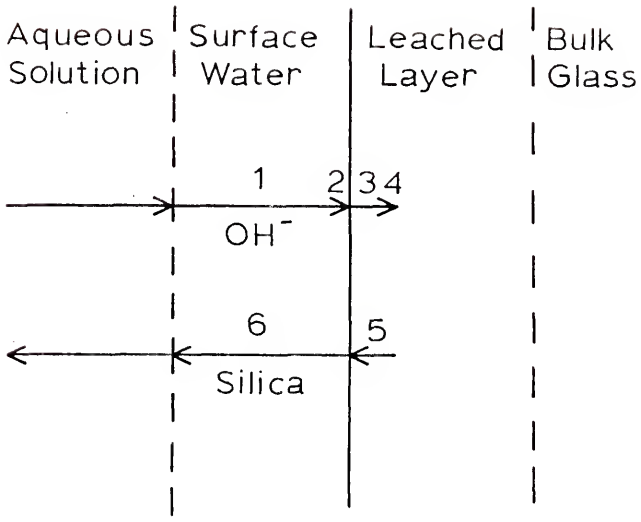

Fig. 7. Schematic representation of the sequence of events necessary for the dissolution of silica.

The rate of silica dissolution of a glass is a function of root time in acidic and neutral solution, so one of the steps 1, 3, 5 or 6 must control the process. The mobility of OH^- ions is much larger in aqueous solution than in a glass so step 3 is slower than step 1. The chemical reaction with the surface leads to the formation of complexes involving Si^{4+}, such as $Si(OH_{1-x} + Na_x) \cdot 2H_2O$.[101] These hydrated complexes are characterized by a large diffusion rate in the solution (at low concentrations) which should rapidly remove the reaction product from the surface so that a fresh surface is always exposed to the solution,[101] so step 5 is slower than step 6.

Doremus said, "A possible mechanism is that dissolution is controlled by diffusion of 'water' molecules a few molecular distances into the silica and their reaction with internal silicon-oxygen bonds."[198] This is probably not precisely correct. A process very similar to Charles' for the attack of the glass network by superheated steam,[196] probably controls the aqueous attack of glass during this stage of glass corrosion. It seems the most probable mechanism for the dissolution of the silica network in solution is, therefore, the diffusion of OH^- ions into the surface of the glass or the diffusion of silica out of the surface. The reaction with the network could be by Eq. 66 or by the combined attack of an H^+ ion (which are present from the ion exchange reaction) and an OH^- by Eq. 65. This diffusion controlled process needs experimental confirmation and will be discussed in Chapter IX.

Interfacial Reaction Controlled Mechanisms

The corrosion of glasses under static conditions (a closed system where the pH increases) results in the change of kinetics from a root time to a linear time regime for both the leaching of alkali ions (modifiers) and the extraction of silica (network formers). This indicates a change from diffusion controlled mechanisms to interfacial reaction mechanisms.

Das and Douglas[49] plotted the log of alkali and silica in solution vs. log corrosion time for several ternary glasses. They wrote, "In general, a series of gentle curves is obtained which, . . ., approach almost asymptotically a slope of ½ at very small times and 1 at large times. It can be seen, however, that over periods of one or two decades the results could be taken to lie on a straight line and thus be expressed as $Q = kt^{a}$ with a having some value intermediate between ½ and 1."[199] They explained the increase in slopes of the curves with time as being due to the development of a highly siliceous layer with channels which increase the effective surface area of the glass allowing more silica to be extracted.

Complex mechanisms and empirical relations have been derived to explain the changeover from root time dependence to linear time dependence. For instance, consider the purely empirical expression published by Douglas and El-Shamy,[19]

$$Q = a\,(t)^{\frac{1}{2}} + bt \tag{69}$$

$$\frac{d\ \log\ Q}{d\ \log\ t} = \frac{a}{2\,(t)^{\frac{1}{2}}} + b\left(\frac{1}{\frac{a}{t} + b}\right) \tag{70}$$

This expression has limiting values of 0.5 as time, t, approaches zero and a value of 1.0 as t approaches infinity. Douglas and El-Shamy explained that over limited times approximately linear plots of ℓog Q vs. $\ell og\ t$ could result and the slopes of these plots would be expected to vary from 0.5 to 1.0 as time and temperature increase. For durable commercial glasses $d(\ell og\ Q)/d(\ell og\ t)$ should usually be nearer 0.5.[19]

Doulgas and El-Shamy[19] proposed a model in which a leached layer forms on the surface of the glass and the silica dissolves at the leached layer water interface while at the same time sodium ions diffused across the leached layer from the glass into the water. They wrote, "The change from root time dependence to linear variation with time might be associated with the fact that as the time elapsed, the diffusion process would gradually slow down as the leached layer became thicker, and when these two reactionsproceeded at equal rates, the diffusion process would become one of steady state diffusion through a layer of constant thickness, although this layer was continuously progressing into the glass."[200]

The above theory is based on the conclusion that the rate at which Na^+ ions diffuse out of the glass and the rate of silica extraction slow down with time and become a linear function of time. Both Rana and Douglas[47] and Douglas and El-Shamy[19] reported such observations. Their data are reproduced in Fig. 8. If one plots all the data for 15N as $\ell og\ [Na_2O]$ vs. $\ell og\ t$ one gets straight lines with slopes close to 0.5 (Fig. 9). It is obvious that the reaction kinetics do not change at longer times as was thought.[19,47] A root time

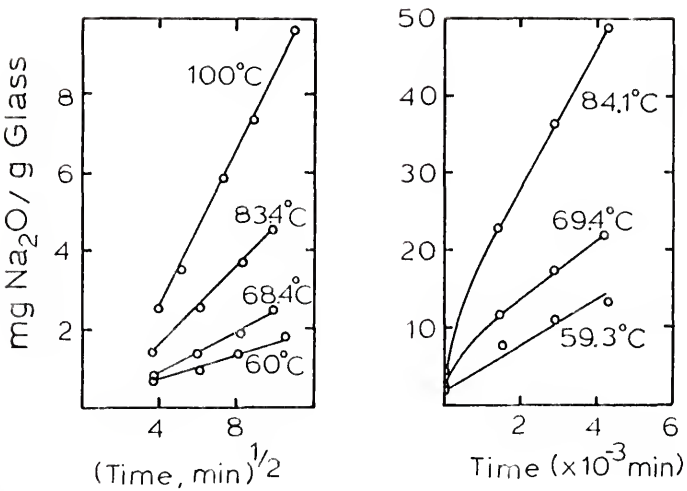

Fig. 8. Short time (A) and long time (B) data for Na^+ ions leaching into water from 15N glass grians. After Douglas and El-Shamy.[19]

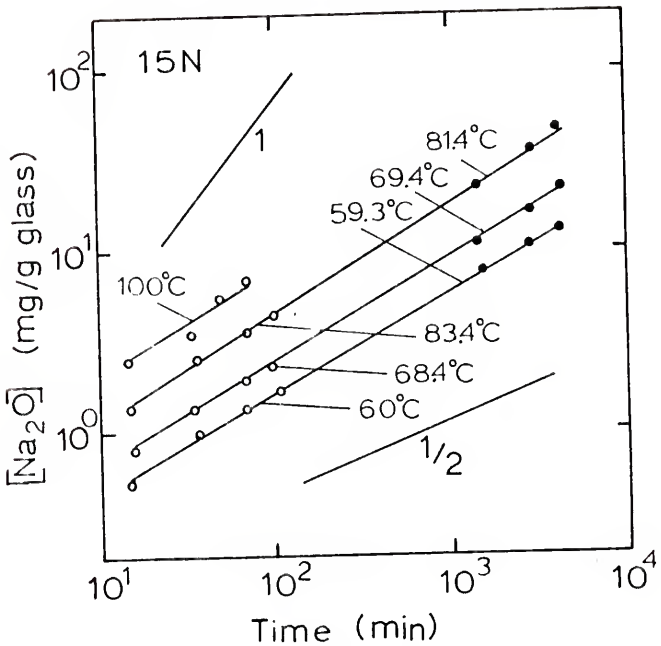

Fig. 9. Replot of Na^+ ion leaching data of Douglas and El-Shamy[19] for 15N glass grains.

dependence must, therefore, continue to control the rate of leaching of Na^+ at the longer times for this experiment. The ionization of surface silanol groups and the resulting formation of an electrical double layer at the glass solution interface at values of pH greater than 9 or 10 led Lewins[201] to postulate that the electrical double layer acts as a barrier which slows down the dealkalization process. Lewins said that the movement of the interdiffusing species across the interface becomes the rate determining step as the pH of the solution exceeds a value of about 9 or 10.[189]

The dealkalization process does slow down with time but it occurs during the root time diffusion controlled regime. For some glasses[19,42] a linear time dependence did develop for the extraction of alkali ions (indicated by a slope close to 1.0 for $\log$ [alkali ions] vs. $\log\ t$), however, an increased rate of alkali and silica extraction resulted. The limiting step described by Lewins[201] is, therefore, incorrect. Charles[40] recognized that since the corrosion rate accelerated, the diffusion process through the surface can play little part in controlling the reaction rate. The reaction rate for the extraction of alkali ions at long times (pH > 10) must be controlled by a reaction at the surface of the glass and is no longer dependent on the supply of reacting species. The increased rate of alkali leaching is, therefore, related to the increased rate of silica extraction.

As long as the silica extraction rate is slower than the rate of leaching, the leaching of alkali ions should follow $t^{\frac{1}{2}}$ kinetics. If the rate of silica extraction becomes equal to or greater than the

alkali leaching rate, the kinetics for the leaching of the alkali ions will be the same as for the silica extraction. Another objective of this dissertation is to examine the corrosion kinetics and changes in the corrosion parameters for the binary alkali silicate glasses in order to determine if the above expalnation of why the rate of alkali leaching becomes a function of $t^{\frac{1}{2}}$ at longer corrosion times is valid.

Geffcken and Berger[186] proposed a mechanism to describe the attack of the network of soda containing glasses by alkaline solutions. They described the reaction as taking place in two steps. First there is a rapid adsorption of NaOH on the glass with the subsequent dissociation of this reactant providing the activation energy for breaking the network,

$$\equiv\text{Si-O-Si}\equiv + \text{NaOH} \rightleftarrows \equiv\text{Si-O-Si}\equiv \quad (71)$$

$$\qquad\qquad\qquad\qquad\qquad\qquad\qquad\quad \text{O-H}$$
$$\qquad\qquad\qquad\qquad\qquad\qquad\qquad\quad |$$
$$\qquad\qquad\qquad\qquad\qquad\qquad\qquad\quad \text{Na}$$

$$\rightleftarrows \equiv\text{Si HO-Si}\equiv$$
$$\qquad\quad |$$
$$\qquad\quad \text{ONa}$$

Equation 71 is very similar to the reaction of water with the silica network described by Budd[196] (Eq. 68). Geffcken and Berger[186] said that Eq. 71 is slow at temperatures less than 100°C so the interfacial step is the slowest step and diffusion effects are secondary. This reaction cannot be slower than the diffusion process if this mechanism is to explain why the reaction kinetics speeds up when the reaction

controlled (t^1) mechanism takes over from the diffusion controlled ($t^{\frac{1}{2}}$) mechanism.

In an earlier section the depolymerization of vitreous silica and silica gel was discussed. This occurs at a pH > 9 and is attributed to the reaction with water. In reference to this Iler said, "The dissolution of solid silica in water involves a simultaneous hydration and depolymerization. Thus, when silica passes into solution, there must be a chemical reaction at the surface of the solid phase with water, whereby the surface layer of SiO_2 is hydrated; and then as each silicon atom with its surrounding oxygen atoms is detached from the surface, further reaction with water occurs and soluble monosilicic acid is formed."[36]

The rate of silica extraction from multicomponent glasses is also related to the pH of the solution. The change in silica extraction is related to the ionization of silanol groups in the glass surface and the production of very polarizable O^{2-} ions. The Si^{4+} ions are more easily screened by the O^{2-} ions making the need for the contrapolarized O^{2-} ions attached to another Si^{4+} ion unnecessary. The Si-O bond is therefore weakened resulting in NaOH or H_2O being sufficiently electronegative to attack the silica network in a reaction such as Eq. 73 or 65. The fact that the surface of corroded glasses is hydrated to some extent by molecular water and a high concentration of water exists at the surface accounts for why the depolymerization reaction (Eq. 65) at the surface can occur quickly and is not controlled by the diffusion of a species to the reaction site.

One would expect a sharper transition from root time kinetics to linear time kinetics if the mechanism described above occurs. The data of Bacon and Burch[130,180] obtained using bottles follows either $t^{\frac{1}{2}}$ or t^{1} kinetics precisely[46] while data obtained with powders[47,19] has $t^{\frac{1}{2}}$ and t^{1} kinetics only as limiting conditions. An objective of this dissertation is to determine how quickly the reaction kinetics change using bulk glass surfaces to eliminate the effects produced by powder tests. If a quick change in kinetics in observed at pH = 9 or 10 it will support the idea that depolymerization of the ≡Si-O-Si≡ groups involving the attack by H_2O on the ionized glass surface is the prime mechanism of network breakdown in corrosion in alkaline solution.

Objectives

The preceding review has shown that a qualitative description of many features of glass corrosion has been achieved by a number of authors. However, as indicated in the review a comprehensive theory cannot be established until several remaining questions are addressed. It is the objective of this dissertation to answer these questions and thereby establish the basis for a general theory of glass corrosion. Specific problems to be addressed are as follows:

1. Compare glass powder tests with bulk surface tests (Chapter IV).

2. Develop a method for examining the effects of varying the A/V ratio on corrosion rates (Chapter V).
3. Propose methods of long term corrosion prediction using plots of the A/V ratio (Chapter V).
4. Determine when and why $t^{\frac{1}{2}}$ kinetics change to t^{1} kinetics with static corrosion tests (Chapter VI).
5. Determine reaction rate constants for the leaching of alkali ions and for the extraction of silica (Chapter VI).
6. Describe the precise sequence of changes which occur at the corroding binary alkali silicate glass surface during the corrosion process using glass corrosion parameters (Chapter VI).
7. Determine the effect of temperature on the glass corrosion kinetics for the binary alkali silicate glasses and relate the effects to Lyle's work[46] (Chapter VI).
8. Determine if elevated temperature corrosion studies can justifiably be used to predict glass corrosion at longer times and lower temperatures (Chapter VI).
9. Examine and interpret the changes in the IRRS spectra of various binary alkali silicate glasses (Chapter VII).
10. Calculate approximate thicknesses for the leached layer on the surface of corroding glasses as a function of time (Chapter VIII).
11. Schematically describe the development of the leached layer on the surface of the different binary alkali silicate glasses and relate the shape to the rate of corrosion (Chapter VIII).

12. Determine interdiffusion coefficients for the leaching of alkali ions, compare them with the work of Das and Douglas[49] and relate them to bulk diffusion rates (Chapter IX).

13. Determine the diffusion coefficients for the rate determining species in silica extraction and propose a mechanism (Chapter IX).

and finally,

14. Describe a general theory for the corrosion of binary alkali silicate glasses (Chapter X).

CHAPTER III

EXPERIMENTAL PROCEDURE

The glasses used in this study were made from reagent grade alkali carbonates and 5.0 μm SiO_2*. Batches were melted at temperatures of 1200°C to 1400°C in covered Pt crucibles and allowed to homogenize for 24 hours. All the glasses except for 46L were cast onto graphite and pressed into a slab about 0.5 cm thick. The 46L samples were quenched on a chilled block of aluminum to prevent crystallization. The glasses were annealed for 4 hours at 475 - 500°C and furnace cooled.

The 10K and 10L samples were prepared by and obtained from Sanders.[25] A compact of 5.0 μm silica,* lithium carbonate and methyl cellulose was sintered at 1250°C and then fused with an oxyacetylene torch. The 14K samples were made by melting a mixture of potassium carbonate and 5.0 μm silica* in an Al_2O_3 crucible at 1550°C for 4 hours and furnace cooled. Samples were sliced out of the center of the solid piece of glass. The IRRS spectra of these 14K samples were identical to those reported by Sanders.[25]

---

*Min-U-Sil, Pennsylvania Glass and Sand Co.

Slabs of each glass were sliced into pieces approximately 2 x 2 x 0.5 cm. These specimens were polished from 120 grit to 600 grit with dry SiC paper. The compositions of the glasses used in this study are listed in Table XI. The number of the code for the glass corresponds to the mole % alkali oxide in the glass and the letter specifies the particular oxide (i.e. 33L = 33 mole % Li_2O with the balance SiO_2).

Glass grains of 33L glass were produced by a procedure described by Sykes.[115] Some of the 33L glass prepared as above was crushed in a porcelain mortar by hand. The crushed glass was emptied into a nest of sieves** (Lid, 4,6,10,20,45,60,100,200, tray). After a momentary shaking, the contents of the 4 sieve were returned to the mortar. The crushing procedure was continued until all the material passed through the 4 sieve. Then the nest of sieves was placed in a shaking apparatus for 1 hour. The contents on the 6, 20, 60 and 200 sieves were saved and stored in a desiccator.

Each range of grains was scoured by a method also described by Sykes.[115] First the grains which passed through the 100 mesh sieve and rested on the 200 mesh sieve (-100 + 200 M) were emptied into a mortar and dry ether was poured over the grains until they were covered. The contents were lightly scoured to break up the agglomerates. After about two minutes of scouring, the ether was decanted off quickly to remove the fine particles. Fresh ether was added and

---

**U.S. Standard Sieve Series, W. S. Tyler Co., Cleveland, Ohio.

Table XI. List of Glass Compositions Used.

Glass	Mole % Li_2O	Mole % SiO_2
10L	10	90
20L	20	80
25L	25	75
30L	30	70
33L	33	67
46L	46	54
	Mole % Na_2O	Mole % SiO_2
15N	15	85
20N	20	80
31N	31	69
38N	38	62
	Mole % K_2O	Mole % SiO_2
10K	10	90
14K	14	86
20K	20	80
25K	25	75

the procedure repeated several times. The ether was permitted to evaporate after which the grains were returned to the sieve nest and shaken for 10 minutes. The -100 + 200 M grains were collected and saved in a desiccator. This same procedure was repeated for each sieve range.

Several different types of corrosion tests were used in this study. Glass grains were corroded for some of the tests, however, most of the data collected in this investigation were obtained using the Sanders' method.[21] Some glasses were corroded using a procedure developed by Clark.[110]

One gram of grains prepared by the Sykes procedure[115] were corroded in nalgene bottles containing 50 ml of deionized water. The bottles were immersed in a water bath at 50°C and intermittently shaken. After a designated time, the solution was collected by filtering.

An approximate surface area for each particle size range was calculated. The particles were assumed to be spherical with a diameter of the average between the upper and lower mesh opening and the surface area and volume for the average particles calculated. The density of the glass was used to calculate the total surface area per gram of glass. The values are calculated and listed in Appendix B.

The Sanders' corrosion procedure[21] exposes a well characterized planar glass surface to a specific volume of solution such that the surface area of glass exposed to the volume of solution is 0.77 cm^{-1}. Teflon corrosion cells, with a cylindrical hole 0.15 cm (3/8 in.)

diameter and 0.2 cm (0.5 in) deep, were filled with deionized water and a specimen freshly abraded to 600 grit was attached over the hole in the cell with rubber bands. Several of the corrosion cells for each time were placed into sealed jars and immersed in a water bath at various temperatures. After the designated times, the corrosion cells were taken from the bath, the glass specimens were removed and the solutions were collected in polystyrene vials.

Several samples of 33L were washed with dry ether before corrosion with the Sanders' method. These samples were polished to 600 grit as above and then immersed in dry ether for 10 minutes. They were then removed from the ether, allowed to evaporate dry and stored in a desiccator until they were corroded.

The third procedure for corroding the glass specimens was developed by Clark.[110] For this procedure samples of glass about 2 x 2 x 0.5 cm were polished on all sides down through 600 grit. The sample was then suspended with a nylon basket in the corrosion solution contained in a nalgene bottle. The surface area of each sample was calculated and enough water was used to make the surface area of glass to volume of solution ratio approximately 0.0339 cm^{-1} to correspond precisely with the ratio used by Clark. The bottles were placed in a water bath at 50°C for the designated times. At various times the pH of the solution was monitored. Separate tests were run to obtain the reaction solution for elemental analysis.

Although distilled and deionized water were used for most of the tests one set of data in Chapter IV was obtained using buffered

solutions. The preparation of the buffered solutions is described in detail by Gomori.[202]

The solutions used to corrode the different glasses were analyzed for corrosion products in solution. Duotest[≠] pH papers and a pH meter[≠≠] were used to determine the pH of each test solution shortly after collection. The concentrations of alkali and silica in solution were determined by atomic emission[≠≠≠] and colorimetry[+] respectively. The detection limits and use of these analytical techniques have been described in detail elsewhere.[40,124]

Many of the glass samples corroded by the Sanders method were examined using infrared reflection spectroscopy (IRRS). After the glass samples were removed from the corrosion cells they were lightly rinsed with deionized water, blotted dry and stored in a desiccator (1 day to 1 week) until they were examined. The arrangement of the IRRS apparatus used in this study is the same as that described by Sanders, et al.[25] A Perkin-Elmer infrared spectrophotometer[*] was used with the angle of incidence of the beam set at 23° for all the spectra. The medium scan rate was used to obtain IRRS spectra over the wavenumber range of 1500 cm^{-1} to 250 cm^{-1}. A freshly abraded 33L sample was used as a standard for adjusting the absolute intensity and for precise wavenumber calibrations.

≠ Gallard-Schlesinger Chem. Mfg. Corp.

≠≠ Coleman, Metrion

≠≠≠ Beckman B

+ Hack Model 585, Hack Chemical Co., Ames, Iowa.

* Perkin-Elmer Model 467.

Samples for scanning electron microscopy[≠] and electron microprobe analysis[≠≠] were connected to aluminum mounts with silver paint and coated with approximately 100 Å of carbon. To minimize the diffusion of alkali from under the electron beam the technique devised by Clark et al.[148,149] was used. With this technique a 100 μm diameter electron beam is moved along the surface at a rate of 150 μm/min parallel to the surface of the sample.

A technique was developed by the author for determining the surface composition of corroded binary alkali silicate glasses (see Appendix C). This technique was then used in a procedure developed for determining the composition profile of thick leached layers on the surface of corroded binary alkali silicate glasses (see Appendix D).

[≠] Cambridge Stereoscan, Kent Cambridge Scientific, Inc.

[≠≠] Acton Lab., Model MS-64.

CHAPTER IV

A COMPARISON OF GLASS POWDER CORROSION METHODS WITH METHODS USING BULK GLASS SURFACES

Introduction

The corrosion behavior of glass has been studied by many investigators. Most of these studies have involved the use of powders ground to a particular range of mesh sizes.[19,44,47,54,112] Alkali leaching and silica dissolution rates for these tests have been characterized by root time ($t^{\frac{1}{2}}$) and linear time (t^{1}) limiting conditions at short and long times. As was discussed in Chapter II many complex theories have been proposed to describe the transition period between ($t^{\frac{1}{2}}$) and (t^{1}) kinetics.

Douglas and El-Shamy[19] proposed that the change from root time behavior to linear time behavior is due to the development of channels throughout the glass surface, making it more porous, effectively increasing the surface area to the attacking solution. The author proposes that the long transition region is due to a concentration cell effect and is an anamolous behavior characteristic of corrosion tests using glass grains.

By comparing the corrosion of glass grains with the corrosion of bulk glass surfaces one of the above two theories should be

confirmed to the exclusion of the other. If a long transition period is observed having $t^{\frac{1}{2}}$ and t^{1} as limiting conditions for the corrosion of glass surfaces, then the glass surface probably does form channels which increase the corrosion kinetics, confirming the Douglas - El-Shamy theory.[19] However, if a relatively short transition region results with the corrosion of bulk glass surfaces, the implication is that the long transition region observed with powders is due to the corrosion test and is not a characteristic of the glass corrosion kinetics since a bulk glass surface would also develop channels. The main objective of this chapter is to determine which mechanism is valid.

The author believes that the Sykes' method[115] of preparing glass grains without agglomerates and fine particles is the best in the literature, however, it involves washing the glass grains with ether. Since this ether treatment might affect the glass corrosion kinetics another objective is to determine if an ether treatment alters the glass corrosion kinetics.

Results and Discussion

The concentration of Li^{+} that leached into the solution for each grain size range of 33L is shown in Fig. 10. As would be expected, one gram of the smaller grains leach more Li^{+} into the 50 ml of solution than the larger grains. Nearly straight lines for the plots of $\log [Li^{+}]$ vs. $\log$ time are observed. The reaction rate exponents,

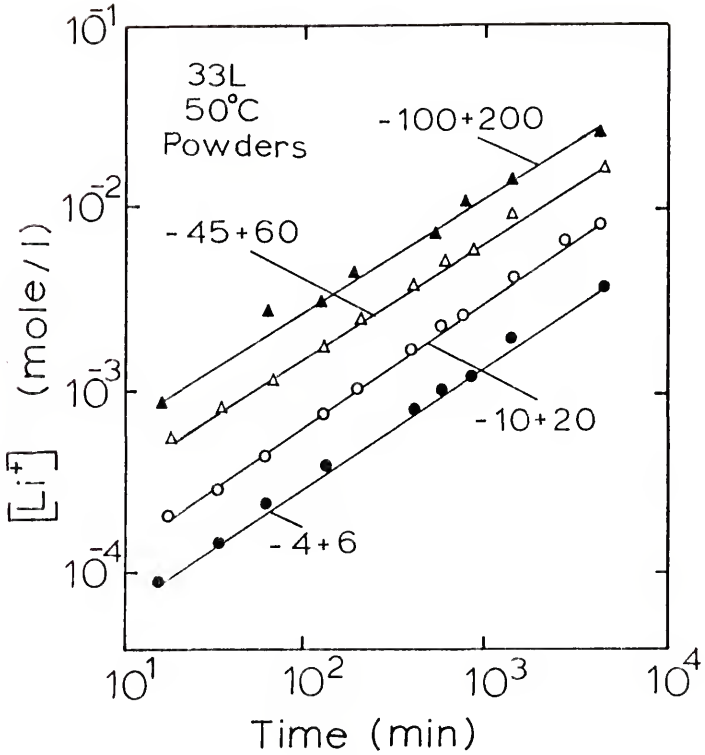

Fig. 10. *Log* concentration of Li^+ in solution (mole/l) as a function of *log* corrosion time (min) for 33L glass grains.

a, for these tests have values between ½ and 1 (see Table XII). The traditional explanation for these results is that the grains are corroding in the transition region between the two extremes ($\frac{1}{2} < a < 1$).

Figure 11 shows a plot of *log* [silica] vs. *log* time for the same series of samples. The silica dissolution behavior for each grain size range is characterized by a curve which bends gently upward with time. The reaction rate exponents, a, at 10 min are approximately ½ while at 5×10^3 min they are very close to 1 (see Table XII). In the region between the extremes $\frac{1}{2} < a < 1$.

A plot of the leaching of Li^+ and the dissolution of silica for 33L using the Sanders[21] and Clark[110] corrosion tests is shown in Fig. 12. Samples tested by the Sanders method were prepared both by freshly polishing the surface and by washing with dry ether. One can see that washing the glass surface with ether prior to corrosion has no effect on the corrosion kinetics. The reaction rate constant, a, for the leaching of Li^+ for both tests is very close to ½ ($t^{\frac{1}{2}}$ kinetics) indicating a diffusion controlled process during the period of observation. This is in contrast with the results with the powders in which the apparent reaction rate exponents, a, were between ½ and 1. The plots of the silica dissolution for these two tests are also different. For both the Sanders method and the Clark method, a is ½ at shorter times and 1 at longer times. There is a very short time for the transition between the two regions (Fig. 12).

Table XII. Reaction Rate Exponents for Corroded 33L Glass Grains.

Grain Size Range	$a^{I}_{Li^+}$	a^{I}_{Si} (t = 10 min)	a^{II}_{Si} ($t = 5 \times 10^3$ min)
-100 + 200	0.56	0.65	0.94
-45 + 60	0.62	0.55	1.03
-10 + 20	0.68	0.50	1.01
-4 + 6	0.66	0.48	0.92

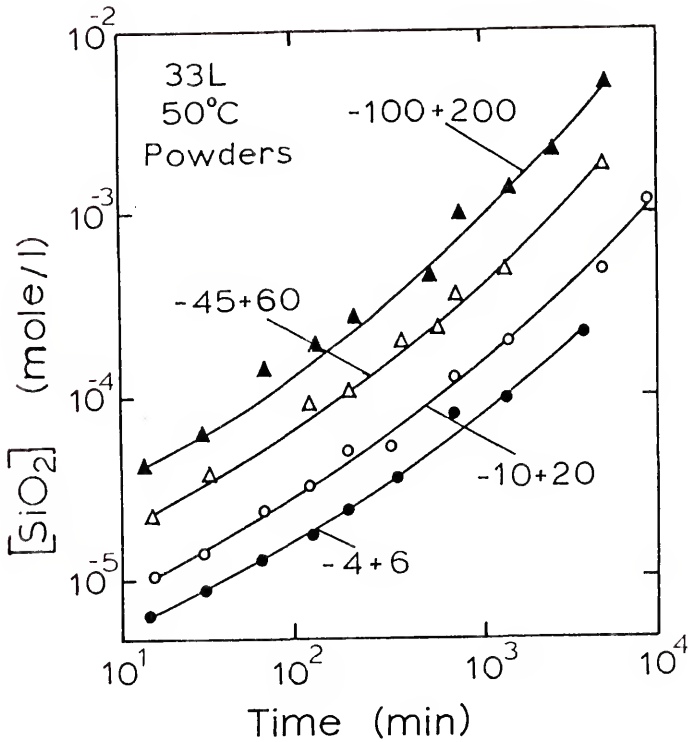

Fig. 11. *Log* concentration of silica in solution (mole/l) as a function of *log* corrosion time (min) for 33L glass grains.

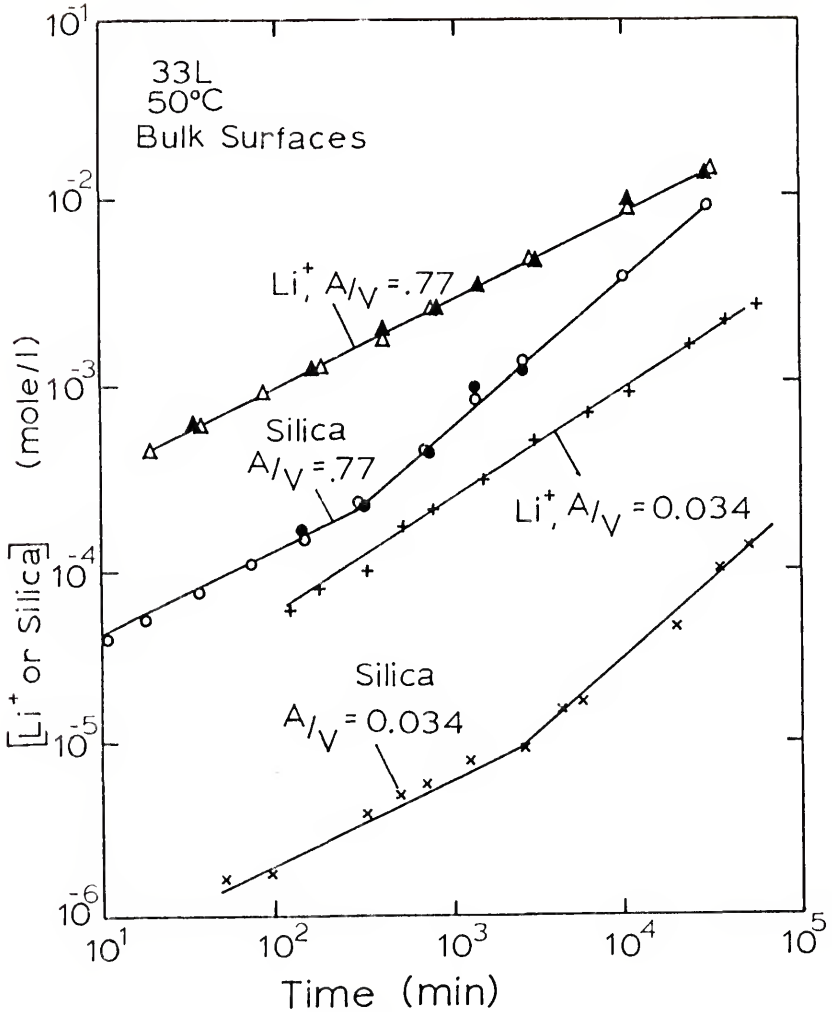

Fig. 12. Leaching of Li^+ and extraction of silica from 33L at 50°C for the Sanders method (A/V = 0.77 cm^{-1}) and Clark method (A/V = 0.034 cm^{-1}). Closed data points indicate ether treated surfaces.

The pH of the solution for each test is given in Fig. 13. Typically, the pH increases with corrosion time and the equilibrium pH at approximately 11.8 is reached with the smaller grains. One can also see that the pH at which the change from $t^{\frac{1}{2}}$ to t^{1} silica dissolution kinetics occurs at a pH of approximately 9.5.

The water corrosion results demonstrate that the theory of the transition region proposed by Douglas and El-Shamy[19] is incorrect and that the transition is an anomolous effect due to the type of corrosion test rather than the glass corrosion kinetics. As the glass grains corrode, the reaction products become concentrated between the grains, locally increasing the effective surface area of glass to volume of corrosion solution (A/V). From Fig. 13 one can see that by increasing A/V the pH of the solution increases faster. Since the silica dissolution kinetics change from $t^{\frac{1}{2}}$ to t^{1} at a pH $\approx$ 9.5, some grains are in this regime of corrosion while other grains are in the $t^{\frac{1}{2}}$ regime of corrosion. The mixture of solution from the grains undergoing the two types of corrosion behavior yields an average reaction rate exponent $\frac{1}{2} \leq a \leq 1$.

The problem with the concentration cell effects does not exist with bulk glass surface corrosion tests (i.e. Sanders[21] and Clark[110] methods). It is possible, therefore, to observe the transition from $t^{\frac{1}{2}}$ to t^{1} silica dissolution kinetics at pH $\approx$ 9.5.

One can see in Fig. 14 the effect of pH on the leaching of Li^{+} and the extraction of silica using the Clark method and buffered solutions. The reaction rate exponent for both processes is precisely $\frac{1}{2}$

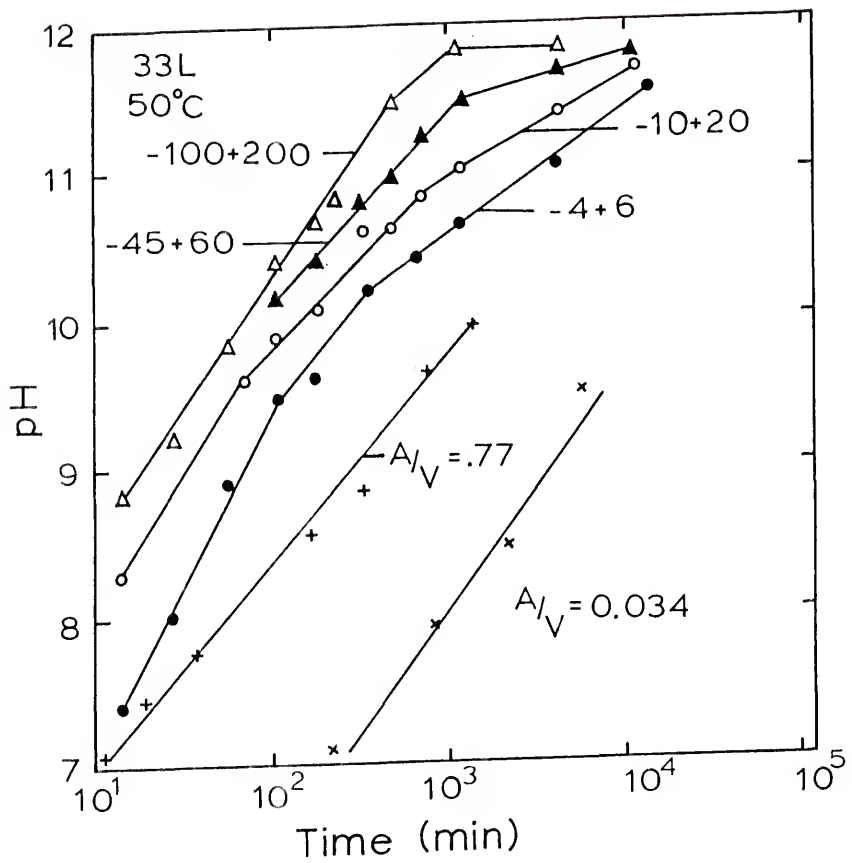

Fig. 13. The pH of the corrosion solutions as a function of *log* corrosion time (min) for 33L glass grains and for bulk glass surfaces.

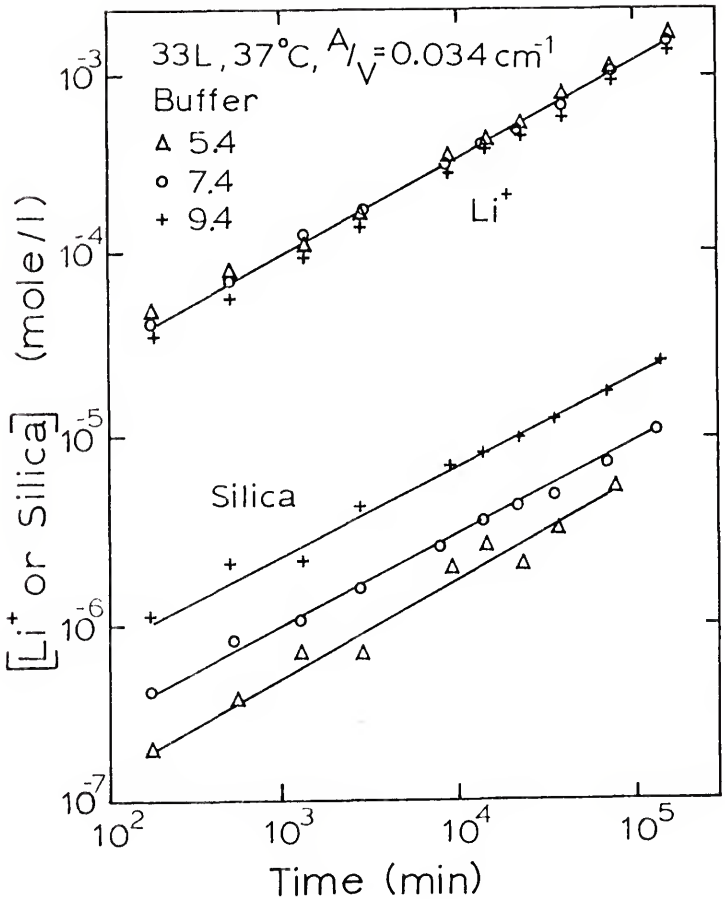

Fig. 14. Leaching of Li^+ and extraction of silica from bulk 33L glass surfaces at 37°C into 5.4 Succinate, 7.4 TAMM and 9.4 Glycine Buffer solutions.

for pH of 5.4, 7.4 and 9.4. The absolute quantities of Li^+ in solution for each of the buffers are slightly different with more Li^+ leaching out at 5.4 than at 7.4 and 9.4. These results are in agreement with Douglas and El-Shamy[19] who observed only a slight pH dependence on the leaching of alkali ions in this range of pH. The rate of silica extraction, however, is much more dependent on the pH of the solution, being greatest at 9.4, less at 7.4 and least at 5.4. Douglas and El-Shamy[19] had similar observations for 14K, but these data indicate that the pH dependence on silica extraction may vary from one glass composition to another.

Summary and Conclusions

The corrosion of glass using glass grains presents problems. Although the limiting conditions of $t^{\frac{1}{2}}$ and t^1 are observed, a long period of transition results. This has led many investigators to develop theories for a process that is the result of the testing procedure and not an actual property of the glass surface. It is demonstrated that a rapid transition from $t^{\frac{1}{2}}$ to t^1 corrosion kinetics results when a bulk 33L glass surface is corroded. The transition occurs at a time when the pH of the solution reaches approximately 9.5 or 10. When bulk glass surfaces are corroded in solutions buffered to pH of 5.4 to 7.5 precisely $t^{\frac{1}{2}}$ corrosion kinetics are observed for both the extraction of alkali and silica. These results

are proof that the transition period for corrosion of glass powders is due to concentration cell effects which locally increase the effective A/V ratio causing a rapid increase in the pH surrounding many of the glass grains. The corrosion kinetics observed for the total solution is, therefore, a mixture of the kinetics for the glass grains having $t^{\frac{1}{2}}$ kinetics with those having t^{1} kinetics.

CHAPTER V

THE RELATIONSHIP OF THE SURFACE AREA OF GLASS TO VOLUME OF SOLUTION ON GLASS CORROSION KINETICS

Introduction

As was stated in Chapter II the only papers in the literature which investigate the effect of changes in the surface area of glass to volume of solution on glass corrosion appear to conflict one another. Dimbleby and Turner[106] found that a four fold increase of the surface area (with a constant solution volume) only doubled the weight loss. El-Shamy and Douglas,[52] on the other hand, found that doubling the surface area of glass grains approximately doubled the quantity of alkali and silica extracted.

The objective of this chapter is to compare the effect of the ratio surface area of glass to volume of solution (A/V) on the corrosion of bulk glass surfaces and glass grains. A mathematical relation will be described which accounts for the discrepancy in the literature. Different ways of examining the effect of the A/V ratio are to be discussed in terms of the long term prediction of glass corrosion.

Bulk Glass Surfaces

Recall the kinetic equation used to model the leaching of glass constituents into solution,

$$Q = k_1 t^a \tag{17}$$

Since the concentration of glass constituent in solution, Q, is a function of reaction rate constant for the extraction, the surface area of the glass, A, and the volume of solution, V, Eq. 17 can be rewritten as,

$$Q = \frac{A}{V} k_2 t^a \tag{72}$$

After taking the logarithm and rearranging one obtains,

$$\log Q = \log (A/V) + \log k_2 + a \log t \tag{73}$$

For concentrations of glass constituent in solution at constant times, Eq. 73 simplifies to,

$$\log Q = \log (A/V) + c_1 \tag{74}$$

where c_1 is a constant. By plotting $\log$ Q (concentration of a glass constituent in solution at a given time) vs. $\log$ (A/V), one should

obtain straight lines with a slope of 1. The quantity of glass constituent in solution should be directly proportional to the A/V ratio, if no other effects are present.

Figure 15 is a plot of the concentration of Li^+ and silica in solution at given times vs. the A/V ratio for the bulk glass surface samples described in Chapter IV (Sanders' test A/V = .77 cm^{-1} and Clark's test A/V = 0.034 cm^{-1}). One can see that at both short times (10 min) when root time kinetics are in effect (a = ½) and at long times when linear time kinetics are in effect (a = 1) the leaching of both alkali ions and the extraction of silica have an A/V dependence with a slope of 1.

A similar relation can be derived for the time to reach a given concentration of glass constituents in solution. Rearranging Eq. 73 one obtains,

$$\log t = -\frac{1}{a} \log (A/V) + c_2 \qquad (75)$$

A plot of $\log t$ (time to reach a constant concentration of glass constituent in solution) vs. $\log$ (A/V) one should obtain straight lines with slopes equal to -2 during the root time dependent regime and -1 during the linear time regime. Figure 16 is such a plot for the extraction of silica from 33L. During the root time controlled regime (a = ½) a straight line with a slope of nearly -2 is obtained while for the linear time controlled regime (a = 1) a slope of approximately -1 is obtained for the bulk glass surfaces. These results

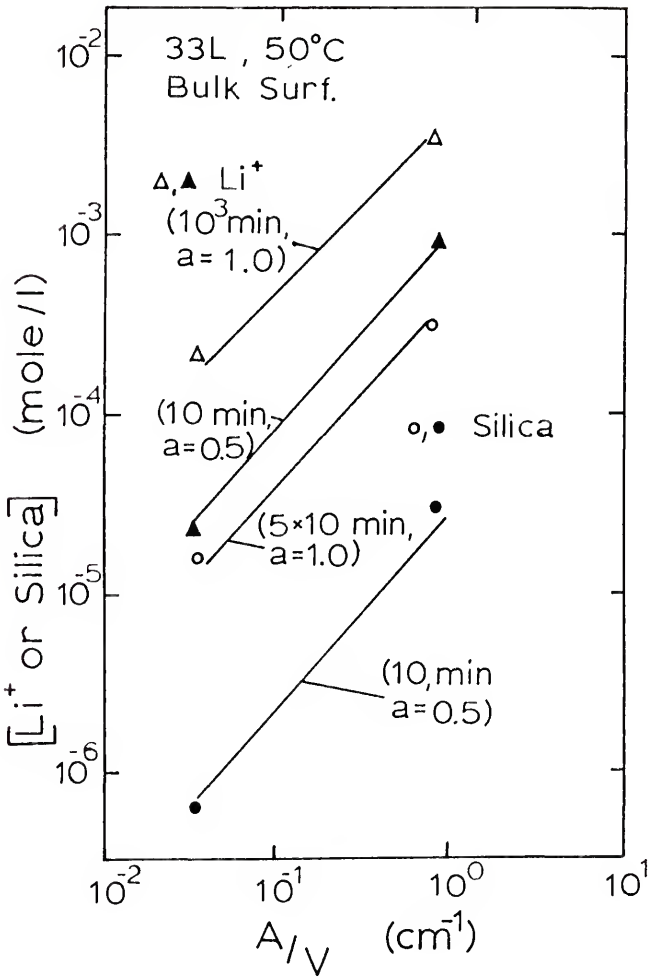

Fig. 15. Concentrations of Li^+ and silica at the given times as a function of the A/V ratio for the bulk 33L glass surfaces.

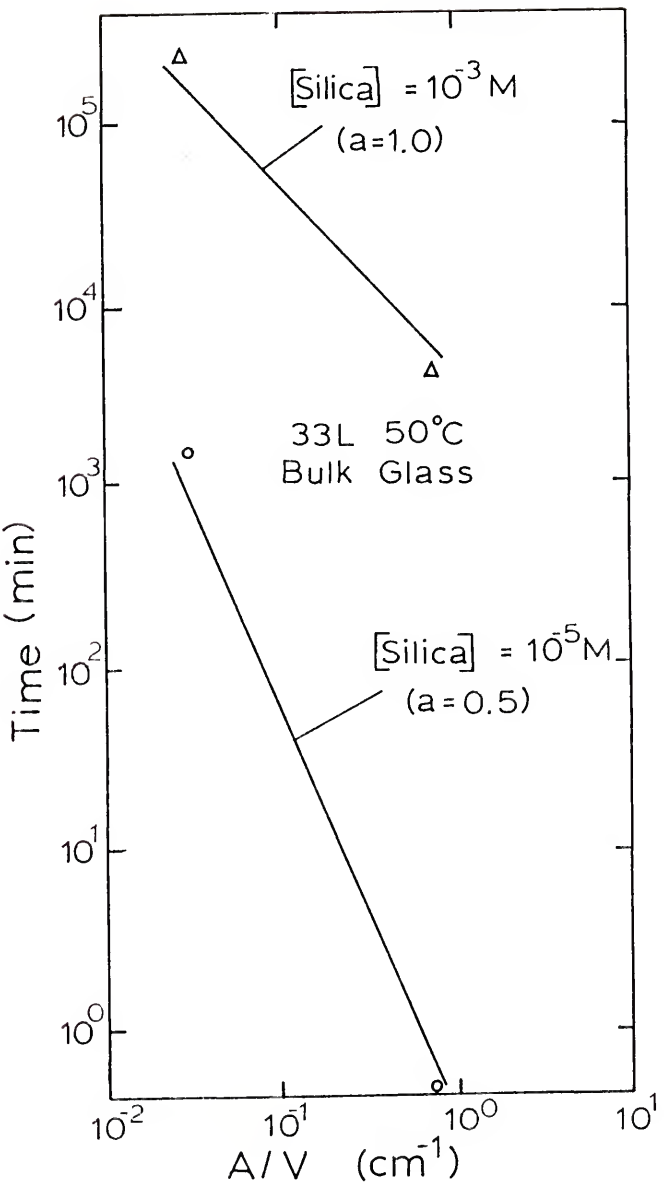

Fig. 16. Time to reach a given concentration of silica vs. the A/V ratio for bulk 33L glass surfaces.

indicate that for the bulk glass surfaces, the only effect produced by the A/V ratio is to make the extraction of glass constituents a direct proportion to the surface area of the glass.

Glass Grains

Different results are obtained if the data for the glass grains from Chapter IV is used. A plot of the concentration of silica in solution at a given time vs. the A/V ratio for the glass grains is given in Fig. 17. At short times during the root time regime ($a = \frac{1}{2}$) a straight line (A/V) relation with a slope of $\frac{1}{2}$ results. At longer times during the linear time regime ($a = 1$) a straight line with a slope of 1 is obtained. Figure 18 is a plot of $\ell og\ t$ (time to reach a constant concentration of glass constituent in solution) vs. ℓog (A/V) for the glass grains corroded in the previous chapter. The data at both a low silica concentration (10^{-5} mole/l, short times) and that at a higher concentration (10^{-3} mole/l, long times) have slopes approximately equal to -1.

The data in Figs. 17 and 18 do not agree with Eqs. 74 and 75, however, they do agree with the results of the previous investigators. During the $t^{\frac{1}{2}}$ regime a four fold increase in the A/V ratio doubles the quantity of silica in solution, in agreement with Dimbleby and Turner.[106] During the t^{1} regime, however, the quantity of glass constituents in solution (at a given time) is directly proportional to the A/V ratio, in agreement with the results of El-Shamy and Douglas.[52]

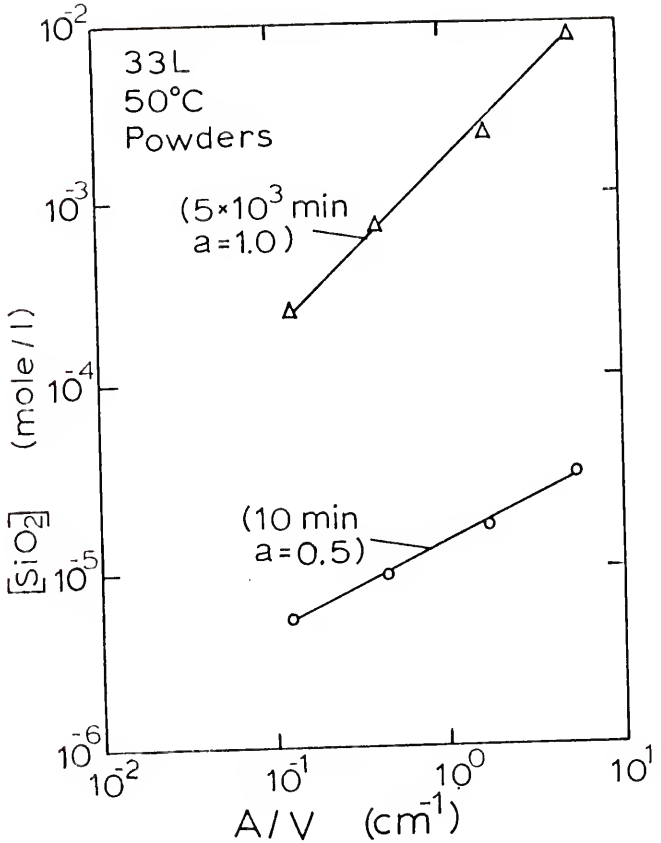

Fig. 17. Concentrations of silica in solution at given times (10 min and 5 x 10^3 min) vs. A/V ratio for 33L glass grains.

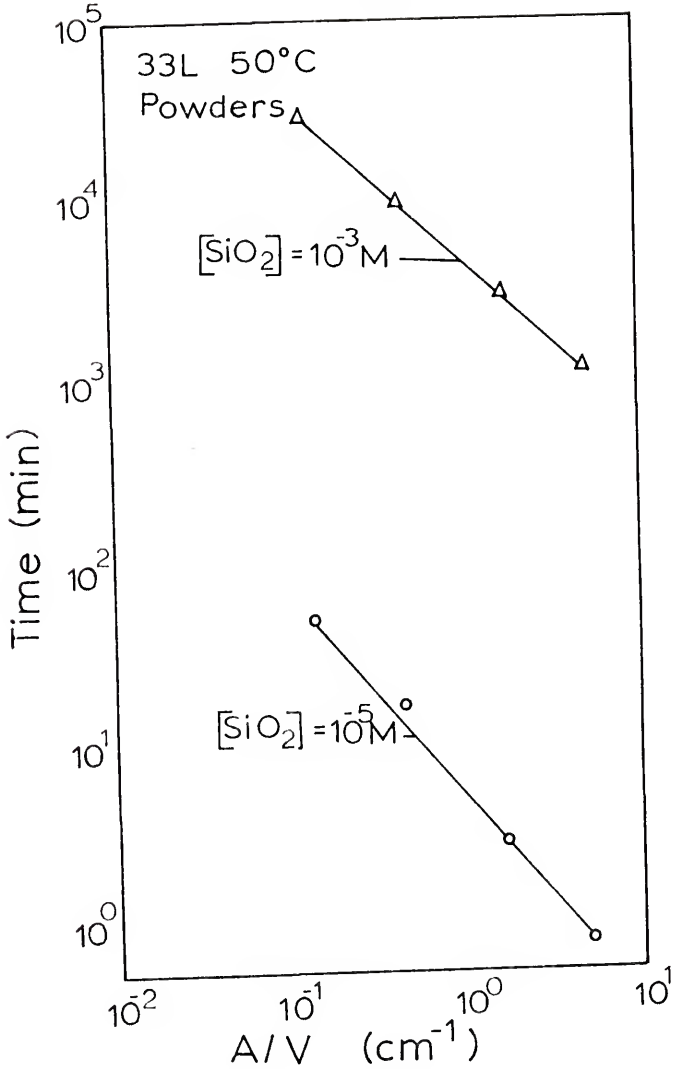

Fig. 18. Time to reach a given silica concentration in solution (10^{-5} mole/l and 10^{-3} mole/l) vs. A/V ratio for 33L glass grains.

The above results for glass grains indicate that the A/V ratio can have an effect on the corrosion process. If one assumes that the A/V ratio does affect glass grain corrosion, a new kinetic equation can be written,

$$Q = k_3 (A/V)^b t^a \tag{76}$$

After taking logarithms and rearranging one gets,

$$\log Q = b \log(A/V) + \log(k_3 t^a) \tag{77}$$

For the concentration of glass constituent in solution at a given time,

$$\log Q = b \log(A/V) + c_3 \tag{78}$$

Equation 78 indicates that the quantity of glass constituent in solution for a given time is related to the A/V ratio by the factor b. The slope of the line in Fig. 17 obtained from short time data ($t^{\frac{1}{2}}$) is 0.5 while that for the long time data (t^1) is 1.0. This indicates that $b = a$.

A similar relation can be derived for an expression between the time to reach a constant concentration of silica. Rearranging Eq. 77 yields,

$$\log t = -\frac{b}{a} \log (A/V) - \frac{1}{a} \log \frac{Q}{k_3} \tag{79}$$

For times to reach a constant concentration of glass constituent in solution this equation becomes,

$$\log t = -\frac{b}{a} \log (A/V) + c_4 \tag{80}$$

The lines for both the short times and long time data have slopes of -1. Again the experimental evidence indicates that $b = a$.

These results indicate that the corrosion of glass grains is dependent on the A/V ratio in some way. It was mentioned in Chapter II that the corrosion of glass grains is complicated by the fact that the surface area of the glass grains decreases with time and is also a function of time. This is confirmed by the above results. Therefore, a relation in which the A/V ratio is a function of time must be included in the kinetic equation for the corrosion of glass grains,

$$(A/V) = k_5 \cdot f(t^b) \tag{81}$$

$$Q = k_5 \cdot f(t^b) \cdot t^a \tag{82}$$

Prediction of Glass Corrosion

The data from bulk glass surfaces for the time to reach a particular extent of corrosion vs. A/V yield straight lines with predictable slopes. This type of representation of the data appears

to offer a means of predicting glass corrosion at different A/V ratios. In principle, one should be able to increase the A/V ratio in a corrosion test and be able to predict the time to reach a similar extent of corrosion for service conditions at longer times and at lower A/V ratios. Because of the very large A/V ratios attainable with glass grains, they offer the greatest potential for predicting corrosion to very long times. This can only be realized, however, when the factors affecting the A/V ratio for glass powders are properly treated. It may be possible to predict the corrosion of glasses for ten orders of magnitude longer time than the test conditions by using very small powders. The usefulness of these techniques as predictors of glass corrosion can be assessed only by further work.

Summary and Conclusions

It is shown that for bulk glass surfaces, the quantity of glass constituent in solution at a given time is directly proportional to the A/V ratio of the test. The time to reach a given concentration of glass constituent in solution for varying A/V ratios depends, however, on the reaction rate exponent, a.

Tests with glass grains, on the other hand, indicate that the quantity of glass constituent going into solution and the time to reach a given concentration of glass constituent in solution for varying A/V ratios depend on the conditions of the test. The results of

varying the A/V ratio on the time to reach a constant concentration of glass constituent in solution or the concentration of a glass constituent in solution are explained as being due to the time dependence of the A/V ratio for glass grains.

A new way of predicting glass corrosion is proposed in which the logarithm of the time to reach a particular extent of corrosion is plotted vs. the logarithm of the A/V ratio. Test conditions at large A/V ratios and short times can be used to predict the extent of corrosion at longer times and smaller A/V ratios.

CHAPTER VI

KINETICS OF STATIC CORROSION OF BINARY ALKALI SILICATE GLASSES I. SOLUTION DATA

Introduction

Douglas and El-Shamy[19] investigated the corrosion of binary alkali silicate glasses. Their corrosion procedure, however, involved the use of glass grains. In Chapter IV it was demonstrated that the use of glass grains to study glass corrosion is inferior to the corrosion of bulk surfaces for several reasons. In fact, tests with glass grains effectively increase the A/V ratio, speeding up the corrosion kinetics of some of the grains producing results which are not typical of the corrosion processes for a bulk glass surface. Because of this, the reaction rate constants calculated by Douglas and El-Shamy are only apparent reaction rate constants. An objective of this chapter is to reexamine the corrosion of the binary alkali silciate glasses using the Sanders' method[4] and to calculate true reaction rate constants for these glasses.

As was stated in Chapter II the only way to truly accelerate a corrosion test of a glass is to increase the corrosion temperatures. Lyle[46] approached this problem empirically and derived an equation relating corrosion time and temperature, Eq. 44. Weyl and Marboe,

however, stated that it is illogical to do glass corrosion studies at temperatures at 100°C when a glass is to be used at room temperature.[16] Another objective of this chapter will be to examine the corrosion behavior of a couple of glasses at three temperatures to determine if accelerated corrosion studies at higher than service temperatures are valid tests.

Corrosion parameters can be calculated from solution data which permit the indirect observation of changes at the corroding glass surface. The two most useful parameters alpha and epsilon were discussed in Chapter II. A third objective of this chapter is to determine the sequence of events occurring at the glass surface in more detail than the hypothetical sequence described by Sanders and Hench[21] for glasses in the three glass systems.

Results

The concentrations of alkali and silica in solution were obtained as a function of corrosion time. The leaching of alkali into solution for the three systems is shown in Figs. 19, 20 and 21. As was expected, the glasses with larger concentrations of alkali oxide are more reactive, leaching much more alkali ions into solution for any given time period. Two distinct regions of leaching are observed. At short times the graphs of $\log [A^+]$ vs. $\log t$ have a slope of ½ (e.g. $t^{\frac{1}{2}}$ kinetics). Although this is not observed for the 38N and 15K glasses it is

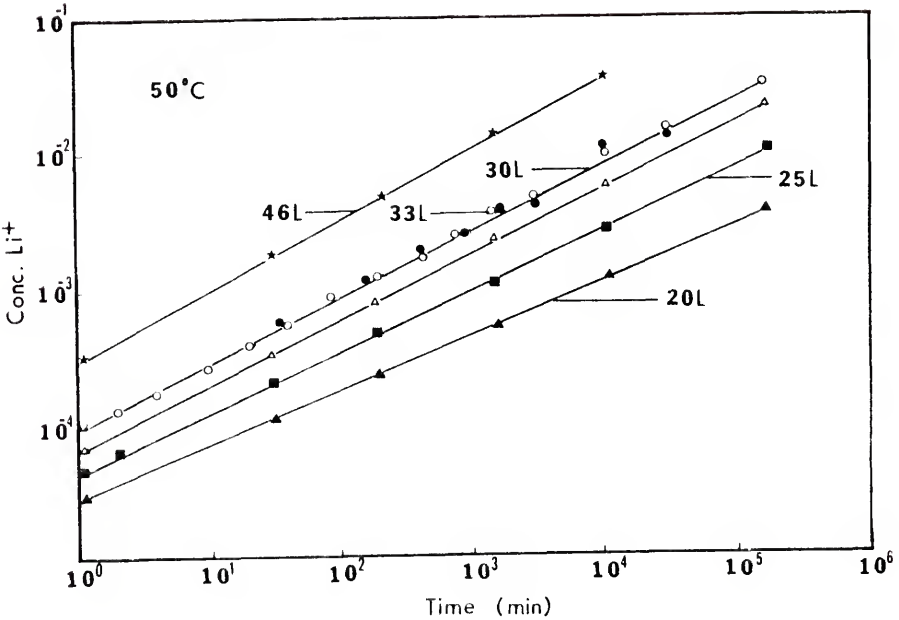

Fig. 19. *Log* Li^+ concentration (mole/l) as a function of *log* corrosion time (min) for various Li_2O-SiO_2 glasses.

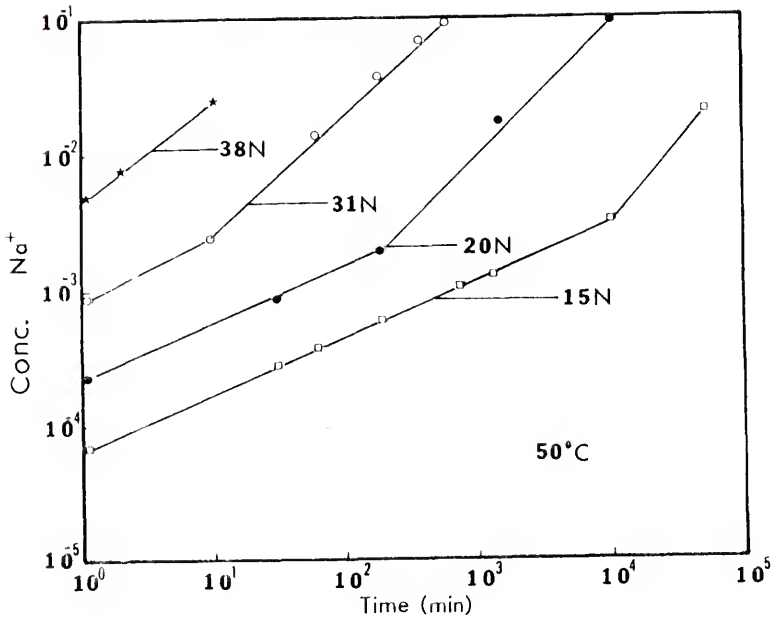

Fig. 20. *Log* Na^+ concentration (mole/l) as a function of *log* corrosion time (min) for various glasses in the Na_2O-SiO_2 system.

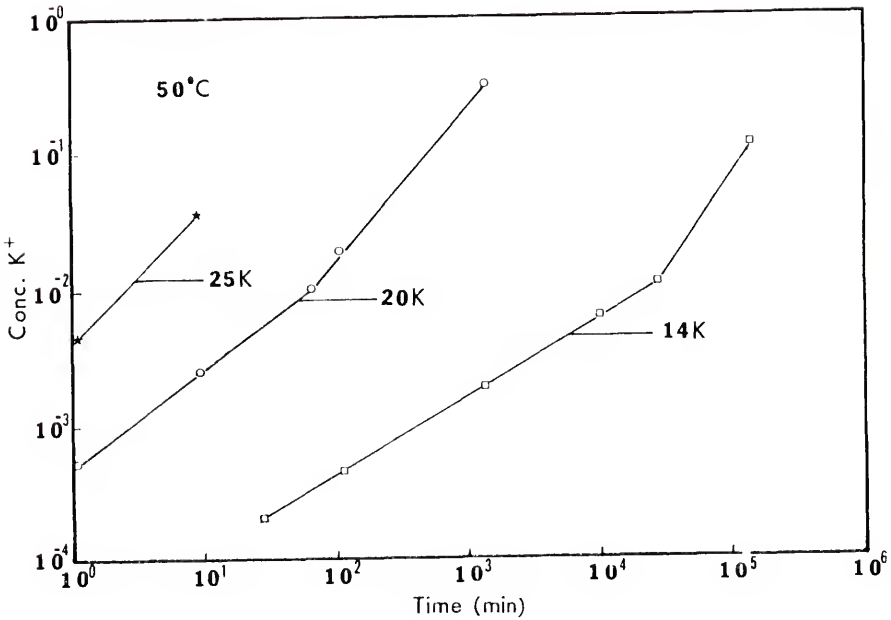

Fig. 21. *Log* K^+ concentration (mole/l) as a function of *log* corrosion time (min) for various K_2O-SiO_2 glasses.

probably due to even the shortest sampling time being too long to observe the $t^{\frac{1}{2}}$ regime. At longer times the slope changes rather abruptly to a value approximately equal to 1 (e.g. t^1 kinetics). Glasses in the Li_2O-SiO_2 system are sufficiently durable that the changeover from $t^{\frac{1}{2}}$ to t^1 kinetics does not occur under these conditions.

The extraction of silica into solution also has a distinct transition from $t^{\frac{1}{2}}$ to t^1 kinetics (see Figs. 22, 23 and 24). The transition for silica occurs at a shorter time than is observed for the leaching of alkali ions and is observed even in the Li_2O system. Within each system the time for the transition from $t^{\frac{1}{2}}$ to t^1 kinetics occurs at higher concentrations of silica in solution for glasses with less alkali oxide in the bulk glass, see Fig. 25a. However, the transition for the extraction of silica occurs within a narrow range of alakli concentrations for each of the three alkali silicate systems, see Fig. 25b.

Two corrosion parameters (alpha and epsilon) were calculated from the solution data. Plots of alpha vs. *log* time for each system are shown in Figs. 26, 27 and 28. For the Li_2O-SiO_2 system (Fig. 26) a relatively constant value for alpha is observed until the time at which the transition from $t^{\frac{1}{2}}$ to t^1 kinetics for silica dissolution occurs. The value for alpha begins to increase at this time and for 46L it reaches a value of one at approximately 1×10^4 min. The trend for the Na_2O- and K_2O-SiO_2 systems is similar. The reaction kinetics for the 25K glass, are so fast, however, that the value for

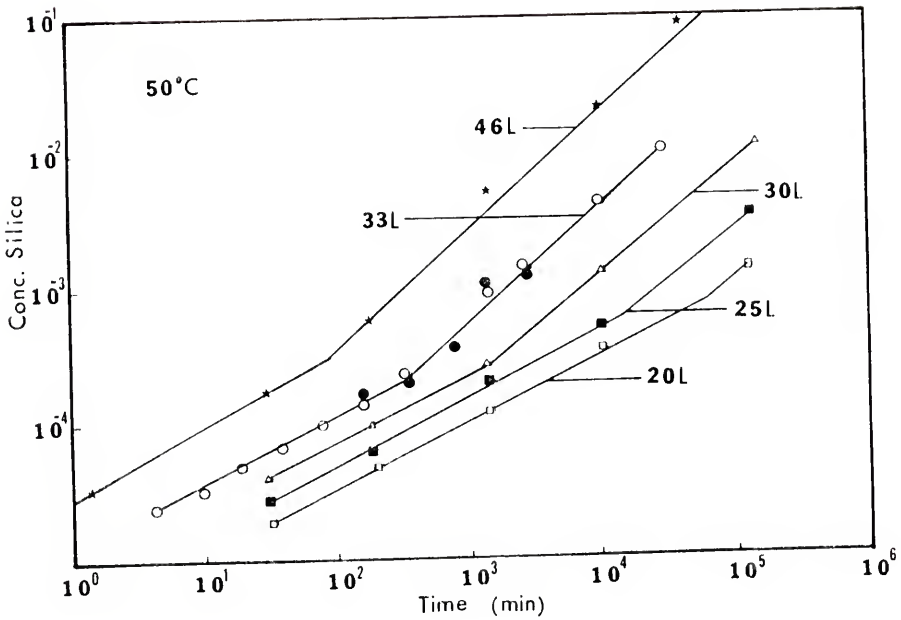

Fig. 22. *Log* silica concentration (mole/l) as a function of *log* corrosion time (min) for various glasses in the Li_2O-SiO_2 system.

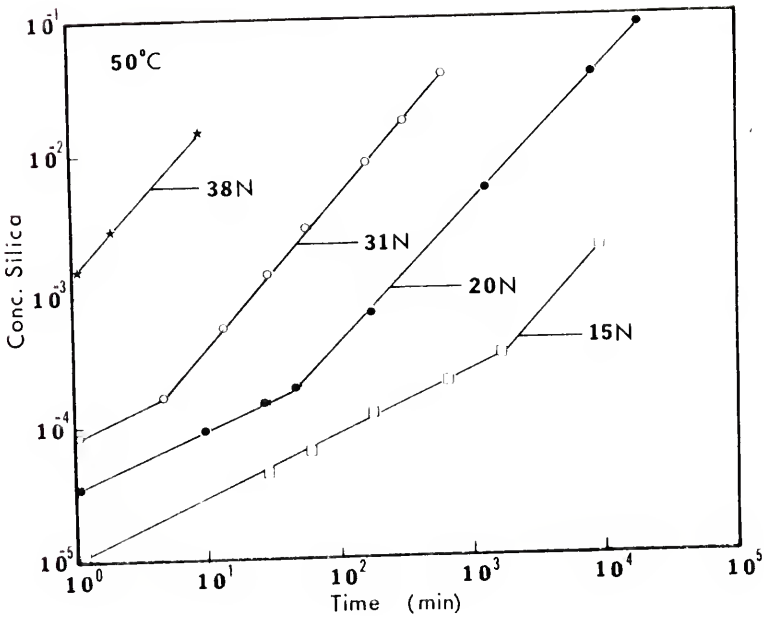

Fig. 23. *Log* silica concentration (mole/l) as a function of *log* corrosion time (min) for various glasses in the Na_2O-SiO_2 system.

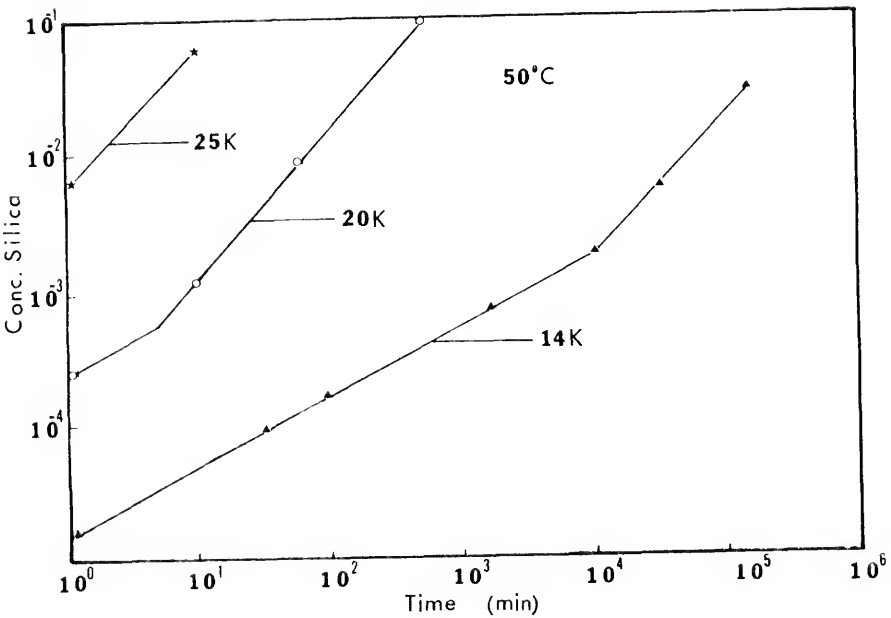

Fig. 24. *Log* silica concentration (mole/l) as a function of *log* corrosion time (min) for various glasses of the K_2O-SiO_2 system.

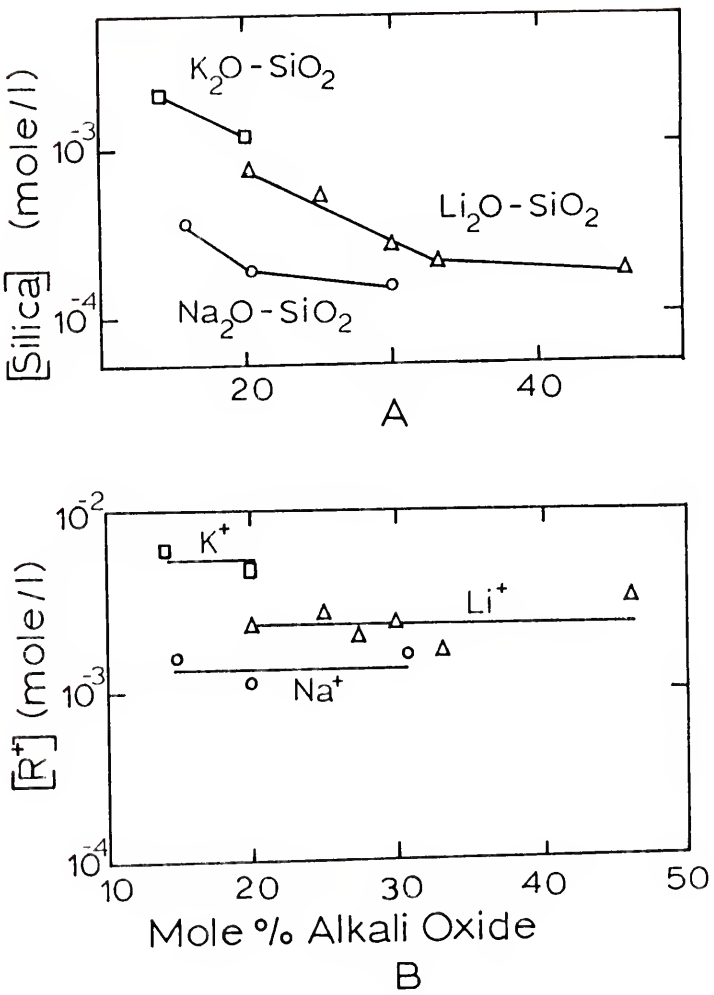

Fig. 25. Concentrations of alkali and silica in solution at the time when the silica dissolution kinetics change from $t^{\frac{1}{2}}$ to t^1 dissolution behavior.

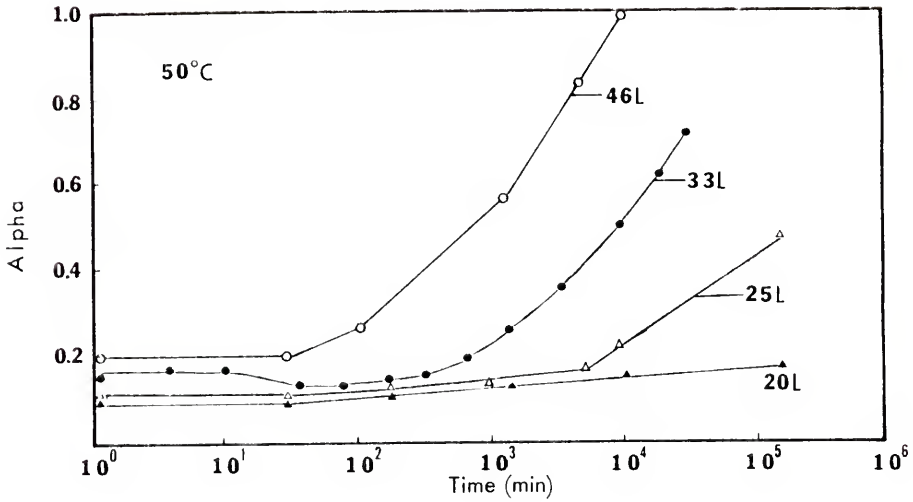

Fig. 26. Alpha as a function of *log* corrosion time (min) for various glasses of the Li_2O-SiO_2 system.

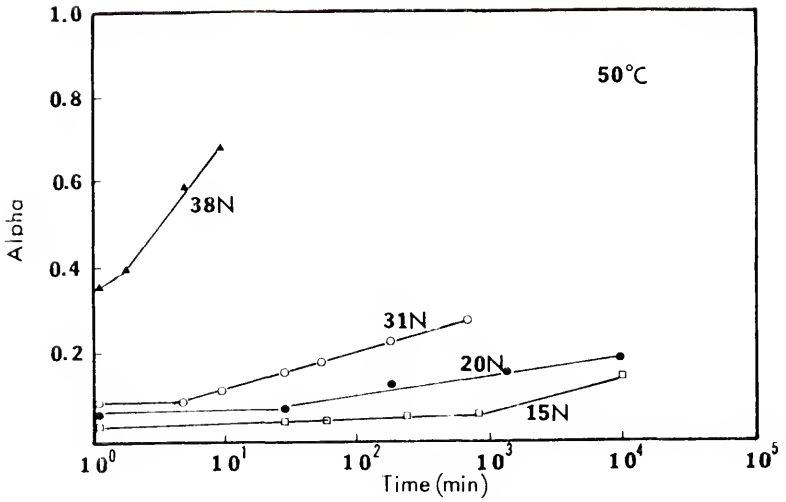

Fig. 27. Alpha as a function of *log* corrosion time (min) for various glasses of the Na_2O-SiO_2 system.

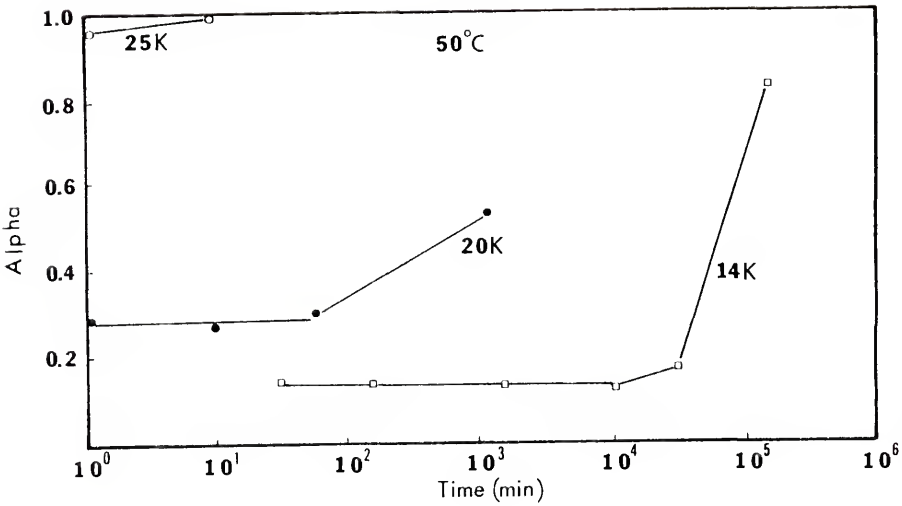

Fig. 28. Alpha as a function of *log* corrosion time (min) for various glasses of the K_2O-SiO_2 system.

alpha becomes equal to 1.0 at a very short time. In general, for the more durable glasses in each system the reaction kinetics are slow enough that relatively constant values of alpha between zero and 0.2 are observed. Alpha remains constant until the transition from $t^{\frac{1}{2}}$ to t^{1} kinetics for silica dissolution occurs. At this time alpha begins increasing and for the less durable glasses alpha is observed to approach a value of one at longer times.

The effect of temperature on the sequence of changes in alpha is shown for 33L and 46L in Figs. 29 and 30 respectively. Increasing the temperature merely speeds up the kinetics so that the sequence of events described above occur at shorter times.

Graphs of epsilon vs. time for the three systems are shown in Figs. 31, 32 and 33. The Li_2O-SiO_2 system (Fig. 31) demonstrates the various types of corrosion behavior that are seen with all three systems. The glasses 20L, 25L and 30L have slow enough reaction kinetics such that epsilon increases within the entire observation period. The more reactive glasses, 33L and 46L, however, reach a maximum value of epsilon. For 33L, epsilon increases up to 10^4 min after which it becomes approximately constant. The most reactive Li_2O-SiO_2 glass tested, 46L, has an epsilon which increases for approximately 7×10^2 min at which time a maximum for epsilon is attained. At longer times epsilon decreases and becomes zero at approximately 10^4 min (at the same time that alpha = 1).

Figure 32 shows values for epsilon for glasses in the Na_2O-SiO_2 system. The value of epsilon increases to very large values but at

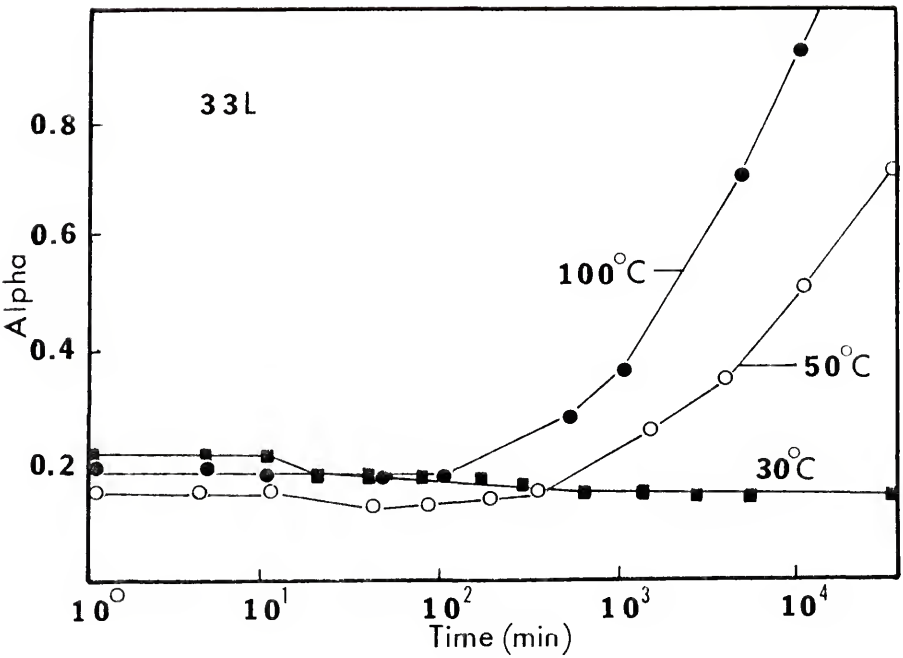

Fig. 29. Alpha as a function of *log* corrosion time (min) for 33L corroded at 30°C, 50°C and 100°C.

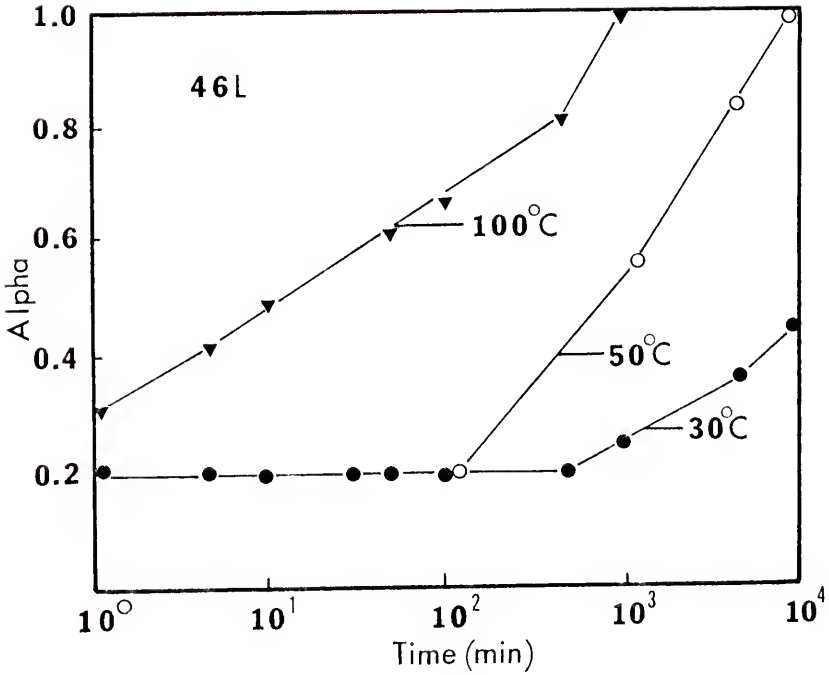

Fig. 30. Alpha as a function of *log* corrosion time (min) for 46L corroded at 30°C, 50°C and 100°C.

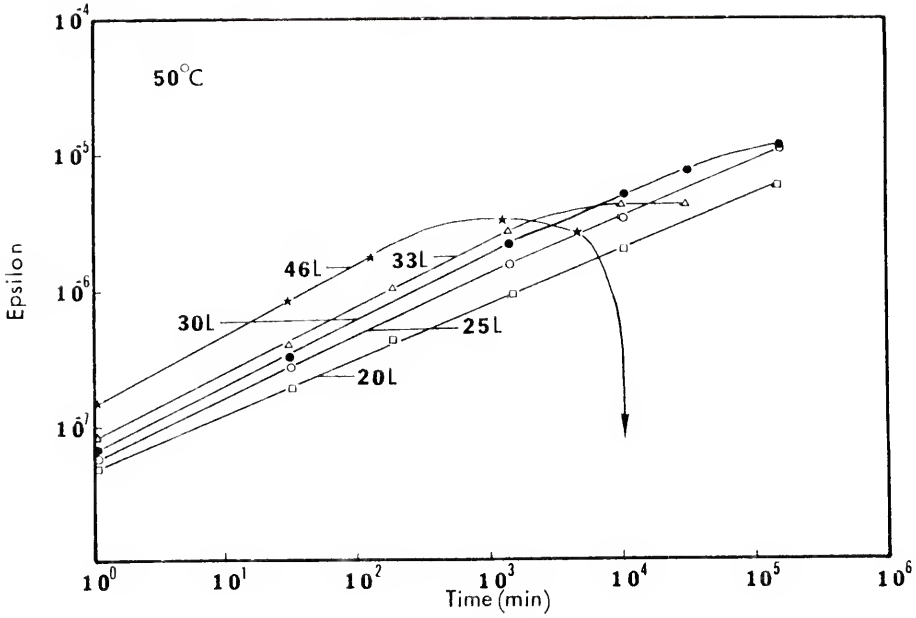

Fig. 31. *Log* epsilon (mole silica/cm^3) as a function of *log* corrosion time (min) for various glasses of the Li_2O-SiO_2 system.

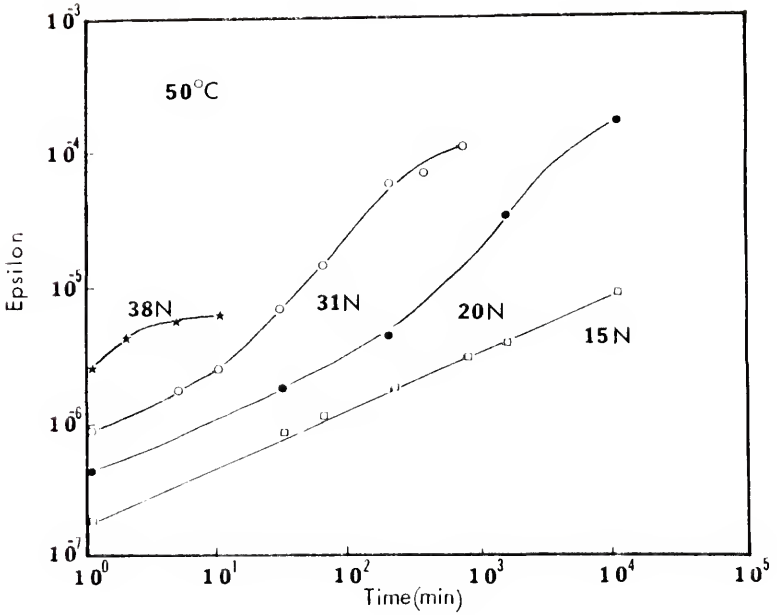

Fig. 32. *Log* epsilon (mole silica/cm^3) as a function of *log* corrosion time (min) for various glasses of the Na_2O-SiO_2 system.

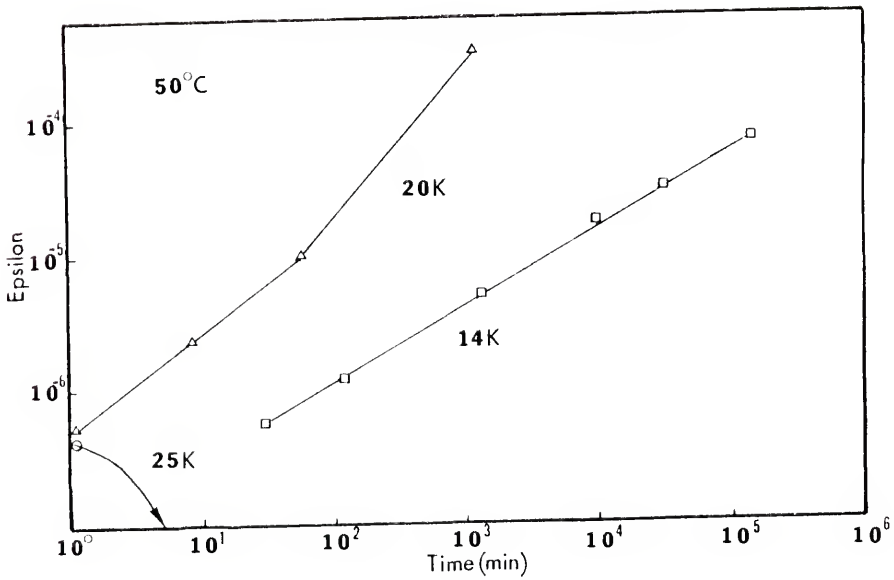

Fig. 33. *Log* epsilon (mole silica/cm^3) as a function of *log* corrosion time (min) for various glasses of the K_2O-SiO_2 system.

long times it appears to be approaching a maximum value for 20N and 31N. The 38N glass has a maximum value for epsilon at a very short time. The K_2O-SiO_2 glasses have very large values for epsilon. In the observed time period epsilon continues to increase for 14K and 20K, however, for the 25K sample the observation time is too short to observe the increase in epsilon and a maximum epsilon value so that only a decreasing epsilon is observed which asymptomically approaches zero at approximately 10 min.

Since increasing the corrosion temperature speeds up the corrosion kinetics, it makes the sequence of changes in epsilon described above occur at shorter times. For 33L corroded at 50°C the value of epsilon reaches a maximum value at approximately 10^4 min. When the temperature is increased to 100°C (see Fig. 34), epsilon reaches a maximum more than an order of magnitude sooner than at 50°C after which it decreases rapidly to zero at approximately 10^4 min. Similarly for 46L (Fig. 35) both the maximum value of epsilon and the point at which it becomes zero occur an order ot magnitude sooner at 100°C than at 50°C. At 30°C, however, a maximum epsilon is not observed for 46L even after 5×10^4 min because of the much slower reaction kinetics at the lower temperature.

Discussion

In Chapter IV it was observed that separate $t^{\frac{1}{2}}$ and t^1 rate dependent regions with a very short transition region could be

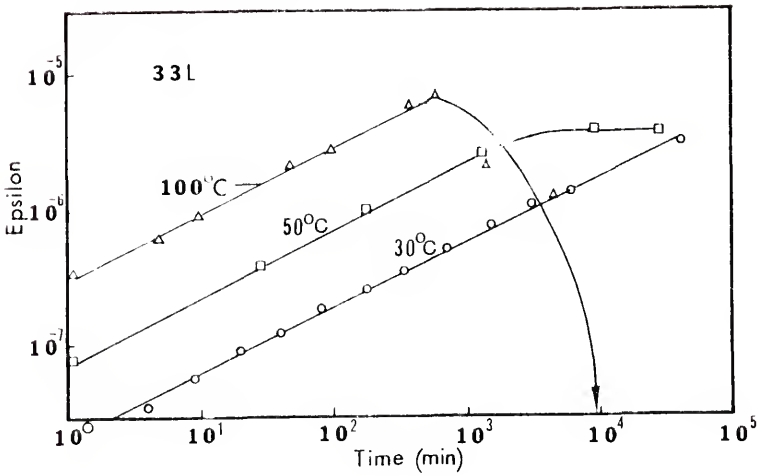

Fig. 34. *Log* epsilon (mole silica/cm^3) as a function of *log* corrosion time (min) for 33L corroded at 30°C, 50°C and 100°C.

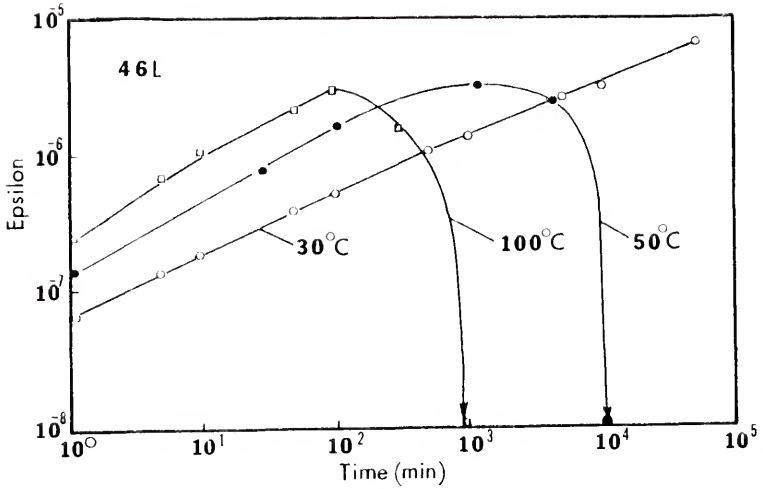

Fig. 35. *Log* epsilon (mole silica/cm^3) as a function of *log* corrosion time (min) for 46L corroded at 30°C, 50°C and 100°C.

distinguished for 33L glass corroded using bulk glass surfaces. In this chapter, the data for the leaching of alkali ions and the extraction of silica into solution confirm this observation. From the slopes of the plots of *log* [silica] vs. *log* time (Figs. 22, 23 and 24) the reaction rate exponents, a, were calculated and are listed in Table XIII. The slopes at shorter times with values approximately equal to 0.5 are designated as a_{Si}^{I}, since they are the reaction rate exponents for the extraction of silica during the first corrosion mechanism ($t^{\frac{1}{2}}$ dependence, see Chapter II). The lines with steeper slopes at longer times are designated as a_{Si}^{II}, since they correspond to the reaction rate exponents for silica extraction during the second corrosion mechanism (t^{1} dependence, see Chapter II). Within experimental error the calculated values for a_{Si}^{I} are approximately equal to 0.5 while those for a_{Si}^{II} are approximately equal to 1.0. These data confirm that for the extraction of silica, the first mechanism, at short times is diffusion controlled while the second mechanism at longer times is controlled by an interfacial reaction mechanism.

The leaching of alkali ions from the glass also has a transition from a $t^{\frac{1}{2}}$ dependence to a t^{1} dependence demonstrated by the reaction rate exponents. These values are also tabulated in Table XIII. The transition for the leaching of alkali ions occurs after the transition for the extraction of silica, however, by an order of magnitude in time (see Table XIV).

Reaction rate constants, k in Eq. 17, for the leaching of alkali, $k_{A^+}^{I}$, and the extraction of silica, k_{Si}^{I}, during the diffusion controlled

Table XIII. Reaction Rate Exponents for the Extraction of Silica and Alkali at Short Times During Mechanism I, a_{Si}^{I} and $a_{R^+}^{I}$, and at Longer Times During Mechanism II, a_{Si}^{II} and $a_{R^+}^{II}$.

Glass	a_{Si}^{I}	a_{Si}^{II}	$a_{R^+}^{I}$	$a_{R^+}^{II}$
20L	0.50	--	0.40	--
25L	0.50	--	0.44	--
30L	0.50	0.90	0.49	--
33L	0.51	0.94	0.48	--
46L	0.51	0.96	0.52	--
15N	0.45	1.02	0.41	1.01
20N	0.45	1.04	0.42	0.98
31N	0.46	1.10	0.42	0.93
38N	--	1.03	--	0.77
14K	0.50	1.05	0.56	1.10
20K	--	1.11	0.62	1.11
25K	--	1.10	--	0.98

Table XIV. Times for the Transition from Mechanism I to Mechanism II at 50°C for the Leaching of Alkali Ions $t_{R^+}^{I\to II}$, and for the Extraction of Silica, $t_{Si}^{I\to II}$, for the Break in Alpha, $t_{\alpha,break}$, for the Time When Alpha Equals One, $t_{\alpha=1}$, for Epsilon to Reach a Maximum, $t_{\varepsilon,max}$, and for Epsilon to Equal Zero, $t_{\varepsilon=0}$.

Glass	$t_{R^+}^{I\to II}$	$t_{Si}^{I\to II}$	$t_{\alpha,break}$	$t_{\alpha=1}$	$t_{\varepsilon,max}$	$t_{\varepsilon=0}$
20L	$>10^5$	7.0×10^4	$>10^5$	$>10^5$	$>10^5$	--
25L	$>10^5$	1.0×10^4	5.0×10^3	$>10^5$	$>10^5$	--
30L	$>10^5$	1.5×10^3	--	$>10^5$	$>10^5$	--
33L	$>10^5$	3.4×10^2	3.5×10^2	--	$>10^4$	$>3 \times 10^4$
46L	$>10^4$	4.5×10^1	1.0×10^2	10^4	10^3	10^4
15N	1.0×10^4	1.8×10^3	8.0×10^2	$>10^4$	$>10^4$	--
20N	2.0×10^2	5.0×10^1	3.0×10^1	$>10^4$	$>10^4$	--
31N	10	5.0	5.0	$>10^3$	$>10^3$	--
38N	<1.0	<1.0	<1.0	>10	≈10	>10
14K	2.3×10^4	1.0×10^4	1.0×10^4	$>10^5$	$>10^5$	--
20K	3.5×10^1	5.0	5.0×10^1	$>10^3$	$>10^3$	--
25K	<1.0	<1.0	<1.0	<10	<1.0	10

first mechanism are listed in Table XV. Unlike the apparent reaction rate constants determined by Douglas and El-Shamy[19] those in Table XV are real since, within experimental error, the values for the reaction rate exponents are equal to 0.5. This is the first time that real reaction rate constants have been determined for the leaching of alkali and for the extraction of silica from these glasses. The reaction rate constants for the diffusion controlled mechanism could not be determined for 38N and 25K, however. These two glasses are so reactive that the interfacial reaction controlled mechanism dominates after just one minute of corrosion time.

The fact that alkali ions leach much more rapidly than silica can be seen from the order of magnitude differences in the reaction rate constants for the two processes (Table XV). This supports the criticism of the theory by Douglas and El-Shamy[19] in Chapter II that the two processes are dependent upon one another and confirms that the extraction of silica and the leaching of alkali ions are independent diffusion controlled processes.

The reaction rate constants are plotted vs. concentration of alkali oxide in the bulk glass in Fig. 36. One can see that the compositional dependence is much greater for the K_2O-SiO_2 system than for the Li_2O-SiO_2 system. There are no discontinuities or inflections for the Li_2O-SiO_2 system across the immiscibility region. Since the Li_2O-SiO_2 system is the most likely to be partially phase separated, this indicates that phase separation has no effect on compositions greater than 20 mole %.

Table XV. Reaction Rate Constants for the Leaching of Alkali Ions, $k^{I}_{R^+}$, and the Extraction of Silica, k^{I}_{Si} During the First Mechanism.

Glass	$k^{I}_{R^+}$ $\frac{\text{mole}}{\text{cm}^3\ \text{sec}^{\frac{1}{2}}} \times 10^{10}$	k^{I}_{Si} $\frac{\text{mole}}{\text{cm}^3\ \text{sec}^{\frac{1}{2}}} \times 10^{10}$
20L	38	4.3
25L	58	6.2
30L	84	8.4
33L	130	16
46L	420	39
15N	91	13
20N	310	43
31N	1170	108
38N	--	--
14K	40	21
20K	700	312
25K	--	--

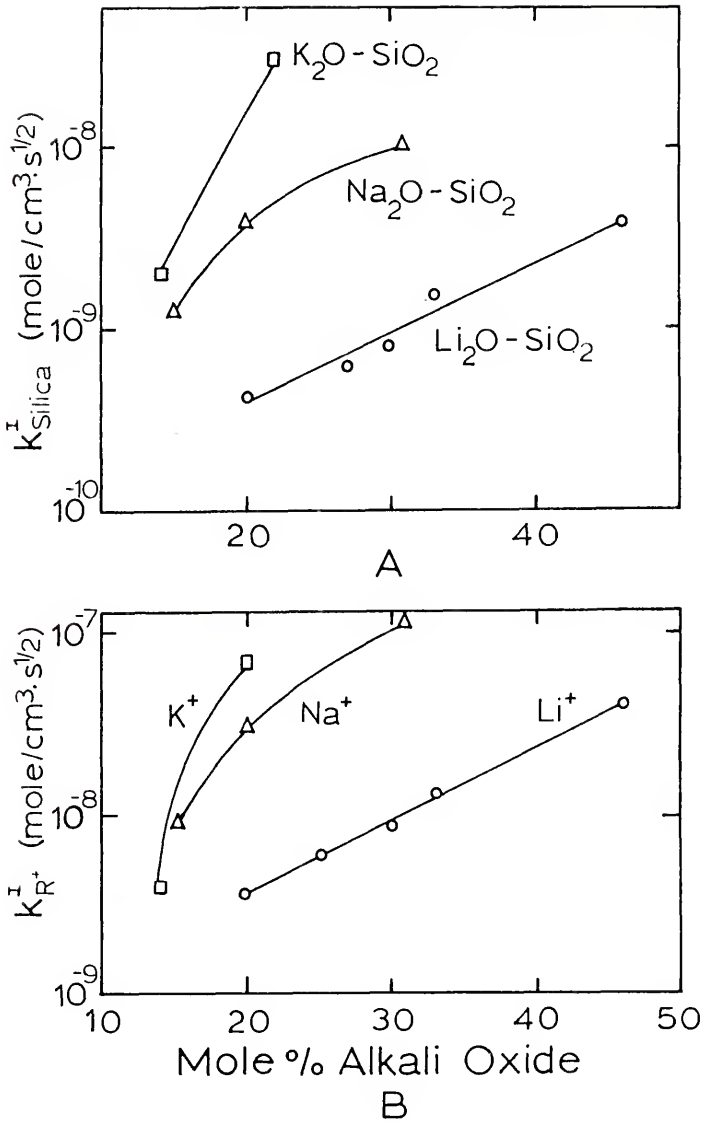

Fig. 36. Reaction rate constants for the extraction of silica (A) and the leaching of alkali ions (B) during the $t^{\frac{1}{2}}$ regime.

In order to obtain a measure of the differences in corrosion behavior of the three systems with higher alkali oxide concentrations in the bulk glass, the time to reach 10^{-3} (mole/l) of silica in solution was plotted vs. the concentration of alkali oxide in the glass (see Fig. 37). For the three systems there are several orders of magnitude difference in the times required to extract the same concentration of silica into solution. An inflection is observed in the curve for the Li_2O-SiO_2 system indicating a possible influence by phase separation. The effect of phase separation in glass corrosion can be assessed only by more systematic work.

A general sequence of events occurs with the corrosion parameters (alpha and epsilon, Figs. 26 - 35). Changes in glass composition as well as changes in the corrosion temperature only shifted the time sequence of events. The corrosion sequence which must occur on the surface of a corroding binary alkali silicate glass surface is modeled schematically in Fig. 38.

The first step in the sequence of corrosion events is the selective leaching of the glass surface (see Fig. 38a). The reaction kinetics are sufficiently slow for all the glasses so that selective leaching is observed at short times. During the selective leaching regime the leaching of alkali ions and the extraction of silica follow a $t^{\frac{1}{2}}$ dependence ($\alpha^{I}_{R^+}$ and $\alpha^{I}_{silica} = 0.5$) and are diffusion controlled. Since the rate at which alkali ions leach from the surface is much greater than the rate of silica extraction ($k^{I}_{A^+} > k^{II}_{silica}$, see Table XIV) a layer leached of alkali ions develops on the surface. A value

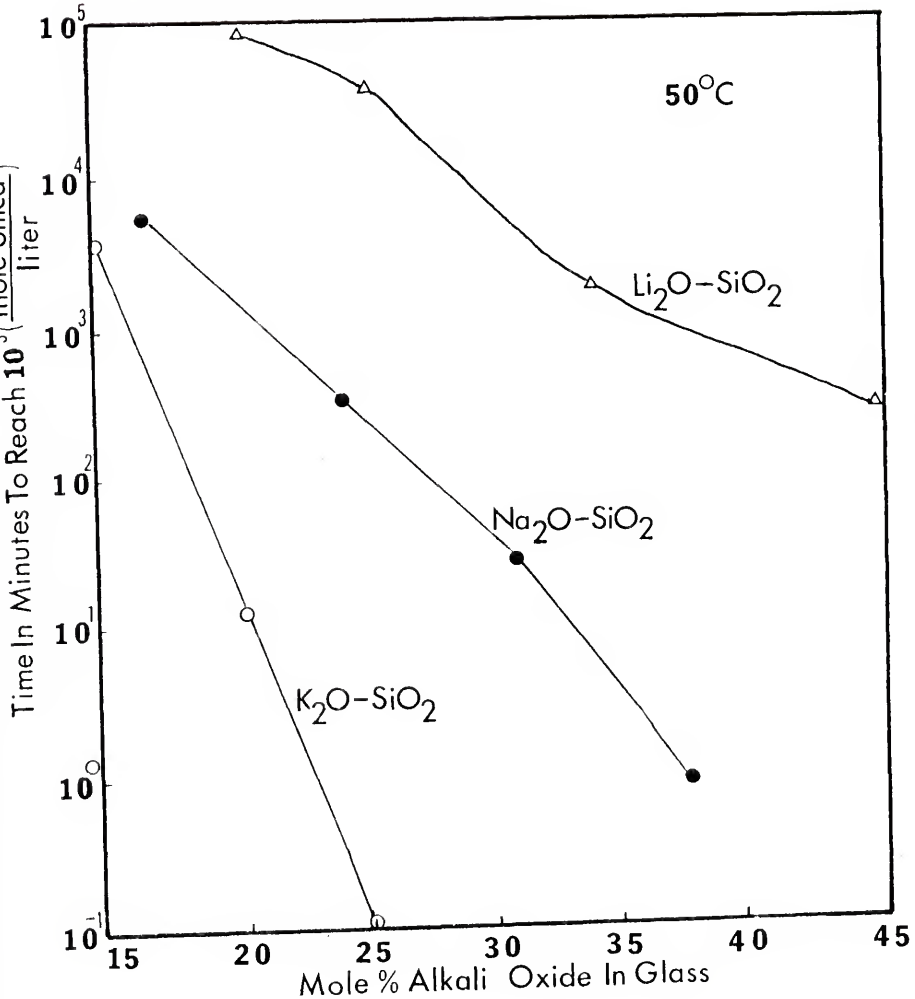

Fig. 37. *Log* of the time (min) to reach 10^{-3} (moles/l) of silica in solution as a function of the composition of the glass for the three systems.

A. Selective Leaching

a^{I}_{silica} = 0.5

$a^{I}_{A^+}$ = 0.5

$k^{I}_{A^+} >> k^{I}_{silica}$

$\alpha << 1$, constant

ε (+) increasing

B. Selective Leaching at a Decreasing Rate

a^{II}_{silica} = 1

$a^{I}_{A^+} \approx 0.5$

$k^{I}_{A^+} > k^{I}_{silica}$

$\alpha < 1$ increasing

ε (+) increasing at a slower rate

C. Steady State

a^{II}_{silica} = 1.0

$a^{II}_{A^+}$ = 1.0

$k^{I}_{A^+} = k^{II}_{silica}$

$\alpha < 1$ increasing

ε = maximum

D. Leached Layer Dissolution

a^{II}_{silica} = 1.0

$a^{II}_{A^+}$ = 1.0

$k^{II}_{A^+} < k^{II}_{silica}$

$\alpha < 1$ approaching 1.0

ε decreasing

E. Congruent Dissolution

a^{II}_{silica} = 1.0

$a^{II}_{A^+}$ = 1.0

$k^{II}_{A^+} = k^{II}_{silica}$

α = 1.0

ε = 0

Figure 38. Sequence of events which occur for the corrosion of binary alkali silicate glasses.

for alpha much less than one and an epsilon with a positive increasing value confirm this process. Since the rate of alkali leaching and silica dissolution are relatively constant for pH < 9 alpha remains constant until the pH of the solution reaches this value.

As the pH of the corrosion solution reaches a pH of approximately 9.5 the silica dissolution rate changes from a $t^{\frac{1}{2}}$ to t^{1} controlled process and the selective leaching progresses at a slower rate (Fig. 38b). This is accompanied by a larger reaction rate constant for the extraction of silica. The rate of alkali leaching remains greater than the rate of silica extraction ($k^{I}_{A+} > k^{II}_{silica}$) however, since alpha remains much less than one. The change in rates of extraction are apparent from the change in the corrosion parameter alpha which begins to increase (see Table XIII).

As the pH of the solution continues to increase to a value greater than 9.5, the rate of silica extraction increases as the rate of alkali leaching decreases. During this time the leaching of alkali approaches the rate of silica dissolution so that no longer is it under diffusion control but rather is controlled by the rate of silica extraction. Eventually a time is reached when the two rates are equal ($k^{II}_{A+} = k^{II}_{silica}$) and a steady state process results (Fig. 38c). At this time the leaching of alkali becomes controlled by the rate of silica extraction ($t^{\frac{1}{2}}_{A+} \rightarrow t^{1}_{A+}$ dependence). Values for the corrosion parameters which characterize this behavior are an alpha that is increasing and epsilon that is constant. It is not known how long epsilon remains at a constant value because the reaction kinetics of many of the glasses

studied are too slow. A maximum in epsilon is observed for 33L (50°C at 10^4 min), 46L (50°C at 10^3 min, 100°C at 2×10^2 min) and for 38N (50°C at 10 min).

After this point in time, an increase in the solution pH makes the rate of alkali extraction less than the rate of silica extraction ($k^{II}_{A^+} < k^{II}_{silica}$). The dissolution of the leached layer begins (Fig. 38d) when alpha rapidly approaches a value of one and epsilon decreases. The eventual outcome is a total dissolution of the leached layer after which congruent dissolution of the glass occurs (Fig. 38e) with alpha equal to one and epsilon equal to zero. Such is the case for 33L (100°C at 10^4 min), 46L (50°C at 5×10^3 min, 100°C at 10^3 min) and 25K (50°C at 10 min).

According to Lyle's empirical equation (Eq. 46) relating the time and temperature of a corrosion test to service conditions it requires approximately 100 and 1,400 times longer to obtain an equivalent extent of corrosion for tests relating 100°C to 50°C and 100°C to 30°C respectively.[46] In this chapter it is observed that for binary alkali silicate glasses an equivalent extent of corrosion (time to reach a maximum epsilon, epsilon = 0, etc.) at two different temperatures requires less of a time difference than the Lyle relation. There is only approximately 10 times difference for tests at 100°C and 50°C.

Lyle derived an equation to relate the time and temperature, of a corrosion test,

$$\log \theta = \frac{b}{T} - C \qquad (44)$$

where θ, is the time to reach an equivalent extent of corrosion at different temperatures and b and C are constants. For the commercial soda lime silicate glasses examined by Lyle, b = 5080.

Figure 39 is a plot of the time required to reach a certain extent of corrosion, θ, for 33L and 46L vs. reciprocal temperature. One can see that for each glass composition the different indicators of the extent of corrosion yield nearly parallel lines. A value for the constant b determined from the indicators $\theta_{Li^+}^{33L}$ and $\theta_{Li^+}^{46L}$ have values of 3553 and 3005 respectively. These two values are much lower than the value (5080) calculated by Lyle for glasses with commercial soda lime silica compositions.

These results confirm the hypothesis of Lyle that corrosion tests may be carried out at elevated temperatures and extrapolated to lower temperature. The same sequence of events occur within the temperature range of 25°C - 100°C with only the time sequence of the events altered. The constant b in Eq. 44, however, must be determined for each glass composition (or small composition range) tested.

Summary and Conclusions

Corrosion studies of the Li_2O-, Na_2O- and K_2O-SiO_2 glass systems using the Sanders' method confirm the hypothesis from Chapter II that there are two independent diffusion controlled mechanisms for the leaching of alkali ions and the extraction of silica at short times.

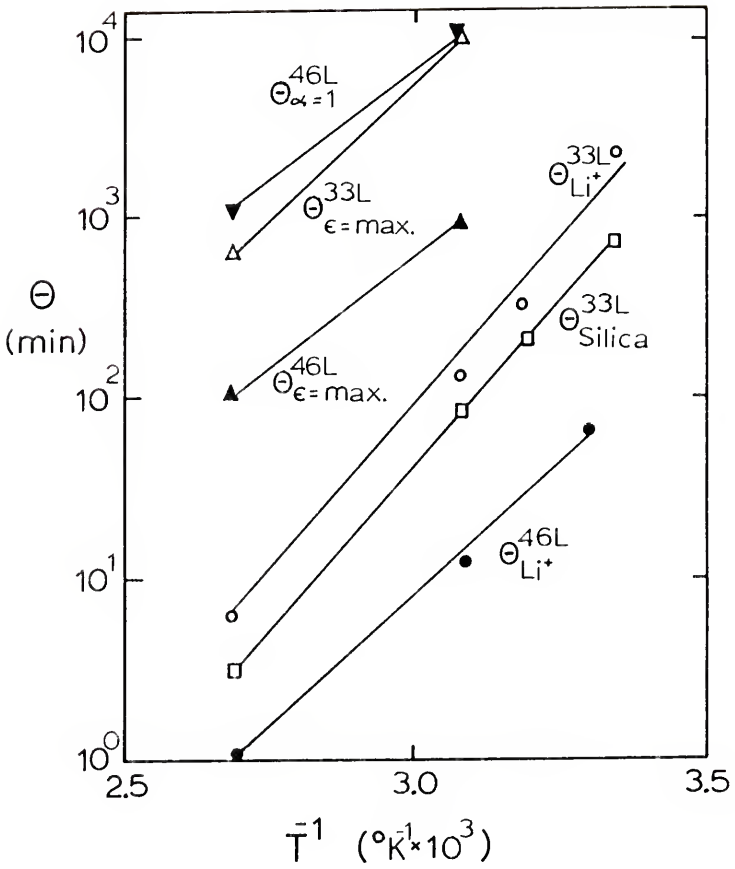

Fig. 39. Plots of *log* Θ vs. reciprocal temperature for 33L and 46L. Where Θ is the time to reach a particular extent of reaction, i.e. 10^{-3} mole/l Li^+ or 10^{-4} mole/l silica in solution, steady state (maximum epsilon), or congruent dissolution (alpha = 1).

The short transition region between the $t^{\frac{1}{2}}$ and t^{1} controlled mechanisms observed in Chapter IV was confirmed for additional glasses in the three systems.

Reaction rate constants for the diffusion controlled leaching of alkali ions and silica extraction were determined for the glasses investigated. There is no discontinuity in the plot of the reaction rate constants vs. concentration of alkali oxide in the glasses of the Li_2O-SiO_2 system which indicates that phase separation has no effect on the corrosion behavior for compositions greater than 20 mole % Li_2O.

A specific description of the sequence of events which occur during binary alkali silicate glass corrosion was given and related to specific glasses.

A time-temperature relationship for the corrosion of glasses was discussed. Values for the constant b in Lyle's equation of 3553 and 3005 for 33L and 46L glasses respectively were determined. The justification for elevated temperature (100°C) corrosion studies to model room temperature corrosion was verified.

CHAPTER VII

KINETICS OF STATIC CORROSION OF BINARY ALKALI SILICATE GLASSES II. INFRARED REFLECTION SPECTRA

Introduction

Infrared spectroscopy is a very useful tool for studying silicate glasses (see Chapter II). This is because it is sensitive to the local positioning of atoms and the strength of the chemical bonds between them.[203] Some investigators have shown how infrared spectroscopy can be used to study glass structure,[165,204] while others have been interested in quantitative studies of the vibrations of the different atoms constituting the glassy network.[25,205] Quantitative analysis of glass compositions has been accomplished using both peak wavenumber shifts and peak height shifts (see Chapter II and Appendix C).

The purpose of this chapter is to describe and interpret the spectral changes which accompany the corrosion of the surface of several glasses from the Li_2O-, Na_2O- and K_2O-SiO_2 systems, most of which have never been examined before.

Results

Glasses from the three systems were corroded for various times. Figure 40 shows several spectra of 20L corroded at 50°C from 1 min to 15 weeks. It can be seen that as the glass is corroded, the silica-bridging oxygen peak (S) increases in intensity and shifts to slightly larger wavenumbers. There is a corresponding decrease of the intensity of the silica-nonbridging oxygen peak (in an alkali environment, NS) indicated by the decrease in intensity of the shoulder at approximately 960 cm^{-1}.

A more complicated series of spectra are observed for 33L corroded at 50°C (Fig. 41). In the early stage of corrosion for this glass there is separation and sharpening of the two peaks (S and NS) for 10 days which is followed by an increase in intensity and shift of the S peak to larger wavenumbers. A corresponding decrease in intensity of the NS peak and a shift to smaller wavenumbers occurs until it slowly disappears after approximately 1 day. After about 1 week the S peak begins to decrease in intensity and at 3 weeks it has decreased to a considerably smaller value. During this time, however, the S peak continues to shift to larger wavenumbers.

When 33L is corroded at 100°C, the same sequence described above for 33L corroded at 50°C, can be seen. However, the sequence occurs in a shorter time (Fig. 42). At 5 seconds and 1 min the peaks begin to separate. However, the intensity of the S peak for the corroded glass is less than the S peak of the freshly abraded 33L surface.

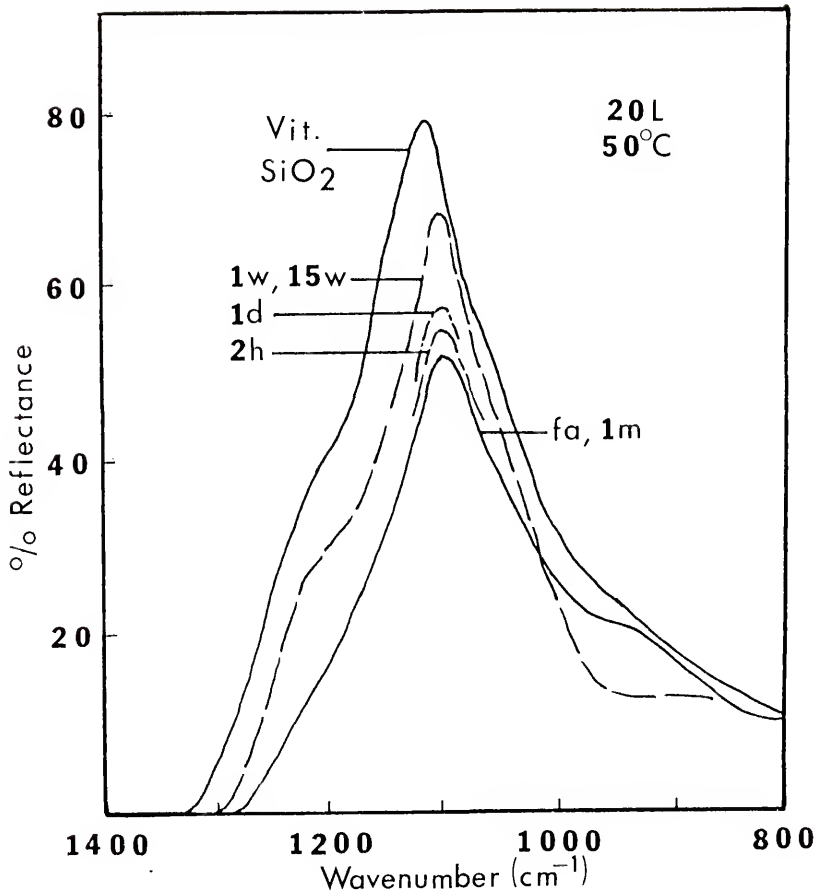

Fig. 40. Infrared reflection spectra (IRRS) for 20L corroded at 50°C for 1 min (m), 2 hours (h), 1 day (d) and 1 and 15 weeks (w).

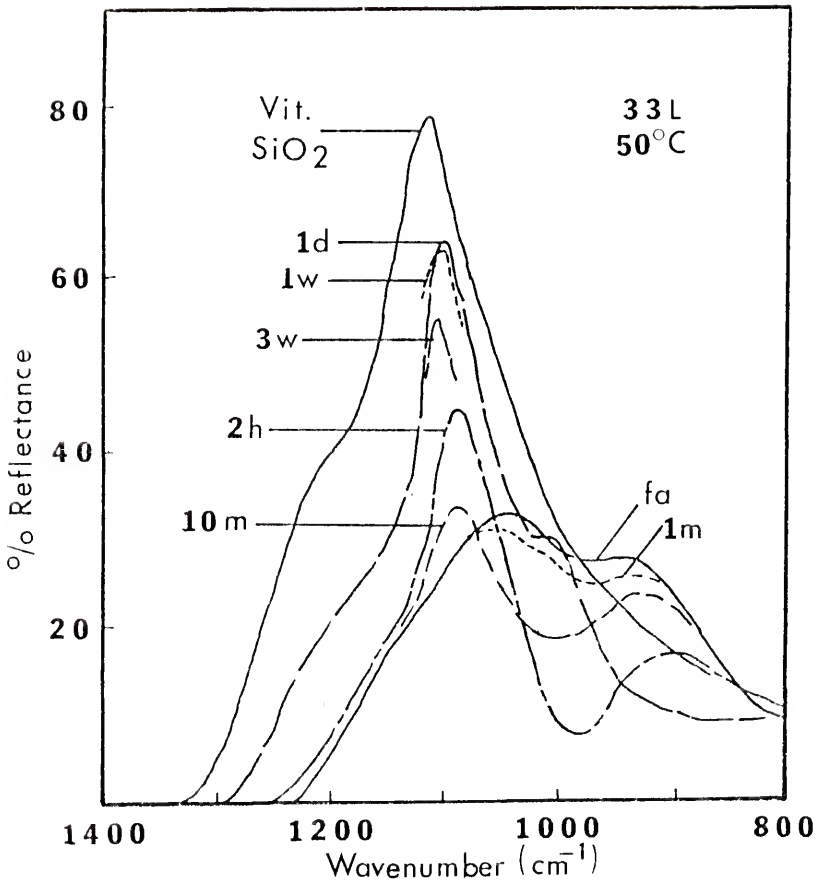

Fig. 41. IRRS for 33L corroded at 50°C for 1 and 10 min, 2 hours, 1 day, and 1 and 3 weeks.

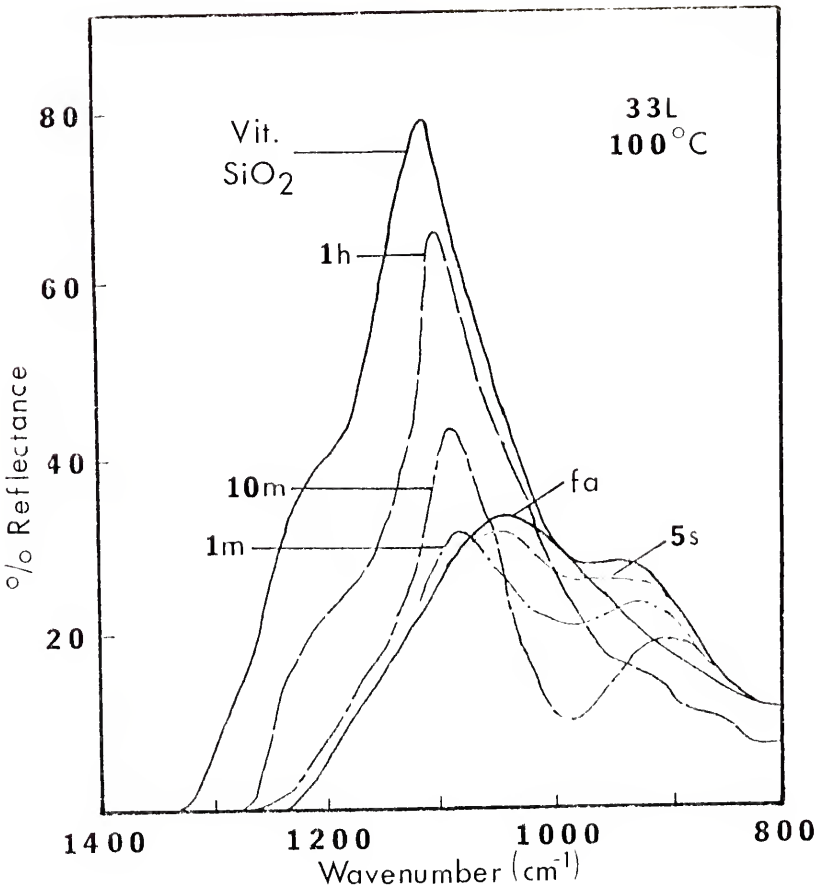

Fig. 42. IRRS for 33L corroded at 100°C for 5 sec (s), 1 and 10 min, and 1 hour.

Corrosion times longer than 1 min cause the S peak to increase until at about 1 hour it reaches a maximum intensity. For corrosion times longer than 1 hour, the S peak intensity decreases (Fig. 43). The wavenumber shift reaches a maximum at about 1 hour also. The wavenumber of the S peak remains at about the same value for 1 day. After this, the wavenumber of the S peak begins to shift back to smaller wavenumbers. At 1 week the NS peak at approximately 920 cm^{-1} begins to reappear. This peak continues to rise until at 2 weeks the spectrum appears very much like the freshly abraded (f.a.) 33L spectrum except for being slightly lower at all points than the freshly abraded 33L spectrum.

The spectra for the corroded 46L glass are similar to those previously discussed. When 46L is corroded at 30°C, the first observation is the separation of the S and NS peaks with a slight reduction in intensity (Fig. 44). Accompanying this there is a very large decrease in intensity of the region between the two peaks and an increase of the intensity and a shift to larger wavenumbers for the S peak. There is no shift back to lower wavenumbers or decrease in intensity even after 4 weeks. Neither the maximum wavenumber nor the maximum intensity of the S peak reaches those seen with 20L or 33L.

When 46L was corroded at 50°C the changes were accelerated (Fig. 45). A maximum in intensity for the S peak occurred at about 1 hour after which the intensity decreases. A maximum wavenumber also occurs at about 1 hour, however, it remains relatively constant until at about 12 hours when the wavenumber begins to decrease again.

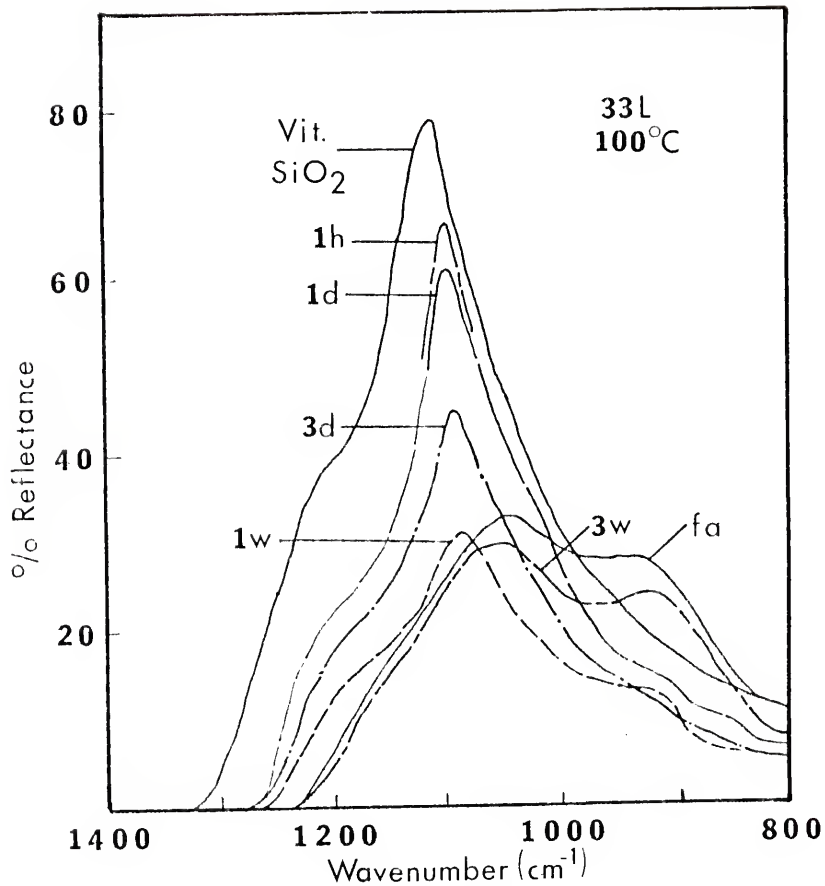

Fig. 43. IRRS for 33L corroded at 100°C for 1 hour, 1 and 3 days, and 1 and 3 weeks.

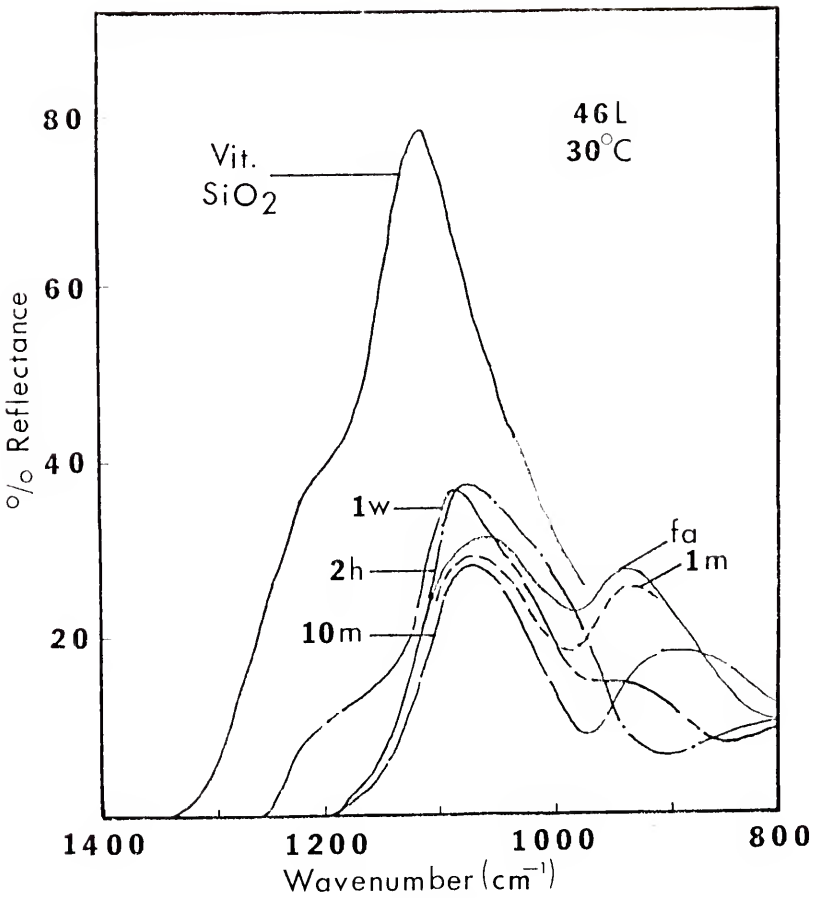

Fig. 44. IRRS for 46L corroded at 30°C for 1 min, 10 min, 2 hours and 1 week.

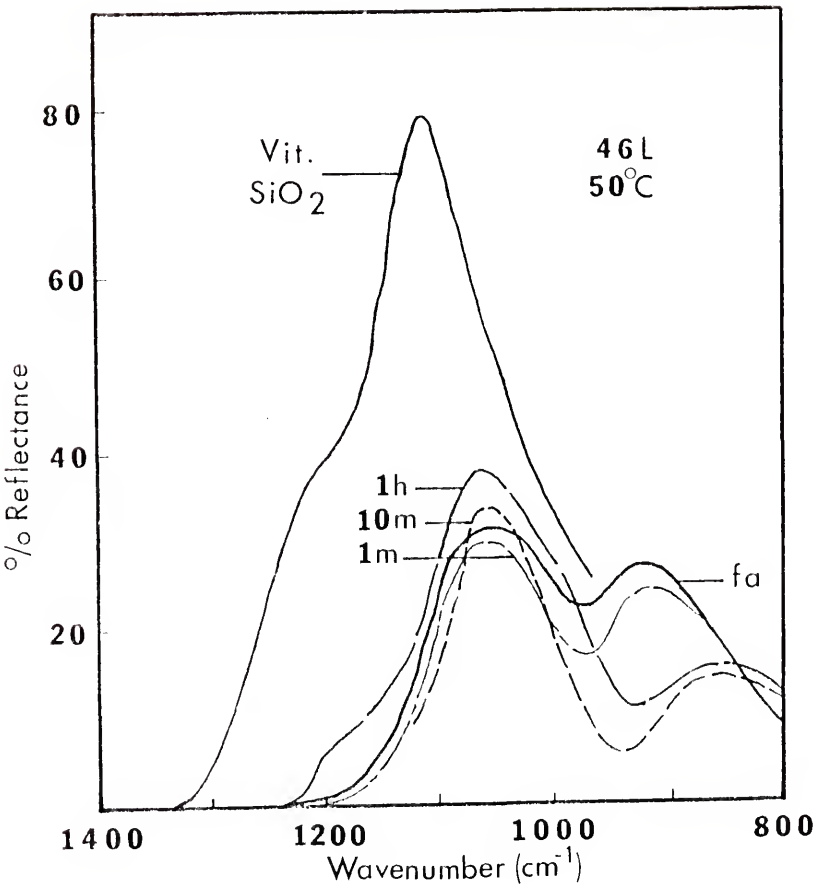

Fig. 45. IRRS for 46L corroded at 50°C for 1 min, 10 min and 1 hour.

As would be expected, the changes in the 46L spectra which accompany glass corrosion are accelerated considerably by raising the temperature to 100°C (Figs. 46 and 47). The changes observed at longer times (Fig. 47) are similar to those for 33L at 100°C (Fig. 43). Eventually the spectra for 46L at 100°C changes back after 1 week to look very much like the freshly abraded 46L spectra except for having a lower intensity at all points.

Similar types of behavior observed above occur when glasses in the Na_2O-SiO_2 system are corroded. Figure 48 shows several spectra of 15N corroded at 50°C for 1, 4 and 6 weeks. The shifts of the S peak are typical. The S peaks move progressively to higher wavenumbers and increase in intensity. Likewise with 20N corroded at 50°C, the same changes are observed (Fig. 49).

A slightly different type of behavior is observed with 31N (Fig. 50). After 15 seconds of corrosion at 50°C, a separation of the S and NS peaks occurs. This separation is similar to that seen with 46L and 33L corroded at 50°C. As corrosion proceeds, the intensity of the S peak increases. The S peak shifts to smaller wavenumbers, however. This is a phenomena which has not been observed in any of the previous spectra. In all the previous cases during the early corrosion times, the wavenumber of the S peak has always shifted to larger wavenumbers.

Figure 51 shows spectra for 14K corroded at 50°C for various times. As has been the case with the other binary glasses with a low percentage of alkali, the spectra of the corroded 14K glasses are rather simple and typical. The S peak intensity and wavenumber increase with corrosion time.

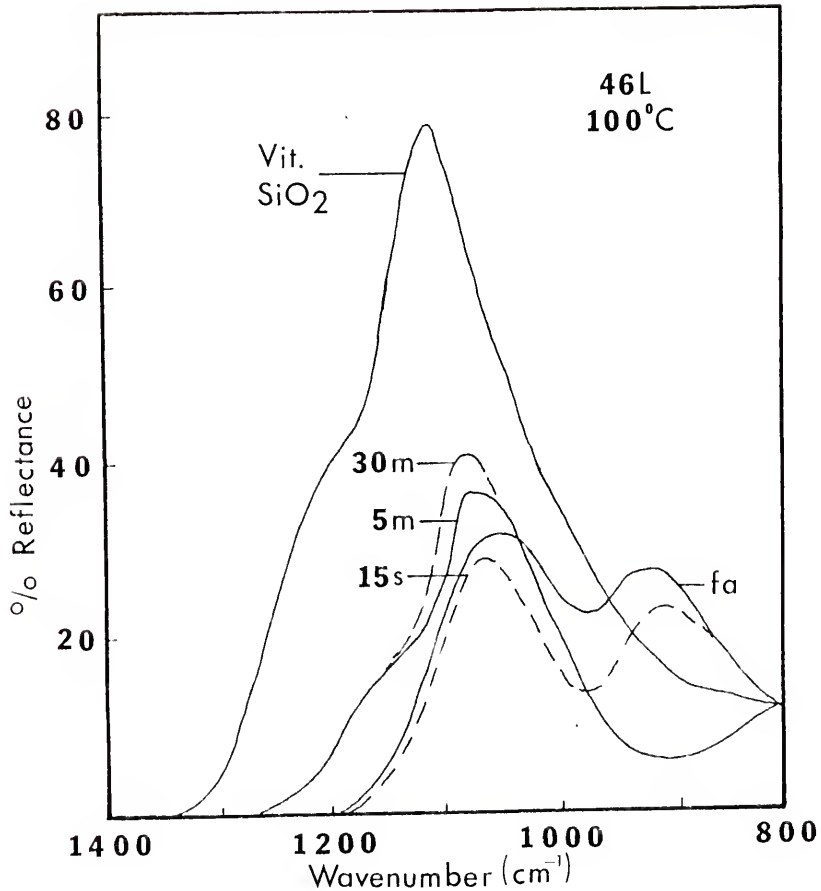

Fig. 46. IRRS for 46L corroded at 100°C for 15 sec, 5 min and 30 min.

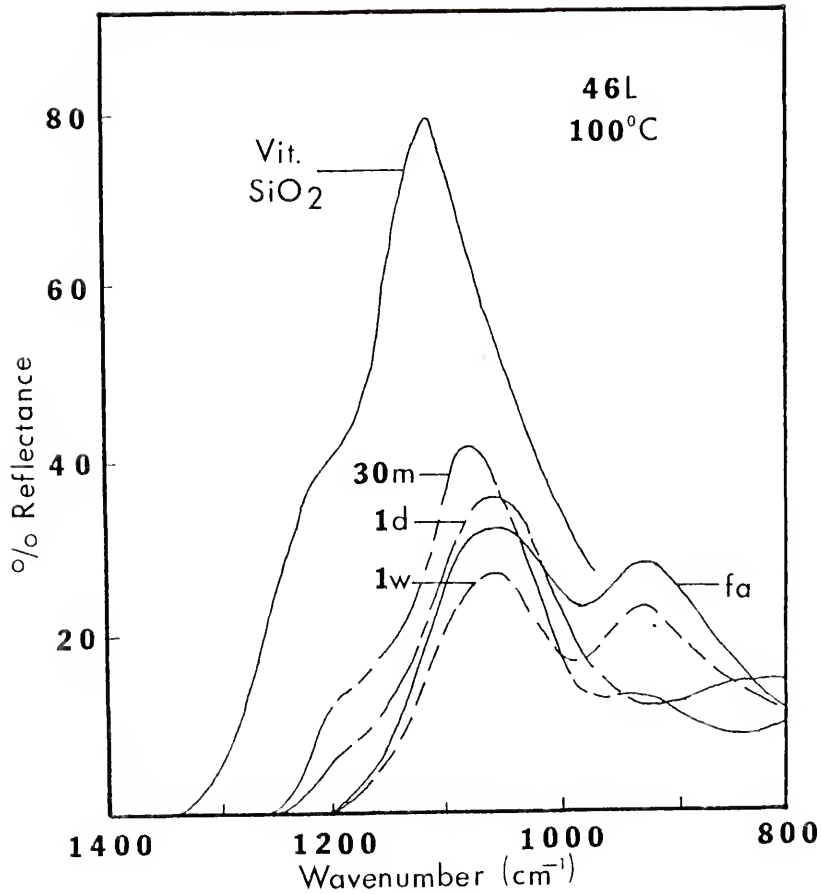

Fig. 47. IRRS for 46L corroded at 100°C for 30 min, 1 day and 1 week.

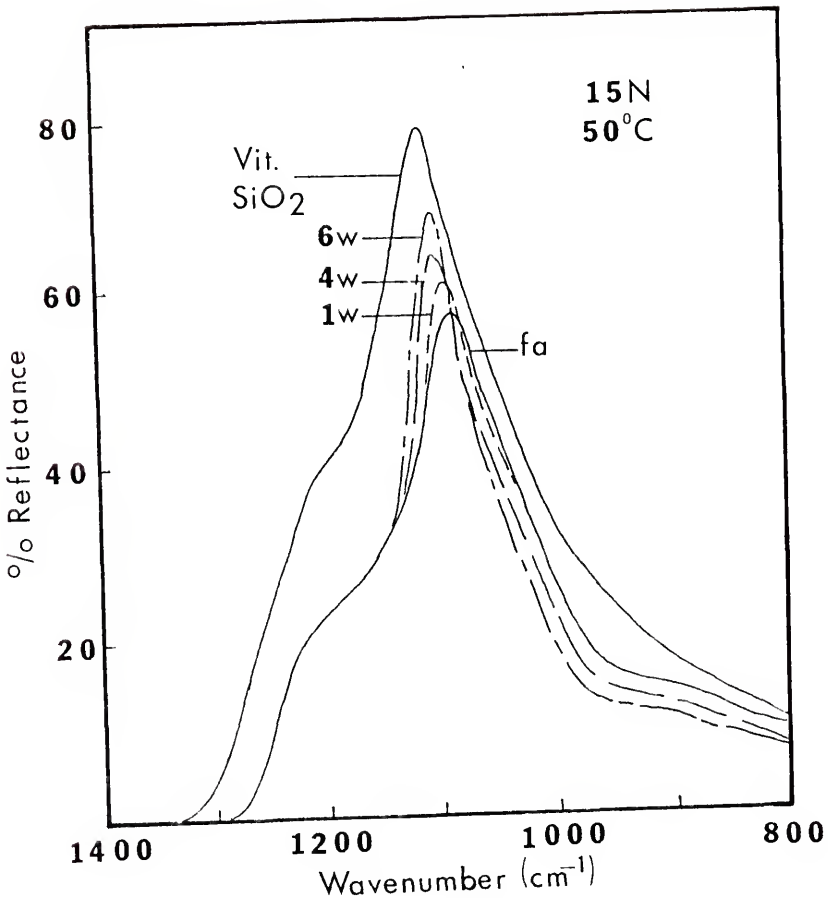

Fig. 48. IRRS for 15N corroded at 50°C for 1, 4 and 6 weeks.

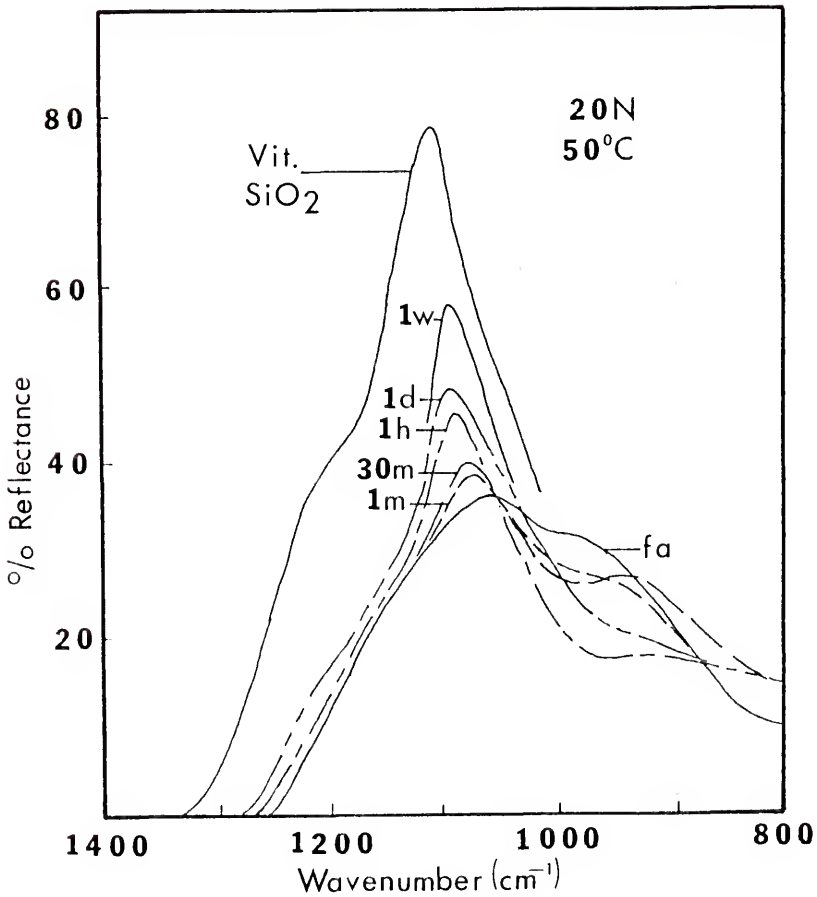

Fig. 49. IRRS for 20N corroded at 50°C for 1 and 30 min, 1 hour, 1 day and 1 week.

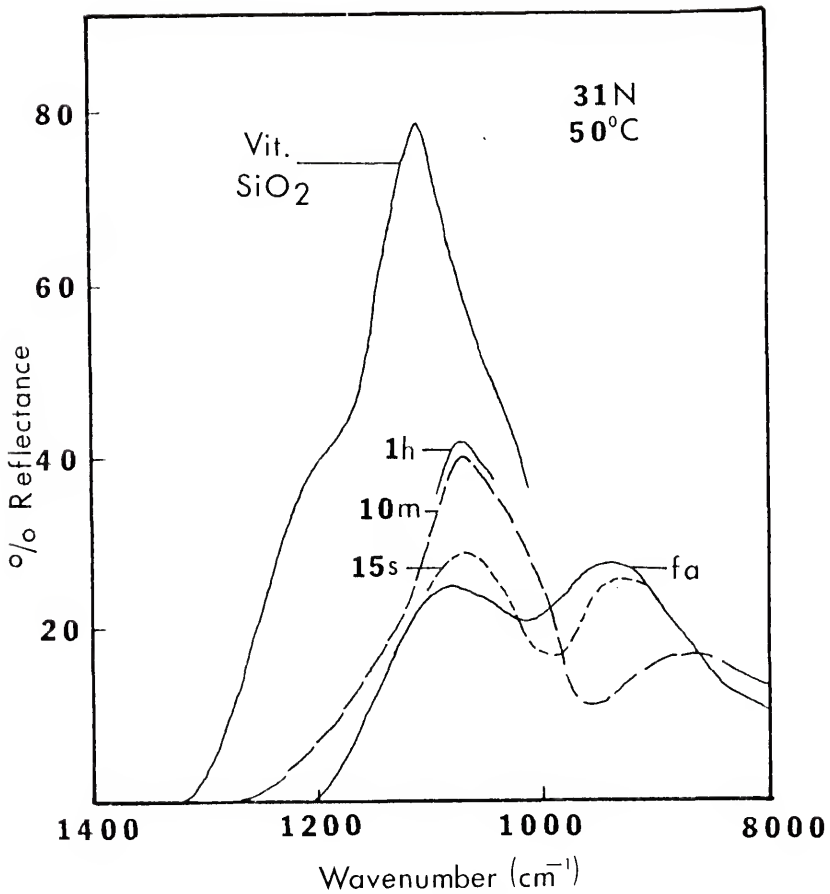

Fig. 50. IRRS for 31N corroded at 50°C for 15 sec, 10 min and 1 hour.

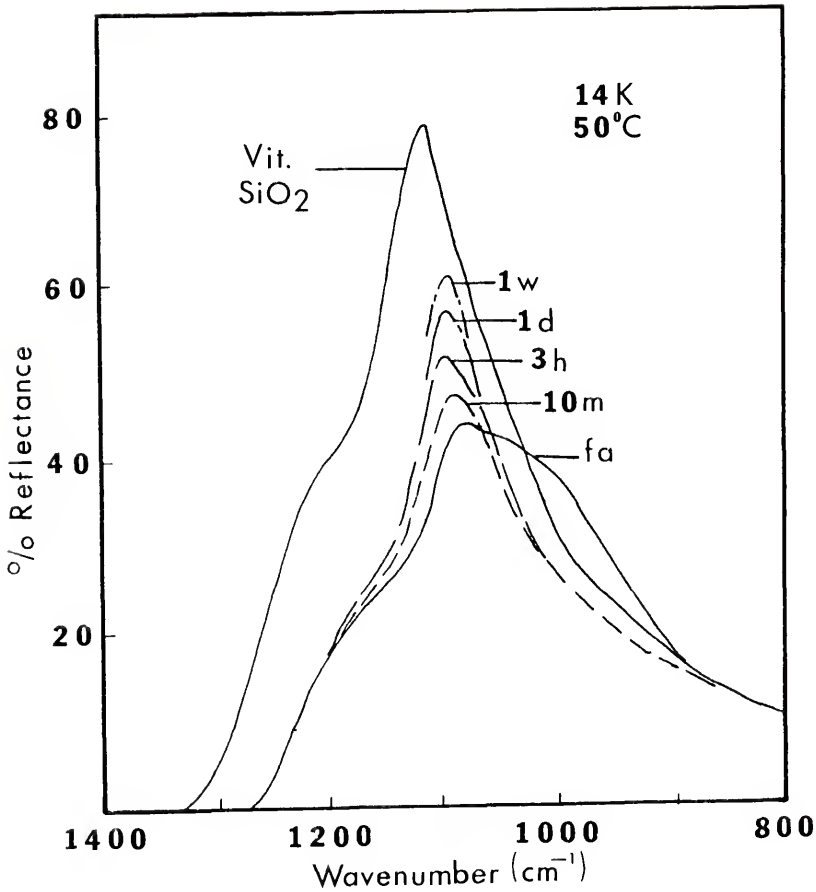

Fig. 51. IRRS for 14K corroded at 50°C for 10 min, 3 hours, 1 day and 1 week.

The corrosion spectra for 20K are also rather simple (Fig. 52). Since the 20K glass is quite soluble in water, the spectral changes occur very rapidly. Neither the S peak intensity nor the wavenumber ever reaches as high a value as is observed for the 14K sample.

Discussion

When glasses containing relatively small initial concentrations of alkali oxide are corroded (20L, 50°C, Fig. 47; 14N, 50°C, Fig. 55; 14K, 50°C, Fig. 58) the resulting spectral changes are very similar and are characterized by increases in intensity and wavenumber of the S peak. This is accompanied by a decrease in intensity of the NS peak at approximately 960 cm^{-1}. This type of spectral change caused by aqueous attack was first observed by Sanders and Hench.[123] They stated that this observation is consistent with the theory that a "silica gel" is formed on the surface of corroded silicate glasses.[16]

Glasses containing a higher concentration of alkali oxide in the bulk glass composition exhibit a characteristic separation and sharpening of the S and the NS peaks at short corrosion times (Figs. 48, 49,51,52,53,57,59) accompanied by a decrease in intensity of the region between the two peaks at about 975 cm^{-1}. The separation and sharpening of the two peaks is due to the decoupling of sodium ions from nonbridging oxygen atoms and their diffusion out of the glass. It is known that the Si-O bond force constant is decreased by

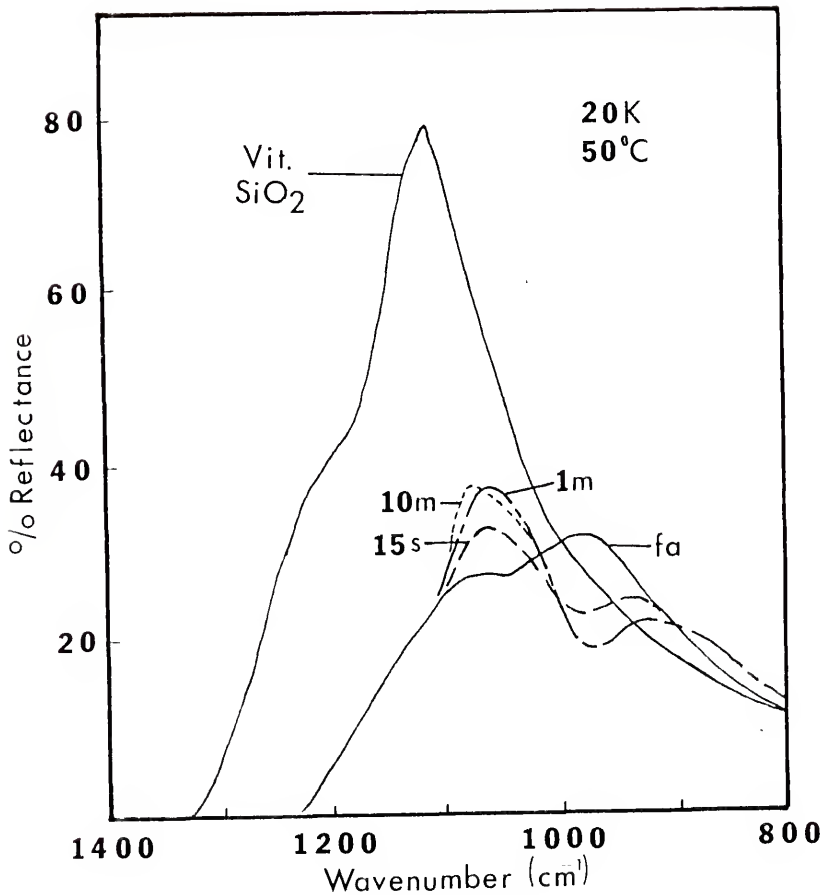

Fig. 52. IRRS for 20K corroded at 50°C for 15 sec, 1 min and 10 min.

the cationic field of the network modifiers.[162,206] The presence of the alkali in the glass also produces a coupling between the S and NS peaks[123] causing a shift of the NS peak to higher wavenumbers. This is accompanied by S peak shifts to lower wavenumbers as alkali oxide is added to vitreous silica.[123] Conversely, if sodium diffuses out of the glass, shifts should occur in the opposite direction and the coupled region between the two peaks should decrease in intensity.

An additional explanation exists for the decrease in intensity of the coupled region during the early stages of corrosion of 46L. For glasses containing greater than 33 mole % alkali oxide, there are on the average more than one nonbridging oxygen per silica tetrahedron. Sanders, et al.[25] reported that at concentrations greater than 36 mole % the number of tetrahedra having more than one nonbridging oxygen becomes significant. When this occurs, two nonbridging oxygens can couple leading to two small satellite peaks on either side of the NS peak. One of these small peaks lies directly under the coupled region between the S and NS peaks. During the early stage of corrosion of 46L, the coupled region decreases in intensity more than with the other lithia silicate glasses. In Fig. 51 one can see this effect on the 10 min spectrum of 46L corroded at 30°C. It can also be seen on the 10 min spectrum of 46L corroded at 50°C (Fig. 52) and the 15 second spectrum of 46L corroded at 100°C (Fig. 53). The decrease in intensity between the S and NS peaks for 46L can, therefore, be due to decoupling of the Li^+ ions plus a decrease in intensity of the satellite peak.

When the less durable glasses are corroded under relatively severe conditions or for long periods of time, another characteristic behavior is observed. If one examines the spectrum for 33L corroded for 100°C, one can see that the S peak intensity begins to decrease after about 1 hour (Fig. 50). The cause of this decrease in intensity is due to a roughening of the surface as is described in Appendix C. The S peak wavenumber remains relatively constant during this period. At longer times, however, the wavenumber of the S peak begins to decrease and eventually the spectrum returns to the same shape as the freshly abraded spectrum. This is observed for 33L corroded at 100°C for 2 weeks (Fig. 50) and 46L corroded for 1 week at 100°C (Fig. 54). These times correspond to the time when congruent dissolution of the surface begins. This provides independent evidence confirming the time sequence for the corrosion behavior described in Chapter VI.

Sanders[4] could have avoided the errors in calculating the solution parameters noted in Chapter II if he had used the independent information available to him. The IRRS spectra and leached layer profile for the 33L sample corroded at 79°C for 17 hours indicated that congruent dissolution had not begun at the time when the incorrect solution data indicated that it had.

The 31N sample corroded at 50°C showed a behavior that deviated from that of all the other glasses studied. As the initial stage of corrosion proceeded, the wavenumber of the S peak decreases. This is the reverse of what is observed with the other glasses. The explanation lies in the fact that a reversal in the dependence of

wavenumber shift vs. composition occurs at about 22 mole % Na_2O (see Appendix C). Since 31N is past this critical concentration, the initial depletion of alkali shifts the S peak to lower wavenumbers. The S peak increases in intensity as the NS peak shifts to lower wavenumbers and decreases in intensity. These observations demonstrate that Na^+ ions are in fact leached from the glass. The fact that alpha is much less than 1.0 and epsilon is quite large confirms this interpretation (see Chapter VI).

There is evidence for another reaction occurring at the surface. This reaction is the polymerization of silanol groups within the leached layer. As corrosion proceeds, alkali ions leach out of the surface and are replaced by H^+. This loss of alkali ions is evidenced by the decrease in intensity of the region of spectrum around 960 cm^{-1} associated with the $Si\text{-}O^-$ bond in an alkali environment. Accompanying this, the Si-O bridging oxygen vibration at about 1100 cm^{-1} increases in intensity. Since the intensity is directly related to the number of vibrators contributing to the peak, this implies that the number of Si-O bridging oxygen atoms increase. This can only result from the polymerization of Si-O nonbridging oxygens through a condensation reaction,

$$2 \equiv Si\text{-}OH \rightarrow \equiv Si\text{-}O\text{-}Si\equiv + H_2O \qquad (39)$$

This reaction in the leached layer is supported by the literature. The esterification of amorphous silica[207] and the polymerization of

silicic acid[37] have been observed. By studying the polymerization of silicic acid Greenberg and Sinclair[37] found that in aqueous solution monomeric silicic acid polymerizes to polysilicic acid. They found that the polymerization reaction proceeds most rapidly when the solution is at a pH of 8.6. At this pH they said that it gelled so fast that they could not measure the polymerization rate. As the reaction continued, polymeric particles aggregated and became transformed into a gel. Slower polymerization rates are observed when the pH increases or decreases from this value, and at high and low pH no polymerization results.

In an X-ray study, Gould and Hill[208] examined 25K powders which were leached in a solution buffered to a pH of 7 with the removal of most of the potassium from the powders. In subsequent X-ray analysis they found that as the leaching proceeds, the diffraction patterns change to look like vitreous silica. The interatomic distances of various atoms of the silica structure also approach those observed for vitreous silica.

Changes in the spectra, for several glasses at long times, indicate that the surface changes back to a composition and structure much like the original bulk glass. This only occurs, however, after the pH of the solution has exceeded a value of 9.5. A depolymerization reaction similar to that proposed by Greenberg[38] for vitreous silica at high pH is indicated at long times. These reactions will be discussed in the general sequence of glass corrosion presented in Chapter X.

Summary and Conclusions

Infrared reflection spectra of many corroded glasses from the three alkali silicate glass systems are presented. These spectra are interpreted in terms of the stages of glass corrosion described in Chapter III. A polymerization reaction in the glass surface involving ≡Si-OH groups occurs during corrosion. At long corrosion times, however, when the pH > 9.5 and the corrosion parameter alpha begins to increase, a depolymerization reaction occurs.

CHAPTER VIII

KINETICS OF STATIC CORROSION OF BINARY ALKALI SILICATE GLASSES III. SURFACE COMPOSITIONAL ANALYSIS

Introduction

An important use for infrared reflection spectroscopy, IRRS, is for quantitative analysis of glass structure.[156,163,164] A technique is developed in Appendix C for determining the surface composition of a corroded glass surface. The purpose of this chapter is to analyze the surface compositional changes for several of the corroded glasses described in Chapter VII and relate the changes to the solution data from Chapter VI. The surface SiO_2 concentration is then used along with the values of epsilon from Chapter VI to calculate approximate leached layer thicknesses. Composition profiles for several corroded glasses can then be calculated and related to each other.

Results and Discussion

Using the techniques developed in Appendix C, the surface composition of several corroded glasses was determined. Figure

53 shows the surface composition vs. time for 33L corroded at 30, 50 and 100°C. One can see that at 100°C the surface SiO_2 concentration rapidly increases to approximately 90%. It remains at this concentration until about 1 day when the surface SiO_2 concentration begins to decrease. At 2×10^4 min (2 weeks) the surface composition approximately equals that of the bulk composition of 33L. This data agrees very well with the solution data for 33L corroded at 100°C given in Chapter VI. At 10^3 min the surface concentration of SiO_2 begins to increase at the same time that the value of alpha increases. At approximately 2×10^4 min the surface composition of the corroded glass returns to the bulk composition (33 mole percent) and corresponds precisely to the time when the value for alpha reaches 1 and epsilon becomes zero (see Chapter VI). Lowering the temperature to 50°C slows down the leaching process such that the surface composition does not reach 90% SiO_2 until 10^4 min (1 week). Corrosion at 30°C proceeds at an even slower rate.

The surface compositions for 46L corroded at the three temperatures are shown in Fig. 54. The surface composition approaches a value of about 74% SiO_2 after which the surface SiO_2 concentration decreases. After 10^3 min at 100°C the surface composition of 46L has a value that is nearly that of the bulk glass. This also agrees with the solution data from Chapter VI in which it is observed that alpha reaches 1.0 and epsilon becomes equal to zero at the same times.

Figure 55 compares the surface compositon of 20L, 33L and 46L corroded at 50°C. One can see that the maximum observed surface SiO_2

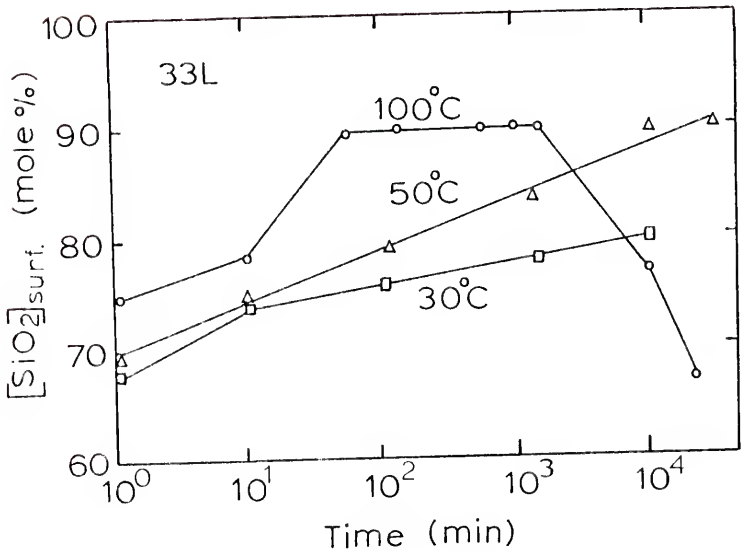

Fig. 53. Surface SiO_2 concentration (mole %) vs. $\log$ corrosion time (min) for 33L corroded at 30°C, 50°C and 100°C.

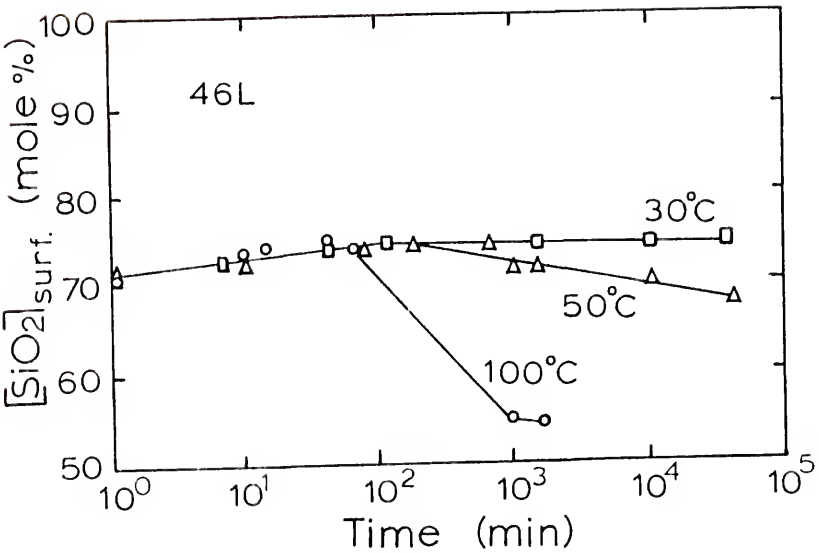

Fig. 54. Surface SiO_2 concentration (mole %) vs. *log* time (min) for 46L corroded at 30°C, 50°C and 100°C.

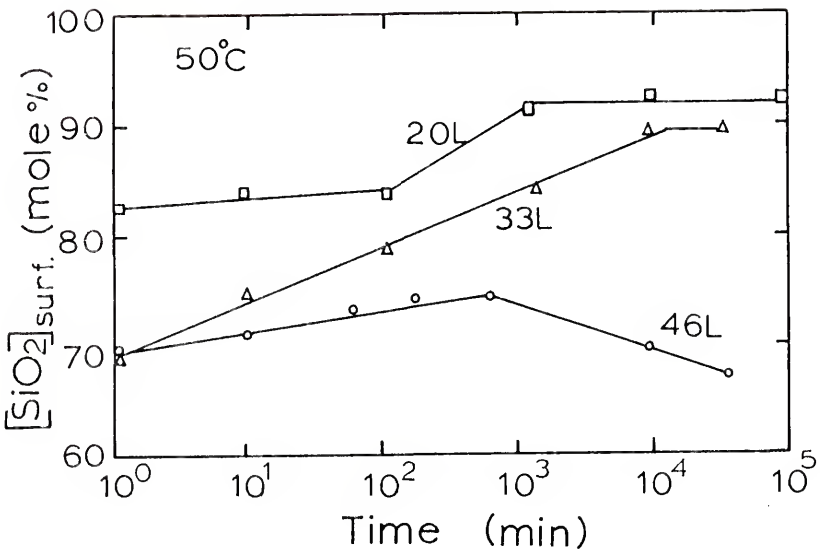

Fig. 55. Surface SiO_2 concentration (mole %) vs. *log* time (min) for 20L, 33L and 46L corroded at 50°C.

concentration is largest for 20L (93% SiO_2) but almost as large for 33L glass, being 90% SiO_2. The 46L glass, on the other hand, did not get above a 75% SiO_2 surface concentration.

A comparison of the surface compositional changes which occur during corrosion of 20 mole % concentrations from the three systems is shown in Fig. 56. The 20L sample gradually increases to a surface SiO_2 concentration of about 93% at 10 weeks (10^5 min). The change is much faster for the 20N sample and the SiO_2 concentration increases to a value of about 94% at about an order of magnitude sooner than for 20L. The reaction kinetics are so fast for the 20K glass that the surface composition never reaches as high of a surface SiO_2 concentration as with 20N and 20K.

A technique is developed in Appendix D for determining the composition profile for thick leached layers on the surface of corroded binary silicate glasses. Figure 57 shows three profiles for 33L glass corroded at 50°C for 1 hour, 1 day and 1 week (60, 1440 and 10,080 min respectively) determined using this technique. One can see that after 1 hour of corrosion an essentially linear profile is obtained corresponding to the Sanders - Hench model.[123] After 1 day, the depth of leaching naturally increases. The profile appears to have a slight plateau at about 76% SiO_2. With the 1 week sample, a plateau of constant SiO_2 concentration is significant. At both ends of the plateau a nearly uniform concentration gradient exists.

Profiles for three glasses within the Li_2O-SiO_2 system corroded at 50°C for 1 hour are shown in Fig. 58. For the 20L sample, the

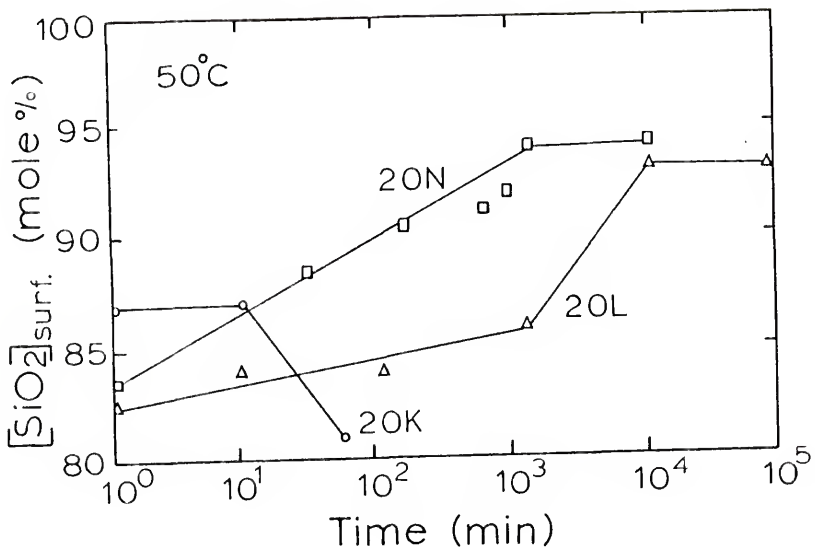

Fig. 56. Surface SiO_2 concentration (mole %) vs. corrosion time (min) for 20L, 20N and 20K corroded at 50°C.

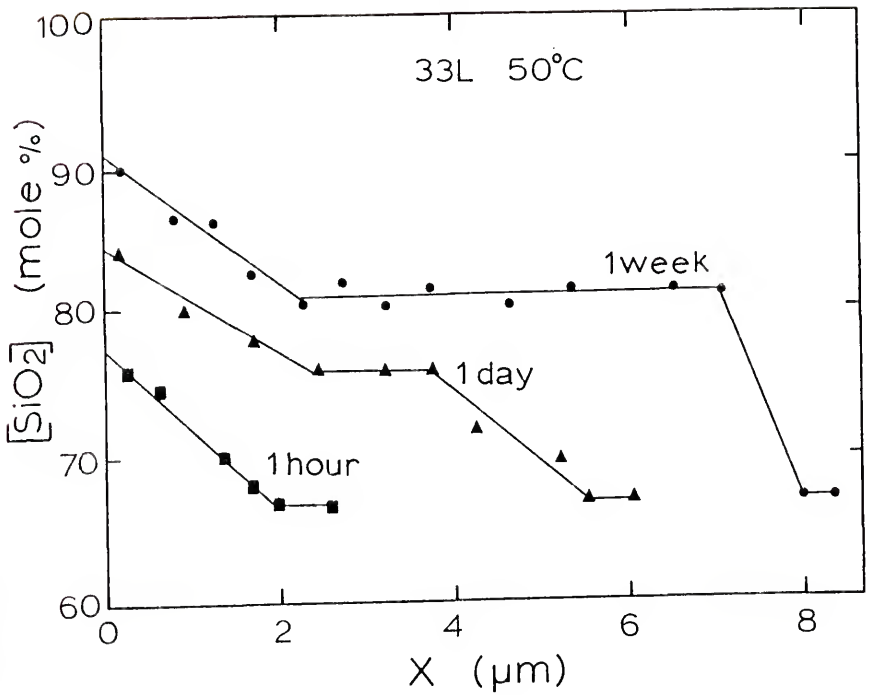

Fig. 57. SiO_2 concentration profile for 33L corroded at 50°C for 1 hour, 1 day and 1 week.

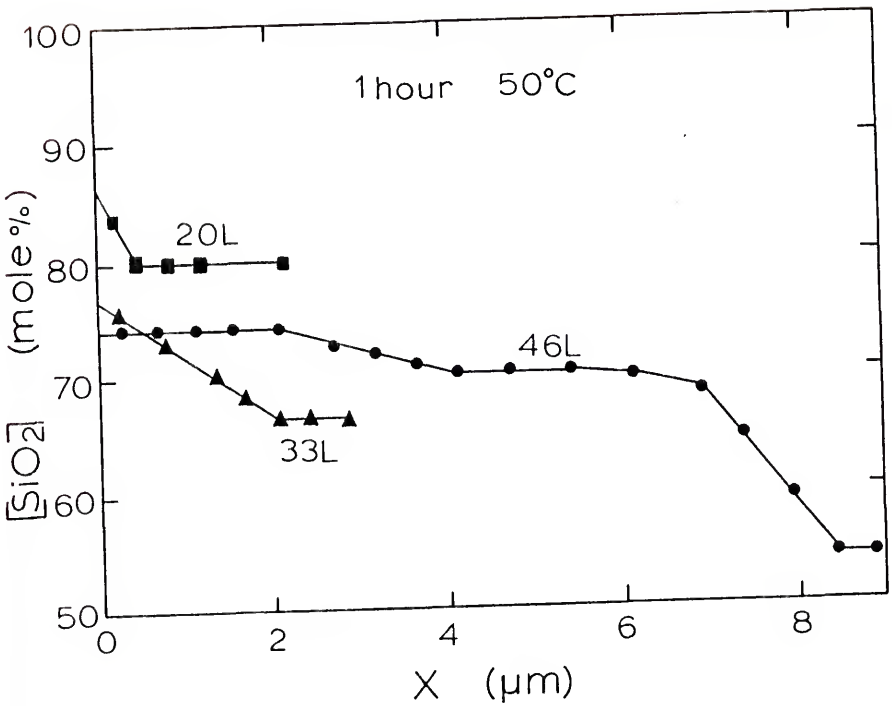

Fig. 58. SiO_2 concentration profiles for 20L, 33L and 46L glass surfaces corroded for 1 hour at 50°C.

leached layer is so thin that the bulk composition is obtained after 1 polish, indicating a leached layer thickness of less than 0.5 μm. The profile for the 33L sample has a constant SiO_2 concentration gradient. For the 46L sample there are two nearly linear regions with that nearest the surface having a smaller concentration gradient than that nearest the bulk glass.

Figure 59 shows scanning electron micrographs of these two glasses. The surface changes very little even after corroding 20L for 15 weeks at 50°C (Fig. 59a). The original polish scratches are still very visible. A marked different behavior is observed with 46L. A thick film forms on the surface of the glass with a large concentration of water which cracks and flakes off the surface after it dehydrates (Fig. 59b).

It was noted in Chapter II that is is possible to calculate the theoretical leached layer thickness from the corrosion parameter epsilon and the surface composition of the corroded glass. If one assumes a uniform concentration gradient, then,

$$\frac{\varepsilon}{(A/V)} = 0.5X\ (C_s - C_o) \qquad (83)$$

where epsilon, ε, is the excess silica in moles silica/cm^3, the surface area of exposed glass to volume of solution ratio, A/V, is cm^{-1}, the film thickness, X, is in cm and $C_s - C_o$ is the difference in the surface and bulk SiO_2 concentration. In Appendix E an equation is derived for

A

B

Fig. 59. (A) SEM of 20L corroded at 50°C for 1 week. (1000X)
(B) SEM of 46L corroded at 50°C for 1 week. (200X)

calculating the thickness of the leached layer, X. Using an A/V ratio of 0.77 and substituting into this equation gives,

$$X = 6.0 \times 10^5 \frac{\varepsilon}{\left(n_S^{SiO_2} - n_B^{SiO_2}\right)} \qquad (84)$$

where $n_S^{SiO_2}$ and $n_B^{SiO_2}$ are the mole fractions of SiO_2 at the glass surface and in the bulk glass respectively.

The theoretical thickness of the leached layer for a number of corroded glasses were calculated from Eq. 84. These thicknesses along with values for epsilon obtained from solution data and $[SiO_2]_S$ from IRRS compositional analysis of the corroded glass surfaces are listed in Table XVI. Values for the thickness of the leached layer determined from the profiles described earlier are also listed. The agreement between the calculated leached layer thickness and the actual thickness ($\pm$ a factor of 2 or 3) is very good considering the assumptions made and the number of times experimental error can enter the calculations and measurements.

By using the solution data to determine epsilon and IRRS data to determine the surface composition of the glass it is possible to model the development of the leached layer on the surface of corroding glasses (see Chapter II and Appendix B). Figure 60 shows a schematic representation of the development of the leached layer on the surface of corroding 20L, 33L and 46L glasses. Comparing Fig. 60 with Fig. 58 one can see that the 20N sample develops a surface much richer in SiO_2 faster than 33L and 46L while 46L develops a much deeper leached layer than 20L.

Table XVI. Calculated and Experimentally Determined Leached Layer Thicknesses.

Glass	Conditions	Epsilon ($mole/cm^3$)	$[SiO_2]_S$ (mole %)	$X_{calc.}$ (μm)	$X_{exp.}$ (μm)
33L	79°C, 17hour	2.0×10^{-5}	92	48	17
20L	50°C, 1hour	3.5×10^{-7}	93	1.6	0.5
33L	50°C, 1hour	5.8×10^{-7}	76	3.8	2.0
33L	50°C, 1day	3.0×10^{-6}	84	10.6	5.0
33L	50°C, 1week	5.2×10^{-6}	90	13.5	8.0
46L	50°C, 1hour	1.2×10^{-6}	74	3.6	8.0

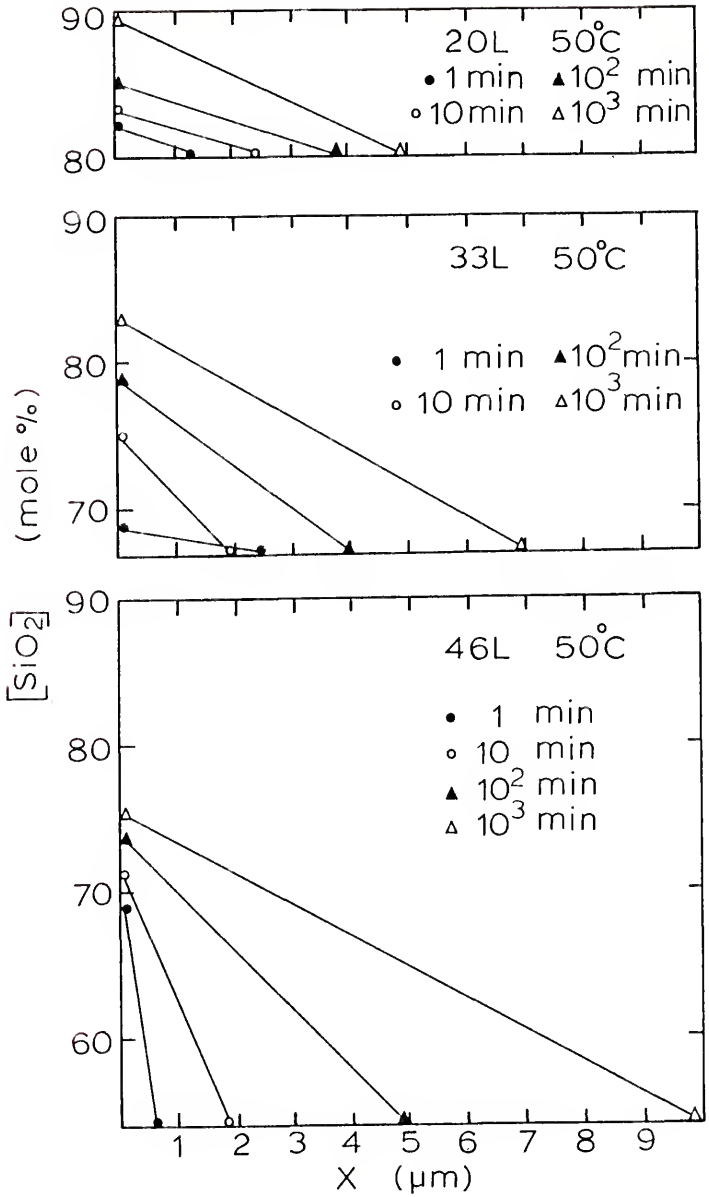

Fig. 60. Schematic SiO_2 concentration profiles for 20L, 33L and 46L corroded at 50°C for various times.

In Chapter VI the effect of temperature on the glass corrosion kinetics was described. Approximate order of magnitude time differences in corrosion rates exist for glasses corroded at 30°C, 50°C and 100°C. The effect of temperature on the development of the leached layer is represented schematically in Figs. 61 and 62. Approximately equivalent leached layers are produced for 33L glasses corroded at 30°C with those corroded 10 times shorter at 50°C and 100 times shorter at 100°C (Fig. 61). Similar results for 46L are observed (Fig. 62). These results are in good agreement with the time-temperature kinetics described in Chapter VI.

Differences in the development of the leached layer for the three alkali silicate systems is represented in Fig. 63. One can see that for the 20L sample the leached layer develops a very large concentration gradient in relation to the 20N and 20K samples while the leached layer becomes very deep for the 20N and 20K samples.

As a glass corrodes, silica also goes into solution and a certain thickness of the glass completely dissolves. This is represented in Fig. 64 where the thickness of glass dissolves is X_1 and the thickness of the leached layer is X. The thickness of glass completely dissolved due to the attack of the silica network can be calculated from the solution data (see Appendix E). Given the composition of the glass and the concentration of silica in solution (moles/l),

$$X_1 = 3.0 \times 10^2 \frac{[SiO_2]}{n^{SiO_2}} \qquad (85)$$

for an A/V ratio of 0.77.

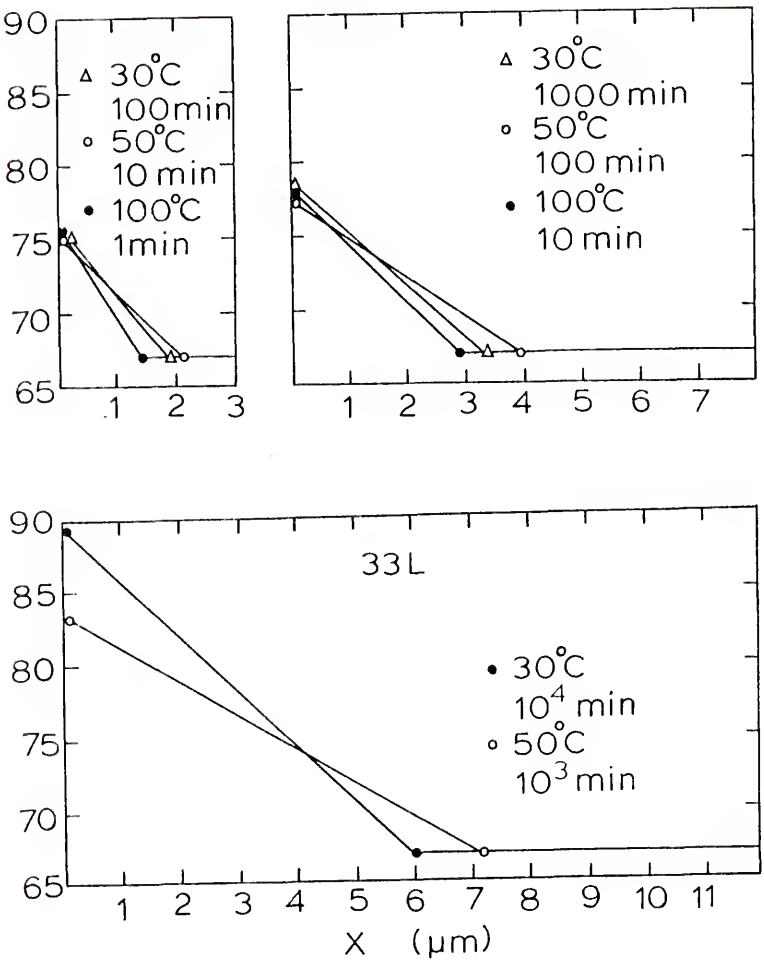

Fig. 61. Schematic SiO_2 concentration profiles for 33L corroded at 30°C, 50°C and 100°C for various times demonstrating nearly equivalent extents of corrosion at combinations of time and temperature.

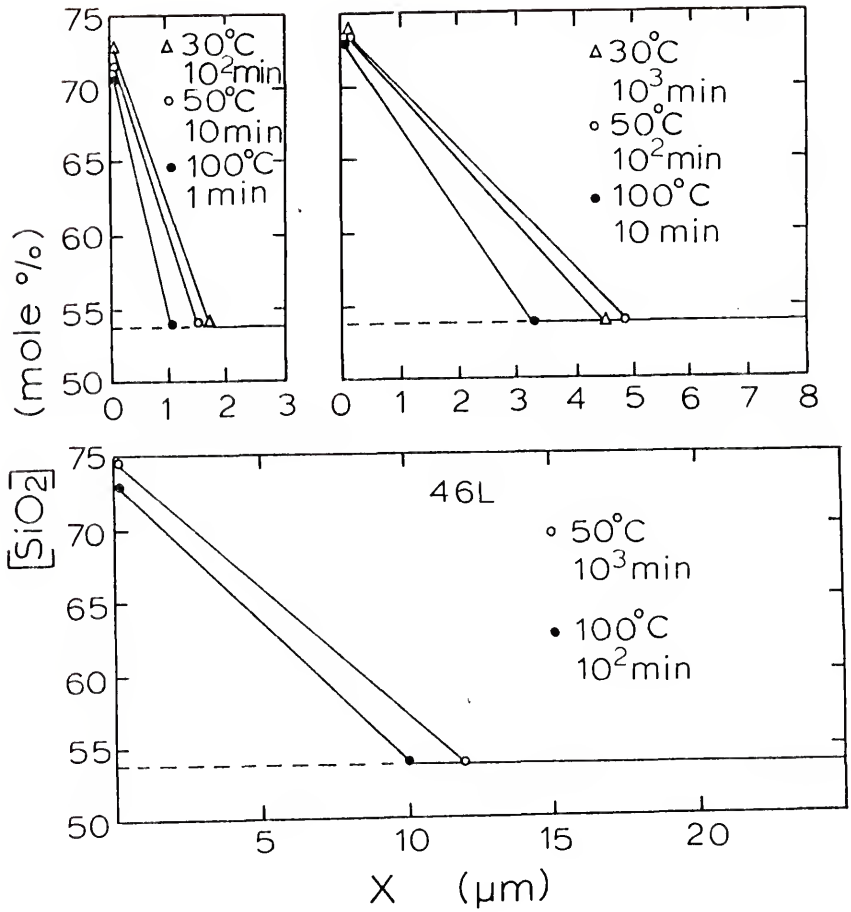

Fig. 62. Schematic SiO_2 concentration profiles for 46L corroded at 30°C, 50°C and 100°C for various times.

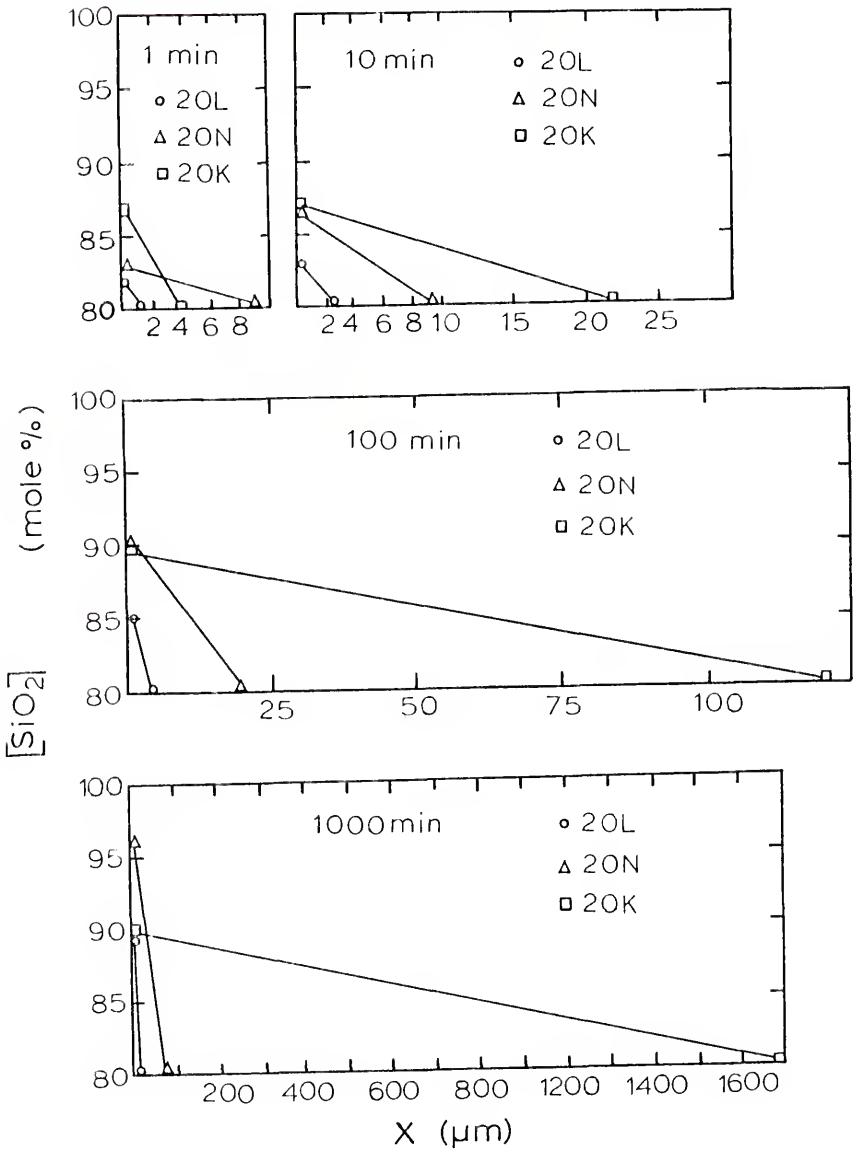

Fig. 63. Schematic SiO_2 concentration profiles for 20L, 20N and 20K corroded at 50°C for various times.

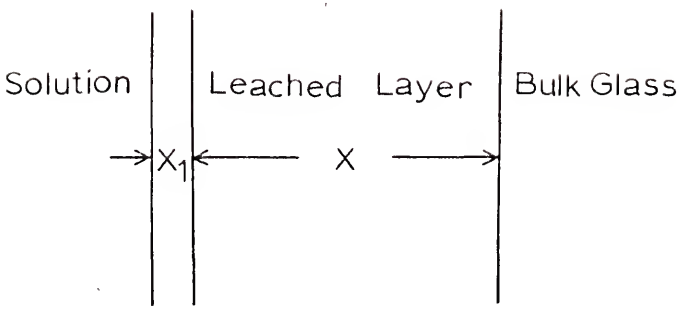

Fig. 64. Schematic representation of a corroding glass surface.

Figure 65a illustrates the changes in X and X_1 during the corrosion of 33L at 30, 50 and 100°C. Both X and X_1 increase with time during most of the corrosion process. At short times for 30°C the ratio X/X_1 decreases and reaches a relatively constant value at 10 min (see Fig. 65b). The same constant value is observed for 33L at 50°C for 1 to 1000 min and for 33L at 100°C for 10 min. Das[90] postulated that when the ratio reached a constant value, the $t^{\frac{1}{2}}$ controlled mechanism would change over to the t^1 mechanism (see Chapter II). This is not the case. The ratio remains constant until the time when the rate of silica extraction accelerates. For 33L at 100°C this occurs at approximately 40 min. The acceleration in the extraction of silica can be observed in the plot of X_1. At time < 40 min the slope is approximately 0.5, however, after 40 min the slope increases to precisely 1.0. The increase in silica extraction is accompanied by a decrease in the X/X_1 ratio. At approximately 10^3 min the value for X reaches a maximum value at precisely the same time that epsilon reaches a maximum (see Chapter VI). After this point in time X decreases and approaches zero at 1.4×10^4 min.

Summary

Quantitative analysis techniques involving peak wavenumbers and peak intensities are used to determine the surface compositions of a number of corroded binary alkali silicate glasses. The changes are

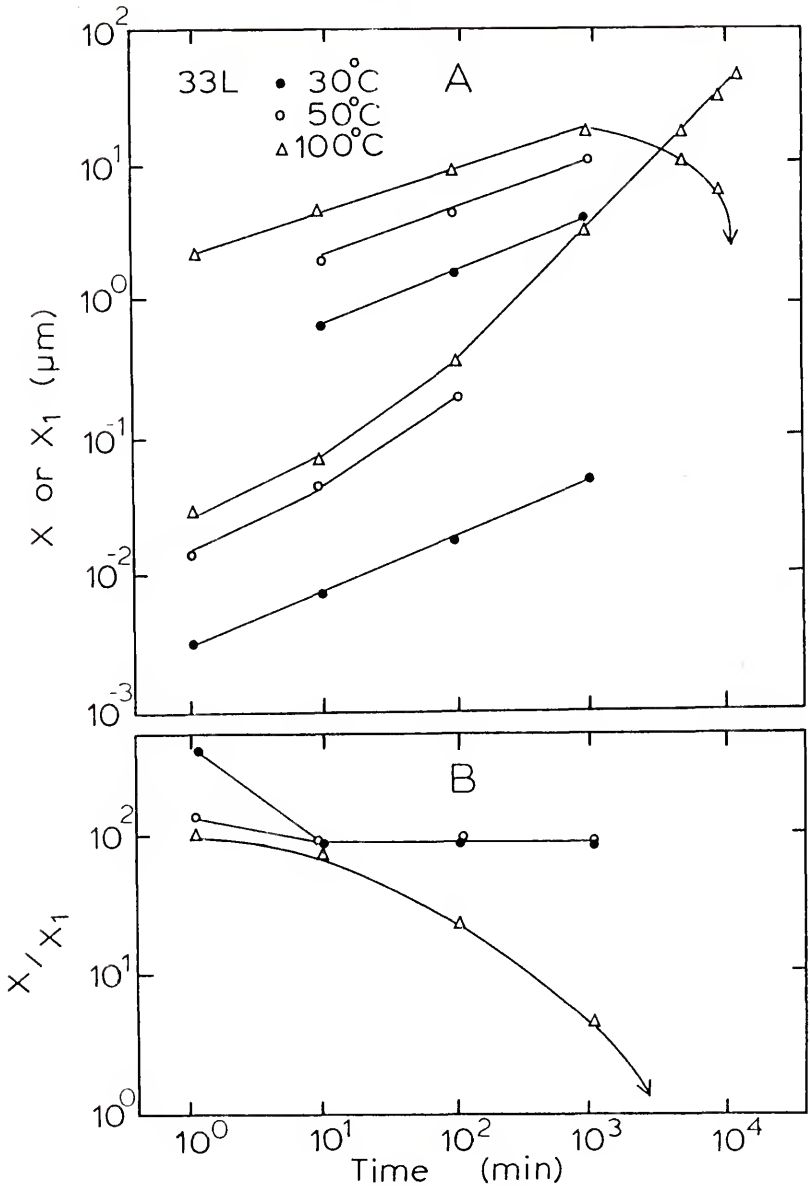

Fig. 65. (A) *Log* thickness of the leached layer, X, and the thickness of the dissolved layer of glass, X_1, (μm) vs. *log* time (min) for 33L corroded at 30°C, 50°C and 100°C.
(B) *Log* vs. (X/X_1) vs. *log* time (min) for the same conditions.

related to the results from Chapter VI. The thickness of the leached layer, X, on the surface of the glasses is calculated and hypothetical composition profiles are related to profiles determined using the new technique from Appendix D. Values are also determined for the thickness of glass completely dissolved, X_1. The X/X_1 ratio is used to describe the changes on the surface of corroding glasses.

CHAPTER IX

MECHANISMS OF BINARY ALKALI SILICATE GLASS CORROSION

Introduction

The state of understanding of the mechanisms of glass corrosion was described in Chapter II. In general the corrosion of glass involves two processes, the selective leaching of some glass constituents (i.e. alkali ions) and the attack of the glass network (i.e. silica). Each of these two processes has a $t^{\frac{1}{2}}$ limiting condition at short times (in acidic and neutral solution) and a t^{1} limiting condition at long times (in alkaline solution).

The short time diffusion controlled process for the leaching of alkali ions involves an ion exchange with the limiting species being either tha alkali ion or the H^{+} (H_3O^{+}) ion. Rana and Douglas[47] calculated the interdiffusion coefficients for the ion exchange process for several glasses (see Tables VI and VII in Chapter II). The large differences between the interdiffusion coefficients and self diffusion coefficients (determined from electrical conductivity measurements) indicate that the surface of the glass undergoes a dramatic change during corrosion. They argued that the use of conductivity or other measurements which determine the diffusion

coefficients of alkali ions are not reliable indicators of the reactivity of a glass to aqueous solutions. An objective of this chapter is to examine the dependence between the bulk composition of glass and the interdiffusion coefficient for glasses in the three binary alkali silicate glass systems in order to determine why the interdiffusion coefficients are much different than the self diffusion coefficients of bulk glasses.

A diffusion controlled process is also implied for the short time extraction of silica into acidic or neutral solution. Doremus[23] speculated that a diffusion controlled process limits the silica extraction rate with the controlling species probably being "H_2O" which penetrates to form two ≡Si-OH groups. In this chapter diffusion coefficients for the limiting step in silica extraction are calculated from the solution data. Deductions are made from the results concerning the species controlling the silica extraction.

Leaching of Alkali Ions

Interdiffusion coefficients can be calculated from the $t^{\frac{1}{2}}$ reaction rate constants for the leaching of the alkali ions (Chapter VI) using Eq. 34 (Chapter II) if it is assumed that the alkali ion is the limiting species. Interdiffusion coefficients for glasses in the binary alkali silicate systems are shown in Fig. 66. The interdiffusion coefficients follow straight lines on a plot of $\ell og\ \bar{D}$ vs. $[SiO_2]$ and they fit the following,

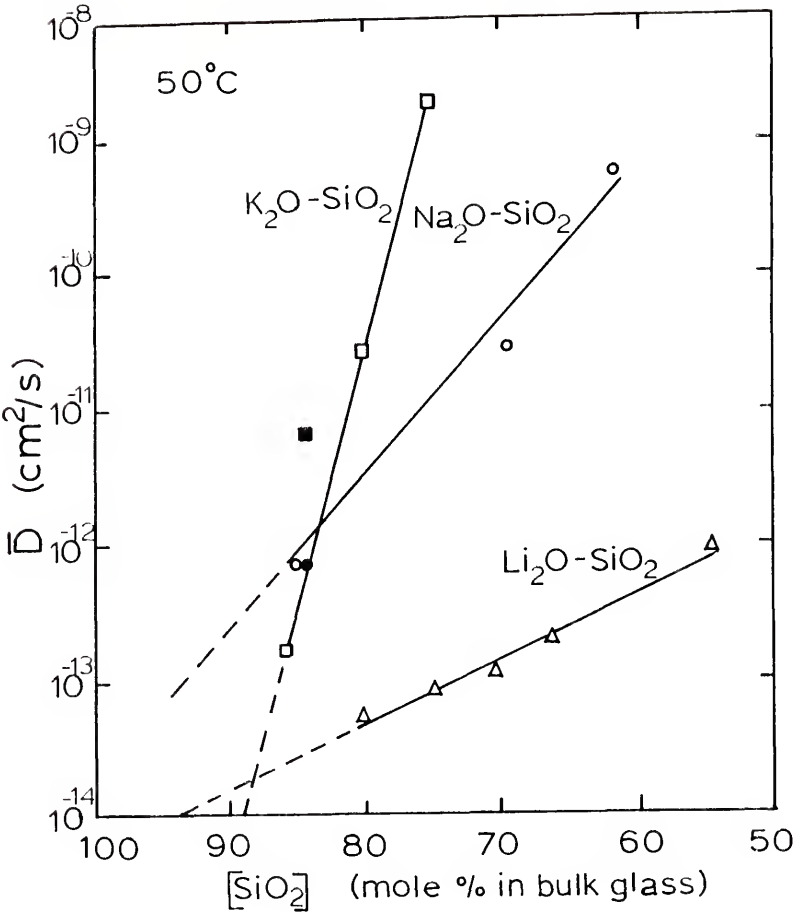

Fig. 66. Interdiffusion coefficients for the ion exchange between the alkali ion and the H^+ (H_3O^+) ion as a function of the composition of the bulk glass.

$$\bar{D} = a \exp(b n_{R_2O}) \qquad (86)$$

where a, and b are constants and n_{R_2O} is the mole fraction of alkali oxide in the bulk glass. For the Li_2O-, Na_2O- and K_2O-SiO_2 glass systems, the values for a are 5.8×10^{-15}, 1.7×10^{-14} and 8.0×10^{-19} respectively and the values for b are 10.9, 26.1 and 86.8 respectively. Equation 86 is similar to Eq. 28 (Chapter II) which describes the sodium concentration dependence on the diffusion coefficient in the bulk glasses.

The interdiffusion coefficients calculated by Rana and Douglas[47] for 15N and 15K are also given in Fig. 66. Their value for 15N corresponds almost exactly with the value determined in this work. Their value for 15K on the other hand, is considerably different from that expected from the line in Fig. 66. Because of the large compositional dependence of $\bar{D}$, a variation in composition by 2.5 mole %, however, would put their value on the line. The concentration dependence of the interdiffusion coefficient is much greater for the K_2O-SiO_2 system than for the Na_2O-SiO_2 system and both are greater than for the Li_2O-SiO_2 system. For binary alkali silicate glasses with greater than 20 mole % alkali oxide, the interdiffusion coefficient increases as the size of the diffusing alkali ion increases.

Values of $\bar{D}/D_c$ can be calculated for the Na_2O- and K_2O-SiO_2 systems. Self diffusion coefficients for Na^+ and K^+ ions in binary alkali silicate listed in Table II (Chapter II) are plotted in Fig. 67. Data in Fig. 66 and 67 yields the values for $\bar{D}/D_c$ in Fig. 68.

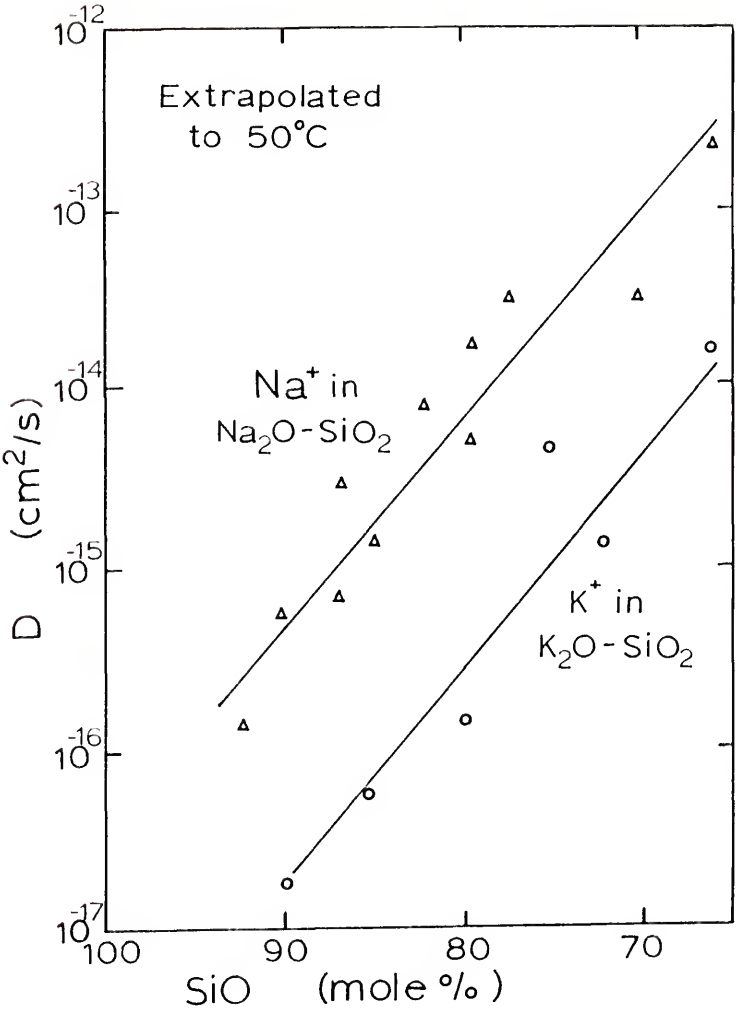

Fig. 67. Tracer diffusion coefficients for Na^+ and K^+ ions in the Na_2O-SiO_2 and K_2O-SiO_2 systems respectively.

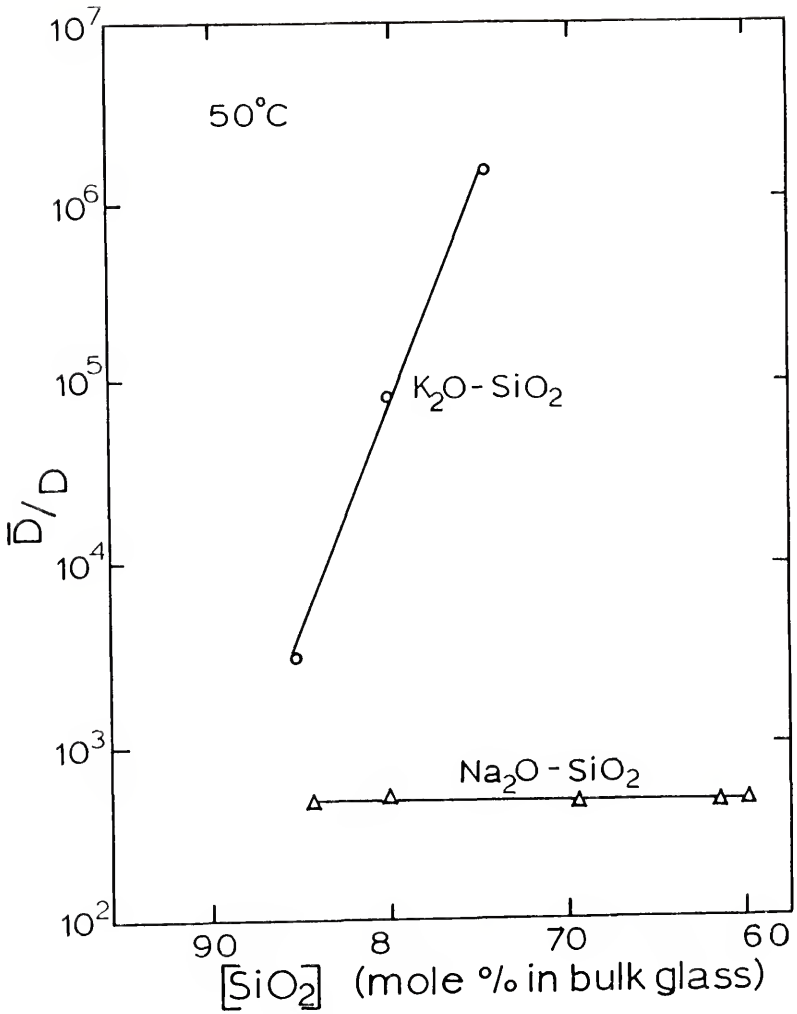

Fig. 68. Values for $\bar{D}/D_c$ as a function of glass composition for the Na_2O- and K_2O-SiO_2 systems.

The glasses in the K_2O-SiO_2 system have a large compositional dependence in the composition range of 15 to 40 mole % Na_2O. The calculation of the interdiffusion coefficient requires the assumption that the diffusion coefficient of the alkali ion is much smaller than that for the interdiffusing species (H^+ or H_3O^+).[45] The corrosion process leading to the extraction of alkali ions involves an ion exchange process with the measured interdiffusion coefficient being a function of the diffusion coefficients of the two interdiffusing species (see Eq. 35). A value for $\bar{D}/D_c > 1$ implies that the tracer diffusion coefficient of the species interdiffusion with the alkali ions is greater than the tracer diffusion coefficient for the alkali ion. These data indicate that the diffusion of the alkali ions is the limiting step in the ion exchange process.

Baucke[81] studied a glass that has a $\bar{D}/D_c < 1$ which implies that the interdiffusing species limits the ion exchange process. A mathematical analysis of the composition profiles on the corroded glass surface confirms that H^+ ions do in fact limit the ion exchange process for these glasses. An ion exchange process for another glass was found by Doremus[209] to be limited by the diffusion of H_3O^+ ions.

It must be remembered that the glasses studied by Baucke[81] and Doremus[209] are multicomponent glasses with a relatively good resistance to attack (as compared with binary alkali silicate glasses). The binary alkali silicate glasses lack the constituents present in the glasses above which stabilize the surface; therefore, they are much less resistant to attack by aqueous solution so they readily become hydrated (produce Si-OH groups) by way of the ion exchange reaction.

When this occurs the H^+ ion mobility increases because the surface becomes a protonic conductor (see Chapter II). For these glasses the interdiffusing species has a mobility greater than that for the alkali ions and $\bar{D}/D_c > 1$.

The diffusion of univalent cations in bulk glasses, D_c, is dependent on two factors, the openness of the structure (size of the cation) and the interaction with O^{2-} ions (ionic field strength of the cation), see Chapter II. The results obtained from calculations of $\bar{D}$, can be explained in terms of the glass surface becoming more open as H^+ ions replace the alkali ions. As the structure becomes more open it affects the glasses with the larger alkali ions the greatest. The larger compositional dependence for alkali ions with larger ionic radii confirms that the glass structure becomes more open during the corrosion process. The absolute values for $\bar{D}$ also increase as the radius of the alkali ion increases. Since the openness of the structure becomes less of an obstacle to the diffusion of the alkali ions, the interaction with the O^{2-} ions becomes more significant. This explains why the glasses with Li^+ ions which interact the most with the network have the lowest $\bar{D}$, while $\bar{D}$ is larger for glasses with Na^+ and K^+.

Extrapolations of the straight lines in Fig. 66 to less than 10 mole % alkali oxide indicate a change in the realtive order of the interdiffusion coefficients. These extrapolated interdiffusion coefficients at very low alkali oxide concentrations are in the same order as the diffusion coefficients in the bulk glasses with Na^+ ions being

the most mobile. The mobility of the Li^+ ions is close to that for Na^+ ions but the K^+ ions have a much lower mobility (see Chapter II). In fact the extrapolation of the line for the K_2O-SiO_2 system to 100% SiO_2 yields precisely the same value (1.2×10^{-18} cm^2/sec) as the extrapolation of the bulk K^+ ion diffusion line (Fig. 67). These data indicate that at low alkali oxide concentrations the surface of the glass undergoes much less change so that the rate of leaching is controlled by both the size of the cation and the field strength of the cation as is the case for bulk ionic diffusion.

The straight line on the $\log (\bar{D}/D_c)$ vs. $[SiO_2]$ graph for the K_2O-SiO_2 system intersects $\bar{D}/D_c$ at a value of precisely 1.0 at 100% SiO_2. This supports the theory that the leached layer on the surface of K_2O-SiO_2 glasses is very open and that the rate of leaching is determined by the openness of the structure.

Silica Extraction

The rapid attack of vitreous silica and multicomponent glasses by chelators and alkaline solutions is controlled by interfacial reaction mechanisms and a t^1 behavior prevails. This is not observed for the extraction of silica from binary and multicomponent glasses in acidic and neutral solutions. It is possible that a diffusional controlled mechanism limits the extraction of silica into these solutions. Doremus[58] speculated that the diffusion of water a few

atomic distances into the glass might be the controlling process but a rigorous model has not been proposed. The diffusion of water into glass and the hydration of glass surfaces were discussed in Chapter II. The hydration of vitreous silica occurs by either the diffusion of molecular water into the glass or by the separate diffusion of H^+ and OH^- ions in the glass.

During glass corrosion H^+ (or H_3O^+) ions must interdiffuse with the alkali ions. These H^+ ions replace alkali ions forming Si-OH groups. It is very unlikely from an energetics standpoint that H^+ ions by themselves would attack the silica network.[196] The glass structure is known to be attacked by OH^- ions, however, and Charles[40] attributed the rapid attack of water vapor on glass to the reaction of OH^- ions with the glass network as in Eq. 66. He wrote that there is a well-defined attacked region in the glass surface which is distinguishable from the unattacked glass. Other authors have written that a transition occurs in the silica rich leached layer on the glass surface.[180] It is possible that the transition in the silica rich leached layer occurs by the polymerization of some Si-OH groups (see Chapter VII) and by the reaction of OH^- ions with weaker Si-O bonds[180] to relieve strains developed by the ion exchange process. The result is a silica rich leached layer in equilibrium with water as Rana and Douglas[84] speculated, however, it more likely resembles a porous vitreous silica structure rather than a pure silica gel (see Chapter VII). During the transformation reaction weakly bound tetrahedra are most likely to be attacked to relieve the strain. Evidence of such

weakly bonded tetrahedra comes from shifts of the S peak in IRRS spectra to a lower frequency,[162] increasing bond lengths from X-ray studies,[208] and decreases in the elastic modulus and strength of glasses[167] as alkali oxide is added. Once attacked, freed silica groups could diffuse through the transformed porous leached layer and out into the solution.

If one assumes that the limiting step for the extraciton of silica is the diffusion of silica through the transformed surface layer diffusion coefficients can be calculated from Eq. 34.

The absolute values of D calculated for the extraction of silica are much lower than those for the leaching of alkali ions. This confirms that the two processes are independent. Values for the diffusion coefficients are plotted in Fig. 69 as a function of the bulk glass composition. The compositional dependence of D is greatest for the K_2O-SiO_2 system and least for the Li_2O-SiO_2 system. Exchange of H^+ ions for K^+ ions results in a more open leached layer and produces the greatest strain facilitating the transformation reaction. The Li_2O-SiO_2 glasses have the lowest values for D. These glasses are also the most stable in aqueous solution. This results from less strain being induced when H^+ ions replace Li^+ ions. Many Si-OH groups are thereby able to polymerize (see Chapter VII) producing a structure which is less open and stronger than the K_2O- and Na_2O-SiO_2 glasses.

These data support the proposed mechanism for the $t^{\frac{1}{2}}$ release of silica into acidic and neutral solutions. This mechanism is not confirmed absolutely, however. If one extrapolates the lines in Fig.

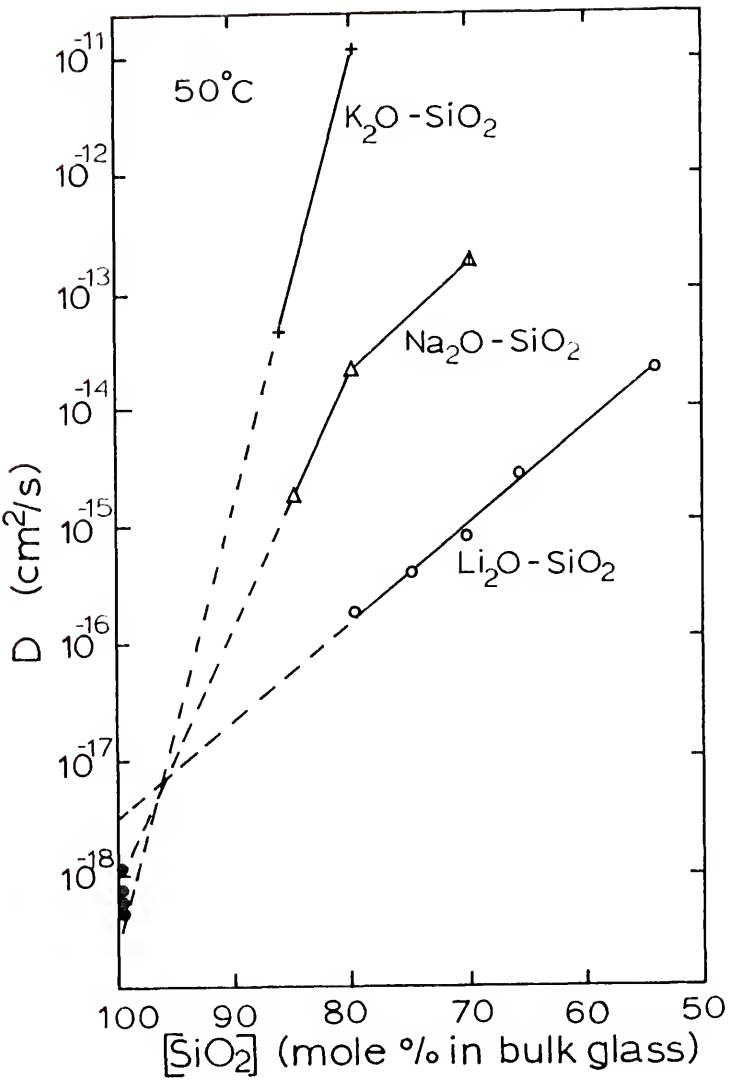

Fig. 69. Diffusion coefficients for the species limiting the extraction of silica into solution (OH^- ion) as a function of the composition of the bulk glass.

69 to 100% SiO_2 the values obtained are very close to the value for the diffusion of OH^- ions into vitreous silica. It seems from these data that the actual limiting mechanism, whether the diffusion of silica groups out of the glass or the diffusion of OH^- ions into the glass, cannot be deduced from this data. Further work is needed to determine the actual mechanism for the $t^{\frac{1}{2}}$ dependent release of silica into solution.

Summary and Conclusions

In this chapter interdiffusion coefficients are calculated for the ion exchange reaction involving alkali ions and H^+ ions for the different glasses in the Li_2O-, Na_2O- and K_2O-SiO_2 systems. The values of $\bar{D}$ are plotted vs. composition of the bulk glass. The increasing compositional dependence of $\bar{D}$ as well as increasing absolute values of $\bar{D}$ with increasing size of the alkali ion indicate that the interdiffusion process is controlled by the diffusion of the alkali ions out of the glass and by the openness of its leached layer.

Values of $\bar{D}/D \gg 1$ indicate that the diffusion of the alkali ions out of the glass is the controlling step and that this is a correct assumption in the calculation of $\bar{D}$.

A model is proposed for the $t^{\frac{1}{2}}$ release of silica into acidic and neutral solutions. Diffusion coefficients are calculated which support a model in which OH^- ions attack the glass network during a

transformation reaction freeing silica groups which diffuse out of the glass surface through the transformed region of the silica rich leached layer.

CHAPTER X

SUMMARY AND SUGGESTIONS FOR CONTINUED RESEARCH

Glass corrosion is such a complex process the state of the corrosion literature is in quite a state of confusion. For this reason a critical review of the corrosion literature and related subjects was presented in Chapter II. There are quite a few generalizations which can be made. Glass corrosion is comprised of basically two types of reactions occurring simultaneously. The glass modifiers (i.e. alkali ions) selectively leach from the surface of the glass by an ion exchange with primarily H^+ ions and to a much lesser extent with H_3O^+ ions. The ion exchange reaction is controlled by the interdiffusion of these ions, resulting in a $t^{\frac{1}{2}}$ dependence for the leaching of alkali ions. Concurrent with the ion exchange reaction is a reaction in which the glass network is attacked. At short times the rate of extraction of silica follows a $t^{\frac{1}{2}}$ dependence indicating that a diffusional process controls the kinetics.

The above processes occur in acidic and neutral solutions; and since the leaching of alkali ions is much greater than the rate of silica extraction, a leached layer develops on the surface of the glass. As corrosion proceeds in a static environment (constant A/V

ratio), the pH increases as a result of the ion exchange reaction. This brings about a general increase in the corrosion kinetics until the leaching of alkali ions and the extraction of silica become linear functions with time.

In Chapter IV it was shown that the gradual increase in reaction kinetics from a $t^{\frac{1}{2}}$ to a t^{1} dependence observed in the literature is a result of tests using glass grains. Tests with bulk glass surfaces, on the other hand, revealed a rather sharp transition from $t^{\frac{1}{2}}$ to t^{1} kinetics for the extraction of silica.

In Chapters IV, VI, VII and VIII the kinetics of static corrosion of binary alkali silicate glasses were discussed. The kinetics were followed by many parameters. The concentrations of alkali ions and silica in solution and the pH of the solutions were monitored vs. time. From these conditions values for alpha and epsilon were calculated. The surface SiO_2 concentration was determined using the method outlined in Appendix C. Theoretical leached layer thicknesses were calculated in Chapter VIII using the procedure described in Appendix E and were checked by experimentally determined surface composition profiles (see Appendix D). The thickness of completely dissolved glass, X_1, was also determined for several glasses and the changes in the X/X_1 ratio were related to the kinetics from the previous chapters.

A general sequence of changes was observed for the binary alkali silicate glasses. At short times the reaction kinetics for the leaching of alkali ions and for the extraction of silica both followed

parabolic courses with time. This is represented by reaction rate exponents, a, approximately equal to 0.5 (see Table XIII, Chapter VI). The reaction rate constants, k, were also determined for the extraction of glass components and are listed in Table XV (Chapter VI). The reaction rate constants are over an order of magnitude smaller for the extraction of silica than for the leaching of alkali ions during this $t^{\frac{1}{2}}$ regime indicating that the ion exchange process is much faster than the silica attack.

The leached layer on the surface of the glasses, therefore, results from the inequity of the extraction rates of the two independent processes. The small values for alpha and the increasing values of epsilon and X with time are indicative of the formation of the leached layer. Infrared reflection spectra from Chapter VII provide additional evidence of the ion exchange reactions occurring during this regime. The S peak increases in intensity and shifts to higher wavenumbers.

As the surface becomes depleted of alkali ions they are replaced by H^+ forming Si-OH groups. A transformation occurs in the surface by an esterification reaction in which two Si-OH groups react to form a new Si-O-Si bond and a molecule of water. The result is an increase in the surface SiO_2 concentration. The transformation does not decrease the diffusion coefficient for the alkali ions, however. This is observed by the low concentration gradients near the surface of the glass (Chapter VII) and by the large interdiffusion coefficients (Chapter IX). The transformation probably occurs to relieve strains

introduced by the ion exchange reaction but in the process it does not completely restrict further diffusion of alkali ions out of the glass. The polymerization of Si-OH groups is more likely for the Li_2O-SiO_2 glasses than for the Na_2O- and K_2O-SiO_2 glasses. This makes glasses in the Li_2O-SiO_2 system resistant to the attack by water for compositions as low as 46 mole % Li_2O. The Na_2O- and K_2O-SiO_2 systems are not nearly as stable at much lower concentrations of alkali oxide. The formation of this silica rich leached layer on the surface of Li_2O-SiO_2 glasses give them their outstanding chemical durability.

In a sense the silica rich surface can be considered a passivation film, in another it cannot. A transformation occurs in the silica rich leached layer which limits the network attack by OH^- ions and the free silica produced by this reaction during the transformation has to diffuse through the silica rich transformed leached layer. The transformed silica rich leached layer is, therefore, a protective film in the sense that it is a diffusion barrier to network breakdown and the release of silica into solution. The silica rich surface does not, however, decrease the interdiffusion coefficient for the ion exchange reaction.

As the corrosion proceeds in a closed system (static corrosion) the pH of the solution increases. It was observed in Chapter IV and confirmed in Chapter VI that the kinetics for the extraction of silica undergo a change when the pH of the solution becomes approximately equal to 9.5. This is due to the ionization of surface silanol groups and the depolymerization of silica groups from the surface in a

reaction with water. The result is a rapid change at this time from $t^{\frac{1}{2}}$ to t^{1} kinetics and a much more rapid rate of silica extraction. As the rate of silica extraction increases it eventually becomes equal to the leaching rate for the alkali ions and a temporary steady state condition is established. This is represented by a maximum value for epsilon, X, and the surface SiO_2 concentration. At this time the leaching of alkali ions changes to follow t^{1} kinetics.

This steady state condition is not like that described by Lyle.[46] Lyle said that for the steady state condition to occur the extraction of alkali ions would decrease until eventually the two rates become equal. If this occurs both extraction rates would continue to follow a $t^{\frac{1}{2}}$ dependence. This type of steady state condition might occur for test conditions where the A/V ratio is very small or for a continuously replenished solution so that the test solution remained acidic or neutral. Additional work is needed to check for this type of steady state condition. This could be accomplished by leaching a glass in a continuously replenished solution. The attainment of a maximum value for epsilon at a time when the rate of leaching of alkali ions and extraction of silica both follow a $t^{\frac{1}{2}}$ dependence would be proof of such a process.

As the pH of the solution continues to increase, the rate of silica extraction exceeds the leaching rate for the alkali ions and the leached layer begins to dissolve. This is demonstrated by a decreasing value of epsilon and a decreasing surface SiO_2 concentration. Concurrently the thickness of the leached layer, X, decreases

and the X/X_1 ratio decreases. Eventually the leached layer becomes completely dissolved with epsilon, X and X/X_1 equal to zero and the surface SiO_2 concentration equal to that of the bulk glass. After this point in time the binary alkali silicate glasses undergo congruent dissolution.

The problem associated with accelerated tests used for corrosion studies of glasses was also examined in this dissertation. The corrosion of glass grains was compared with the corrosion of bulk glass surfaces in Chapter IV. The conclusion was that typical glass grain tests have several factors which make them inferior to the bulk glass tests. The most significant of these factors is the concentration cell effect which locally increases the A/V ratio of some grains. The net analysis of these tests are, therefore, a mixture of the effects of the different conditions to which the grains are exposed. This was shown to be an effect which complicates the interpretation of glass corrosion kinetics.

In Chapter V a new way was demonstrated for presenting glass corrosion data in terms of the A/V ratio. The data from bulk corrosion tests was found to agree with mathematical relations derived from the kinetic equation. Data from glass grain corrosion tests, however, could only be interpreted in terms of the surface area of the grains being a function of time.

In Chapter VI it was shown that the transition from $t^{\frac{1}{2}}$ to t^1 kinetics for the dissolution of silica occurs at a relatively constant concentration of alkali ion in solution for a particular glass system.

Since the processes become greatly accelerated when the t^{1} regime of silica network attack occurs. The time to reach this concentration of alkali ion is, therefore, a critical time in the corrosion of these glasses. Before the critical time the corrosion processes are diffusionally controlled and have the lowest reaction rate constants. After this critical time the rapid attack of the silica network results. A plot of the time to reach this critical time vs. the A/V ratio can be used to predict corrosion at different A/V conditions. Once the critical times are determined for bulk glass surfaces one can extrapolate to determine the time to reach the critical conditions for conditions with much larger A/V ratios (crack tip corrosion) or much smaller A/V ratios (continuously replenished solution with a constant rate of replenishment).

The use of glass powders enables one to examine glass corrosion at very large A/V ratios. Under these conditions the time required to reach a critical condition is many orders of magnitude smaller than conditions under which the glass will be used in service. The corrosion of glass powders, therefore, offers the opportunity to examine the corrosion of very durable glasses in much shorter times. Problems associated with the corrosion of glass powders, however, make critical time vs. A/V analysis much more difficult. More work is needed to completely characterize all of the effects associated with the corrosion of glass powders. When the corrosion of glass powders becomes completely predictable, then plots of the critical time vs. A/V ratio for glass grains will become a very useful

prediction technique. By using short time very large A/V ratio it should be possible to extrapolate to very long time in service A/V ratio conditions.

This type of analysis could be used to predict the behavior of glasses used to contain nuclear wastes. Another problem is encountered with these glasses, however. Since they are invert glasses their simple corrosion characteristics are not known. A change in corrosion kinetics may not occur at a pH = 9.5 for these glasses. It would be necessary, therefore, to examine in detail the corrosion kinetics of a representative composition of these invert glasses. After a critical corrosion parameter is determined it would be possible to use the critical time vs. A/V method to predict their corrosion behavior.

As was noted in Chapters VI, VII and VIII, the primary effect of temperature on the corrosion of binary alkali silicate glasses is to shift the time sequence of events which occur during the corrosion process. Tests at elevated temperatures, therefore, offer the advantage of accelerating the corrosion processes by orders of magnitude. After the proper constants are determined it is possible to extrapolate from high temperature short time tests to lower temperature long time in service conditions to predict the time to corrode to an equivalent extent of corrosion.

An analysis involving elevated temperatures and very large A/V test conditions will most likely be needed to predict the behavior of the nuclear containment glasses. This type of research is needed and hopefully the problems with long term prediction can be worked out.

Appendix A

DERIVATION OF ALPHA

Sanders[4] calculated values for alpha and epsilon from solution data using an incorrect formula for alpha. For this reason the author feels it is worthwhile to present correct derivation of alpha which will be used throughout this study.

Define the congruent dissolution of glass to be that corrosion process in which no glass constituent leaches preferentially in relation to any other glass constituent. Also, define alpha to equal one for congruent dissolution. If congruent dissolution occurs, the ratio of silica to alkali atoms (or ions) in solution must equal the ratio in the glass,

$$\frac{[\text{Silica}]}{[R_2O]} = \frac{[\text{Silica}]}{\frac{1}{2}[R^+]} = \frac{1-m}{m} \qquad (87)$$

where the glass composition is $mR_2O \cdot (m\text{-}1)SiO_2$ and the terms in brackets represent molar concentrations in solution. Rearranging terms one gets,

$$1 = \frac{[\text{Silica}]}{2[R^+]} \cdot \frac{m}{1-m} = \alpha \qquad (88)$$

Since alpha equals one under these conditions, Eq. 88 is by definition the equation for alpha.

The corrosion process of dealkalization is common for most glasses for the early stages of corrosion, such that the ratio of silicon to alkali atoms (ions) in solution is much smaller than in the glass. Under these conditions alpha has a value $0 < \alpha \leq 1$. The value of alpha, therefore, gives a measure of the extent of selective leaching of glass constituents from the surface.

A value of alpha > 1 has no significance in aqueous glass corrosion processes since the selective leaching of alkali ions is prevalent and selective leaching of silica is not observed.

It should be noted that alpha could have been defined as,

$$\alpha = \frac{2[R^+]}{[\text{Silica}]} \cdot \frac{1-m}{m} \qquad (89)$$

however, Eq. 89 yields alpha in the range of $1 < \alpha < \infty$ for the selective leaching regime. Equation 88 is, therefore, preferred since it provides normalized values for alpha between 0 and 1.

Appendix B

CALCULATION OF GLASS GRAIN SURFACE AREAS

The surface area of the glass grains used in Chapter IV were calculated by a procedure used by Budd and Frankiewicz.[53] Assume the glass grains are spheres with a diameter equal to an average of the limiting screen sizes. The radii of the spheres appears in Table XVII.

The density of the glass is approximately 2.4 g/cm^3 so the volume of one gram of glass is 0.417 cm^3/g.

The number of spheres per gram of glass, N, is equal to the volume of one gram of glass divided by the volume of the sphere,

$$N = \frac{V\ (1\ g)}{V\ (\text{each sphere})} = (9.95 \times 10^{-2}\ cm^3)\ \frac{1}{r^3} \qquad (90)$$

The number of spheres for one gram of each mesh range is given in Table XVII.

The total surface area per gram of glass, A, equals the number of spheres, N, times the surface area of each sphere, S_s,

$$A\ (1\ g) = N \cdot S_s = (9.95 \times 10^{-2}\ cm^3)\ \frac{1}{r^3}\ (12.6)r^2 \qquad (91)$$

$$A\ (1\ g) = 1.25\ \frac{1}{r} \qquad (92)$$

Table XVII. Values Used to Calculate Glass Grain Surface Areas.

Mesh Range	r (cm)	N	A (cm^2/g)	A/V (cm^{-1})	Reference
-4 + 6	2.03×10^{-1}	11.8	6.16	0.123	
-10 + 20	5.10×10^{-2}	7.5×10^{3}	24.5	0.430	
-45 + 60	1.51×10^{-2}	2.9×10^{4}	82.8	1.66	
-100 + 200	5.6×10^{-2}	5.7×10^{5}	223	4.46	
-25 + 60			38 - 62		47
-240 + 300			450		53

The total surface area per gram of glass of each mesh range is given in Table XVII. Values for other mesh ranges used by Rana and Douglas[47] and Budd and Frankiewicz[53] are included for comparison. The surface area of glass to volume of solution, A/V, ratios used to corrode the glass grains in Chapter IV (1 g glass/50 ml solution) are also listed in Table XVII.

Appendix C

QUANTITATIVE ANALYSIS OF CORRODED GLASSES UTILIZING INFRARED REFLECTION SPECTROSCOPY

Introduction

Infrared reflection spectroscopy (IRRS) is a very useful tool for studying glass surfaces as was discussed in Chapter II. One important use for IRRS is for quantitative analysis of glass surfaces. Shifts in peak frequencies[156,163] as well as changes in peak intensity[164] have linear relations with the glass composition. Sanders et al.[25] stated that the linear behavior of reflectance vs. composition makes IRRS an excellent nondestructive analytical tool for the determination of the alkali concentration of alkali silicate glasses. Infrared reflection spectroscopy is especially useful for Li_2O-SiO_2 glasses since lithium has a low atomic number and is not easily detected using X-ray techniques.

Sanders and Hench[21] described qualitatively the changes in a 33L glass surface as it undergoes dealkalization during glass corrosion. The changes in the spectra (see Chapter II) verify the formation of a leached layer on the surface of the glass which is rich in silica. Recently Clark et al.[155] developed a quantitative analysis

technique utilizing frequency shifts to determine the surface composition of corroded soda containing glasses.

The purpose of this appendix is to examine the use of peak frequency shifts and intensity changes as quantitative analysis techniques for determining the surface composition of corroded glasses. Analytical problems associated with corroded glass surfaces will be discussed.

Results and Discussion

Certain changes in the IRRS spectrum are observed when alkali oxide is added to vitreous silica (see Chapter II). Of particular interest is the silicon bridging oxygen (S) peak. In Fig. 70 one can see that for the Na_2O-SiO_2 system, as the concentration of Na_2O in the glass increases (concentration of SiO_2 decreases), the wavenumber and the intensity of the S peak decrease.

The relationship between the wavenumber of the S peak and the concentration of alkali oxide in the glass for the three systems is shown in Fig. 71. A linear relation exists for the Na_2O-SiO_2 system to about 22% Na_2O. Beyond this composition a reversal occurs in which the wavenumber begins to increase again. This is in agreement with other investigators who attributed the reversal to a critical nonbridging oxygen concentration.[156,163] There are two separate linear regions for the Li_2O-SiO_2 system with a break at approximately

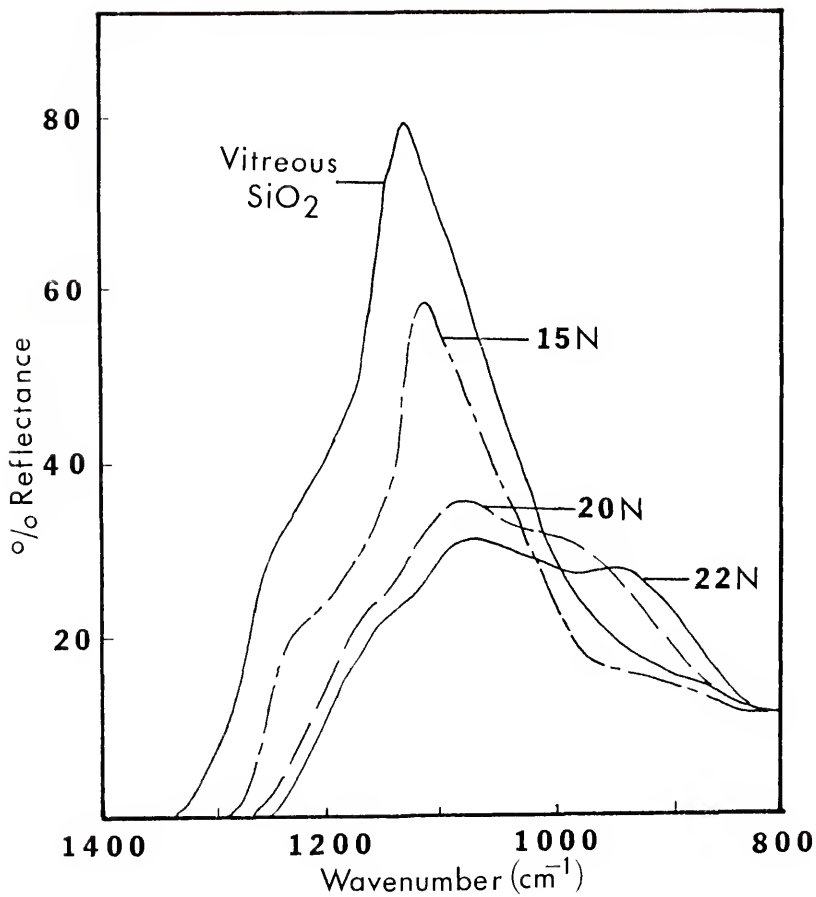

Fig. 70. IRRS for several glasses in the Na_2O-SiO_2 system.

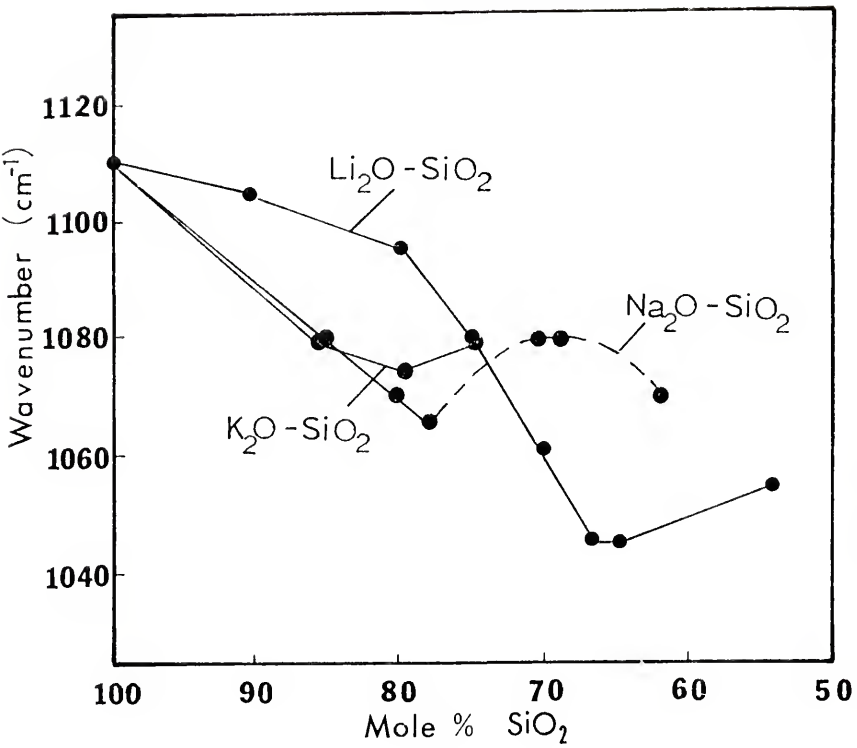

Fig. 71. Wavenumbers of the S peak as a function of the concentration of SiO_2 in the glass for the Li_2O-, Na_2O- and K_2O-SiO_2 systems.

20% Li_2O. At a Li_2O concentration of 30% a reversal occurs which is similar to that with the Na_2O-SiO_2 system. The dependence in the K_2O-SiO_2 system is not as clearly established. A general decrease in the wavenumber of the S peak is observed down to approximately 20% K_2O, after which a reversal occurs.

Figure 72 shows the relationship between the S peak height and the concentration of alkali oxide in the glass. Two linear regions are apparent for the Li_2O-SiO_2 and Na_2O-SiO_2 systems with discontinuities at 24% Na_2O and 30% Li_2O. A linear relation also exists down to 22% K_2O for the K_2O-SiO_2 system. Higher concentrations of K_2O, however, make the glass so reactive with atmospheric water that spectra for these glasses are unrepresentative of the true spectra, see Sanders et al.[25]

This data is in agreement with Sanders et al.[25] who demonstrated that the S peak intensity is directly related to the silica concentration in the glass. Surface roughness, on the other hand, is inversely related to the peak intensity.[155] Figure 73 shows the effect of surface roughness on the intensity of the IRRS spectra for 33L. The intensity of the spectra increases as the polish becomes smoother up to the polish with 600 grit. A further increase in the intensity of the spectra is not observed with finer polishing since there is very little scatter.

When a glass is corroded in water definite changes occur in the IRRS spectra. Figure 74 shows IRRS of the 20N glass corroded with deionized water at 100°C for the indicated times. It can be seen that

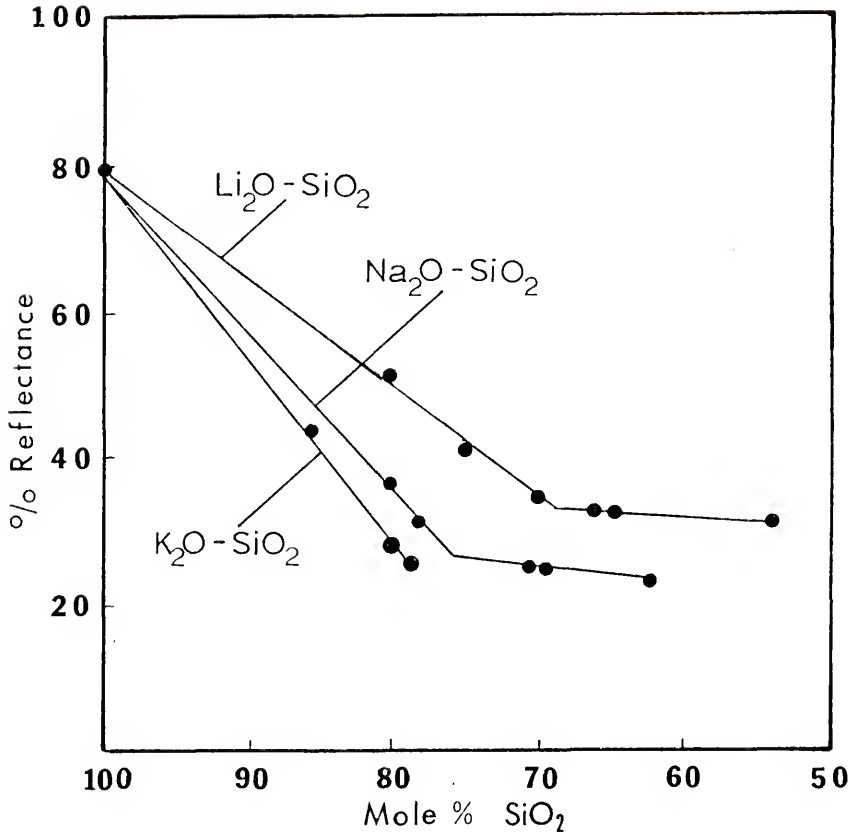

Fig. 72. Intensity of the S peak as a function of the concentration of SiO_2 in the glass for the Li_2O-, Na_2O- and K_2O-SiO_2 systems.

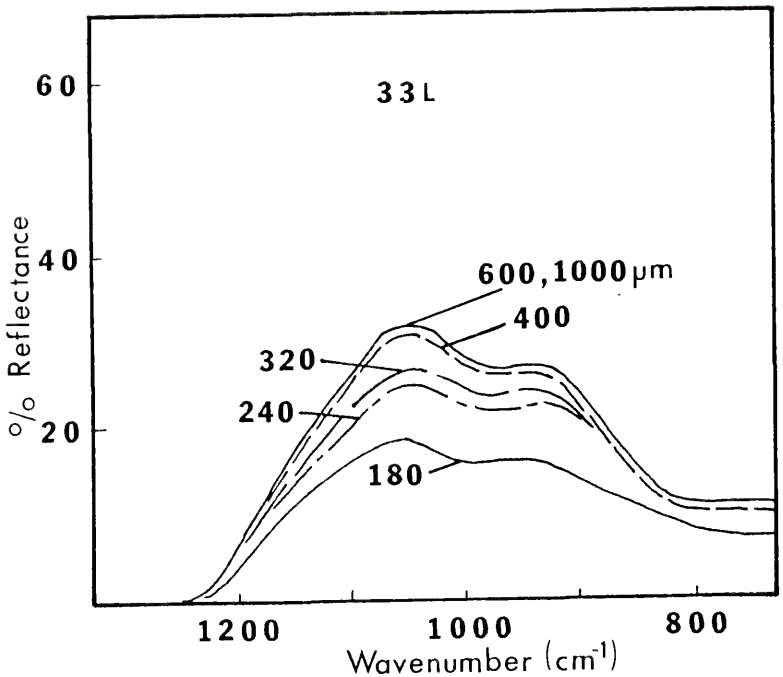

Fig. 73. IRRS for 33L polished with 1000 μm diamond paste and with 600, 400, 320, 240 and 180 grit dry SiC paper.

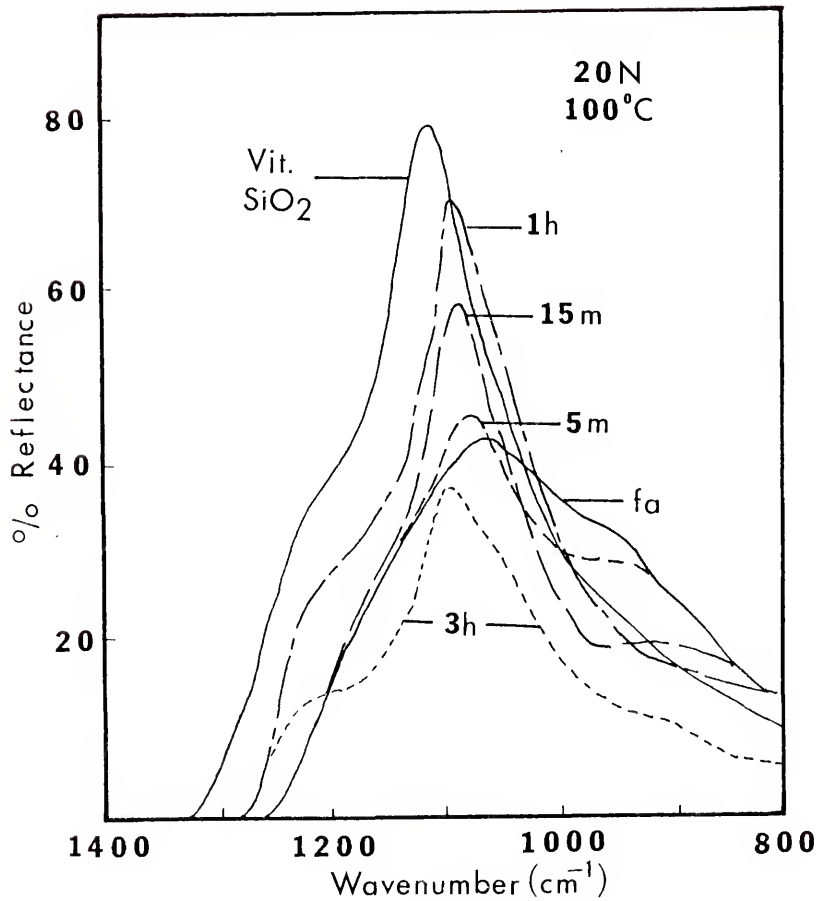

Fig. 74. IRRS for 20N corroded at 100°C for 5 min, 15 min, 1 hour and 3 hours.

the S peak increases in intensity and moves to higher wavenumbers as the corrosion time increases to one hour. This shift in the S peak is attributed to the diffusion of sodium from the glass into solution[21,148] forming an alkali depleted region on the surface of the glass.

The surface composition of a corroded 20N glass was determined by Clark et al.[148] using a frequency shift technique. In this procedure the wavenumber of the S peak of a corroded 20N glass is obtained from the IRRS spectrum. IRRS data from bulk glasses (as that for Na_2O-SiO_2 is Fig. 71) are used to prepare a calibration curve for the determination of the surface composition.

In Chapter VII a condensation reaction within the leached layer is proposed to account for the increase in intensity and wavenumber of the S peak. Since the quantitative analysis techniques developed by Sanders et al.[21] and Clark et al.[148] rely on the S peak, it is more significant to quantify the SiO_2 concentration (number of silicon bridging oxygen groups) rather than alkali oxide concentration (number of silicon nonbridging oxygen groups). Silanol groups, ≡Si-OH, probably also exist within the leached layer and since they produce an NS peak at precisely the same wavenumber as the ≡Si-O-alkali groups is is difficult to distinguish the two from IRRS spectra. The balance from the calculation of the SiO_2 concentration, therefore, consists of R_2O (where R is an alkali oxide ion in the form of two ≡Si-OA groups) and H_2O (in the form of two ≡Si-OH groups).

Using the S peak frequency shift procedure of Clark et al.[148] the author determined the surface SiO_2 concentrations as a function of time for glasses corroded at several temperatures. This data appears in Fig. 75. A similar approach can be applied to the S peak intensity. Using Fig. 72 as a calibration curve, S peak intensities from different IRRS spectra of corroded 20N were used to obtain surface compositions (see Fig. 75). In the early stage of corrosion when the amount of Na^+ that has leached from the surface is small, the two procedures yield identical surface compositions. As corrosion proceeds a difference in composition is obtained with the two techniques. When the frequency shift procedure indicates that the surface composition is approximately 90 or 93.5% SiO_2, the peak intensity procedure indicates that the surface composition is 88.5 and 91% respectively (see Fig. 75).

It should be noted that the surface composition could not be determined for 20N corroded at 100°C for three hours using the S peak intensity. The spectrum obtained for these conditions has a marked decrease in intensity for the entire spectrum. This is due to roughening of the surface (Fig. 76) which scatters the IR beam reflected from the surface.

The differences in the surface compositions for the other conditions in Fig. 75 are also due to surface roughening. Since surface roughening decreases the peak intensity at longer times, an overestimate of the surface composition results when the intensity is used to obtain the composition from the calibration curve.

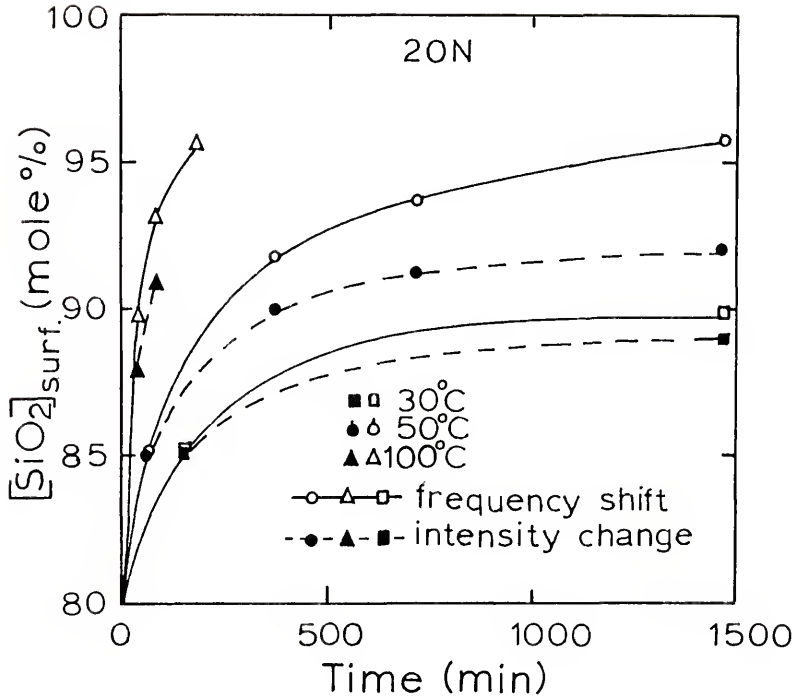

Fig. 75. Surface SiO_2 concentration of 20N corroded at 30°C, 50°C and 100°C as a function of corrosion time determined by S peak wavenumber shifts and by S peak intensity changes.

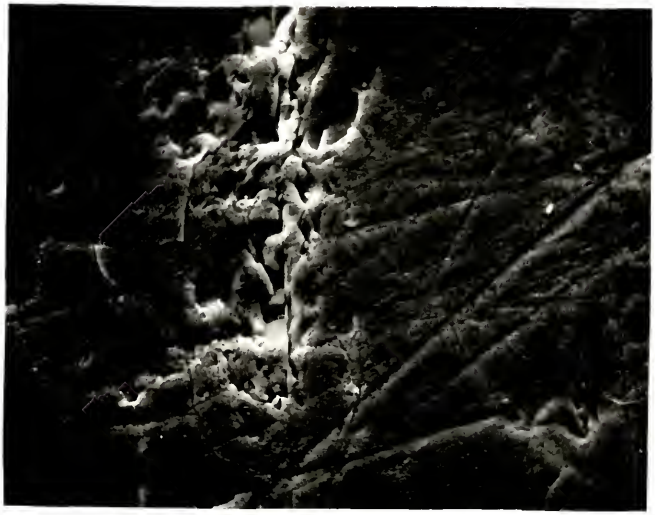

Fig. 76. SEM of 20N corroded at 100°C for 2.5 (620X).

However, by calibrating IRRS data such as shown in Fig. 73 with a profilimeter, the differences shown in Fig. 75 can be used to calculate average surface roughness from the IRRS measurements. Electron probe microanalysis has been used to verify the surface compositions determined from the frequency shift technique.[40]

The changes in the IRRS spectra are more complicated for 14K corroded at 100°C (Fig. 77). After one min of corrosion the S peak intensity decreases slightly over the entire band. The peak frequency, however, remains at the same value. After 30 min the S peak sharpens, increases in intensity and shifts to larger wavenumbers. At 3 and 6 hours the S peak decreases in intensity; however, the frequency remains constant.

Using calibration curves for the K_2O-SiO_2 system (Figs. 71 and 72) the surface compositions were determined by the two methods described previously (see Fig. 78). Except for the apparent decrease in SiO_2 concentration at one min using the peak intensity method, the two procedures yield identical compositions to about 30 min. This indicates that the decrease in intensity at one min is not due to surface roughening but rather the initial decoupling of K^+ ions from the O^{2-} ions since the two quantitative analysis techniques yield identical values at 15 and 30 min.

After 30 min the wavenumber shift procedure indicates that a constant surface SiO_2 concentration is reached. Surface roughening causes the whole spectrum to decrease in intensity after 30 min so that the peak intensity procedure indicates an erroneous decrease in the concentration of SiO_2 in the surface.

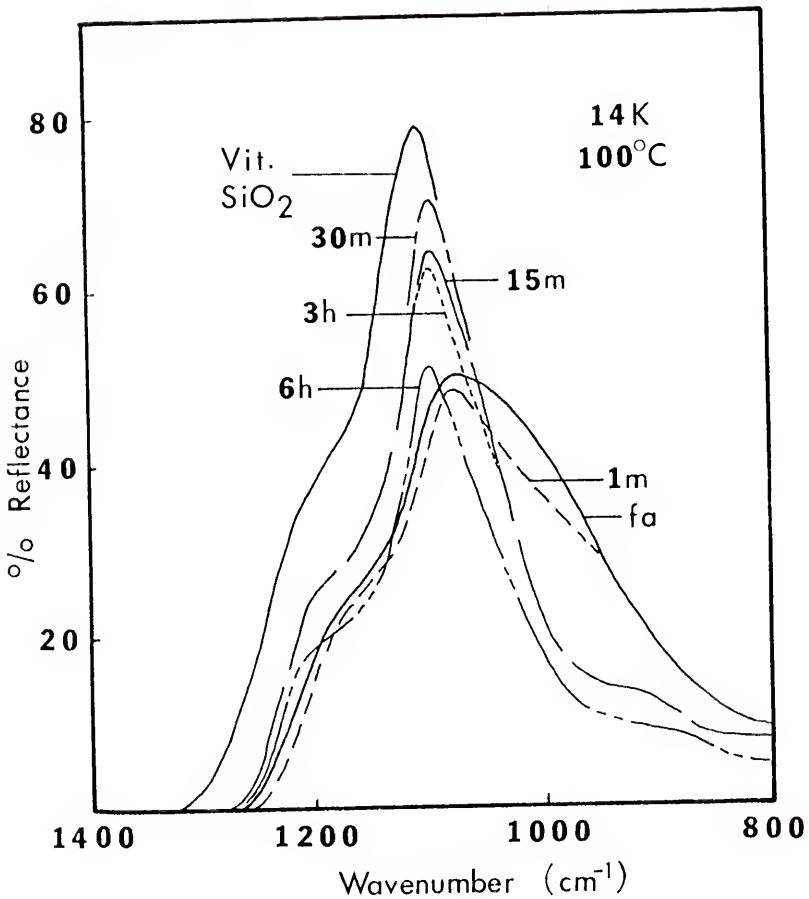

Fig. 77. IRRS for 14K corroded at 100°C for 1 min, 15 min, 30 min, 3 hours and 6 hours.

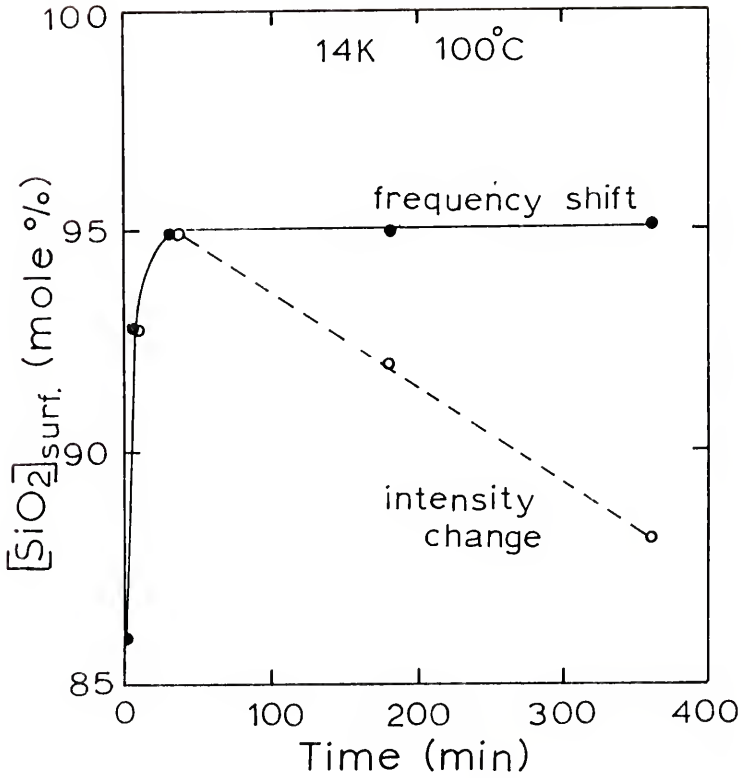

Fig. 78. Surface SiO_2 concentrations for 14K corroded at 100°C determined using S peak wavenumber shifts and S peak intensity changes.

The two procedures give similar results for the Li_2O-SiO_2 system. This will be demonstrated in the next appendix (Appendix D).

Conclusions

Two possible procedures exist for the quantitative analysis of binary alkali silicate glasses. Except for the initial decoupling of alkali ions from the structure producing a decrease in intensity, both the S peak frequency shift method and the S peak intensity change method yield equal surface concentrations of SiO_2 at short times (when the surface SiO_2 concentration has increased less than 5 mole % over the original SiO_2 concentration). During this time it is advantageous to use the peak intensity procedure since larger changes in the spectra permit the surface composition determination with less experimental error.

At longer times (when the surface SiO_2 composition has increased over more than 5% of the original SiO_2 concentration) surface roughening causes more scatter of the IR beam from the sample. This causes the whole spectrum to have a lower intensity, producing erroneous results with the peak intensity procedure. The peak wavenumber procedure, however, is not affected by surface roughening and the compositions determined agree very well with electron microprobe analysis.

Appendix D

COMPOSITION PROFILES OF CORRODED GLASSES UTILIZING INFRARED REFLECTION SPECTROSCOPY

Introduction

There are several existing techniques for determining compositional profiles of corroded glass surfaces. Auger electron spectroscopy combined with ion milling can examine leached layers 40-50 Å thick.[150,160] Grinding techniques and HF etching techniques can be used to remove and analyze 2-3 μm thick layers respectively.[22] Electron probe microanalysis can also be used to obtain composition profiles on a μm scale.[21]

The purpose of this appendix is to demonstrate how a grinding procedure coupled with IRRS can be used to obtain composition profiles from corroded binary alkali silicate glass surfaces by analyzing layers approximately 0.5 μm thick.

Results and Discussion

A 33L sample was corroded at 79°C for 17 hours using the Sanders method. IRRS spectra obtained after corrosion and after successive

polishing of the corroded glass are shown in Fig. 79. The numbers on the spectra designate the particular polishing step with zero being the corroded surface. One can see that as the polish procedure continues, the intensity of the S peak decreases and its wavenumber decreases. Likewise, the intensity of the region around 960 cm^{-1} increases in intensity until finally by the seventh polish the spectrum is identical to the freshly abraded specturm. These changes with polishing demonstrate the decreasing concentration of silica as one polishes through the leached layer. Using the S peak frequency shift procedure described in Appendix C, the concentration of Si_2O in the successive layers in the glass surface were determined. These values appear in Table XVIII.

The thickness removed by each polishing step can be determined from the change in weight of the sample. The sample was prepared in a rectangular shape with all sides normal to one another. The change in thickness of the sample for each polish is, therefore, related to the change in weight by,

$$\Delta X_i = \Delta W_i = \frac{W_o - W_i}{W_o} \tag{93}$$

assuming a uniform density. Since the corroded area on the sample is significantly smaller than the total area polished, any change in density of the corroded area should not affect the results appreciably. The absolute change in thickness is,

$$\Delta X_i = X_o \cdot (\Delta X) \tag{94}$$

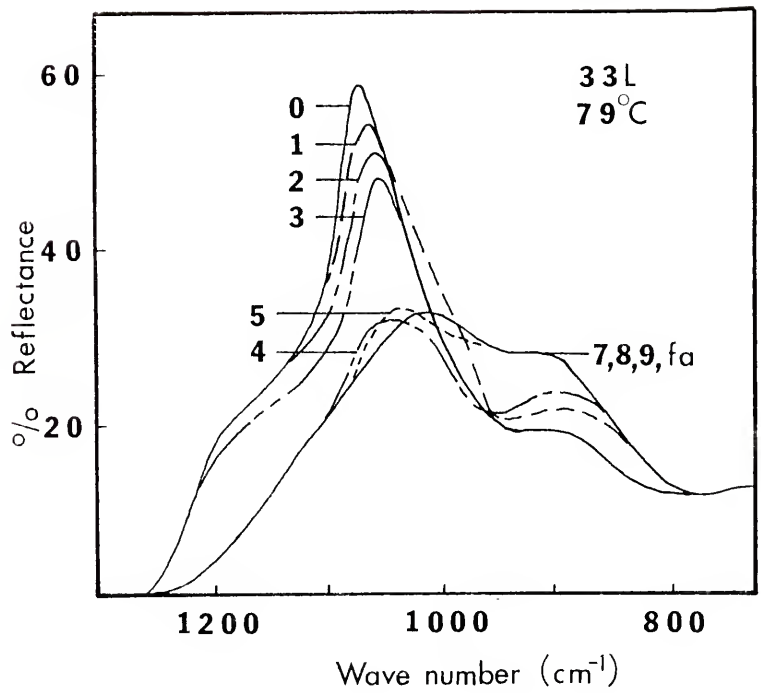

Fig. 79. IRRS for 33L corroded at 79°C with successive polishes.

Table XVIII. Experimental Measurements Used to Calculate the SiO_2 Concentration Profile for a 33L Sample Corroded at 79°C for 17 Hours.

Polish (i)	Weight (average of before and after IR)	Δw_i ($X10^4$ g)	ΔX_i (μm)	Total ΔX (μm)	Wavenumber (cm^{-1})	Si_2O (mole %)
0	1.3789				1097	84
1	1.3780	9	2.18	2.18	1090	78
2	1.3773	7	1.70	3.88	1085	76
3	1.3765	8	1.94	5.82	1080	75
4	1.3754	9	2.18	8.00	1070	73
5	1.3748	6	1.45	9.45	1065	71
6	1.3743	5	1.21	10.66	1050	68
7	1.3735	8	1.94	12.60	1045	67

t_i = 0.313 cm

Δt = 12.6 μm

With this technique the corroded sample was weighed on a Mettler* balance to 1 x 10^{-4} g four times and the weights averaged. An IRRS spectrum was then obtained after which the sample was reweighed four times and averaged with the measurement made before the IRRS was taken. The corroded sample surface was then lightly polished with dry 600 grit SiC paper to remove approximately 5 x 10^{-4} g of glass. A new weight was taken (average of 4 measurements) and another IRRS spectra obtained. This procedure was repeated until the IRRS spectra corresponded to a normal freshly abraded sample. At all times the sample was handled with tweezers and rubber gloves. The change in weight for each polish is also listed in Table XVIII. From these values the change in thickness and the distance from the surface were determined.

The composition profile for this sample is given in Fig. 80 along with the profile determined by Sanders and Hench[21] using electron probe microanalysis (EMP). Close agreement exists for the two procedures. The profile determined by Sanders and Hench has a slightly larger SiO_2 concentration in the surface. Clark et al.[149] found that when EMP is used for compositional analysis of a corroded glass surface, care must be exercised to prevent the diffusion of alkali ions from under the electron beam. Since this was not known when Sanders and Hench determined their profile they did not take proper steps to prevent the diffusion of lithium from under the sample. The diffusion of lithium from under the electron beam caused an overestimate of the

*Mettler H10, Mettler Instrument Corp.

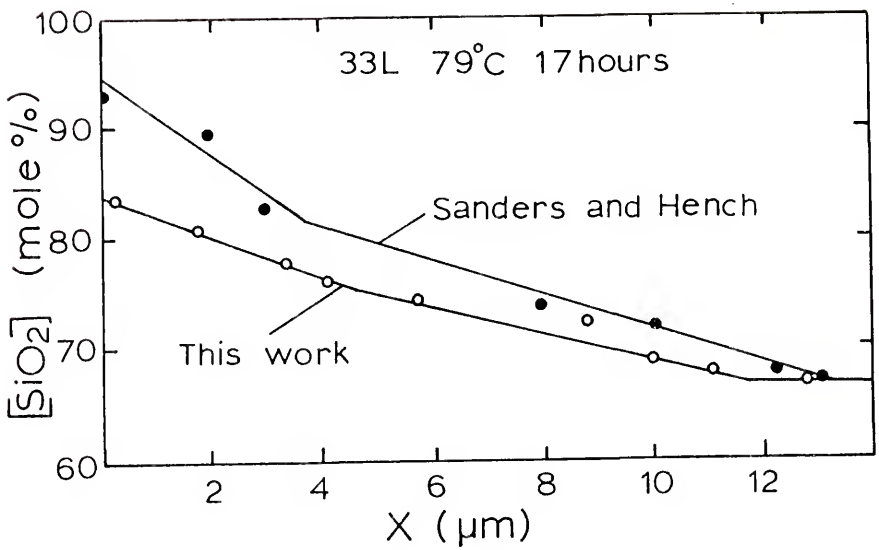

Fig. 80. Concentration of SiO_2 (mole %) vs. distance into the glass (μm) for 33L corroded at 79°C for 17 hours.

concentration of silica in the surface. The overestimate is greatest at the surface since alkali ions tend to diffuse much more rapidly on the surface or a corroded glass than further in the leached layer.[149]

These results confirm the quantitative analysis techniques using IRRS developed in the previous Appendix (C) as well as the procedure for obtaining composition profiles of the thick leached layers on the surface of binary alkali silicate glasses.

Summary and Conclusion

A technique was developed for determining the composition profile of the leached layer on the surface of corroded binary alkali silicate glasses.

Appendix E

CALCULATION OF LEACHED LAYER THICKNESSES FROM EPSILON AND THE SURFACE SiO_2 CONCENTRATION

In Chapter II it was shown how epsilon is proportional to the area under the SiO_2 composition profile. One can write,

$$\varepsilon \frac{\frac{\text{mole } SiO_2}{cm^3}}{(A/V)\ (cm^{-1})} = \tfrac{1}{2} \times (\mu m)\ \frac{10^{-4} cm}{\mu m} \left([SiO_2]_S - [SiO_2]_B \right) \frac{\text{mole } SiO_2}{cm^3} \tag{95}$$

where $[SiO_2]_S - [SiO_2]_B$ is the percent difference in molar concentration of SiO_2 between the surface and the bulk glass. This quantity equals,

$$[SiO_2]_S - [SiO_2]_B = (n_S^{SiO_2} - n_B^{SiO_2}) \frac{\rho(g/cm^3)}{MW_{SiO_2}\ (g/mole)} \tag{96}$$

$$= (4.0 \times 10^{-2})\ (m_S^{SiO_2} - m_B^{SiO_2})\ (mole/cm^3) \tag{97}$$

where $n_S^{SiO_2}$ and $n_B^{SiO_2}$ are the mole fractions of SiO_2 at the surface and the bulk respectively. Substituting Eq. 97 into Eq. 95 and solving for the leached layer thickness, X, gives,

$$X = (5.0 \times 10^5) \frac{\varepsilon}{(A/V)\ (n_S^{SiO_2} - n_B^{SiO_2})} \qquad (98)$$

for X in μm, ε in mole SiO_2/cm^3, (A/V) in cm^{-1} and $n_S^{SiO_2}$ and $n_B^{SiO_2}$ unitless fractions.

The thickness of glass completely dissolved from the surface of a glass can also be calculated from solution data,

$$X_l = \frac{[SiO_2]\left(\frac{\text{moles}}{l}\right)\left(\frac{10^{-3}l}{cm^3}\right) MW_{SiO_2}\left(\frac{g}{\text{mole}}\right)}{(A/V)\ (cm^{-1}) m_B^{SiO_2}\left(\rho\frac{g}{cm^3}\right)} \left(\frac{10^4\ \mu m}{cm}\right) \qquad (99)$$

Substituting in and rearranging gives,

$$X_l = (2.5 \times 10^2) \frac{[SiO_2]}{n_B^{SiO_2}\ (A/V)} \qquad (100)$$

for the thickness of completely dissolved glass, X_l, in μm, concentration of silica in solution, $[SiO_2]$, in moles/l, and the surface area of glass exposed to volume of solution, (A/V), in cm^{-1}.

REFERENCES

1. A.S.T.M. Designation C 162-166, "Standard Definitions of Terms Relating to Glass and Glass Products," American Society for Testing Materials ASTM Std. Part 13, p. 115 (1967).

2. L. Holland, The Properties of Glass Surfaces, Chapman and Hall, London (1964).

3. Frank R. Bacon, "The Chemical Durability of Silicate Glass," Glass Ind. 49:494-9, 554-9, (1968).

4. David M. Sanders, "Structure and Kinetics of Glass Corrosion," Ph.D. Thesis, Univ. of Fla. (1973).

5. L. L. Hench, R. J. Splinter, W. C. Allen and T. K. Greenlee, Jr., "Bonding Mechanisms at the Interface of Ceramic Prosthetic Materials," J. Biomed. Mater. Res. Symp. 2:117-141 (1971).

6. L. L. Hench and H. A. Paschall, "Direct Chemical Bond of Bioactive Glass-Ceramic Materials to Bone and Muscle," J. Biomed. Mater. Res. Symp. 4:27-45 (1973).

7. A. E. Clark, L. L. Hench and H. A. Paschall, "The Influence of Surface Chemistry on Implant Interface Histology: A Theoretical Basis for Implant Materials Selection," J. Biomed. Mater. Res. 10:161-174 (1976).

8. C. A. Beckham, T. K. Greenlee, Jr. and A. R. Crebo, "Bone Formation at a Ceramic Implant Interface," Calc. Tiss. Res. 8:165-171 (1971).

9. H. R. Stanley, L. L. Hench, R. Going, C. Bennett, S. J. Chellemi, C. King, N. Ingersol, E. Ethridge and K. Kreutziger, "The Implantation of Natural Tooth Form Bioglasses in Baboons," Oral Surg. 42:339-356 (1976).

10. Edwin C. Ethridge, "The Effect of Different Dental Implant Materials on Oral Tissue Compatibility," J. Metals 28:14-21 (1976).

11. Reference 1, p. 126

12. G. W. Morey, "Solubility and Decomposition in Complex Systems," J. Soc. Glass Tech. 6:20-29 (1922).

13. G. W. Morey, The Properties of Glass, Reinhold, N.Y. (1954).

14. Y. Oishi, A. R. Cooper, Jr. and W. D. Kingery, "Dissolution in Ceramic Systems: III Boundary Layer Concentration Gradients," J. Am. Ceram. Soc. 48:88-95 (1965).

15. A. R. Cooper, "Corrosion of Ceramics," Personal communication.

16. Woldemar A. Weyl and Evelyn Chostner Marboe, The Constitution of Glasses: A Dynamic Interpretation, Volume II: Part 2, Interscience Pub. N.Y. (1967).

17. W. A. Weyl, "The Significance of the Co-ordination Requirements of the Cations in the Constitution of Glass. I. Basic concepts and the constitution of Alkali Silicate Glasses," J. Soc. Gl. Tech. 35:421-447 (1951).

18. C. R. Das, "A Review of the Chemical Resistance of Glass," Indian Ceram. Soc. Trans. 24:p. 22 (1965).

19. R. W. Douglas and T. M. El-Shamy, "Reactions of Glasses with Aqueous Solutions," J. Am. Ceram. Soc. 50:1-8 (1967).

20. D. M. Sanders and L. L. Hench, "Surface Roughness and Glass Corrosion," Bull. Am. Ceram. Soc. 52:666-669 (1973).

21. D. M. Sanders and L. L. Hench, "Mechanisms of Glass Corrosion," J. Am. Ceram. Soc. 56:373-377 (1973).

22. Z. Boksay, G. Bouquet and S. Dobos, "Diffusion Processes in the Surface Layer of Glass," Phys. Chem. Glass 8:140-144 (1967).

23. Robert H. Doremus, Glass Science, John Wiley & Sons, N.Y. (1973).

24. Mushtag Ahmad Rana and R. W. Douglas, "The Reaction Between Glass and Water. Part 2: Discussion of the Results," Phys. Chem. Glass. 2:p. 205 (1961).

25. D. M. Sanders, W. B. Person and L. L. Hench, "Quantitative Analysis of Glass Structure with the Use of Infrared Reflection Spectra," App. Spect. 28:247-256 (1974).

26. G. H. Frischat, Ionic Diffusion in Oxide Glasses, Diffusion Monograph Series, Trans. Tech. Publications, Bay Village, Ohio (1975).

27. W. H. Zachariasen, "The Atomic Arrangement in Glass," J. Am. Chem. Soc. 54:3841-3851 (1932). Chem. Ab. 26:5800 (1932).

28. Reference 17, p. 423

29. Reference 17, p. 429

30. G. B. Alexander, W. M. Heston and R. K. Iler, "The Solubility of Amorphous Silica in Water," J. Phys. Chem. 58:453-455 (1954).

31. Paul S. Roller and Guy Ervin, Jr., "The System Calcium Oxide-Silica-Water at 30°C. The Association of Silicate Ion in Dilute Alkaline Solution," J. Am. Chem. Soc. 62:461-471 (1940).

32. S. A. Greenberg and E. W. Price, "The Solubility of Silica in Soluitons of Electrolytes," J. Phy. Chem. 61:1539-1541 (1957).

33. T. L. O'Connor and S. A. Greenberg, "The Kinetics of the Solution of Silica in Aqueous Solution," J. Phy. Chem. 62:1195-1198 (1958).

34. C. C. Lucas and M. E. Doland, "The Solubility of Quartz and Silicates," J. Can. Med. Assoc. 40:126-134 (1939).

35. S. Storgaard Jörgensen, "Solubility and Dissolution Kinetics of Precipitated Amorphous Silica in 1M $NaClO_4$ at 25°C," Acta. Chem. Scand. 22:335-341 (1968).

36. R. K. Iler, The Colloid Chemistry of Silica and Silicates, Cornell University Press, N.Y. (1955).

37. Sidney A. Greenberg and David Sinclair, "The Polymerization of Silicic Acid," J. Phy. Chem. 57:435-440 (1957).

38. Sidney A. Greenberg, "The Depolymerization of Silica in Sodium Hydroxide Solutions," J. Phy. Chem. 61:960-965 (1957).

39. Charles B. Hurd, Renato C. Pomatti, John H. Spittle and Frank J. Alois, "Studies on Silicic Acid Gels. XV. The Effect of Temperature upon the Time of Set of Alkaline Gel Mixtures," J. Am. Chem. Soc. 66:388-390 (1944).

40. R. J. Charles, "Static Fatigue of Glass I," J. App. Phys. 29:1549-1553 (1958).

41. E. Rexer, Keramische Rundschen 38:421-425 (1930).

42. P. Tietze, P., Jr., Sprechsaal 60:813-814 (1927).

43. M. Nagaoka, Glastech. Ber. 17:327-329 (1939).

44. Frank R. Bacon and O. G. Burch, "Resistance of Glass Bottles to Neutral Alcoholic Solutions," J. Am. Ceram. Soc. 23:147-151 (1940).

45. G. H. Frischat, Ionic Diffusion in Oxide Glasses, Diffusion Monograph Series, Trans. Tech. Publications, Bay Village, Ohio (1975).

46. A. K. Lyle, "Theoretical Aspects of Chemical Attack of Glasses by Water," J. Am. Ceram. Soc. 26:201-204 (1943).

47. Mushtag Ahmad Rana and R. W. Douglas, "The Reaction Between Glass and Water. Part I: Experimental Methods and Observations," Phys. Chem. Glass. 2:179-195 (1961).

48. L. Zagar and L. Schillmöller, Glastech. Ber. 33:117-121 (1960).

49. C. R. Das and R. W. Douglas, "Studies on the Reaction Between Water and Glass. Part 3," Phys. Chem. of Glass. 8:178-184 (1967).

50. Frank R. Bacon and O. G. Burch, "Effect of Time and Temperature on Accelerated Chemical Durability Tests Made on Commercial Glass Bottles, I," J. Am. Ceram. Soc. 23(1):1-9 (1940); correction 23(2): 56 (1940).

51. Frank R. Bacon and O. G. Burch, "Effect of Time and Temperature on Accelerated Chemical Durability Tests Made on Commercial Glass Bottles, II," J. Am. Ceram. Soc. 24:29-35 (1941).

52. T. M. El-Shamy and R. W. Douglas, "Kinetics of the Reaction of Water with Glass," Glass Tech. 13:77-80 (1972).

53. S. M. Budd and J. Frankiewicz, "The Mechanisms of Chemical Reaction Between Silicate Glass and Attacking Agents. Part II: Chemical Equilibrium at Glass - Solution Interface," Phys. Chem. Glass. 2: 115-118 (1961).

54. C. R. Das, "Study of the Equilibrium pH of some Commercial and Experimental Glasses and their Relationship with Chemical Durability," Indian Ceram. Soc. Trans. 27:41-45 (1968).

55. G. Keppeler and M. Thomas-Welzow, Glastech. Ber. 11:205-208 (1939).

56. G. Keppeler, Glastech. Ber. 12:366-372 (1939).

57. P. Ehrmann, M. deBilly and J. Zarzycki, Verres Refrac. 18:164 (1964).

58. Robert H. Doremus, Glass Science, John Wiley & Sons, N.Y. (1973).

59. G. H. Frischat, Glastech. Ber. 42:351-358 (1969).

60. G. H. Frischat, Glastech. Ber. 43:482-488 (1970).

61. K. K. Evstrop'ev and V. K. Pavlovskii, Inorg. Mater. 3:592-596 (1967).

62. R. Terai, "Self-Diffusion of Sodium Ions and Electrical Conductivity in Sodium Aluminosilicate Glasses," Phys. Chem. Glass. 10:146-152 (1969).

63. K. K. Evstrop'ev, Struct. Glass 2:237-240 (1960).

64. H. Hayami and R. Terai, "Diffusion of Alkali Ions in Na_2O-Cs_2O-SiO_2 Glasses," Phys. Chem. Glass. 13:102-106 (1972).

65. P. J. Bray and J. G. O'Keefe, "Nuclear Magnetic Resonance Investigations of the Structure of Alkali Borate Glasses," Phys. Chem. Glass. 4:37-46 (1963).

66. V. V. Moiseev and V. A. Zhabrev, Inorg. Mat. 5:793-796 (1969).

67. Gary L. McVay and Delbert E. Day, "Diffusion and Internal Friction in Na-Rb Silicate Glasses," J. Am. Ceram. Soc. 53:508-513 (1970).

68. James W. Fleming, Jr. and Delbert E. Day, "Relation of Alkali Mobility and Mechanical Relaxation in Mixed-Alkali Silicate Glasses," J. Am. Ceram. Soc. 55:186-192 (1972).

69. G. H. Frischat, Glastech. Ber. 44:93-98 (1971).

70. W. Müller-Warmuth, R. Krämer and H. Dutz, IX^{e} Congrés Intern. du Verre, Section A1. 2, 303-318, Versailles (1971).

71. L. Bartha and I. Hangos, Mag. Kem. Foly. 29:210-212 (1973).

72. I. Burn and J. P. Roberts, "Influences of Hydroxyl Content on the Diffusion of Water in Silica Glass," Phys. Chem. Glass. 11:106-114 (1970).

73. A. J. Moulson and J. P. Roberts, "Water in Silica Glass," Trans. Brit. Ceram. Soc. 59:388-394 (1960).

74. A. J. Moulson and J. P. Roberts, "Water in Silica Glass," Trans. Faraday Soc. 57:1208-1216 (1961).

75. James R. Johnston, Robert H. Bristow and Henry H. Blau, "Diffusion of Ions in Some Simple Glasses," J. Am. Ceram. Soc. 34:165-172 (1951).

76. R. H. Doremus, "Electrical Conductivity and Electrolysis of Alkali Ions in Silicate Glass," Phys. Chem. Glass. 10:28-33 (1969).

77. G. Hetherington, K. H. Jack and M. W. Ramsay, "The High-Temperature Electrolysis of Vitreous Silica. Part I. Oxidation, Ultra-Violet induced Fluorescence, and Irradiation colour," Phys. Chem. Glass. 6:6-15 (1965).

78. K. K. Evstrop'ev, in The Structure of Glass, Vol. II, p. 237, Consultants Bureau, N.Y. (1960).

79. H. Hayami and R. Terai, "Diffusion of Alkali Ions in Na_2O-Cs_2O-SiO_2 Glasses," Phys. Chem. Glass. 13:102-106 (1972).

80. Alfred Sendt, "Ion Exchange and Diffusion Processes in Glass," Adv. Glass Tech., Tech. Papers Intern. Cong. Glass, 6th, Wash., D.C., Part 1: 307-32 Plenum Press (1962); Chem. Ab. 58:326f (1963).

81. F. G. K. Baucke, "Investigation of Surface Layers, Formed on Glass Electrode Membranes in Aqueous Solutions, By Means of an Ion Sputtering Method," J. of Non-Crystalline Solids 14:13-31 (1974).

82. Woldemar A. Weyl and Evelyn C. Marboe, The Constitution of Glasses: A Dynamic Interpretation, Volume I, Interscience Pub., N.Y. (1962).

83. R. W. Douglas and J. O. Isard, "The Action of Water and of Sulphur Dioxide on Glass Surfaces," J. Soc. Glass. Tech. 33:289-335T (1949).

84. Mushtag Ahmad Rana and R. W. Douglas, "The Reaction Between Glass and Water. Part 2: Discussion of the Results," Phys. Chem. Glass. 2:196-205 (1961).

85. I. R. Beattie, "The Reaction Between Water and Vitreous Silicates," Faraday Soc. Trans. 49:1059-1065 (1953).

86. F. Mylius and F. Foerster, Ber. D. Deutsch. Chem. Ges. 22:1092 (1889).

87. F. Mylius and F. Foerster, Zeitschr. f. Instrum. 9:117 (1889).

88. J. I. E. Corney, Thesis, University of Sheffield (1956).

89. Reference 45, p. 90

90. Chitta Ranjan Das, "Theoretical Aspects of the Corrosion of Glass," Glass Ind. 50:422-427 (1969).

91. Reference 90, p. 426

92. T. Drury, G. J. Roberts and J. P. Roberts, "Diffusion of "Water" in Silica Glass," Adv. Glass Tech., Tech. Papers Inter. Cong. Glass, 6th, Wash. D.C., Part 1: 307-32 Plenum Press (1962).

93. Reference 92, p. 251

94. J. Crank, Mathematics of Diffusion, Oxford University Press, London (1956).

95. Carl Wagner, "Diffusion of Lead Chloride Dissolved in Solid Silver Chloride," J. Chem. Phys. 18:1227-1230 (1950).

96. G. J. Roberts and J. P. Roberts, "Influence of Thermal History on the Solubility and Diffusion of 'water' in Silica Glass," Phys. Chem. Glasses 5:26-32 (1964).

97. G. J. Roberts and J. P. Roberts, "An Oxygen Tracer Investigation of the Diffusion of 'water' in Silica Glass," Phys. Chem. Glasses 7:82-89 (1966).

98. R. V. Adams, "Infra-red Absorption Due to Water in Glass," Phys. Chem. Glass. 2:39-49 (1961).

99. V. F. Kokorina, "Influence of Oxides of Alkaline Earth Metals on the Chemical Resistance of Glass," Conf. Glassy State, Proc. 3rd, All Union Cong. Str. Glass, Leningrad, Nov. 16-20, 1959; Consultants Bureau, N.Y. 2:385-387 (1960).

100. W. A. Weyl, "The Significance of the Co-ordination Requirements of the Cations in the Constitution of Glass. III. The Chemical Durability of Glass," J. Soc. Gl. Tech. 35:462-468 (1951).

101. Johann Enss, Glastech. Ber. 5:27 (1928).

102. C. R. Das, "Theoretical Aspects of the Corrosion of Glass: Conclusion," Glass Ind. 50:483-485 (1969).

103. A. Tielsch and E. Zschimmer, Sprechsaal Keram. Glas Email 66:285-286, 303-306, 319-322, 334-337 (1933).

104. A. Cousen and C. J. Peddle, "A Critical Examination of the Standard Test for Chemical Durability of Glass Bottles," J. Soc. Glass Tech. 20:418-427 (1936).

105. A. Cousen and C. J. Peddle, "Notes on Annealing Lehrs," J. Soc. Glass Tech. 21:177-186 (1937).

106. Violet Dimbleby and W. E. S. Turner, "The Relationship Between Chemical Composition and the Resistance of Glasses to the Action of Chemical Reagents. Part I," J. Soc. Glass Tech. 10:304-363 (1926).

107. H. S. Williams and W. A. Weyl, "Surface Dealkalization of Finished Glassware: I," Glass. Ind. 26:275-77, 290-92, 301, 339, 341-44 (1945).

108. Reference 83, p. 299

109. Frank R. Bacon and Glenn L. Calcamuggio, "Effect of Heat Treatment in Moist and Dry Atmospheres on Chemical Durability of Soda-Lime Glass Bottles," Bull. Am. Ceram. Soc. 46:850-855 (1967).

110. Carlo G. Pantano, "Compositional Analysis of Glass Surfaces and Their Reaction in Aqueous Environments," Ph.D. Thesis, University of Florida (1976).

111. Reference 16, p. 1102

112. Chemical Durability Committee, "A Comparison of Two Methods for Testing the Resistance of Glass to Attack by H_2O," Glass Tech. 7:181-182 (1966).

113. Report of Committee on Chemical Durability of Glass., Bull. Am. Ceram. Soc. 14:181-184 (1935).

114. V. Dimbleby and W. E. S. Turner, "The Relationship Between Chemical Composition and Resistance of Glasses to the Action of Chemical Reagent," J. Soc. Glass Tech. 10:T304 (1926).

115. R. F. R. Sykes, "The Preparation of Glass Grain Samples for Durability Tests," Glass Tech. 6:178-183 (1965).

116. E. Wiegel, Glastech. Ber. 34:259-268 (1961).

117. E. Wiegel, Glastech. Ber. 37:141-147 (1964).

118. A. Herman, "Factors Influencing Autoclave Chemical Durability Tests of Glass Containers," J. Am. Ceram. Soc. 24:323-327 (1941).

119. David E. Clark, "A Durability Evaluation of Soda-Lime-Silica Glasses Using Electron Microprobe Analysis, Infrared Reflection Spectroscopy and Other Techniques," Ph.D. Thesis, Univ. of Florida (1976).

120. G. W. Morey, R. O. Fournier and J. J. Rowe, "The Solubility of Quartz in Water in the Internal From 25°C to 300°C," Geochim. Cosmo. Acta. 26:1029 (1962).

121. F. R. Bacon and R. C. Raggon, "Promotion of Attack on Glass and Silica by Citrate and Other Anions in Natural Solution," J. Am. Ceram. Soc. 42:199-205 (1959).

122. Reference 16, p. 1106

123. D. M. Sanders and L. L. Hench, "Environmental Effects on Glass Corrosion Kinetics," Gull. Am. Ceram. Soc. 52:662-665, 669 (1973).

124. Morris F. Dilmore, "Chemical Durability of Multicomponent Silicate Glasses," Ph.D. Thesis, University of Florida (1977).

125. E. Rexer, Keram. Fundschau. 38:389 (1930).

126. C. R. Das, "A Review of the Chemical Resistance of Glass," Indian Ceram. Soc. Trans. 24:12-23, 34 (1965).

127. S. Sen and F. V. Tooley, "Determination of Calcium, Sodium, and Silicate Ions in Extracts from Chemical Durability Tests on Glass," J. Am. Ceram. Soc. 33:178-180 (1950).

128. R. W. Harman, "Aqueous Solutions of Sodium Silicates. Part VIII. General Summary and Theory of Constitution. Sodium Silicates as Colloidal Electrolytes," J. Phy. Chem. 32:44-60 (1928).

129. R. H. Bogue, "Hydrolysis of the Silicates of Sodium," J. Am. Chem. Soc. 42:2575-82 (1920).

130. Franklin Fu-Yen Wang and F. V. Tooley, "Detection of Reaction Products Between Water and Soda-Lime-Glass," J. Am. Ceram. Soc. 41:467-469 (1958).

131. R. Jagitsch, Glassteknisk Tidskraft 11:127 (1956).

132. F. Y. Wang and F. V. Tooley, "Influence of Reaction Products on Reaction Between Water and Soda-Lime-Silica Glass," J. Am. Ceram. Soc. 41:521-524 (1958).

133. Yu A. Schmidt, "Structure of Glass," 1:253-254 (1958), Translated from Russian by E. B. Uvarov, Consultants Bureau, N.Y.

134. I. E. Berger, Glastech. Ber. 14:351-60 (1936); Chem. Ab. 31:513[5] (1937).

135. S. Glasston, Textbook of Physical Chemistry, Macmillan, p. 884 (1943).

136. K. C. Lyon, "The Effect of Rinsing on the Chemical Durability of a Container Glass," J. Am. Ceram. Soc. 32:46-48 (1949).

137. J. S. Owens and E. C. Emanuel, "Variable Factors in Accelerated Autoclave Chemical Durability Tests," J. Am. Ceram. Soc. 25:143-49 (1942).

138. H. Deveaux and E. Aubel, Compt. Rend. Acad. Sci. 184:601 (1927).

139. R. K. Iler, "Effect of Adsorbed Alumina on the Solubility of Amorphous Silica in Water," J. Coll. Inter. Sci. 43:399-408 (1973).

140. W. Geffcken, "Chemical Attack by Alkaline Liquids and the Effect of Soluble Ions on Its Action I," Kolloid. Z. 86:11-15 (1939); Chem. Ab. 33:2665^3 (1939).

141. W. A. Weyl, "Some Practical Aspects of the Surface Chemistry of Glass: IV," Glass Ind. 28:408-12, 428-32 (1947); Ceram. Ab. 27:127g (1948).

142. George A. Hudson and Frank R. Bacon, "Inhibition of Alkaline Attack on Soda-Lime Glass," Bull. Am. Ceram. Soc. 37:185-188 (1958).

143. Reference 139, p. 408

144. F. M. Ernsberger, "Attack of Glass by Chelating Agents," J. Am. Ceram. Soc. 42:373-375 (1959).

145. Reference 144, p. 373

146. Reference 121, p. 205

147. Reference 144, p. 375

148. D. E. Clark, M. F. Dilmore, E. C. Ethridge and L. L. Hench, "Aqueous Corrosion of Soda-Silica and Soda-Lime-Silica Glass," J. Am. Ceram. Soc. 59:62-65 (1976).

149. D. E. Clark, L. L. Hench and W. A. Acree, "Electron Microprobe Analysis of Na_2O-CaO-SiO_2 Glass," J. Am. Ceram. Soc. 58:531-532 (1975).

150. Carlo G. Pantano, Arthur E. Clark, Jr. and L. L. Hench, "Multilayer Corrosion Films on Bioglass Surfaces," J. Am. Ceram. Soc. 57:412-413 (1974).

151. H. E. Simpson, "Study of Surface Structure of Glass as Related to its Durability," J. Am. Ceram. Soc. 41:43-49 (1958).

152. H. R. Persson, "Improvement of the Chemical Durability of Soda-Lime-Silica Glass Bottles by Treating with Various Agents," Glass Tech. 3:17-35 (1962).

153. R. M. Tichane, "The Initial Stages of the Weathering Process on a Soda-Lime-Glass Surface," Glass Tech. 7:26-29 (1966).

154. E. Brueche, and H. Poppa, Glastech. Ber. 30:163-175 (1957).

155. D. E. Clark, E. C. Ethridge, M. F. Dilmore and L. L. Hench, "Quantitative Analysis of Corroded Glass Utilizing Infrared Frequency Shifts," Accepted by Phys. Chem. Glass.

156. D. Crozier and R. W. Douglas, "Study of Sodium Silicate Glasses in the Infra-Red by means of Thin Films," Phys. Chem. Glass. 6:240-245 (1965).

157. Reuter Wilhad, "Electron Probe Microanalysis," Surface Science 25:80-119 (1971).

158. Patrick J. Rynd and Aril K. Rastogi, "Auger Electron Spectroscopy--a New Tool in the Characterization of Glass Fiber Surfaces," Bull. Am. Ceram. Soc. 53:631-637 (1974).

159. Bernard Goldstein and David E. Carlson, "Determination of the Composition of Glass Surfaces by Auger Spectroscopy," J. Am. Ceram. Soc. 55:51-52 (1972).

160. C. J. Pantano, Jr., D. B. Dove and G. Y. Onoda, Jr., "AES Analysis of Sodium in Corroded Bioglass Using a Low-Temperature Technique," App. Phys. Letters 26:601-602 (1975).

161. H. Bach, "Distortion of Na^+ Concentration Profiles in Thin Glassy Surface Layers by ion Bombardment," Radiation Effects 28:215-226 (1976).

162. I. Simon and H. O. McMahon, "Study of Some Binary Silicate Glasses by Means of Reflection in Infrared," J. Am. Ceram. Soc. 36:160-164 (1953).

163. J. R. Sweet and W. B. White, "Study of Sodium Silicate Glasses and Liquids by Infrared Reflection Spectroscopy," Phys. Chem. Glass. 10:246-251 (1969).

164. K. K. Evstrop'ev and V. K. Pavlovskii, Inorg. Mater. 3:592-596 (1967).

165. Scott Anderson, "Investigation of Structure of Glasses by Their Infrared Reflection Spectra," J. Am. Ceram. Soc. 33:45-51 (1950).

166. R. J. Charles, "Activities in Li_2O-, Na_2O-, and K_2O-SiO_2 Solutions," J. Am. Ceram. Soc. 50:631-641 (1967).

167. John R. Ferraro and Murli H. Manghnani, "Infrared Absorption Spectra of Sodium Silicate Glasses at High Pressure," J. Appl. Phys. 43:4595-4599 (1972).

168. L. L. Hench and M. F. Dilmore, "Infrared Reflection Spectra of Lead Germanate Glasses," Personal communication.

169. Murli H. Manghnani, John R. Ferraro and L. J. Basile, "A Study of Na_2O-TiO_2-SiO_2 Glasses by Infrared Spectroscopy," App. Spec. 28:256-259 (1974).

170. J. Zarzycki and F. Naudin, J. Chem. Phys. 58:830 (1961).

171. H. Scholze, Glastech. Ber. 32:81-88 (1959).

172. H. Scholze, Glastech. Ber. 32:142-152 (1959).

173. B. A. Morrow and I. A. Cody, "Infrared Spectra of the Isolated Hydroxyl Groups in Silica," J. Phy. Chem. 77:1465-1469 (1973).

174. Michael L. Hair and William Hertl, "Acidity of Surface Hydroxyl Groups," J. Phy. Chem. 74:91-94 (1970).

175. H. Scholze, Glastech. Ber. 32:81, 142, 278, 314 (1959).

176. R. V. Adams, "The Absorption of Infrared Radiation and the Structure and Composition of Various Oxide Glasses with Special Reference to the Bonds Due to 'Water'" Ph.D. Thesis, University of Sheffield (1960).

177. M. S. Hill, "An X-Ray Investigation of Interatomic Distances in Potassium Silicate Glass," Master's Thesis, University of Florida (1972).

178. R. W. Gould and M. S. Hill, "An X-Ray Amorphous Scattering Investigation of the Corrosion of a Potassium Silicate Glass K_2O-$3SiO_2$," Adv. X-Ray Anal. 17:384-394 (1973).

179. C. V. Gokularathnam, R. W. Gould and L. L. Hench, "Effect of 'Water' on the Structure of Vitreous Silica," Phys. Chem. Glass. 16:13-16 (1975).

180. L. L. Hench, "Characterization of Glass Corrosion and Durability," J. Non-Crystalline Solids 19:27-39 (1975).

181. E. L. Mochel, M. E. Nordberg and T. H. Elmer, "Strengthening of Glass Surfaces by Sulfur Trioxide Treatment," J. Am. Ceram. Soc. 49:585-89 (1966).

182. Reference 90, p. 425

183. S. Dobos, Acta. Chim. Acad. Sci. Hung. 69:43-48 (1971); Chem. Ab. 75:80627w (1971).

184. S. Dobos, Acta. Chim. Acad. Sci. Hung. 69:49-57 (1971); Chem. Ab. 75:80624t (1971).

185. Z. Boksay and G. Bouquet, "On the Reaction of Water Molecules with the Silicate Network in the Glass Phase," Phys. Chem. Glass. 16:81-82 (1975).

186. W. Geffcken and E. Berger, "Fundamental Investigations on the Chemical Stability of Glasses. II," Glastech. Ber. 16:296-304 (1938); Chem. Ab. 33:8251 (1939).

187. S. M. Budd and J. Frankiewiez, "The Mechansims of Chemical Reaction Between Silicate Glass and Attacking Agents. Part III: Equilibrium pH of some Na_2O-CaO-SiO_2 Glasses and its Relationship with Chemical Reactivity," Phys. Chem. Glass. 3:116-120; Correction, Phys. Chem. Glass. 5:32 (1964).

188. Reference 49, p. 179

189. T. M. El-Shamy, "The Rate Determining Step in the Dealkalization of Silicate Glass," Phys. Chem. Glass. 14:18-19 (1973).

190. A. Woldemar Weyl and Evelyn C. Marboe, The Constitution of Glasses: A Dynamic Interpretation, Volume II: Part 1, Interscience Pub., N.Y. (1964).

191. G. Eisenman, Glass Electrodes for Hydrogen and Other Cations, G. Eisenman, Ed., M. Dekker, N.Y. (1967).

192. P. Ehrmann, M. deBilly and J. Zarzycki, Verres Refrac. 18:169 (1964).

193. Reference 19, p. 4

194. Reference 19, p. 5

195. Evelyn C. Marboe and W. A. Weyl, "Staining of Glass Containers in Contact with Iron," J. Am. Ceram. Soc. 30:320-322 (1947).

196. S. M. Budd, "The Mechanisms of Chemical Reaction Between Silicate Glass and Attacking Agents. Part I: Electrophilic and Nucleophilic Mechanisms of Attack," Phys. Chem. Glass. 2:111-114 (1961).

197. Eugene W. Sucov, "Diffusion of Oxygen in Vitreous Silica," J. Am. Ceram. Soc. 46:14-20 (1963).

198. Reference 23, p. 131

199. Reference 49, p. 181

200. Reference 19, p. 2

201. Lewins, J., Ph.D. Thesis, Department of Glass Technology, University of Sheffield (1965).

202. G. Gomori, "Preparation of Buffers for use in Enzyme Studies," Meth. Enzymology 1:138-146 (1955).

203. E. B. Wilson, J. C. Pecius and P. C. Cross, Molecular Vibrations, McGraw-Hill, New York (1955).

204. Rinoud Hann, "The Structure of Sodium Silicate Glasses and Their Far-Infrared Absorption Spectra," J. Phy. Chem. 69:3846-3849 (1965).

205. R. H. Doremus, "Internal Hydroxyl Groups Near the Surface of Silica," J. Phy. Chem. 75:3147-3148 (1971).

206. Rinoud Hana and G-J Su, "Infrared Absorption Spectra of Sodium Silicate Glasses from 4 to 30 μ," J. Am. Ceram. Soc. 47:597-600 (1964).

207. C. C. Ballard, E. C. Broge, R. K. Iler, D. S. St. John and J. R. McWhorter, "Esterification of the Surface of Amorphous Silica," J. Phy. Chem. 65:20-25 (1961).

208. R. W. Gould and M. S. Hill, "An X-Ray Amorphous Scattering Investigation of the Corrosion of a Potassium Silicate Glass K_2O-$3SiO_2$," Adv. X-Ray Anal. 17:384-394 (1973).

209. R. H. Doremus, "Interdiffusion of Hydrogen and Alkali Ions in a Glass Surface," J. Non-Cry. Solids 19:137-144 (1975).

BIOGRAPHICAL SKETCH

Edwin Clark Ethridge was born June 29, 1950, in Meridian, Mississippi. After living his preschool years in several small Mississippi towns, his parents moved to Florida where he received most of his elementary education. In 1960 he moved to Hollywood, Florida, where he finished his public school education and graduated from McArthur High School in June 1968. While in high school the author participated in track and Cross Country. In the fall of 1968 he entered the University of Florida. Majoring in Engineering-Premed. he graduated magna cum laude in June 1973 from the Department of Materials Science and Engineering. While an undergraduate he pursued many extra curricula activities including being an active member in the Premed. Service Organization (PSO), Delta Chi Social Fraternity, and the University United Methodist Church. He also worked as a lab technician in his department.

In June 1973 he started his graduate studies, receiving his Master of Science in August 1975 and Doctor of Philosophy in June 1977, both degrees in Materials Science and Engineering. During his graduate studies, the author worked on an interdisciplinary study between the Department of Materials Science and Engineering and the College of Dentistry on the development of dental implants. He has authored and

coauthored several papers on dental implants, biomaterials, and glass corrosion during his academic studies as well as writing papers that won the National AIME Student Undergraduate and Graduate Paperwriting Contests.

Recently in September 1976 he was married to Julie McLouth.

The author is a member of AIME, Am. Ceram. Soc., and Soc. Biomaterials professional societies as well as Tau Alpha Sigma, Sigma Tau, Tau Beta Pi, Alpha Sigma Mu, and Sigma Xi honorary fraternities. Unrelated interests include running, camping, traveling, rockhounding, gardening, coin collecting, genealogy, woodworking, and ceramic art.

I certify that I have read this study and that in my opinion it conforms to acceptable standards of scholarly presentation and is fully adequate, in scope and quality, as a dissertation for the degree of Doctor of Philosophy.

Larry L. Hench, Chairman
Professor and Head of Ceramics Division

I certify that I have read this study and that in my opinion it conforms to acceptable standards of scholarly presentation and is fully adequate, in scope and quality, as a dissertation for the degree of Doctor of Philosophy.

George Y. Onoda, Jr.
Associate Professor, Materials Science and Engineering

I certify that I have read this study and that in my opinion it conforms to acceptable standards of scholarly presentation and is fully adequate, in scope and quality, as a dissertation for the degree of Doctor of Philosophy.

Ronald E. Loehman
Associate Professor, Materials Science and Engineering

I certify that I have read this study and that in my opinion it conforms to acceptable standards of scholarly presentation and is fully adequate, in scope and quality, as a dissertation for the degree of Doctor of Philosophy.

Dinesh O. Shah
Professor, Chemical Engineering

This dissertation was submitted to the Graduate Faculty of the College of Engineering and to the Graduate Council, and was accepted as partial fulfillment of the requirements for the degree of Doctor of Philosophy.

June, 1977

Dean, College of Engineering

Dean, Graduate School